TAL
TECH

DOCTORAL THESIS

Decision Support Tools for the Management of Eastern Baltic Sea Coasts

Mojtaba Barzehkar

Decision Support Tools for the Management of Eastern Baltic Sea Coasts

MOJTABA BARZEHKAR

**TAL
TECH**
PRESS

TALLINN UNIVERSITY OF TECHNOLOGY
School of Science
Department of Cybernetics
Wave Engineering Laboratory
This dissertation was accepted for the defence of the degree 19/11/2024

Supervisor:	Prof. Dr. Kevin Ellis Parnell Department of Cybernetics, School of Science Tallinn University of Technology Tallinn, Estonia
Co-supervisor:	Prof. Dr. Tarmo Soomere Department of Cybernetics, School of Science Tallinn University of Technology Tallinn, Estonia
Opponents:	Prof. Dr. habil. Gerald Schernewski Head of the Research Unit - Coastal Seas & Society Leibniz-Institute for Baltic Sea Research (IOW) Rostock-Warnemünde, Germany
	Marine Research Institute, Klaipėda University, Klaipėda, Lithuania
	Prof. Mehdi Maanan Head of the Earth Sciences Department Ain Chock Faculty of Sciences Hassan II University Casablanca, Morocco

Defence of the thesis: 16/12/2024, Tallinn

Declaration:
Hereby I declare that this doctoral thesis, my original investigation and achievement, submitted for the doctoral degree at Tallinn University of Technology has not been submitted for doctoral or equivalent academic degree.

Mojtaba Barzehkar

----
                                                                  signature

Läänemere idaranniku haldamise otsuste tugivahendid

MOJTABA BARZEHKAR

Contents

List of publications

The list of author's publications, on the basis of which the thesis has been prepared:

I   Barzehkar, M., Parnell, K.E., Soomere, T., Dragovich, D., Engström, J. 2021. Decision support tools, systems and indices for sustainable coastal planning and management: A review. Ocean and Coastal Management, 212, 105813, doi: 10.1016/j.ocecoaman.2021.105813.

II   Barzehkar, M., Parnell, K., Soomere, T., Koivisto, M. 2024. Offshore wind power plant site selection in the Baltic Sea. Regional Studies in Marine Science, 73, 103469, doi: 10.1016/j.rsma.2024.103469.

III   Barzehkar, M., Parnell, K., Soomere, T. 2024. Extending multi-criteria coastal vulnerability assessment to low-lying inland areas: examples from Estonia, eastern Baltic Sea. Estuarine, Coastal and Shelf Science, 311, 109014, doi: 10.1016/j.ecss.2024.109014.

IV   Barzehkar, M., Parnell, K., Soomere, T. 2024. Incorporating a machine learning approach into an established decision support system for coastal vulnerability in the eastern Baltic Sea. Journal of Coastal Research, Special Issue 113, 58–62, doi: 10.2112/JCR-SI113-012.1.

V   Soomere, T., Bagdanavičiūtė, I., Barzehkar, M., Parnell, K.E. 2024. Towards implementing water level variations into Coastal Vulnerability Indexes in microtidal seas. Journal of Coastal Research, Special Issue 113, 48–52, doi: 10.2112/JCR-SI113-010.1.

VI   Barzehkar, M., Parnell, K.E., Dinan, N.M, Brodie, G. 2020. Decision support tools for wind and solar farm site selection in Isfahan Province, Iran. Clean Technologies and Environmental Policy, 23 (4), 1179–1195, doi: 10.1007/s10098-020-01978-w.

Author's contribution to the publications

Contribution to the papers in this thesis are:

Paper I   Contributed to the literature review, synthesised findings, and assisted in drafting and revising the manuscript concerning the applications of decision support tools for coastal planning and management.

Paper II   Participated in methodology design, performed spatial data analysis for offshore wind farm site selection in the Baltic Sea, and contributed to writing data analysis and results sections.

Paper III   Provided expertise in multi-criteria decision analysis (MCDA) for coastal vulnerability assessment in Estonia, guided the integration of new assessment criteria, and reviewed the manuscript.

Paper IV   Developed machine learning models, analysed data outputs, and contributed to methodology and model validation sections of the manuscript regarding coastal vulnerability assessment in Estonia.

Paper V   Applied MCDA expertise to analyse extreme water level, shoreline change, and geomorphology data, to provide a robust framework for the coastal vulnerability assessment of the Lithuanian coastline.

Paper VI   Designed the study, conducted data collection and analysis, developed decision support tools for wind and solar farm site selection in inland areas, and wrote the manuscript.

Introduction

Coastal and nearshore areas develop under the influence of a large number of different drivers of greatly varying magnitude, duration and scale. Coastal areas are perceived as having high value, including their economic value, their amenity and their aesthetics. Given the range of values, benefits and services it is natural that coastal areas are among the most densely populated regions in the world. These areas are also one of the most dynamic and fastest changing environments, the health and status of which is often not well understood. This situation gives rise to a multitude of contradictory and often rapidly changing desires and expectations of different people, communities, companies, governments and other groups of stakeholders with interest in the coast. As a natural consequence, the use, planning and management of coastal and nearshore areas usually functions in an extremely complicated "landscape" of conflicting perceptions, interests, visions and goals where decision-making must take into account not only instantaneous impacts but also delayed and threshold-based reactions, and long-term and cumulative influences.

This situation naturally calls for the development and implementation of advanced tools that make it possible to gather, compare, analyse and interpret information from fundamentally different sources at different spatio-temporal resolutions to be used for informed decision-making. These tools, often called decision support systems (DSS), have to be able to merge fundamentally different kinds of information, from time series of totally quantitative hydrometeorological and geological variables, to perceptions and personal values associated with people's relationships with the coast. On the one hand, the use of data and the outcome of using such tools, ideally, should be transparent and clearly related to the input information in order to be of real use in the described "landscape" of perceptions, to convince society that the offered solution is the best. On the other hand, such tools should naturally employ the most advanced methods of data analysis and synthesis that are sometimes incomprehensible even to highly qualified experts.

This thesis attempts to address the described challenges by providing a systematic overview of existing DSSs and their main components. Based on this information, several more specialised versions of DSSs are developed and implemented to address decisions associated with the selection of locations for wind energy production in marginal seas, and options for the quantification of coastal vulnerability on a country scale. Another implementation addresses a sister problem of wind and solar energy site selection challenges in inland areas.

The nearshore and coasts under increasing pressure

The problems addressed are evident worldwide. The environmental challenges present specific threats to nations and adversely affect global communities. They are globally augmented by climate change that is an environmental issue with significant impacts on both humans and non-human species (Al-Masri et al., 2023). Climate change poses a significant threat to coastal regions worldwide (IPCC, 2022). There is strong evidence that climate change is likely to increase extreme sea levels, accelerate sea level rise, reduce sea ice cover, and enhance wave heights (Hünicke et al., 2015; von Storch et al., 2015; Farquharson et al., 2018; Nerem et al., 2018). These changes commonly lead to other adverse effects such as higher or more frequent storm surges, increased erosion rates, and flooding of low-lying areas (Nicholls et al., 2007). In densely populated coastal

areas, these hazards cause substantial damage to infrastructure and human livelihoods (Nichols et al., 2019; Tanner et al., 2014). Climate-related hazards also can destroy ecosystem services, impact biodiversity and disrupt the functioning of ecosystems in marine and coastal environments (Myers et al., 2019). Coastal areas are particularly vulnerable to hazards triggered by extreme events (Easterling et al., 2000), and pressures on coastal resources are expected to intensify due to climate change (Nursey-Bray et al., 2014). The vulnerability of these areas and the exposure of human infrastructure to flooding and wave impacts shape the impact of these events (Maanan et al., 2018). The construction of coastal structures also significantly increases the risk of coastal erosion in neighbouring segments of shoreline (Mentaschi et al., 2018; Bagdanavičiūtė et al., 2019).

The production and consumption of energy are responsible for approximately 80% of greenhouse gas emissions (Edenhofer et al., 2014). Renewable energy resources like wind, wave or solar energy are abundant in many locations. Using these resources for electricity production can greatly decrease greenhouse gas emissions. Also, their use produces no air pollution during the maintenance phase, making them environmentally friendly in particularly vulnerable areas (Wang and Qiu, 2009). Many countries have redirected their energy policies to focus on renewable energy systems to support economic growth and tackle environmental issues simultaneously (Aydin et al., 2010). The vast potential of these renewable energy sources needs to be explored, environmental concerns addressed, and economic implications considered, alongside an emphasis on sustainable development (Omer, 2008).

These aspects signal that the rapid increase in renewable energy production increases pressure on the marine environment, the nearshore and the coast. On the one hand, the development of offshore wind farms, especially in regions with optimal wind conditions, has proven to be a viable option for reducing carbon emissions-induced climate change (Cali et al., 2024). On the other hand, their development interferes with other marine and coastal activities such as shipping, tourism, commercial fishing, or seabed resource exploitation. There are also concerns about their impact on wildlife (European MSP Platform, 2018a) and their impact on aesthetics (Zhou et al., 2022).

An important aspect in handling this challenge is the need to ensure sustainable development, defined as progress that satisfies current demands without jeopardizing the ability of future generations to meet their needs (Steele, 1997). This approach not only emphasises economic growth but also supports practices that are economically viable, environmentally beneficial, and socially acceptable (Bhattacharyya, 2012). The selection of sites for renewable energy plants is a critical component in achieving this goal (Aghaloo et al., 2023) as it significantly affects electricity production capacity and socio-economic benefits (Shao et al., 2020).

Environmental, social, economic, technical, and infrastructure considerations influence the suitability of locations for renewable energy technologies. Many of the issues associated with the construction of offshore wind farms are also encountered by onshore wind farm sites (Wang and Wang, 2015). For example, land use conflicts can lead to social and political challenges (Brannstrom et al., 2017; Díaz-Cuevas et al., 2019; González et al., 2016; Scholten and Bosman, 2016). As the site selection process seeks to reduce environmental impacts and optimise economic benefits (Golestani et al., 2021; Nedjati et al., 2021) while also being acceptable to communities, it is crucial to establish effective site selection criteria and assessment methods.

Decision support tools for coastal planning and management

The described issues necessitate a complex planning process that considers environmental, social, and economic factors (Tercan et al., 2020; Virtanen et al., 2022). In other words, this highlights the importance of decision support systems (DSSs) in addressing the related environmental challenges (Walling and Vaneeckhaute, 2020; Wong-Parodi et al., 2020).

DSSs for environmental management have become increasingly popular in recent years (Walling and Vaneeckhaute, 2020; Wong-Parodi et al., 2020). By integrating computer-based tools into environmental management and long-term planning, these systems facilitate decision-making and provide a variety of problem-solving approaches, in both coastal and inland areas that aim to achieve both environmental sustainability and development goals (Wong-Parodi et al., 2020). The incorporation of DSSs into planning allows decision-makers to assess risk levels and prioritise areas requiring urgent mitigation and adaptation measures (Torresan et al., 2016). By mapping or modelling the interaction between hazards and exposures, a DSS enhances decision-makers' understanding of management options. One obvious objective is to identify appropriate buffer zones for areas of high environmental value and for infrastructure projects that may have significant impact (Wong-Parodi et al., 2020).

DSS outputs, such as classification maps or predictive models, contribute to managing coastal hazards (Zanuttigh et al., 2014; Torresan et al., 2016). These technologies have become essential tools in addressing challenges posed by climate change and environmental pressures (Zhu et al., 2010). Tools ranging from models to databases and visualisation platforms support decision-making processes with critical information and analysis (Mysiak et al., 2005; Giupponi, 2007).

A DSS commonly uses several computer-based decision support tools (DSTs) designed to facilitate decision-making, including geographical information systems (GIS), multi-criteria decision analysis (MCDA), artificial neural networks (ANN), Google Earth Engine (GEE), and model-driven techniques (Yarian et al., 2020). As discussed in this thesis, integrating multiple DSTs tends to provide better results compared to using a single tool. In particular, robust and user-friendly DSTs are needed to facilitate effective and equitable coastal management strategies under climate change impacts (Nicholls et al., 2007).

DSS rely heavily on GIS tools due to their ability to represent, analyse, and visualise spatial data (Ahmed et al., 2022; Armenio et al., 2021; Hoque et al., 2019; Rehman et al., 2022) by combining multiple parameters (Thirumurthy et al., 2022). While GIS provides a systematic framework for processing, and managing spatial data, allowing the inclusion of diverse parameters (Díaz-Cuevas et al., 2019), MCDA assigns context-based values to evaluation parameters and combines qualitative and quantitative attributes, including the opinions of experts, to prioritise different parameters and locations (Mytilinou et al., 2018). The integration of MCDA and GIS provides an effective framework for incorporating spatial data and expert opinions to generate actionable insights (Malczewski and Rinner, 2015) in various site selection studies (Gil-García et al., 2022; Genç et al., 2021; Li et al., 2022), especially in large-scale marine spatial planning (Tercan et al., 2020). This integration helps enhance the understanding of outputs through the inclusion of expert opinions and trade-offs among decision goals (Bell et al., 2003).

A DSS is useful for generating decision support indices (DSIs) to quantify coastal vulnerability, which can be used for coastal adaptation planning (Gargiulo et al., 2020). A DSI usually incorporates environmental and socioeconomic variables that reflect

vulnerability, risk, and resilience (Furlan et al., 2021). Assessing coastal vulnerability is essential for developing effective strategies to mitigate and adapt to the impacts of climate change and human activities on coastal regions. Several indices have been developed to provide comprehensive evaluations of coastal vulnerability, each addressing different aspects and dimensions of the issue. For example, the Coastal Vulnerability Index (CVI) combines physical, ecological, and socioeconomic data to assess coastal vulnerability, identifying hotspots for targeted mitigation and implementation of adaptation strategies (McLaughlin and Cooper, 2010; Ramieri et al., 2011). The CVI supports the development of strategies that promote human well-being while balancing environmental sustainability (IPCC, 2019; Wong-Parodi et al., 2020).

Renewable energy farm site selection in offshore and inland areas

The pervasive use of fossil fuels is the principal contributor to global warming, with CO_2 and other greenhouse gases being emitted into the atmosphere (IPCC, 2021). In response, renewable energy technologies are increasingly favoured for electricity production as a response to climate change. The utilization of renewable energy systems plays a vital role in mitigating the effects of greenhouse gas emissions (Alsema, 2000). Renewable energy plants are gradually becoming more cost-efficient than those using traditional energy sources (IRENA, 2020).

The global demand for renewable energy is increasing as fossil fuel use declines. Projections indicate that by 2050, renewable sources could account for approximately two-thirds of global energy demand (Gielen et al., 2019). The European Union has implemented multiple strategies to transition to a more efficient and diverse energy model, which involves not only reducing greenhouse gas emissions but also using renewable energy resources efficiently and improving energy efficiency (Díaz-Cuevas et al., 2019). Energy distribution in renewable energy facilities has primarily been based on resource availability and access to an electrical grid, often overlooking broader factors of location suitability or the potential for integrating multiple energy sources (Díaz, 2013). For example, renewable energy farms should be located in geologically suitable places, away from protected areas, acceptable in terms of other marine space and land use, far from marine traffic but close to land-based transport networks. The analysis of these factors aims to balance multiple considerations: maximise economic benefits, minimise negative environmental impacts, enhance energy efficiency (Díaz-Cuevas et al., 2019) while minimising social impacts (Department for Energy Security and Net Zero, 2022).

Wind energy is cost-effective, safe, and environmentally beneficial (Noorollahi et al., 2016a; Gielen et al., 2019). In recent decades, the adoption of wind power has significantly increased, primarily driven by reduced generation costs (Osman et al., 2022; Guchhait and Sarkar, 2023). Offshore wind power plants offer substantial advantages over onshore farms, including higher energy yields and reduced aesthetic and noise impacts (Bilgili et al., 2011; Wu et al., 2018). They also benefit from greater flexibility for the installation of devices in marine environment. Critical factors in the construction of foundations and cable connections include water depth, distance from shore, and port accessibility (Khan et al., 2021). Although deeper water and remote locations require more expensive infrastructure, these areas often offer optimal wind conditions as demonstrated in Paper II.

The last few years have seen a rapid increase in the interest in wind power generation in the Baltic Sea, particularly in its southern parts. This has led to extensive

studies on the technical aspects of such developments (Klinge Jacobsen et al., 2019; Scolaro and Kittner, 2022; Ziemba, 2022). Due to the significant reduction of energy supply from the Russian Federation, it is important to increase energy production capacity in the European Union (European Commission, 2022). It is well known that effective site selection for renewable power plants significantly impacts energy production and installation costs (Shafiee, 2022). However, these developments also impact not only marine ecosystems but a range of existing human activities in the Baltic Sea, including fisheries, shipping routes, coastal tourism, and several socioeconomic factors (Reckermann et al., 2022). Therefore, it is crucial to evaluate optimal locations for offshore wind power plants by integrating technical, social, economic, and environmental factors to mitigate environmental concerns and enhance energy production (Tercan et al., 2020). In particular, it is imperative to identify and prioritise suitable offshore wind power plant sites to maximise energy productivity, minimise costs, reduce environmental impacts, and enhance social benefits as the offshore wind power industry grows and evolves.

It is therefore natural that the site selection process for offshore wind power plants involves a complex planning approach that is able to balance minimizing environmental disruptions with maximizing economic benefits (Golestani et al., 2021; Nedjati et al., 2021). Therefore, comprehensive and adequate analysis of potential power plant locations using advanced DSSs becomes essential to systematically incorporate environmental, economic, and social considerations into the decision-making process, thus promoting the development of a sustainable energy infrastructure and effectively responding to the complex dynamics of renewable energy management. In this context, various single decision support tools incorporating GIS techniques are essential for identifying optimal locations for renewable energy infrastructure both onshore and offshore (Aydin et al., 2010; Tegou et al., 2010; Vagiona and Karanikolas, 2012; Emeksiz and Demirci, 2019; González and Connell, 2022). The best results commonly combine the use of GIS with other appropriate tools, such as multi-criteria decision analysis (MCDA) (Gašparović and Gašparović, 2019).

Another approach for offshore wind site selection is the levelised cost of energy (LCOE) method. This method evaluates the economic feasibility of potential sites by calculating the ratio of total energy production costs to the total energy generated over the project's lifetime (Johnston et al., 2020). By considering both initial investment expenses and recurring operational costs, LCOE provides an average cost per unit of energy output (Johnston et al., 2020). It is thus most useful for identifying the most cost-effective locations for offshore wind farms. However, as sustainable development and exploitation of offshore wind energy resources require a comprehensive understanding of how environmental, economic, and social factors interact (Fetanat and Khorasaninejad, 2015; Vagiona et al., 2018), it is essential to use the LCOE technique simultaneously with approaches that take into account existing space usage and environmental and social aspects. Doing so promotes the reliability and accuracy of the site selection results.

The same tools are appropriate for inland locations. This versatility is demonstrated by presenting results from a study incorporating both wind and solar renewable energy farm locations in Iran. The main goal is to identify and develop a robust methodology for evaluating potential sites for renewable energy facilities based on local and regional characteristics and a variety of parameters that must be thoroughly examined before construction (Gašparović and Gašparović, 2019).

Coastal vulnerability assessment in the Baltic Sea

As discussed above, climate change induced coastal hazards threaten the physical environment, human infrastructure, livelihoods, and biodiversity worldwide (IPCC, 2022; Torresan et al., 2008). Enhancing the resilience of coastal communities and mitigating potential damage necessitates a thorough understanding and addressing of the related risks. Identifying and assessing the susceptibility of coastal areas to various hazards has become crucial. A large part of this work comes from coastal vulnerability assessments that consider both natural and human-induced factors, assisting coastal managers and planners in evaluating the vulnerability of specific locations (Adger et al., 2005).

Such assessments are vital for several reasons. They help identify and prioritise high-risk areas, ensuring effective resource allocation and disaster prevention. They also provide valuable data for infrastructure planning and development, improving the design of new projects to account for potential hazards. This helps coastal communities avoid costly damage and enhances their safety and sustainability. Furthermore, by highlighting regions where natural habitats and ecosystems are at risk, these assessments support environmental conservation efforts by protecting biodiversity and maintaining ecosystem services.

By integrating various parameters, the Coastal Vulnerability Index (CVI) helps prioritise the vulnerability of different coastlines (Rangel-Buitrago et al., 2020). In terms of evaluating the likelihood of socioeconomically valuable features being affected by hazards such as flooding, the Coastal Exposure Index (CEI) is used. The CEI utilises flood maps from hydrodynamic models to determine exposure levels (Bagdanavičiūtė et al., 2019). The combination of CVI and CEI constitutes the Coastal Risk Index (CRI) (Bagdanavičiūtė et al., 2019). For land-use planning to prioritise areas for coastal protection, the Coastal Area Index (CAI) is used. It considers parameters like elevation, coastal slope, and land use to balance conservation and development (Dhiman et al., 2019). To estimate the capacity of coastal areas to respond to hazards, the Coastal Resilience Index (CoRI) is used. It focuses on factors such as distance from the coastline, elevation, and human activities, integrating them into coastal planning (Gargiulo et al., 2020).

The Analytical Hierarchy Process (AHP) is widely used to assess coastal vulnerability in the frame of GIS-MCDA applications. Recently, machine learning algorithms have become popular for mapping hazard susceptibility. Techniques like Random Forest are effective in handling large datasets and complex interactions (Wang et al., 2016). Incorporating GIS, MCDA, and machine learning models into coastal vulnerability assessments offers a more comprehensive view of coastal hazards and robust methodologies for coastal vulnerability assessments. Both methods provide a valuable insight into coastal vulnerability, essential for informed decision-making and effective adaptation While MCDA provides a structured approach that incorporates expert opinions, machine learning techniques handle complex datasets and interactions more efficiently. It is thus necessary to compare GIS-MCDA techniques with other approaches, such as machine learning methods, to evaluate their strengths, weaknesses, and applicability to regions with complex coastal characteristics, like the eastern Baltic Sea.

The assessment of coastal vulnerability is particularly important in the eastern Baltic Sea region, especially in Estonia, due to its complex shoreline characteristics and increasing threats posed by climate change-induced hazards (Orviku et al., 2003;

Rosentau et al., 2017). The low-lying coastal areas, dominated by fine sediment and easily erodible moraine deposits, are highly susceptible to erosion, storm surges, and sea level rise (Łabuz, 2015; Orviku, 2018). The gently sloping shores of islands of Hiiumaa and Saaremaa and low-lying shores of Western Estonia are especially vulnerable (Suursaar et al., 2008). Storm surges in the Baltic Sea, partially driven by excess water volume lasting up to several weeks (Andrée et al., 2023), strong winds, and wave action, pose a significant threat to the Estonian coast (Hünicke et al., 2015). Certain wind directions lead to high wave setup on specific coastal sections (Pindsoo and Soomere, 2015). Coastal flooding is exacerbated by sea level rise, shorter winter ice cover, and increased storm frequency (Orviku et al., 2003; Harff et al., 2017). These hazards are likely to worsen many current and future social, economic, and environmental problems (Rosentau et al., 2017). The vulnerability of coastal regions to extreme events, amplified by sea level rise and storm frequency, necessitates proactive adaptation measures (Harff et al., 2017).

By incorporating a variety of tools, systems, and indices, and considering also less obvious variables such as nature protection areas, land tenure, and setbacks through high-resolution maps, this thesis aims to provide a comprehensive assessment of coastal vulnerability, risk, and resilience, contributing to the development of effective and sustainable coastal management strategies. This integrated approach will help identify priority areas for intervention and inform decision-making processes to enhance the resilience of coastal communities by delivering accurate and comprehensive vulnerability assessments, crucial for informed decisions and effective adaptation measures.

The objective and outline of the thesis
The primary objective of this thesis is to develop and implement an appropriate decision support system to evaluate the optimal locations for offshore wind farm installations in the Baltic Sea region, to perform an assessment of coastal vulnerability in eastern Baltic Sea, and explore options of applications of this system in different environments, including for solar and wind farm site selection in inland areas. The study uses Geographic Information Systems (GIS), multi-criteria decision analysis (MCDA), and machine learning using the Random Forest (RF) technique to improve decision-making processes in coastal planning and management, sustainable offshore wind infrastructure development, coastal vulnerability assessment, and renewable energy site assessment in inland areas. A comprehensive set of parameters, including those often overlooked in previous studies, is considered alongside existing and potential wind farm locations.

The main objectives are to:
- Provide a comprehensible view on existing implementations of decision support tools (DSTs) for coastal planning and management, which incorporates GIS, MCDA, and machine learning to promote coastal decision-making process.
- Analyse the potential economic viability and environmental suitability of offshore wind farm locations using GIS-MCDA and GIS-based levelised cost of energy models for the entire Baltic Sea.
- Combine of two-dimensional and one-dimensional parameters to analyse coastal vulnerability for the whole of Estonian coast using, in parallel, the classic GIS-MCDA technique and machine learning applications.

- Explore the options for integration of different measures of water level variability to improve the classic estimates of coastal vulnerability assessment.
- Demonstrate that the established DSSs are applicable to a different environment by examining wind and solar farm site selection in inland areas based on GIS and MCDA.

To achieve these objectives, Chapter 1 explores the application of decision support tools (DSTs) to coastal planning and management. An integrated approach to coastal management is presented that combines GIS, MCDA, and machine learning. This chapter emphasises the significance of these tools in contributing to a sustainable coastal development and assessing coastal vulnerability.

Chapter 2 discusses the application of DSTs for selection of offshore wind farms in the Baltic Sea. The environmental suitability and economic viability of offshore wind farm locations is evaluated using in parallel the GIS-MCDA technique and GIS-based levelised cost of energy (LCOE) models. It emphasises the importance of selecting an optimal site in order to minimise negative environmental impacts and maximise economic benefits.

Chapter 3 discusses the application of DSTs for coastal vulnerability assessment in the eastern Baltic Sea region. A GIS-MCDA is used in order to assess coastal vulnerability for the entire nearshore of Estonia. A new development is the analysis of vulnerability up to 2 km inland. The aim is to provide coastal managers and decision-makers with valuable insights into comprehensive vulnerability analyses based on several different approaches.

Chapter 4 discusses benefits from integration of a machine learning technology, based on Random Forest technique, into the evaluation of vulnerability of Estonian coasts and the inclusion of water level variations into estimates of coastal vulnerability along the Lithuanian shoreline. As an example of wide applicability of the presented techniques, Chapter 4 also examines how to select the best site for wind and solar farms in inland areas, taking into account environmental, social, economic, technical, and infrastructure factors.

Presentation of the results to scientific community
These basic results have been presented by the author at the following scientific conferences:

Oral presentations:
Barzehkar, M., Parnell, K., Soomere, T. 2024. Integrating multi-criteria decision analysis and GIS for coastal vulnerability assessment: a case study in Estonia, Eastern Baltic Sea. Nordic Geographers Meeting in Copenhagen (24–27 June 2024, Copenhagen, Denmark).

Barzehkar, M., Koivisto, M., Parnell, K.E., Soomere, T. 2022. An integrated decision support system for offshore wind farm site selection in the Baltic Sea. 18th European Academy of Wind Energy (EAWE) PhD Seminar in Wind Energy (2–4 November 2022, Bruges, Belgium).

Barzehkar, M., Parnell, K.E., Soomere, T. 2021. An integrated decision support system for the resilience assessment of eastern Baltic Sea coasts. CoastGIS 2021: Sustainable Coastal Management in a Changing World (16–17 September 2021, Raseborg, Finland, online).

Poster presentations:

Barzehkar, M., Parnell, K.E., Soomere, T. 2020. Decision support tools for the management of eastern Baltic Sea coasts. 3rd Baltic Earth Conference "Earth system changes and Baltic Sea coasts (2–3 June 2020, Jastarnia, Hel Peninsula, Poland, online).

Oral presentations by co-authors:

Soomere, T. (presenter), Barzehkar, M., Parnell, K., Bagdanavičiūtė, I. 2024. In search for suitable parameters quantifying the contribution of water level variations into coastal vulnerability index of microtidal seas. 5th Baltic Earth Conference "New Challenges for Baltic Sea: Earth System Research" (13–17 May 2024, Jūrmala, Latvia).

Soomere, T. (presenter), Bagdanavičiūtė, I., Barzehkar, M., Parnell, K.E. 2024. Towards implementing water level variations into coastal vulnerability index of microtidal seas. 17th International Coastal Symposium (ICS2024) "Coastlines Under Global Change" (24–27 September 2024, Doha, Qatar).

Barzehkar, M., Parnell, K.E. (presenter), Soomere, T. 2024. Incorporating a machine learning approach as an established decision support system for coastal vulnerability in the Eastern Baltic Sea. 17th International Coastal Symposium (ICS2024) "Coastlines Under Global Change" (24–27 September 2024, Doha, Qatar).

Abbreviations

AHP	Analytical Hierarchy Process
ANN	Artificial Neural Network
CAPEX	Capital Expenditure
CAI	Coastal Area Index
CEI	Coastal Exposure Index
CRI	Coastal Risk Index
CVI	Coastal Vulnerability Index
CoRI	Coastal Resilience Index
DSI	Decision Support Index
DSS	Decision Support System
DST	Decision Support Tool
GEE	Google Earth Engine
GIS	Geographical Information System
IPCC	Intergovernmental Panel on Climate Change
LCOE	Levelised Cost of Energy
MCDA	Multi-Criteria Decision Analysis
OPEX	Operational Expenditure
RF	Random Forest

1 Decision support tools for coastal planning and management

A selection of decision support tools (DSTs), decision support systems (DSSs), and decision support indices (DSIs) is discussed in this chapter in order to highlight the basic properties of their constituents and known limitations and experience of their implementation. On the one hand, this kind of information is eventually useful to assist with coastal planning and management for a sustainable coastal environment and for infrastructure development. The focus for these tools is handling of extreme water levels, inundation, and coastal erosion. On the other hand, this material serves as important input for development of more specialised applications in the subsequent chapters.

This chapter also explores the importance of effective DSTs and DSSs for calculating indices such as the Coastal Vulnerability Index (CVI), Coastal Exposure Index (CEI), Coastal Risk Index (CRI), and Coastal Resilience Index (CoRI) (Paper II). As a means of coastal vulnerability and resilience assessment, multi-criteria decision analysis (MCDA), geographical information systems (GIS), and artificial neural networks (ANNs) are integrated. The analytical hierarchy process (AHP), fuzzy standardisation and logic, and weighted linear combination (WLC) are MCDA approaches that incorporate expert preferences. A geographical information system (GIS) assists in storing, displaying, and analysing spatial data, mapping vulnerable coastal areas, and supporting long-term planning (Malczewski and Rinner, 2015; Gargiulo et al., 2020) while ANNs are used to classify maps, detect features associated with vulnerable ecosystems, and predict environmental changes (Rumson et al., 2020).

There have been numerous applications of DSTs in environmental hazard assessment, employing tools such as GIS, MCDA, and ANN (Jena et al., 2020; Yariyan et al., 2020a; Arabameri et al., 2021; Pham et al., 2021). Although clear advancements have been made, many studies lack a formal justification for selecting or combining these tools. Paper I aimed to fill this gap by systematically evaluating a variety of DSTs, DSSs, and DSIs to guide managers and decision-makers in choosing the most appropriate tools. This Chapter largely follows the material presented in Paper I. The detailed characteristics and contributions of various implementations of DSTs, DSSs, and DSIs towards strengthening coastal management planning are presented in Tables 1 and 2 of Paper I.

1.1 Decision support tools and systems

Contemporary informed decision-making ideally relies on the best available information that is properly quantified, analysed and put into an appropriate context. Any decision-making process thus start from the identification of necessary information, selection of important parameters, choice of spatio-temporal resolution and collection of necessary data from various sources, from research papers to classic maps. Alternatively, the necessary information is often generated using various numerical models tuned specifically to provide the best data stream for solving a particular management problem.

As much of this information in coastal and marine areas is presented in the form of (raster) maps, tools like GIS form an intrinsic constituent of the process. Subsequently, the data from various sources have to be converted into a usable form for further

analysis. This is often done using so-called fuzzy normalisation. Different drivers and parameters generally have a different impact on the decision. Therefore, the weight of each parameter should be estimated as adequately as possible. Finally, the compound estimate for decision-making (e.g., normalised vulnerability index) is commonly reached using these weights.

1.1.1 Numerical models

The numerical models are now a common tool to simulate factors such as wind, waves, and other physical processes that affect coastal areas (Coelho et al., 2020; Glover et al., 2011). They provide atmospheric variables (Hersbach et al., 2020), and wave variations and properties both globally (Morim et al., 2022) and locally (e.g., Björkqvist et al., 2018). Based on wind data, it is possible to configure and run contemporary wave models such as SWAN (Booji et al., 1999) and WAM (Komen et al., 1994), or user-friendly implementations, such as MIKE 21 (DHI, 2017) for the region of interest to simulate and estimate wind-generated waves. If it is too time-consuming and computationally demanding to run these models locally, as it is often the case (Chini and Stansby, 2015), databases such as the Copernicus or ERA5 sources (https://cds.climate.copernicus.eu/) provide ready-to-use data. The data can be used with local wave models to calculate storm surge levels (Lorenz and Gräwe, 2023), wave setup (Soomere et al., 2020), and runup (Marsooli and Lin, 2018).

Models such as the MIKE 21 model are also able to estimate sediment transport and coastal morphology (DHI, 2017), and model shoreline changes at local and regional scales (Coelho et al., 2020). In this respect, a number of challenges must be addressed, including determining accurate boundary conditions, managing external waves, and dealing with energy dissipation (Masselink et al., 2011). The modelled data sets can be complemented with extensive sources of information derived using various remote sensing applications, e.g., the worldwide map of coastline changes (Luijendijk et al., 2018) that also covers the entire Baltic Sea.

1.1.2 Geographical information system (GIS) and Google Earth Engine (GEE)

A GIS is essential for the storage, display, and analysis of spatial data, making it a cost-efficient tool for spatial planning in general, and for coastal planning in particular over the long term (Pan et al., 2005). The integration of different approaches that support decision-making with GIS promotes the process by prioritizing and weighting map data (Malczewski and Rinner, 2015). For example, an analysis of vulnerable coastal areas is commonly carried out using GIS for the evaluation of indices such as the Coastal Vulnerability Index (CVI, Section 1.4) and Coastal Resilience Index (CoRI, Section 1.4) (Hoque et al., 2019; Gargiulo et al., 2020). It provides managers and the public with accessible maps (Iyalomhe et al., 2013; Aporta et al., 2020) that support informed decisions (Rangel-Buitrago et al., 2017, 2020b). Tools such as DESYCO and THESEUS were developed to raise public awareness and assess risks through GIS. The DESYCO system provides adaptable risk assessments for sea level rise and coastal erosion (Santoro et al., 2013; Torresan et al., 2016). Based on analytical models and expert opinions, THESEUS assesses coastal risks and mitigation options (Kane et al., 2014; Zanuttigh et al., 2014).

Google Earth Engine (GEE) is a cloud-based platform for processing large geospatial datasets. To analyse regional and global satellite imagery, JavaScript and Python algorithms are used (Vos et al., 2019; Tamiminia et al., 2020). The GEE provides access

to extensive satellite image collections, such as Landsat-8 and Sentinel-2, which can be used for geospatial analyses of various features, such as shoreline position changes and land use changes (Chu et al., 2020; Arruda et al., 2021). The CoastSat application of GEE creates time-series data to classify coastline changes over the past 30 years (Vos et al., 2019).

1.2 Multi-criteria decision analysis (MCDA) approaches

To reach rational and informed decisions and to determine management goals, more generally, to operationalise the management process (Townend et al., 2021), it is necessary to put the environmental and socioeconomic parameters selected and gathered for decision-making into context. This includes their quantification (e.g., via GIS and/or GEE), normalisation, weighting, and ranking (Mafi-Gholami et al., 2019). An effective tool for complex coastal management decisions (Uhde et al., 2015) is the multi-criteria decision analysis (MCDA) that helps to prioritise vulnerable locations and risk areas based on various parameters (Johnston et al., 2014) and makes it possible to incorporate expert preferences and expertise into coastal decision-making (Haque, 2016; Adem Esmail and Geneletti, 2017). MCDA incorporates fuzzy logic standardisation, analytical hierarchy process (AHP), and weighted linear combination (WLC) methods (Malczewski and Rinner, 2015).

1.2.1 Fuzzy standardisation and fuzzy logic

Input information on the properties of coastal and nearshore areas as well as the description of various hydrometeorological drivers is often available or presented as raster maps. Because these maps are intrinsically measured with different units and scales, it is crucial to normalise their numerical values before combining them (e.g., Eastman, 2009). Fuzzy logic is commonly used in the MCDA process to standardise raster map pixels, reduce uncertainties and normalise data variability (Paper I). The range of normalised variables from 0 to 1 is used as a standard, where 0 represents very low and 1 very high vulnerability (e.g., Araya-Muñoz et al., 2017). A linear scale is the most common method for normalizing raster layers, which is often based on minimum and maximum values (e.g., Cheng et al., 2023). This range is usually divided into subranges that characterise very low (values from 0 to 0.2), low (0.2, 0.4), medium (0.4, 0.6), high (0.6, 0.8), and very high (0.8, 1) vulnerability with respect to a particular parameter (e.g., Hoque et al., 2021). In a similar way, resilience and other parameters can be standardised

An intrinsic feature of environmental parameters is that, for some of them increasing values indicate an increase in vulnerability (e.g., extreme water level, sea level rise rate, maximum significant wave height, called increasing functions) while for others a larger value means lower vulnerability (e.g., land elevation, coastal slope, called decreasing functions). Moreover, frequently values over a certain threshold R_{max} (or below another threshold R_{min}) do not further increase or decrease the associated vulnerability. The level of vulnerability is thus constant (1 or 0) for such input values. Such features are usually accommodated using the following piecewise linear transformations

$$X_1(i) = \frac{R_i - R_{min}}{R_{max} - R_{min}}, \quad X_1(i) = 0 \text{ if } R_i < R_{min}, \quad X_1(i) = 1 \text{ if } R_i > R_{min} \quad (1)$$

for increasing functions and

$$X_2(i) = \frac{R_{\max} - R_i}{R_{\max} - R_{\min}}, \quad X_2(i) = 0 \text{ if } R_i > R_{\max}, \quad X_1(i) = 1 \text{ if } R_i < R_{\min} \tag{2}$$

for decreasing functions (e.g., Kao, 2010).

While the classic fuzzy logic captures a continuum of values between 0 and 1 (e.g., Zarin et al., 2021), another class of its input functions form custom user-defined discrete functions. They are expressed as discrete estimates that characterise, e.g., vulnerability associated with geomorphology, type of sediment, presence or absence of nature protection areas or coastal protection structures, land use, and land tenure (see Paper III for examples and references). On some occasions (e.g., presence or absence of nature protection areas or coastal protection structures) the input for fuzzy logic is like a Heaviside function with only two values 0 and 1.

1.2.2 Analytical Hierarchy Process (AHP)

AHP is a widely used pairwise comparison method where each parameter is weighted against others to determine the relative significance of all parameters (Chai et al., 2013; Mu and Pereyra-Rojas, 2018). It is often used as part of coastal vulnerability, risk, and resilience assessments (Ishtiaque et al., 2019; Hadipour et al., 2020b; Sekovski et al., 2020). It allows for the quantitative analysis of parameters that affect CVI, CRI, and CoRI (Mani Murali et al., 2018). The weighting and prioritisation are performed based on expert assessments. Each factor is ranked using a pairwise comparison matrix (see, e.g., Table 7 in Paper III). The selected parameters are usually weighted on a scale from 1 to 9, where 9 indicates extreme importance (or influence), 7 very strong importance, 5 strong importance, 3 moderate importance, and 1 minimum importance, with intermediate values also used (Saaty and Tran, 2007; De Serio et al., 2018). The pairwise comparison matrix is completed by inserting reciprocal values (e.g., 1/3, 1/5, 1/7, 1/9) into the transposed positions (Saaty and Tran, 2007).

The consistency in the weighting process is characterised by the so-called consistency ratio CR (Saaty and Tran, 2007; Gargiulo et al., 2020)

$$CR = \frac{CI}{RI}, \tag{3}$$

that is a ratio of consistency index CI to the Random Index RI. The consistency index CI defined by Saaty and Tran (2007) is computed as (e.g., Klutho, 2013):

$$CI = \frac{\lambda_{max} - N}{N - 1}, \tag{4}$$

where $\lambda_{\max}$ is the largest eigenvalue of the pairwise comparison matrix, and N is its size, equivalently, the number of parameters or attributes being compared. The random index RI is found using the same equation as the usual value for the totally random pairwise comparison matrix (Saaty and Tran, 2007). The RI values, evaluated from a large number of randomly filled matrices, increase to about 1.5 as N increases from 1 to 10 and level off around 1.6 for larger values of N (Aguarón and Moreno-Jiménez, 2003; Saaty and Tran, 2007). The AHP results are consistent if $CR \leq 0.1$. This condition is routinely checked in studies based on the AHP method (e.g., Diaz-Cuevas et al., 2020). The AHP method is used in Papers II, III, and IV as described below.

1.2.3 Weighted linear combination (WLC)

WLC is a common tool to integrate various environmental and socioeconomic data for calculating coastal DSIs, ranking vulnerabilities and risks across different areas (Hadipour et al., 2020a, 2020b) in situations where different components may have different importance, priority or impact. WLC assessment can be effectively accomplished with GIS using map algebra (Tomlin, 1990; Malczewski, 2000). In essence, WLC is a direct generalisation of the simple sum or direct average of single estimates of, e.g., vulnerability driven by some factor X_j by means of assigning weights (or ranks) W_j to each component X_j of normalised data using fuzzy standardisation, to obtain a weighted estimate:

$$WLC = \sum_{j=1}^{n} X_j W_j. \tag{5}$$

The users of this method often call the addressed components or parameters attributes (Ghosh and Lepcha, 2019). In coastal studies, examples of attributes are elevation, slope, geology, shoreline change rate, or land use.

1.3 Advanced methods

Paper I also presents an overview of several advanced, rapidly developing techniques in decision making in coastal matters that have not been implemented in the studies presented below.

1.3.1 Artificial Neural Networks (ANNs)

The ANNs are based on biological neural networks and are used to model environmental hazards for more than two decades (e.g., Chen et al., 2004; Gokceoglu et al., 2005). This approach has provided reasonably good estimates without fully understanding the underlying processes in, for example, hydrological applications (Gudiyangada Nachappa et al., 2020). On many occasions, e.g., to predict coastal erosion, the benefits of GIS and ANN are combined (Peponi et al., 2019). To identify vulnerable coastal ecosystems, ANNs have been used to classify images and maps (Rumson et al., 2020).

ANNs are based on neurons, where the output of one layer becomes the input for the next (Ahmadlou et al., 2020). A multi-layer perceptron (MLP) is the most common ANN for coastal change classification, which uses supervised classification with input, hidden, and output layers (Goldstein et al., 2019). A backpropagation algorithm (BPA) is used for MLP training to minimise mean-square errors between output and expected values (Ghorbanzadeh et al., 2019a). The complexity of a problem determines how many hidden layers are needed. For MLP, random samples are selected to represent hazards and non-hazards (Dao et al., 2020). Yariyan et al. (2020b) divided 101 hazard and 101 non-hazard locations 70:30 for training and testing. Depending on the study scope and desired accuracy, sample size and ratio may vary (Thi Ngo et al., 2021).

1.3.2 Bayesian Networks (BN)

In environments with limited data, various graphical probabilistic models provide additional resources for the analysis and synthesis of existing information (e.g., Ben-Gal, 2008). Among these, Bayesian networks (BN) have become increasingly popular since

about 2000. They often rely on Bayesian statistics for the posterior probability of forecast

$$p(F_i|O_j) = \frac{p(O_j|F_i)p(F_i)}{p(O_j)}, \tag{6}$$

where $p(F_i|O_j)$ is the posterior probability of forecast F_i given observations O_j, $p(O_j|F_i)$ is the likelihood of observations O_j given forecast F_i, $p(F_i)$ is the prior probability of F_i, and $p(O_j)$ is the prior probability of O_j. However, the use of BN does not necessarily imply the use of Bayesian statistics (Ben-Gal., 2008).

In essence, BN models provide graphic representations of probability distributions of e.g. coastal hazards (Sahin et al., 2019) based on predictive modelling. This technology is increasingly being used to model coastal vulnerability and risk assessments in the face of significant uncertainty (Sahin et al., 2019; Guo et al., 2020). The BN outcome shows the probability distribution of hazards graphically (Sahin et al., 2019), commonly forecasting erosion and accretion rates in relation to sea level rise. The nodes of the BN can be used to represent factors such as coastal response, boundary conditions, location, hazards, and wave properties, with undirected or directed edges (arrows) showing their interconnections (Plomaritis et al., 2018).

Another way of implementation of the BN technique is the use of a directed acyclic graph (DAG), for example, to demonstrate causal relationships between parameters that are associated with coastal hazards (Giardino et al., 2019). Multiple variables are integrated into BNs to provide robust data-driven or model-driven forecasts (Giardino et al., 2019). A BN model can provide alternatives to numerical models when assessing the effects of coastal hazards on infrastructure and ecosystems (Plomaritis et al., 2018).

1.4 Decision Support Indices (DSIs)

The concept of vulnerability refers to a system's susceptibility and inability to deal with adverse effects (Adger, 2006). A coastal vulnerability index (CVI) quantifies coastal segments to identify those that may be more vulnerable with respect to the joint impact of a multitude of drivers and thus may require protection for community resilience (Bagdanavičiūtė et al., 2015; Hoque et al., 2019; Koroglu et al., 2019).

While the first application of a CVI incorporated only a small number of variables (elevation, lithology, geomorphology, relative sea level change, shoreline displacement, tidal range and wave heights; Gornitz, 1991), most of contemporary studies include >10 parameters and Paper III addresses 16 parameters. It is customary to normalise the numerical values of CVI index into the range from 0 to 1 and divide the areas into five classes similar to the outcome of the fuzzy standardisation in Section 1.2.1.

A CVI may be split into or be considered as a set of multiple sub-indices, including the coastal characteristics vulnerability index (CCVI), the coastal forcing vulnerability index (CFVI), and the socioeconomic vulnerability index (SEVI). The factors contributing to the SEVI include population density, infrastructure, cultural heritage, land use, and land cover (Mullick et al., 2019; Ng et al., 2019; McLaughlin et al., 2010).

Various coastal exposure indices (CEI) have been developed for the evaluation of socioeconomically important areas in terms of their vulnerability to hazards such as flooding (Bagdanavičiūtė et al., 2019). They may employ both land-based (e.g., heavy precipitation or river flooding) and marine sources of coastal flooding, such as storm surges, tsunamis, and high waves. The CEI is often evaluated based on hydrodynamic

models that predict maximum water levels for the creation of flood maps (Bagdanavičiūtė et al., 2019). In these maps, extreme water level return periods are evaluated, recognizing that predictions may change over time (Mucerino et al., 2019).

Based on the CVI and CEI, the coastal risk index CRI can be developed that quantifies hazards impacting coastal sectors (Bagdanavičiūtė et al., 2019). Various implementations of CRI assist to identify the most vulnerable locations, for example, with respect to climate change (Bagdanavičiūtė et al., 2019). Another example is the flood exposure map used to assess the susceptibility of infrastructure and communities to flooding (Chaib et al., 2020). Using this approach, strategies to enhance infrastructure resilience and coastal disaster protection plans can be developed in response to climate change-induced hazards (Chaib et al., 2020).

Different coastal area indices (CAI) assist in land-use planning by prioritising coastal protection zones, especially in development zones (Dhiman et al., 2019). They are commonly designed to provide decision-makers with a quantitative means of classifying coastal areas on the basis of their vulnerability to infrastructure development (Dhiman et al., 2019). As part of the CAI, factors such as elevation, coastal slope, shoreline change rate, geological formation, soil texture, vegetation, land use, and land cover are taken into account (Dhiman et al., 2018). Based on this index, coastal management can be balanced between conservation and sustainable development (Dhiman et al., 2018, 2019).

A coastal resilience index (CoRI) assesses a coastal area's ability to withstand climate-related hazards, assisting in the development of adaptation strategies (Gargiulo et al., 2020). Resilience is influenced by factors such as distance of a particular location from the coast, elevation, and human activities, with low-lying, densely populated regions being especially vulnerable (Roy et al., 2019; Gargiulo et al., 2020). Coastal resilience can further be reduced by tourism and urbanisation (Kim et al., 2017). The use of this kind of assessment makes it possible to highlight also sustainable development goals and propose potential solutions (Sajjad et al., 2020).

1.5 Organisation of workflow for coastal planning and management

The main conclusions from the overview in Paper I are mostly straightforward. First of all, an effective method for coastal management involves integrating different decision support tools (DSTs) into the decision support system (DSS) and calculating decision support indices (DSIs). A recommended combination of DSTs to be implemented in
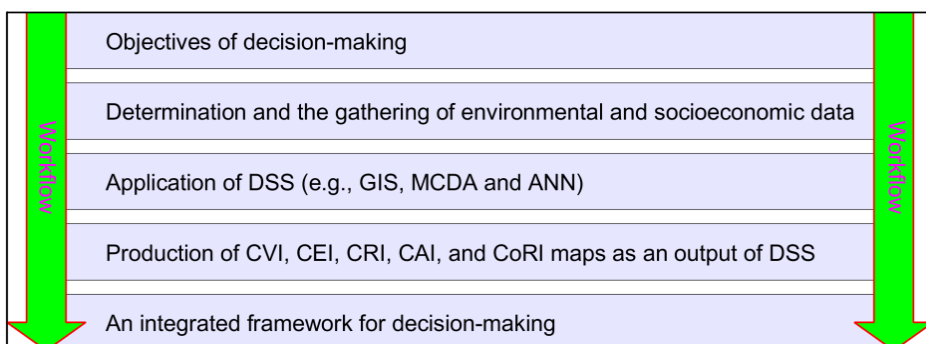

Workflow	Objectives of decision-making	Workflow
	Determination and the gathering of environmental and socioeconomic data	
	Application of DSS (e.g., GIS, MCDA and ANN)	
	Production of CVI, CEI, CRI, CAI, and CoRI maps as an output of DSS	
	An integrated framework for decision-making	

Figure 1. Systematic steps for applying an integrated DSS in coastal planning and management. Adapted from Paper I.

coastal planning and management is shown in Figure 1. The use of the steps of MCDA, fuzzy standardisation followed by the analytical hierarchy process (AHP) to standardise and prioritise environmental and socioeconomic data, makes it possible to combine them using a weighted linear combination (WLC) method in GIS (as described below in Chapters 2 and 3). An example expanded workflow for steps 2 and 3 of the process in Figure 1 is shown in Figure 2. GIS and MCDA tools have traditionally been preferred in this step (Hadipour et al., 2020a; Tercan et al., 2020). Finally, it is important to classify or validate the results using other means, such as artificial neural networks (ANN) (Yariyan et al., 2020b; Pham et al., 2021) (Figure 2). Even though large datasets and computational resources are necessary (Dao et al., 2020), ANN methods have become valuable for classifying and ranking environmental hazards. Rumson et al. (2020) demonstrate that a comprehensive assessment of coastal risks and resilience can be obtained by integrating MCDA, GIS, and potentially ANN. It is likely that this combination improves coastal adaptation planning, hazard mitigation, and resilience initiatives (Kontopoulos et al., 2021).

The overall perception in the literature is that a combination of DSTs provides several advantages for the implemented DSS for coastal planning and management (Figure 3). The outcome can be used to generate effective coastal protection maps,
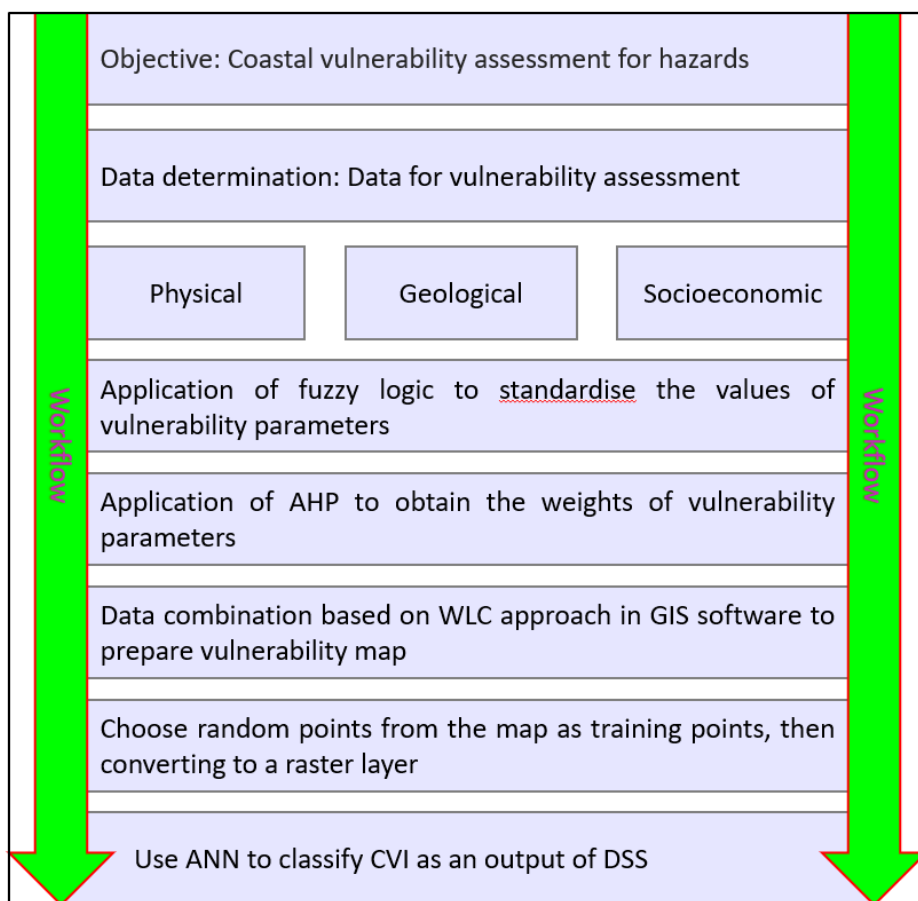

Figure 2. An integrated DSS workflow for a coastal vulnerability assessment using GIS-MCDA-ANN. Adapted from Paper I.

An integrated DSS framework	
Involves the production of maps	Outputs for stakeholder engagement
Consideration of variable results	Enables consideration of uncertainty
Produces high-quality results	Requires human-machine interaction
Facilitates long-term applicability and monitoring	

Figure 3. Benefits from using a DSS for coastal planning and management. Adapted from Paper I.

such as setting appropriate setback zones for erosion and inundation control. As part of this integrated approach, coastal planners can determine the optimal width of buffer zones, establish infrastructure setback distances, and develop construction projects management plans. In particular, the outcome can also assist in specifying floor heights for buildings and identifying shoreline sections that require specific interventions to mitigate erosion, such as sea walls or beach nourishment. Examples of combining these tools in a coastal management system are presented in Bagdanavičiūtė et al. (2019), Mullick et al. (2019) and Hadipour et al. (2020a). It is clear that sea level rise and human activities are increasingly impacting coastal areas, and individual tools are often limited in their long-term functionality (Schumacher et al., 2018). By considering vulnerability, risk, and resilience changes at finer scales, an integrated approach commonly leads to more precise assessments (Mullick et al., 2019).

The assessment of error and uncertainty is critical in such projections. The use of single methods like AHP can cause rankings to differ, whereas an integrated DSS reduces inconsistencies by applying expert knowledge to calibration and validation (Paper VI), which is similar to ensemble methods used in statistics and machine learning (Berk, 2006). The described integrated methods enable the identification and minimization of these errors (Yariyan et al., 2020a). It is particularly helpful to use ANN methods to analyse uncertainty and perform sensitivity analyses to ensure that the model is well-fitted to reality (Bayat et al., 2019; Peponi et al., 2019; Yariyan et al., 2020a).

Using DSTs and developing DSS require human-machine interaction. To interpret data effectively, experts must ensure accurate data inputs and reliable outputs (Rumson et al., 2020; Yun et al., 2021). Experts are able to break complex decisions down into manageable segments despite the fact that DSSs cannot do so independently (Rashidi et al., 2018).

1.6 Experience with applications of integrated DSSs in coastal planning and management

The ultimate task of a DSS for coastal matters is to create a framework integrating environmental and socioeconomic data for coastal planning and management. Combining various DSTs enhances decision-making for coastal issues. The integration of GIS and MCDA is well-established in the literature (Bagdanavičiūtė et al., 2019; Hadipour et al., 2020a; Tercan et al., 2020; Masoudi et al., 2021). Effective combinations like GIS-MCDA, GIS-ANN, GEE-ANN, GIS-MCDA-ANN, and GIS-BN have been also reported in the literature (Peponi et al., 2019; Guo et al., 2020; Hadipour et al., 2020a; Yariyan et al., 2020a; Arruda et al., 2021).

Recent studies emphasise the effectiveness of applying ANN for sensitivity and error analysis. For the majority of environmental applications, combination of GIS-MCDA (fuzzy logic, AHP and WLC) with ANN methods create an effective DSS (Jena et al., 2020; Yariyan et al., 2020a; Pham et al., 2021). These approaches generate visual products that assist public perception of environmental hazards and can be used to raise awareness of coastal sustainability and facilitate expert discussions. Despite the lack of strict conclusions, comparing different approaches reveals several practical implications.

A combination of DSTs addresses various environmental management challenges, such as environmental risk and hazard classification, site selection, land-use zoning, and resilience classification (Table 3 in Paper I). MCDA tools are beneficial for incorporating environmental, social, and economic objectives into decision-making (Tercan et al., 2020; Masoudi et al., 2021). Scientists and stakeholders provide useful inputs, which promote the decision-making process with their expertise (Uhde et al., 2015). ANNs methods contribute to a validation of results by considering future conditions alongside the present situation (Peponi et al., 2019), especially in areas with large datasets (Lamba et al., 2019; Yariyan et al., 2020a). However, implementation of ANNs without MCDA may lead to a lack of expert knowledge in determining the relationships between datasets (Sarbayev et al., 2019).

Bayesian network methods are effective for predicting environmental changes but are computationally complex and require high expertise (Sahin et al., 2019), and are less community-friendly (Guo et al., 2020). The use of tools like Google Earth Engine are effective when it integrated with ANN for analysing publicly available large satellite datasets (Arruda et al., 2021), which require specialised skills to apply.

GIS and MCDA tools are popular due to their widespread availability and ease of use (Malczewski and Rinner, 2015). ANN methods require extensive training, but their accessibility is improving across many fields particularly for environmental specialists (Lamba et al., 2019; Pham et al., 2021). The applications of GIS-MCDA-ANN combinations are expected to become standard for DSS investigations in situations where large input data are available. However, there may be situations where such a combination is not appropriate. This may happen if there is not enough input data available or if the data cannot be generated (Jena et al., 2020). Importantly, outputs from GIS-MCDA or GIS-MCDA-ANN combinations, whenever applicable, can be easily interpreted by managers, decision-makers and stakeholders (Yariyan et al., 2020a).

2 Offshore wind farm site selection

A global shift to renewable energy resources is driven by a need to reduce fossil fuel dependence (e.g., Moriarty and Honnery, 2012) and mitigate climate change impacts (e.g., Bogdanov et al., 2019). An important resource for renewable energy is wind energy, which is a cost-effective, environmentally friendly, and sustainable source of electricity on both a global scale (Ang et al., 2022) and at country level (Baban and Parry, 2001; Latinopoulos and Kechagia, 2015). Due to significant reductions in generation costs (Osman et al., 2022) and the ability to provide power near load centres, wind energy is becoming increasingly popular (Chang et al., 2022). A number of advantages exist for offshore wind power plants over onshore installations (Fernández-Guillamón et al., 2019), including higher wind speeds, fewer visual impacts, and reduced noise (Bilgili et al., 2011; Wu et al., 2018).

Choosing suitable offshore wind power plant sites is crucial for optimizing energy production and minimizing costs (Arrambide et al., 2019). This selection process must take into account a variety of environmental, social, and economic factors (Gil-García et al., 2022; Tercan et al., 2020). Many studies of offshore wind farm development typically concentrate on relatively small sea areas, such as the waters around Denmark (Moller et al., 2012), the United Kingdom renewable energy zone (Cavazzi and Dutton, 2016), Canarian waters (Schallenberg-Rodríguez and Montesdeoca, 2018), Turkey's seas (Genç et al., 2021), or the Gulf of Maine (Gil-García et al., 2022).

According to some estimates (Samuelsson, 2020), in Europe, the North Sea accounts for 77% of all cumulative off-shore wind capacity, the Irish Sea 13%, and the Baltic Sea 10%. The reason is that the Baltic Sea is located within the so-called North Atlantic storm track (Rogers, 1997), along which low pressure systems move from the Atlantic Ocean to the east. The Baltic Sea offers ideal conditions for offshore wind power development because of its favourable wind conditions and extensive coastal regions (Hasager et al., 2011; Rusu, 2020). There is a need for increased energy production capacity in response to the significant decrease in energy supplies from the Russian Federation (European Commission, 2022). However, site suitability assessments for offshore renewable energy in the Baltic Sea region are limited and focus primarily on seabed characteristics (Nyberg et al., 2022). Paper II attempts to close this gap by using different decision support tools (DSTs) to assess the suitability of offshore wind farms in the entire Baltic Sea (Baltic-wide approach). This Chapter mainly follows the material discussed in Paper II. To provide a detailed spatial analysis at a high spatial resolution, this study combines geographic information systems (GIS) with multi-criteria decision analysis (MCDA) as described in Chapter 1 with a levelised cost of energy (LCOE) model by taking into consideration a variety of parameters for offshore wind farm site selection.

2.1 Study area

The Baltic Sea (Figure 4) is a body of water in Northern Europe that is partially enclosed. This area borders Finland, Estonia, Lithuania, Latvia, Denmark, Sweden, Germany, Poland, and Russia. It covers 392,978 km^2 with an average depth of 54 m and a brackish water ecosystem (Leppäranta and Myrberg, 2009). Various human activities and pressures impact the Baltic Sea, including massive discharge of nutrients and pollution that creates pressures on the entire ecosystem, fisheries, extremely intense shipping, and increasing levels of tourism (Reckermann et al., 2022). These activities, if not

handled properly, may exert a negative impact on marine ecosystems, coastal tourism, fisheries, and socioeconomic conditions in all Baltic Sea countries (Reckermann et al., 2022). The development of wind farms will eventually add to this pressure. It is therefore important to take into account technical, socioeconomic, and environmental factors when planning offshore wind farms (Tercan et al., 2020).

The presence of extensive relatively shallow areas in the Baltic Sea is favourable for the installation of wind turbines and the properties of the seabed in these areas are generally known (Nyberg et al., 2022). The installed generation devices and associated infrastructure will be impacted by several types of hydrometeorological drivers.

The Baltic Sea is microtidal, with the maximum range of tidal-driven water level variations being only a few centimetres (Leppäranta and Myrberg, 2009). The water level of the entire sea may still exert substantial atmospheric-driven variations, up to 0.5 m as monthly mean (Johansson and Kahma, 2016) and up to 0.8 m for a few weeks (Soomere and Pindsoo, 2016). It is uncommon that wind speed reaches hurricane level; however, a 10-min average wind speed 32.5 m/s was recorded on 02 January 2019 in the Sea of Bothnia (Björkqvist et al., 2020). The majority of moderate and strong winds blow from the south-west or west but there is evidence that the strongest ever winds could blow from the north-north-west (Soomere, 2001) or north (Björkqvist et al., 2020).
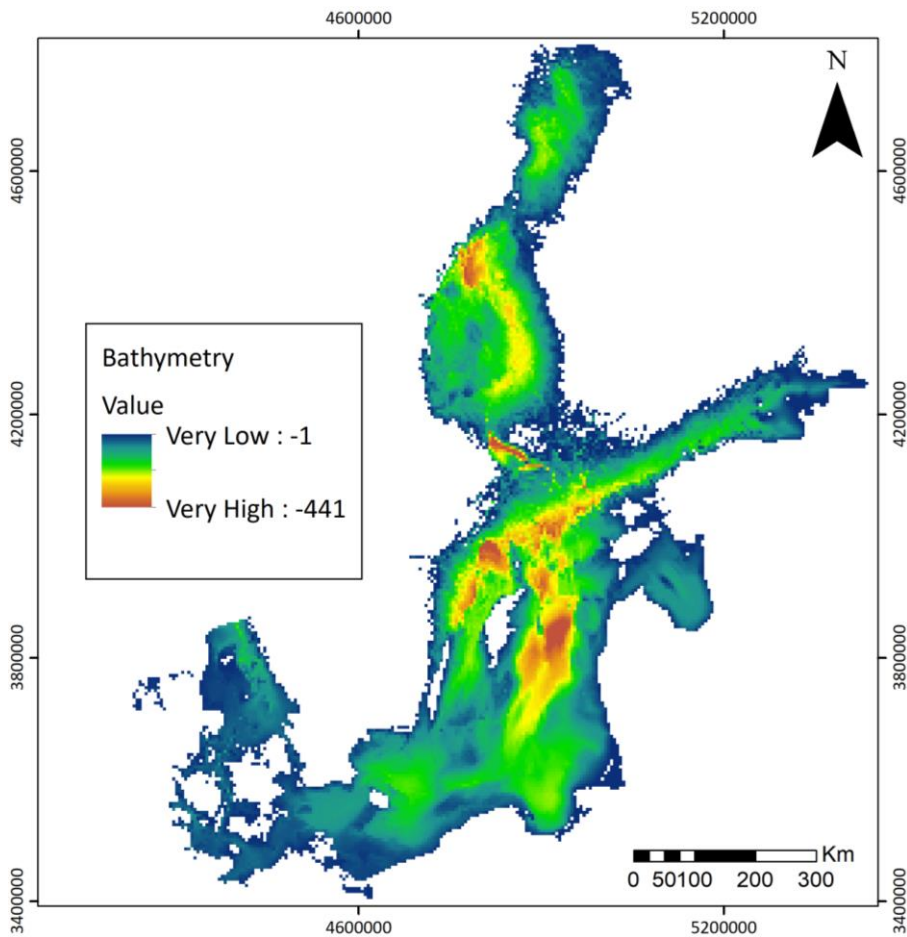

Figure 4. The bathymetry of the Baltic Sea.

The wave climate of the Baltic Sea is generally mild, with long-term average significant wave height slightly exceeding 1 m only in the central part of the open Baltic Sea (Baltic proper) and Sea of Bothnia (Björkqvist et al., 2018). The complex shape of the sea gives rise to extensive variability in the wave properties in different parts of the sea (Björkqvist et al., 2018; Giudici et al., 2023). The wave climate, however, is extremely intermittent (Soomere and Eelsalu, 2014): some 30% of the annual wave energy flux arrives within the stormiest week and about 50% within the two stormiest weeks. Also, some parts of the sea may host extremely severe wave conditions, with significant wave height close to 10 m (Soomere et al., 2008; Björkqvist et al., 2018). The maximum recorded significant wave height to date is 8.2 m (Björkqvist et al., 2017).

Perhaps the most problematic driver is seasonal sea ice. In extreme cases the entire sea may freeze (Leppäranta and Myrberg, 2009). Even though the duration of ice season and the extent of sea ice cover have considerably shortened (Haapala et al., 2015), ice is still common in the nearshore also in southern parts of the sea.

2.2 Methods

2.2.1 Levelised Cost of Energy (LCOE) model

Paper II addresses the problem of offshore wind farm site selection in the Baltic Sea from the viewpoint of the levelised cost of energy (LCOE). This parameter provides a comprehensive measure of the economic feasibility of projects in the energy sector (Johnston et al., 2020). In essence, it expresses a ratio between the total costs of energy production and the total energy expected to be produced over the project's lifetime. It is thus a natural measure of the cost-effectiveness of various energy sources over their entire lifetimes, and technologies are often compared using this model.

The calculations of LCOE take into account both initial investment ($CAPEX$) and recurring operational costs ($OPEX$). The generic expression for LCOE is (Johnston et al., 2020):

$$LCOE = \frac{\hat{C}}{\hat{E}} = \frac{\sum_{t=0}^{t=\text{end}} C}{\sum_{t=0}^{t=\text{end}} E}, \tag{7}$$

where $\hat{C}$ is the total cost over the project lifetime and $\hat{E}$ is the total energy output. Both quantities are expressed as the sum of the relevant costs or energy output from the start of the project $t = 0$ until the end of the lifetime $t = \text{end}$. The costs include but are not limited to the initial investment, planning, feasibility studies, permits, legal fees, development, and decommissioning, and recurring costs like maintenance and fuel. The LCOE for the Baltic Sea study in Paper II incorporates critical factors such as water depth, distance to shore, and wind capacity factor, all of which affect foundation and grid connection costs.

The total cost is traditionally divided into the investment cost I_t in a specific year t, operations and maintenance expenditures M_t, and fuel cost F_t. The costs of fuel for offshore wind turbines (F_t) are negligible except for fuel used for maintenance. The LCOE is commonly estimated based on annual costs and taking into account annual discount rates as follows:

$$\hat{C} = \sum_{t=1}^{t=\text{LT}} \frac{I_t + M_t + F_t}{(1+r)^t}, \quad \hat{E} = \sum_{t=1}^{t=\text{LT}} \frac{E_t}{(1+r)^t}, \tag{8}$$

where t now has the meaning of single years, the lifecycle is LT years and discount rate r (in %) is constant (Johnston et al., 2020). In more complex systems, such as those incorporating a battery bank, and processes with various properties, Eq. (8) can be expanded to include the capital cost of each component (e.g., wind turbine, battery bank, civil works, inverter, miscellaneous expenses), and adjustments for escalation (e.g., Genç et al., 2012). In such cases, Eq. (8) becomes more complex:

$$LCOE = \frac{\sum_{i=1}^{n}(C_i \times CRF_i) + C_{om}}{E_p}, \tag{9}$$

where C_i represents the capital cost of each component:

$$C_i = I_{we} \times P_r, \tag{10}$$

I_{we} is the product of the specific cost of each component, and P_r is the rated power, which is the maximum power output a wind turbine can generate under optimal conditions. E_p represents the total output, similar to Eq. (8), which is essentially the potential maximum output multiplied by the capacity factor. This representation addresses the variability in capital recovery factors CRF_i of individual components, which may have different discount rates r and lifetime n (Genç et al., 2012):

$$CRF_i = \frac{(1+r)^n \times r}{(1+r)^n - 1}. \tag{11}$$

This method also accounts for the escalation of operation and maintenance costs M_t [€/year], which are adjusted for escalation as follows:

$$\widehat{M}_t = C_{om-esc} = \frac{C_{om}}{r - e_{om}} \left[1 - \frac{(1+e_{om})^n}{(1+r)^n}\right], \tag{12}$$

where the term C_{om-esc} represents the escalated operation and maintenance cost, taking into account the increase in these costs over the system's lifetime, $C_{om} = M_1$ is the initial operation and maintenance cost for the first year, and e_{om} is the escalation ratio of operation and maintenance costs. The escalation ratio from 2015 to 2020 is approximately 0.986, indicating a 0.986% decrease in operational and maintenance costs over this period. Different from Genç et al. (2012), Paper II does not include scenarios where a wind turbine or farm is sold or bought.

2.2.2 LCOE model for the Baltic Sea
The model described in Section 2.2.1 is adapted in Paper II to the entire Baltic Sea to identify the spatial pattern of LCOE across different sea areas, taking into account environmental conditions, but assuming the start of a project remains constant. In this way, the model is simplified, making it more practical for large-scale geographic analysis. This framework simplifies the expression for LCOE to:

$$LCOE = \frac{\sum_{t=1}^{LT} \frac{CAPEX(t) + OPEX(t)}{(1+r)^t}}{\sum_{t=1}^{LT} \frac{E(t)}{(1+r)^t}}, \tag{13}$$

where $CAPEX(t)$ includes the capital expenditures during the year t, $OPEX(t)$ represents the operational and maintenance expenditures during the same year, and $E(t)$ is the energy generation during this year.

The LCOE model application in a GIS environment is illustrated in Figure 5. The Baltic Sea was divided into pixels of 5000 m by 5000 m for standardised data analysis. As described in Chapter 1, ArcGIS software was used to extract key parameters such as

capacity factor, water depth, and distance from shore into raster layers used in the LCOE calculation. The Global Wind Atlas (2022) provided high-resolution wind climate data, and the HELCOM portal provided shoreline data. Cost data for the Baltic Sea region are derived from the DEA Technology Data Catalogue (Danish Energy Agency DEA, 2016). Next, the initial $CAPEX$ was calculated based on rotor diameter, hub height, generating capacity, specific power, and area coverage of wind turbines (Table 1) based on Danish Energy Agency DEA guidelines that represent typically used turbines in the Baltic Sea. The total $CAPEX$ was calculated by summing the initial $CAPEX$ in the first year 2020, the foundation costs (dependent on the depth of the water), and the grid connection costs (dependent on the distance from the shore). The foundation costs increase rapidly for larger depths but have become considerably less expensive in the period 2015–2020 (DEA, 2016). For the base case depth of 20 m they were 0.74 M€/MW in 2015 and 0.42 M€/MW in 2020 (see Table 2 in Paper II).

The expected total grid connection costs in 2015 prices were derived from Energinet, (2017), detailing the costs associated with connecting the latest four projects in the Baltic Sea (HR2, Rødsand 2, Anholt, and HR3). These costs were estimated as 0.4 M€/MW for offshore wind power plants that have an on-site transformer station, out of which the estimated offshore platform cost 0.16 M€/MW, project management and environmental assessment 0.027 M€/MW, transformer station onshore 0.016 M€/MW and sea/land cable costs 0.00269/0.00134 M€/km/MW (Table 3 and Table 4 in Paper II). These projected costs for each pixel were assessed by comparing differences in water depth and distance to shore in each pixel from the base case (water depth 20 m; distance to shore 30 km, land cable 50 km). For every 1 m deviation from the depth of 20 m, foundation costs were modified by 0.0206 M€. These estimates apply to power plants with capacities between 400 and 600 MW (DEA, 2016).

A fixed and variable OPEX was then calculated for 2020 using data provided by the Danish Energy Agency DEA (2016) (Table 1). These costs cover the entire project lifetime and do not vary based on water depth or distance from shore. Using the capacity factor multiplied by 8760 hours per year, energy production was calculated.
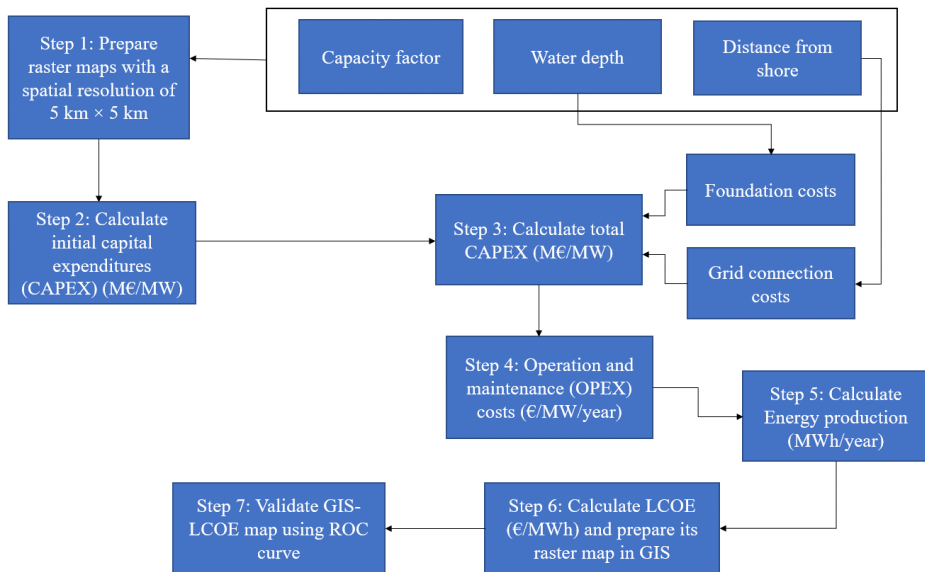

Figure 5. Flowchart for offshore wind farm site selection methodology using GIS-LCOE. From Paper II.

Table 1. Technical and financial data related to large offshore wind turbines costs in 2020 for the base case 20 m water depth and 30 km distance to shore (Danish Energy Agency DEA, 2016).

		Year of investment decision		
		2015	2020	
	Generation capacity for one unit (MW)	8	10	
	Average annual full-load hours (MWh)	4400	4500	
	Technical lifetime (years)	25	27	
	Rotor diameter (m)	164	190	
	Hub height (m)	103	115	
	Specific power (W/m^2)	379	353	
	Specific area coverage (MW/km^2)	5.4	4.5	
	Nominal investment (M€/MW)	2.86	2.13	
	of which equipment	*1.11*	*0.79*	
	of which installation	*1.35*	*0.96*	
	of which grid connection	*0.40*	*0.38*	
	Fixed operation and maintenance (€/MW/year)	57,300	40,059	
	Variable operation and maintenance (€/MWh)	4.3	3.0	

The generation of electricity was projected annually between 2020 and 2047, including power losses of 10%. The LCOE values for each pixel were calculated using the total costs divided by total energy generation over a 27-year project lifetime, with a discount rate of 8%.

2.2.3 Steps of GIS-multi-criteria decision analysis (MCDA)
Site selection for offshore wind power plants using GIS-MCDA involves several steps (Figure 6) as described in Section 1.2. The first step is to specify constraints and identify potential locations based on various data sources, from research and technical literature, various databases, national regulations, etc. The input data used in Paper II use information about wind resources, physical/environmental and socioeconomic aspects. The necessary information was retrieved from DEA standards and databases (Danish Energy Agency DEA, 2016), the European Maritime Spatial Planning platform
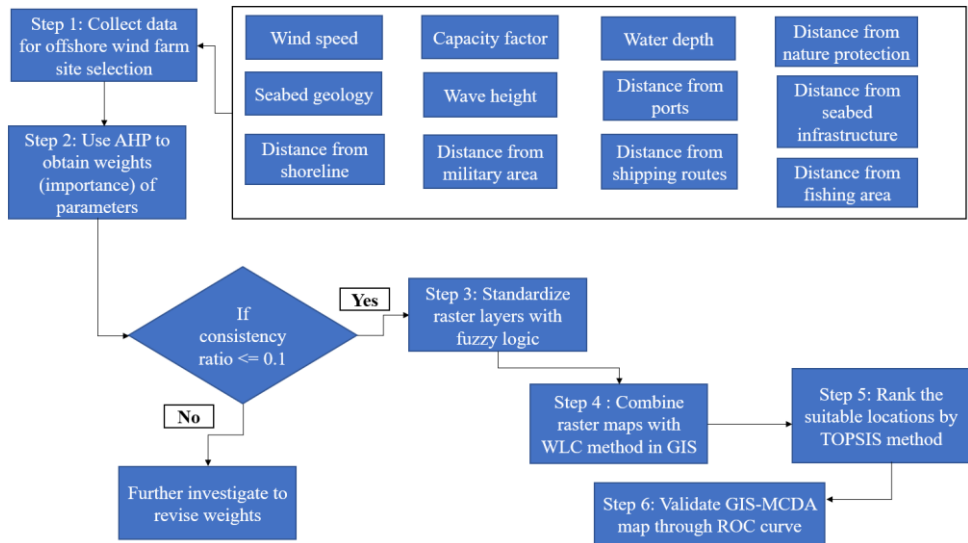

Figure 6. Flowchart for offshore wind farm site selection methodology using GIS-MCDA. From Paper II.

(European MSP Platform, 2018a,b,c,d) and European Commission (2020). The estimates of Gil-García et al. (2022) were used for wave information.

The list of parameters used in the analysis include wind speed (threshold values for fuzzy logic standardisation $R_{\min} = 7$ m/s and $R_{\max} = 10$ m/s, increasing function), capacity factor (35% and 55%, increasing, Figure 7), water depth (10 m and 50 m, decreasing), distance from nature protection areas (2 km and 5 km, increasing), seabed geology (0 for rocks and boulders, 1 for muddy seabed), wave height (<10 m, decreasing), and distance from various objects: ports (10 km and 80 km, decreasing), seabed infrastructure (0.5 km and 5 km, increasing), shoreline (10 km and 80 km, decreasing), military areas (0.5 km and 5 km, increasing), shipping routes (3.7 km and 5 km, increasing), and fishing areas (0.5 km and 5 km, increasing) (Table 5 in Paper II). The derived information about these parameters was identified and quantified with a spatial resolution (pixel size) of 5000 × 5000 m pixels using ArcGIS based on the
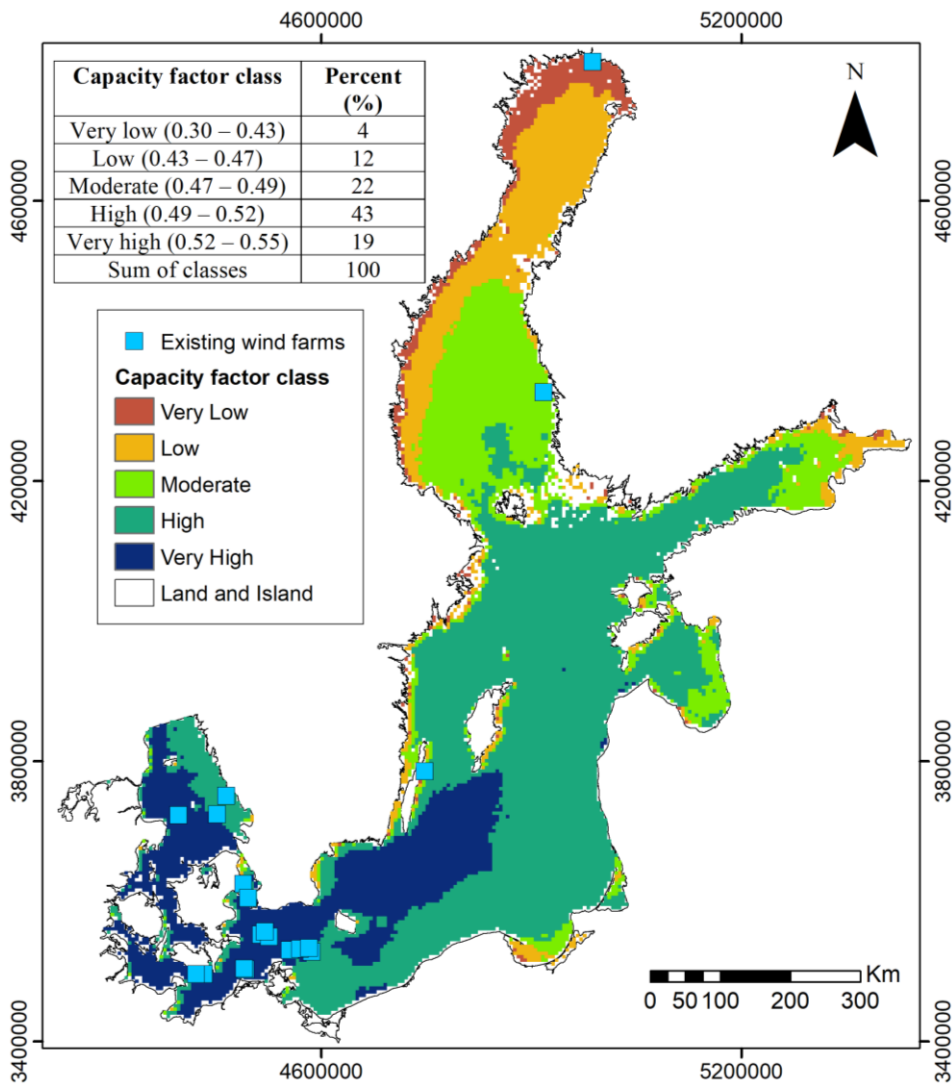

Capacity factor class	Percent (%)
Very low (0.30 – 0.43)	4
Low (0.43 – 0.47)	12
Moderate (0.47 – 0.49)	22
High (0.49 – 0.52)	43
Very high (0.52 – 0.55)	19
Sum of classes	100

Figure 7. Capacity factor for offshore wind power plant site suitability. From Paper II.

ETRS_1989_LAEA reference coordinate system (Annoni et al., 2003).

In the second step of the MCDA process, raster layer values were standardised to facilitate quantitative assessments of site suitability (e.g., Noorollahi et al., 2022) using a fuzzy logic algorithm to reclassify data across layers, that is to convert the values of the pixels of raster maps into a scale from 0 to 1 (Section 1.2.1). As described in Section 1.2.1, any value below the lower threshold R_{min} represents the least appropriate value, and any value above the upper threshold R_{max} is considered optimal (increasing function) (e.g., Latinopoulos and Kechagia, 2015). For example, a minimum acceptable distance from a nature protection area is set at 2 km and R_{max} is set to 5 km. Thus, all locations within 2 km are assigned a suitability value of 0, whereas locations more than 5 km away are assigned a suitability value of 1. Water depth is an example of a decreasing function: depths <10 m are rated as highly suitable, while values >50 m are rated as unsuitable. The fuzzy membership functions $X_1(i)$ and $X_2(i)$ are defined in Eqs. (1) and (2) (Section 1.2.2).

The third step in the MCDA design involves specifying the contribution of various parameters to wind farm site suitability using the Analytical Hierarchy Process (AHP) (Section 1.2.2). For the study in Paper II, expert opinions were gathered from 10 specialists with expertise in coastal management. The geometric mean was used to aggregate their judgments, effectively balancing the differences in their opinions (Mu and Pereyra-Rojas, 2018).

The pairwise comparison matrix (see Table 7 in Paper II) was normalised columnwise. The row sums were then averaged to calculate the weights of each parameter, following Vasileiou et al. (2017) and Mahdy and Bahaj (2018). For the matrix size $N = 12$, the Random Index $RI = 1.54$ (Aguarón and Moreno-Jiménez, 2003) and the consistency index (Section 1.2.2) $CI = 0.04$. The assigned weights are presented graphically in Figure 8.

The fourth step involves combining raster maps within a GIS environment to generate a site suitability map (Section 2.3). The Weighted Linear Combination (WLC) method (Section 1.2.3) is used in the GIS environment, following the implementation of
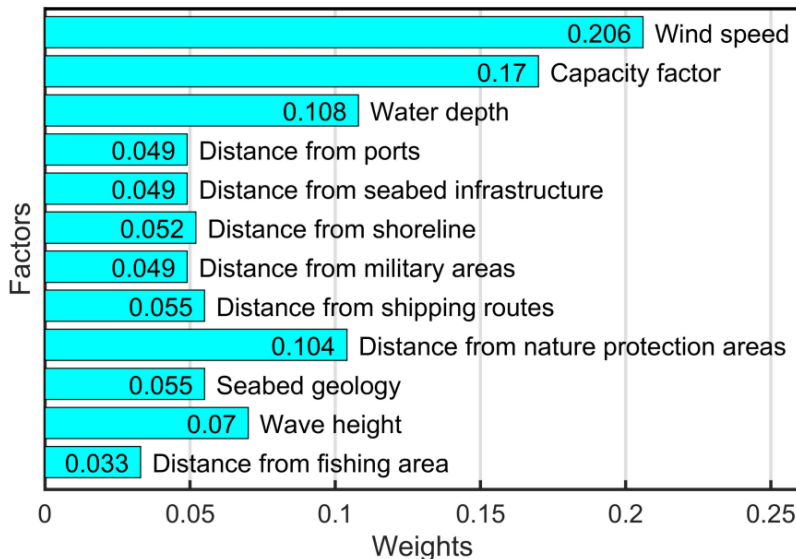

Figure 8. Weights assigned to the factors using the AHP method. From Paper II.

the map algebra techniques in Malczewski and Rinner (2015) to combine raster maps for calculation of site suitability (Díaz-Cuevas et al., 2019). In the output layer, a rank of 1 is the most appropriate.

2.2.4 Technique for Order of Preference by Similarity to Ideal Solution (TOPSIS)

Paper II employs the Technique for Order of Preference by Similarity to Ideal Solution (TOPSIS) to enhance confidence in the results by ranking suitable locations. This technique is an efficient method for selecting the best option among multiple alternatives (Vagiona et al., 2022). This approach is based on the idea that the optimal alternative should be closest to the positive ideal solution and farthest from the negative ideal solution (Sindhu et al., 2017). The positive ideal solution represents the maximum benefit, while the negative ideal solution signifies the minimum benefit (Díaz and Guedes Soares, 2021).

Initially, a decision matrix was constructed with $J = 15$ alternatives (locations A1 to A15, Figure 11) and $N = 12$ criteria, representing each criterion i and alternative j as x_{ij}. The decision matrix was then normalised (Konstantinos et al., 2019):

$$r_{ij} = \frac{x_{ij}}{\sqrt{\sum_{j=1}^{J} x_{ij}^2}}. \tag{14}$$

Next, weighted normalised values v_{ij} were computed (Vagiona et al., 2022):

$$v_{ij} = w_j r_{ij}, \quad i = 1, 2, \dots, N; \quad j = 1,2, \dots J. \tag{15}$$

The positive ideal solution (V_j^+) and negative ideal solution (V_j^-) were identified following Vagiona et al. (2022):

$$A^+ = \{V_1^+, \dots, V_N^+\}, \ V_j^+ = \{(\max(v_{ij}), j \in J'), \ (\min(v_{ij}), \ j \in J'')\}. \tag{16}$$

$$A^- = \{V_1^-, \dots, V_N^-\}, \ V_j^- = \{(\min(v_{ij}), j \in J'), \ (\max(v_{ij}), \ j \in J'')\}. \tag{17}$$

In this context, J' represents the set of indices from $1, 2, \dots, J$ associated with benefit criteria and J'' represents a similar set related to the cost criteria (Vagiona et al., 2022). The study in Paper II uses for evaluation only benefit-oriented criteria, concentrating on positive impacts and improvements rather than negative aspects. Therefore Eqs. (16) and (17) were simplified via setting $J' = \{1, 2, \dots, J\}$ and $J'' = \emptyset$. The differences of the alternatives from the positive S_i^+ and negative S_i^- ideal solutions were calculated (Foroozesh et al., 2022):

$$S_i^+ = \sqrt{\sum_{j=1}^{n}(v_{ij} - V_j^+)^2}, \quad i = 1, 2, \dots, m; \tag{18}$$

$$S_i^- = \sqrt{\sum_{j=1}^{n}(v_{ij} - V_j^-)^2}, \quad i = 1, 2, \dots, m. \tag{19}$$

In the final step, the calculation of the relative closeness to the positive ideal solution for site selection was calculated as in Vagiona and Kamilakis (2018) in terms of how far from the ideal the realistic locations are:

$$C_j^+ = \frac{S_i^+}{S_i^+ + S_i^-}, \ j = 1, 2, \dots, J. \tag{20}$$

2.2.5 Validation

A receiver operating characteristic (ROC) curve (Figure 9) is used in this step to confirm the accuracy of the model's predictions (Ghorbanzadeh et al., 2019b). The GIS-LCOE and GIS-MCDA models were both used for this analysis. In the ROC curve, the x-axis represents the cumulative distribution function of the false-positive rate and the y-axis indicates the sensitivity (Chen et al., 2018). By plotting the false positive rate against the true positive rate, a curve is generated (Pourghasemi et al., 2016).

The true positive rate was determined by existing wind farms, whereas the false positive rate was determined by locations from GIS-LCOE and GIS-MCDA maps with no wind farms. An area under the curve (AUC) value of 1 indicates a perfect suitability map, and a value of 0.5 indicates poor performance (Orhan, 2021). The model's sensitivity, specificity, and accuracy were calculated as follows (Tien Bui et al., 2016; Chen et al., 2017):

$$\text{Sensitivity} = \frac{TP}{TP + FN}, \quad \text{Specificity} = \frac{TN}{FP + TN}, \quad \text{Accuracy} = \frac{TP + TN}{TP + FP + TN + FN}. \quad (20)$$

Validation of the model outputs was conducted using a receiver operating characteristic curve (ROC curve). Figure 9 illustrates how false-positive rates are compared with true-positive rates in this method for assessing model predictions. True positive rates were determined by existing wind power plants (Figure 7), and false positive rates were determined by potential sites identified by the models. Area under the curve (AUC) values for both LCOE and Fuzzy logic-AHP-WLC maps were over 92%, which indicates a high level of accuracy in location prediction. TOPSIS had an AUC of 82%, which was slightly lower than LCOE and Fuzzy logic-AHP-WLC.

2.3 Mapping site suitability based on LCOE, MCDA and capacity factor

There are several parameters that determine the most suitable areas in the south and east of the Baltic Sea, including high wind speeds, fine seabed sediments, shallow waters, and suitable distances from pipelines, shipping routes, military areas, and
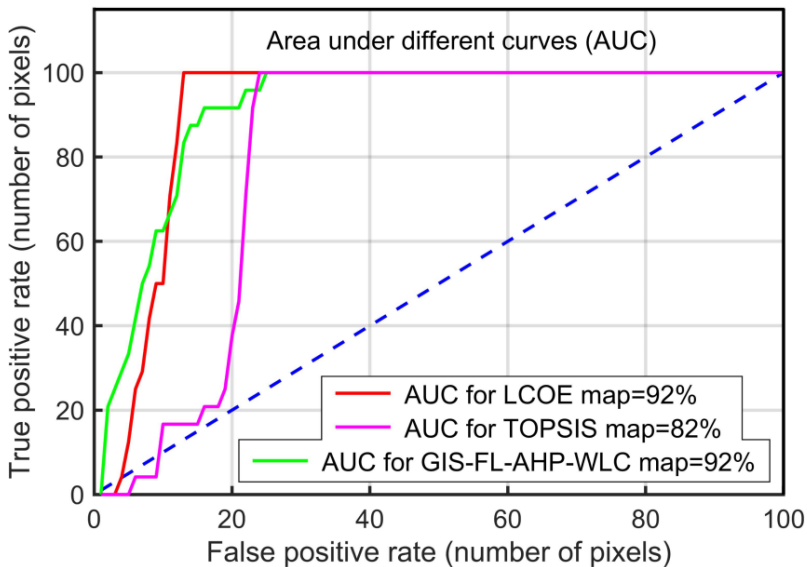

Figure 9. Validation of results using the ROC model. From Paper II.

nature protection areas (Section 2.2). The LCOE maps and the GIS-MCDA techniques treat these parameters very differently. Still, some similarities exist between the outcome of the GIS-LCOE (Figure 10) and GIS-MCDA (Figure 11) models for identifying suitable offshore wind sites in the Baltic Sea. This feature supports the conjecture that both methods can be used to identify sites with high wind speeds and low energy costs, based on the Danish Energy Agency and the European Maritime Spatial Planning platform guidelines.

The GIS-LCOE analysis identifies locations with low LCOE values, generally near Danish shores. This feature mirrors the presence of high wind speeds, large capacity factors and shallow water depths in these locations. These areas have also lower capital expenditures because of shorter electrical cables and lower construction costs.

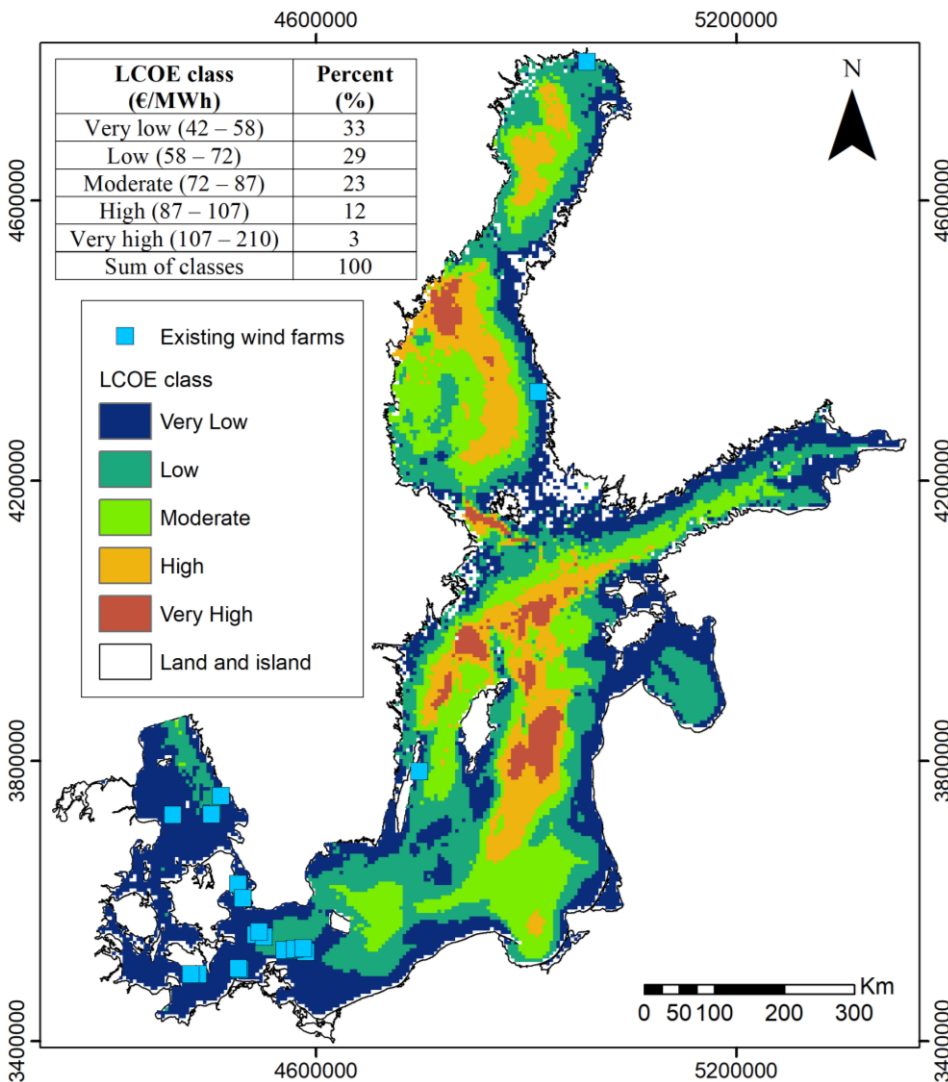| LCOE class (€/MWh)	Percent (%)
Very low (42 – 58)	33
Low (58 – 72)	29
Moderate (72 – 87)	23
High (87 – 107)	12
Very high (107 – 210)	3
Sum of classes	100

Figure 10. Offshore wind power plant site suitability based on the GIS-LCOE. Lower LCOE values indicate better suitability, and higher values indicate less suitability. From Paper II.

In contrast, locations such as the Gulf of Bothnia, offshore areas of the Baltic proper far from Polish and German shores, and the central Gulf of Riga with lower wind speeds and deeper waters have higher LCOE values. The outcome of the GIS-MCDA analysis, which incorporates AHP, fuzzy logic, and WLC (Section 1.2), supports these findings (Figure 11), emphasizing locations near the shore with shallow water and high wind speeds, but away from nature protection areas, seabed infrastructure, military zones, shipping routes, and fishing areas.

The spatial distribution of the capacity factor (Figure 7) reveals high energy output areas (capacity factor > 50%) mainly in the nearshore of Denmark, Sweden, Germany, and Poland. Consequently, the locations in the southern Baltic Sea have greater capacity to meet the energy demands of communities.
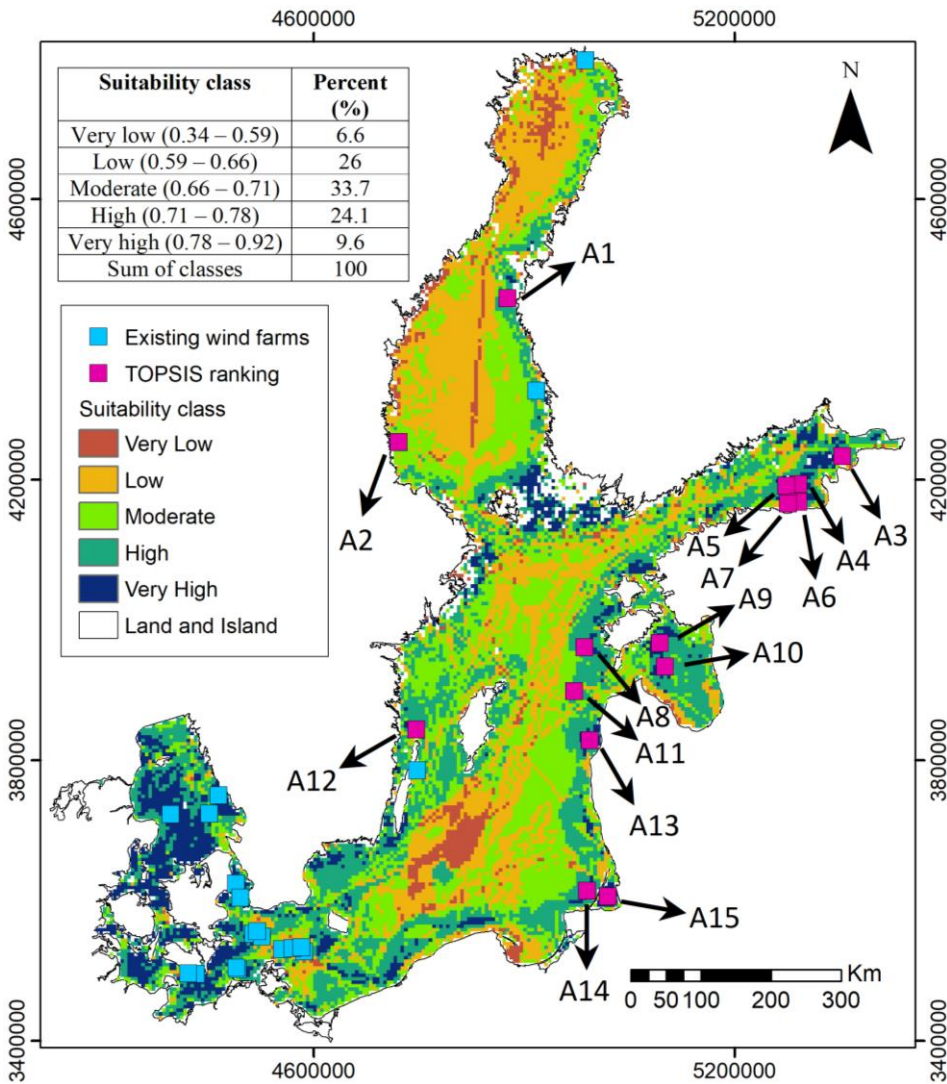

Figure 11. Offshore wind power plant site suitability based on the GIS-MCDA. The labels A1 to A15 indicate the ranking of suitable sites based on the TOPSIS method. Higher MCDA values indicate better suitability, and lower values indicate less suitability). From Paper II.

In terms of the best 20% of the relevant estimates, the most suitable areas according to the long-term energy cost (Figure 10) have LCOE values of 42–58 €/MWh (33% of the total sea area) while the most suitable areas in terms of MCDA (Figure 11) have relevant normalised values of 0.78–0.92 (9.6%), and the most suitable areas in terms of capacity factors (Figure 7) have this factor in the range of 0.52–0.55 (19%). The 20% least suitable areas have LCOE values between 107 and 210 €/MWh (3%), normalised MCDA values between 0.34 and 0.59 (6.6%), and capacity factor values between 0.30 and 0.43 (4%). The northern Baltic Sea is generally less suitable for wind farm development due to lower capacity factors (< 50%). There are, however, certain locations near Finnish coasts that may be suitable because of their close proximity to shorelines and ports.

2.4 Application of the TOPSIS technique in site suitability

To finalise the analysis in Paper II, the technique for order of preference by similarity to ideal solution (TOPSIS) was applied to prioritise and rank the most suitable locations identified by GIS-MCDA (Figure 11). TOPSIS was assessed using an initial matrix (Table 9 of Paper II), which provides a list of numerical values for the parameters listed in Section 2.2.3 across the top 15 sites A1 to A15 (Figure 11). The geometric distances of these sites from the positive and negative ideal solutions (Section 2.2.4) were then determined using Eqs. (18), (19) and (20). The rankings (see Table 10 of Paper II) reveal that distance from military areas significantly contributes to the higher rankings of sites A1 and A2. The distance from fishing areas played a crucial role for sites A3 and A4. Both the distance from nature protection areas and the geology of the seabed impacted the rankings of sites A5, A6, and A7. The winds speed and capacity factor were the main factors contributing to the higher rankings of sites A8, A11, and A13. Distance from the seabed infrastructure and proximity to ports were significant parameters influencing the rankings of sites A10 and A15.

The TOPSIS methodology focuses primarily on parameters with the highest distance from the negative ideal solutions or the lowest distance from the positive ideal solutions (Azadeh et al., 2011). In this way, sites that are further away from nature protection zones, military areas, or seabed infrastructure are more suitable from the viewpoint of this technique. In contrast, the GIS-MDCA (Fuzzy-AHP-WLC) approach adheres to buffer requirements based on national guidelines and standards. This comparison in Paper II suggests that GIS integrated with fuzzy logic, AHP, and WLC techniques provides a more consistent and balanced approach for standardisation, weighting, and combining of parameters. It is likely that this feature is invariant with respect to the particular sources of input information (the European Maritime Spatial Planning platform, Danish Energy Agency standards, and experts' perspectives in Paper II). The application of the TOPSIS model for suitability analysis provides additional confidence in the results by validating the suitability rankings. This means that integrating both approaches can promote the robustness and reliability of the offshore wind energy site selection process.

2.5 Further analysis of offshore wind farm site suitability

The map outcome of the GIS-MCDA technique (Figure 11) clearly show line features that correspond to shipping routes and pipelines. These areas are definitely not suitable for wind power plant development even though the relevant map usually indicates only low suitability. There are nature protection areas in the Swedish, Latvian, Polish, and German nearshore and in the offshore of these countries, which are also inappropriate as wind farm sites. Even though the close proximity to the shore may be generally preferred for wind power plants based on the criteria used, they are often excluded because of noise generation and visual disturbance constraints.

To account for these considerations, Paper II continued the analysis of estimates presented in Figure 10 (GIS-LCOE) and Figure 11 (GIS-MCDA) towards the inclusion into these maps restrictions related to marine protected areas and locations within 4 km of the shore. Also, areas with water depths > 50 m were excluded as the high LCOE costs
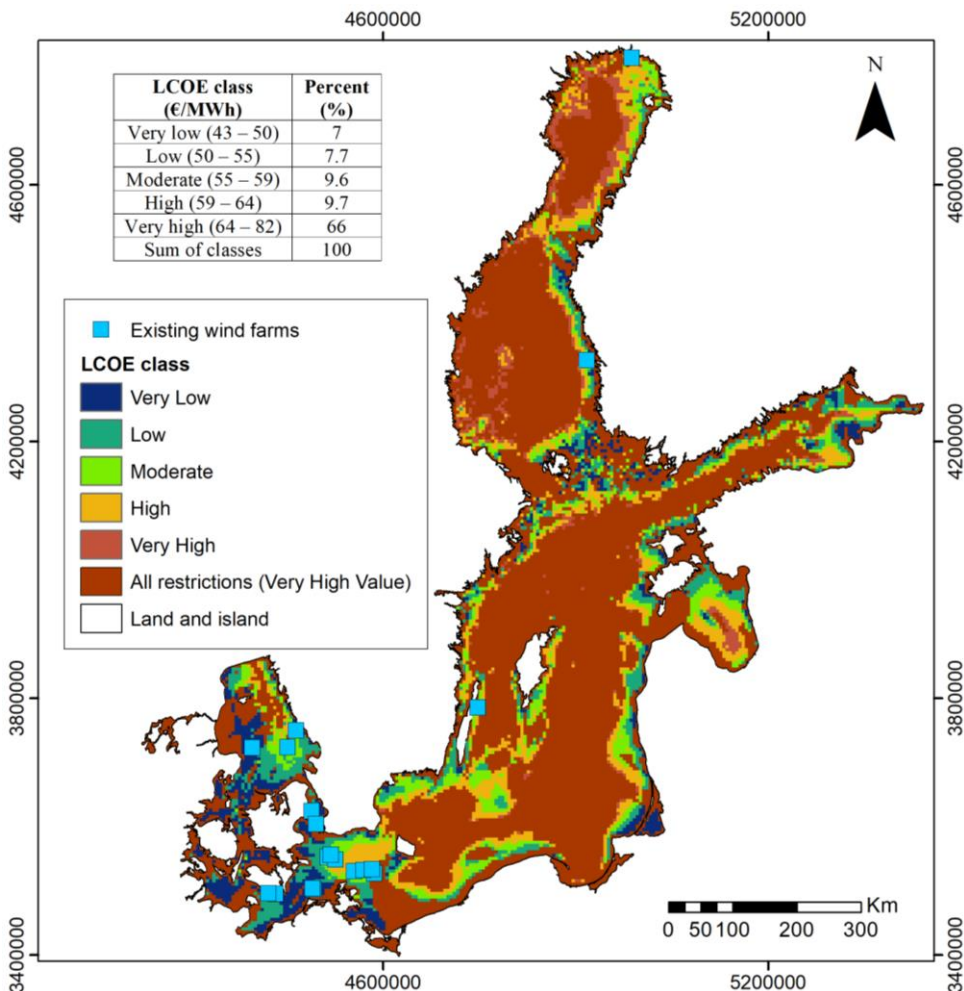

Figure 12. Offshore wind power plant site suitability based on the GIS-LCOE, with marine protected areas, locations within 4 km of the shore and, and areas with water depths greater than 50 m coloured into brown. From Paper II.

render energy produced in such areas non-competitive. With these restrictions included, the results of both analyses (Figure 12, Figure 13) show clear similarity.

A comparison of the above results with the map of capacity factor map (Figure 7) that incorporates these restrictions (Figure 14) shows that, not unexpectedly, areas with high capacity factors are commonly associated with lower LCOE values, indicating lower electricity production costs.

The experts consulted for this study identified wind speed, capacity factor, and water depth as the most important site suitability parameters (Section 2.2.3, Figure 8). Distance from nature protection areas, wave height, seabed geology, and distance from shipping routes were also significant, but to a lesser extent. Expert judgments were reliable and consistent, as indicated by a consistency ratio of 0.03 (Section 2.2.3), which is well below the acceptable threshold of 0.1. However, most experts involved in the study reported by Paper II placed a greater emphasis on environmental parameters
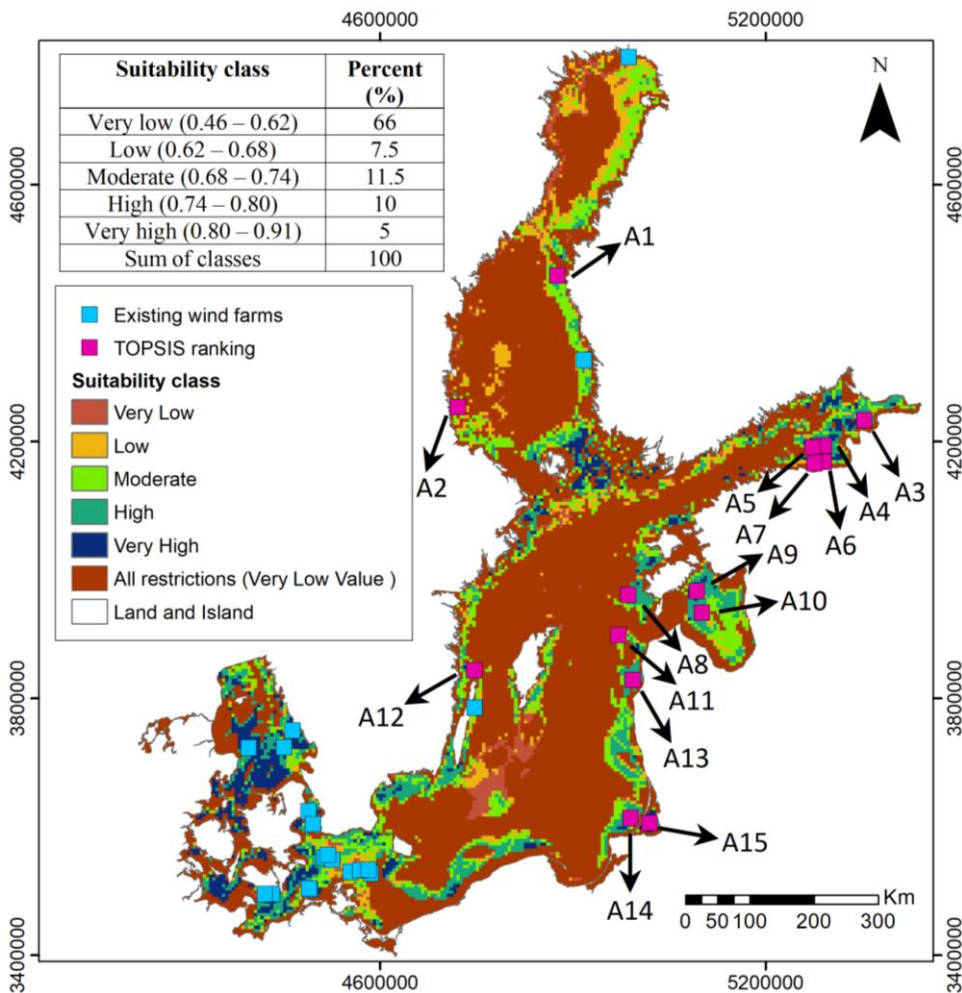

Figure 13. Offshore wind power plant site suitability based on the GIS-MCDA, with marine protected areas, locations within 4 km of the shore and, and areas with water depths greater than 50 m coloured into brown. The labels A1 to A15 indicate the ranking of suitable sites based on the TOPSIS method. From Paper II.

over wind power generation parameters and assigned parameter weights using only
half of the available scale – values from 1 to 5 of the maximum of 9. A different
approach was taken for renewable energy site selection in Iran (Paper VI; see
Chapter 4), where energy generation parameters were prioritised by experts who used
full scale of weighting for parameters from 1 to 9. This discrepancy indicates that
European experts tend to prioritise environmental concerns more strongly than
economic considerations for renewable power generation.

In conclusion, a variety of parameters and methodologies were used to identify
offshore wind farm sites in the Baltic Sea in Paper II and described in this chapter.
By employing LCOE, Fuzzy logic-AHP-WLC, and the TOPSIS technique, the analysis
provided robust and reliable assessments, considering both environmental and
economic parameters. The integration of these techniques within a GIS framework
facilitates marine spatial planning and decision-making, which provide a comprehensive
approach to optimise offshore wind farm site selection in the Baltic Sea.
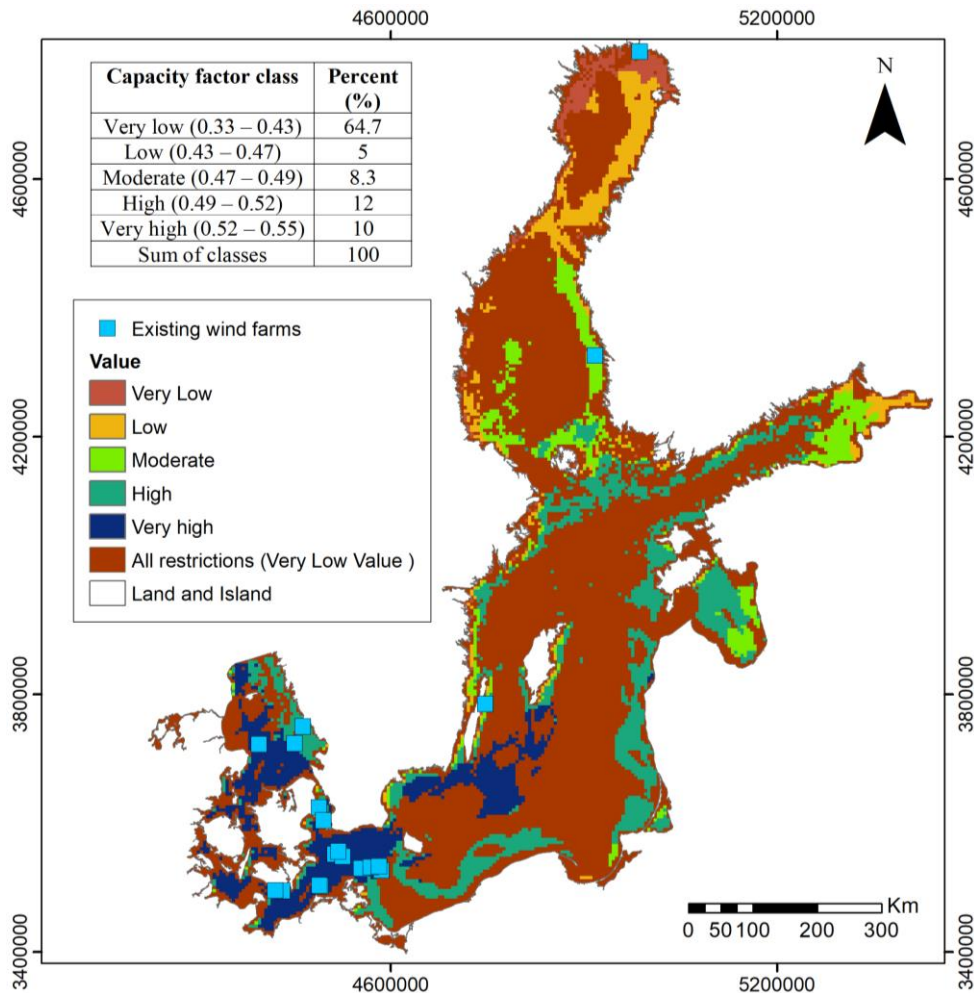

*Figure 14. Offshore wind power plant site suitability based on the capacity factor, with marine
protected areas, locations within 4 km of the shore and, and areas with water depths greater
than 50 m coloured into brown. From Paper II.*

The integration of multiple methodologies, particularly multi-criteria decision analysis (MCDA) and the method of levelised cost of energy (LCOE), enhances the reliability of the outcomes by using diverse datasets. Incorporating the analytical hierarchy process (AHP) into the MCDA framework effectively integrates expert opinions into parameter weighting, and thus contributes to knowledge-based decision-making for site suitability assessment. The MCDA approach reveals significant variations in the importance of different parameters across the study area. For example, the northern Baltic Sea benefits from high wind speeds, however, parameters such as proximity to shore and ports are influential, primarily due to the distance to grid connection points, as noted by Martinez and Iglesias (2022). Seabed substrate suitability is also crucial near the shores of Denmark, Germany, and Poland.

The use of GIS to implement LCOE model for offshore wind farm site selection offers several advantages, including the inclusion of buffers and exclusion zones and easy comparison to other methodologies. This study takes a broader view of parameters than seen in previous studies (Caceoğlu et al., 2022; Gil-García et al., 2022; Gkeka-Serpetsidaki and Tsoutsos, 2022; Salvador et al., 2022). It adheres to the latest industrial standards and environmental policies from the Danish Energy Agency and European Maritime Spatial Planning Platform. The use of two well-established techniques and multiple datasets improves the accuracy and efficiency of the analysis. The LCOE and MCDA approaches provide managers and decision-makers with evidence-based considerations when planning future wind farm installations in the Baltic Sea. The combination of GIS with fuzzy logic-AHP-WLC, TOPSIS, and GIS with LCOE provides better results than single-technology studies. It enables the selection of suitable locations from both an environmental and economic perspective, assisting in balancing these objectives for long-term wind farm development.

Although Vagiona and Kamilakis (2018) found that combining GIS with AHP and TOPSIS methods is useful for hierarchical ranking, the analysis in Paper II suggests that TOPSIS does not significantly enhance the analysis, aligning with Gil-García et al. (2022) in the Gulf of Maine context. A limitation of the presented analysis and the underlying study in Paper II is the lack of data on potential grid connections. Based on discussions in Estonia, this feature may have a significant impact on the selection of wind farm sites in the Baltic Sea. A close proximity to grid connection points is preferred because power transfer costs are lower.

3 Coastal vulnerability assessment for Estonia

Coastal regions globally are increasingly vulnerable to hazards induced by climate change (IPCC, 2022), such as sea level rise, storm surges, and the subsequent flooding of low-lying areas (Nicholls et al., 2007; Torresan et al., 2008). These hazards can adversely impact infrastructure and human livelihoods (Tanner et al., 2014; Nichols et al., 2019) and contribute to the loss of ecosystem services and biodiversity (Myers et al., 2019). Specifying the causes and impacts of marine-driven threats (Rutgersson et al., 2022) enables communities to effectively manage these hazards, enhance social well-being, and minimise economic damage.

One effective planning strategy to strengthen coastal communities' resilience to hazards is vulnerability assessment (Adger et al., 2005). It is essential to include climate change-induced hazards, human-induced environmental changes, and socio-economic developments in these assessments (Ramieri et al., 2011). The Coastal Vulnerability Index (CVI) is a tool used to estimate coastal vulnerability (Rangel-Buitrago et al., 2020). Its streamlined format enhances its effectiveness as a practical management tool (Ramieri et al., 2011). While various alternative indices have been proposed (Mullick et al., 2019; Alcántara-Carrió, 2024), the CVI introduced by Gornitz et al. (1991) remains the most widely used method for evaluating coastal vulnerability (Rangel-Buitrago et al., 2020). This broad applicability is one of the main reasons that this tool is used in this analysis.

As described in Chapter 1 and Chapter 2, decision support tools (DSTs) assist in integrating these estimates into coastal adaptation planning strategies (Gargiulo et al., 2020) and Geographical Information Systems (GIS) enable the integration of various parameters in vulnerability assessment (Thirumurthy et al., 2022).

Multi-criteria decision analysis (MCDA, Section 1.2) employs spatial data and expert priorities to produce information for the decision-making process (Malczewski and Rinner, 2015). It facilitates trade-offs between different decision goals (Bell et al., 2003). All these techniques and approaches are proven to be effective along relatively straight coastlines. However, the situation becomes significantly more complicated in areas with intricate geometry, morphology, and geology, especially in locations with diverse coastal engineering structures. A coastal vulnerability assessment of the Estonian coast was conducted using MCDA techniques, especially fuzzy logic, AHP, and WLC, integrated with GIS, in Paper III. The evaluation covers a land strip extending up to 2 km inland and takes into account various factors not addressed in Chapter 1 and Chapter 2, such as vulnerable infrastructure and population density across a broad coastal area. The core new feature in Paper III and in the presentation in this chapter is an extension of classic one-dimensional vulnerability analysis into a quasi-two-dimensional situation.

3.1 Study area

The area addressed in Paper III and in this Chapter is the entire coastline of Estonia and its large islands. Large parts of Estonia's coastline are characterised by low elevations and are primarily composed of moraine deposits, encompassing various types of sedimentary coasts such as gravels, sands, and silts, along with regions of limestone coastal cliffs (Tõnisson et al., 2013; Łabuz, 2015; Orviku, 2018). The western islands usually have narrow gravel beaches and commonly show visible signs of erosion (Suursaar et al., 2008), some of which are extremely rapid (Suursaar et al., 2015).

Landforms along the Estonian coast are significantly shaped by land uplift, leading to general progradation in the past. However, many areas suffer from deficit of fine sediment, which greatly increases their vulnerability to present and anticipated climate changes (Tõnisson et al., 2013; Łabuz, 2015).

As discussed in Section 2.1, in the Baltic Sea, storm surges are primarily driven by the sea's water volume, strong winds, and wave action (Hünicke et al., 2015). Water levels across the entire Baltic Sea can increase by up to 0.8 m above the long-term average for several weeks (Soomere and Pindsoo, 2016) due to significant changes in water volume (Weisse et al., 2021), known as preconditioning (Andrée et al., 2023). The local impact of storms can be significantly intensified by the high water level background, potentially leading to catastrophic surges in the eastern Baltic Sea (Suursaar et al., 2006).

Wave conditions are typically influenced by wind speed and direction, and long-period remote swell waves are almost non-existent (Björkqvist et al., 2018). The wind direction is capable of intensifying wave set-up along specific coastal sections (Pindsoo and Soomere, 2015), which supports the formation of extremely high water levels in some locations (Eelsalu et al., 2014). The most significant recorded storm surges in Pärnu, for example, occurred in 2005 and 1967, where water levels reached 2.75 m and 2.53 m above approximate long-term mean water level based on the Kronstadt datum, respectively, with massive damage in populated areas (Suursaar et al., 2006; Suursaar and Sooäär, 2007). An increase in storm frequency, along with sea level rise and a shorter duration of winter ice cover, are other contributing factors that influence coastal flooding (Harff et al., 2017). Thus, climate change-driven extreme events can severely impact coastal communities along the Estonian coast (Kont et al., 2003).
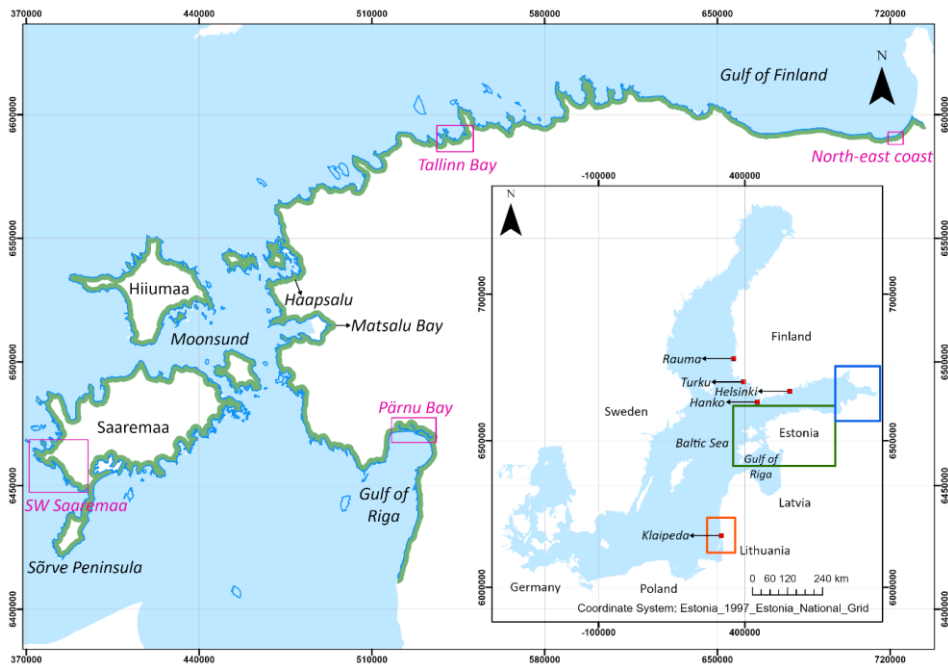

Figure 15. The coast of Estonia. The axis units are in metres. The study area (wide green line) extends 2 km inland from the contour that describes the approximate long-term mean sea level (0 m in EH2000 datum). Pink boxes indicate sub-areas discussed later. From Paper III.

3.2 Steps in the vulnerability analysis

As discussed in Section 1.1, the identification of parameters to be included in a vulnerability assessment is a crucial initial step in the analysis (see Figure 2 and Table 1 in Paper III). The traditional method proposed by Gornitz et al. (1991) incorporates five categories: geomorphology, relative sea level change, shoreline displacement, tidal range, and wave heights and seven parameters used in the analysis: elevation, lithology, geomorphology, relative sea level change, shoreline displacement, tidal range and wave heights. However, in the microtidal Baltic Sea, the tidal range is not a pertinent factor, and relative sea level change may show minimal variation within a small nation (for example, Lithuania; Bagdanavičiūtė et al. (2015)). Subsequently, Gornitz et al. (1994) expanded the number of parameters to 13.

The contemporary perception is that coastal vulnerability is determined by three main elements: exposure, sensitivity, and resilience. This framework was developed by Turner et al. (2003) and applied by Adger (2006), El-Shahat et al. (2021) and many others. This study utilises 16 parameters (Figures 16–23) that collectively represent the essential elements of exposure, sensitivity, and resilience (Turner et al., 2003) (Table 1, Paper III). Exposure relates to the intensity, duration, and extent of hazards affecting a system and encompasses both environmental and socio-political pressures. The exposure factors consist of land surface elevation above mean sea level (MSL), beach slope, underwater slope, shoreline change, closure depth, extreme water level above MSL, relative sea level change, and the maximum significant wave height. The selection of exposure parameters (Figures 16–19) in this study aligns with a well-established set of parameters that have been shown to effectively characterise vulnerability across diverse conditions (see, for example, Bagdanavičiūtė et al., 2015, and Kovaleva et al., 2022 in the context of the Baltic Sea).
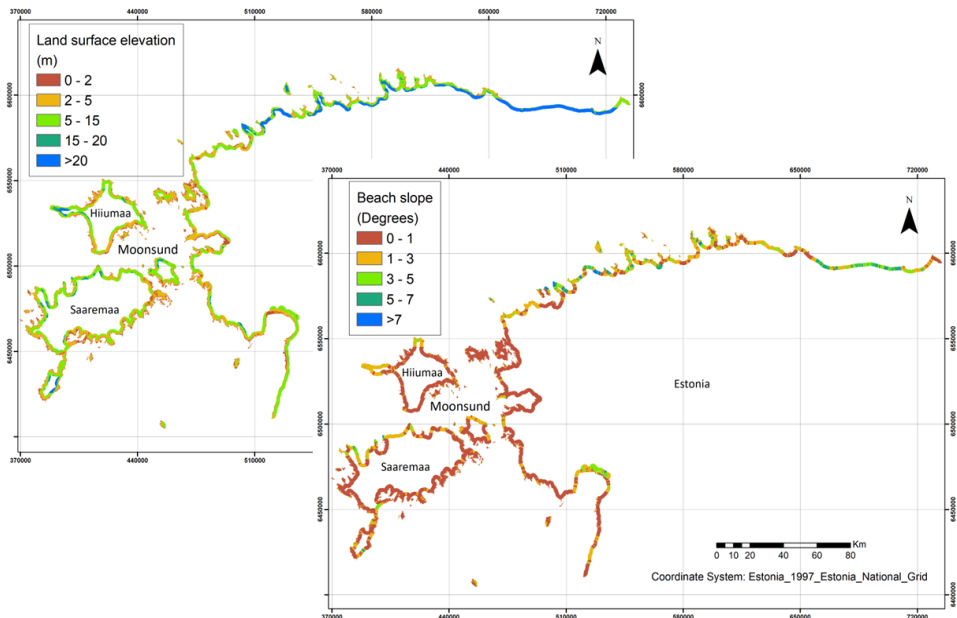

Figure 16. Land surface elevation (left) and beach slope (right). From Paper III.
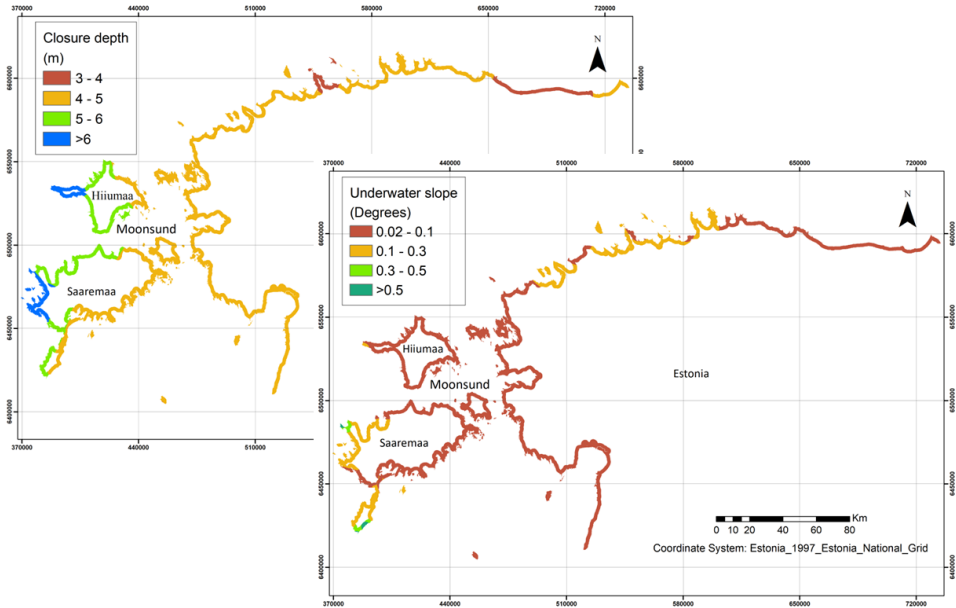
Figure 17. Closure depth (left) and underwater slope (right). From Paper III.
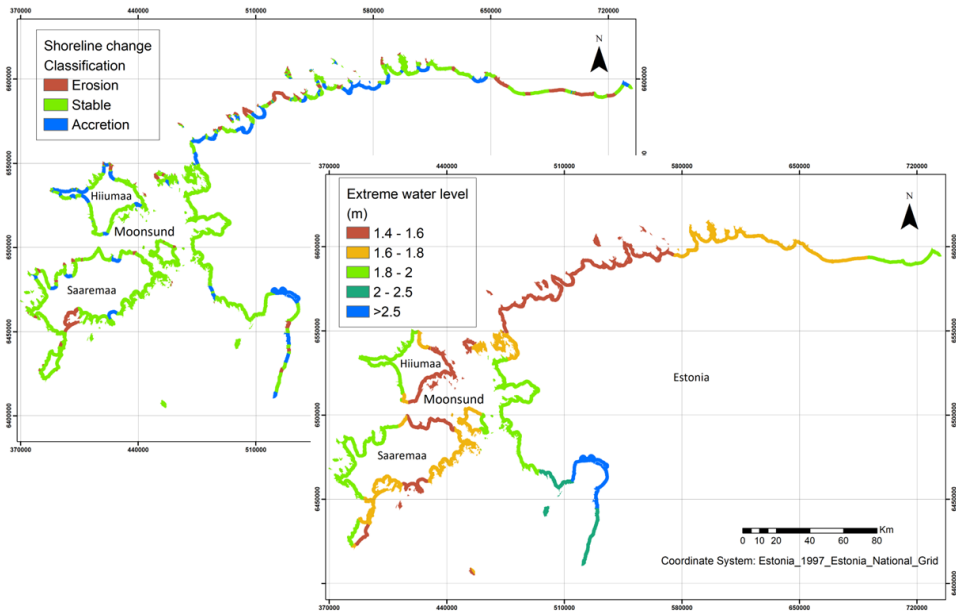

Figure 18. Shoreline change (left) and extreme water level (right). From Paper III.

Sensitivity assumes that the resource is subjected to the hazard and describes the relative impacts of that exposure (Feng et al., 2021). The parameters used to assess sensitivity include geomorphology, sediment type, the existence of nature protection areas, land use and land cover types, land tenure, and population density. The selection of sensitivity parameters (Figures 20–22) is influenced by the specific coastal type and the intended scope of the vulnerability assessment.
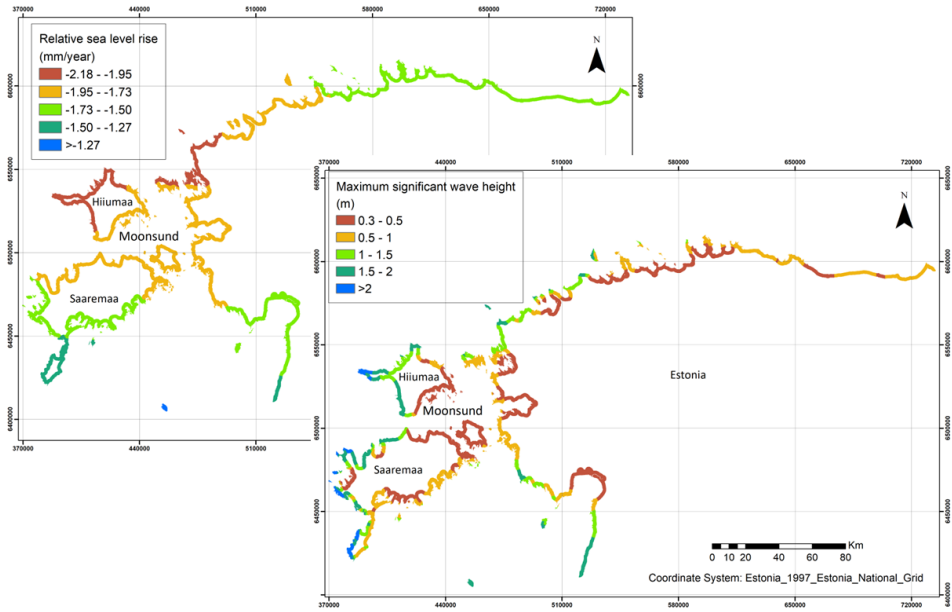
Figure 19. Relative sea level rise (left) and maximum significant wave height (right). From Paper III.
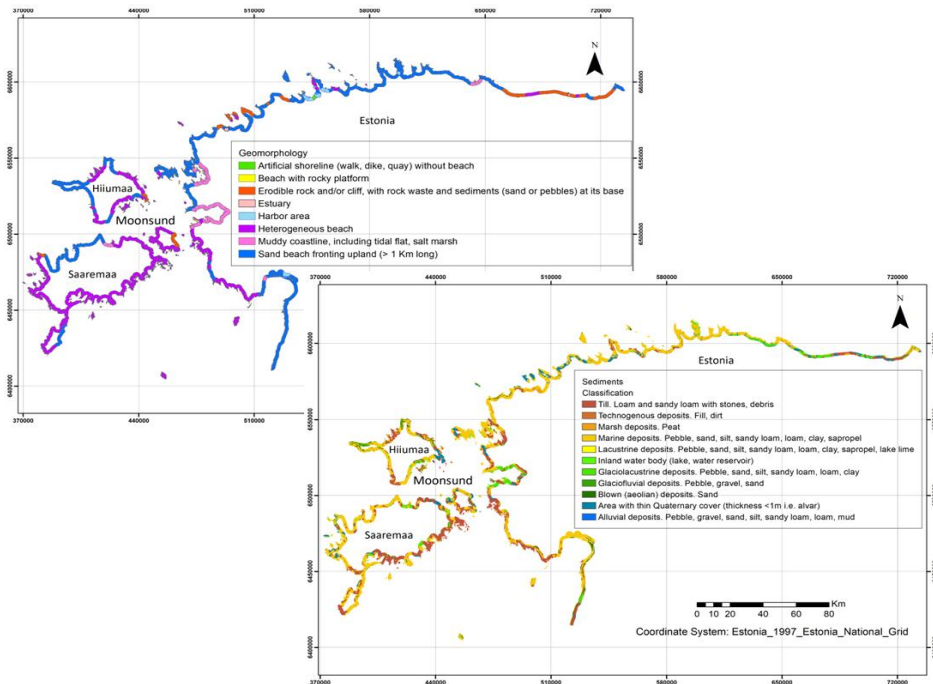

Figure 20. Geomorphology (left) and sediments (right). From Paper III.

This may involve assessing only the shoreline from a societal perspective or extending the analysis inland to incorporate ecological values. The parameter choices aim to expand the Coastal Vulnerability Index (CVI) analysis into a quasi-two-dimensional framework, seeking a broader perspective without substantially increasing the number of parameters compared to classic studies, such as those by Gornitz et al. (1994).
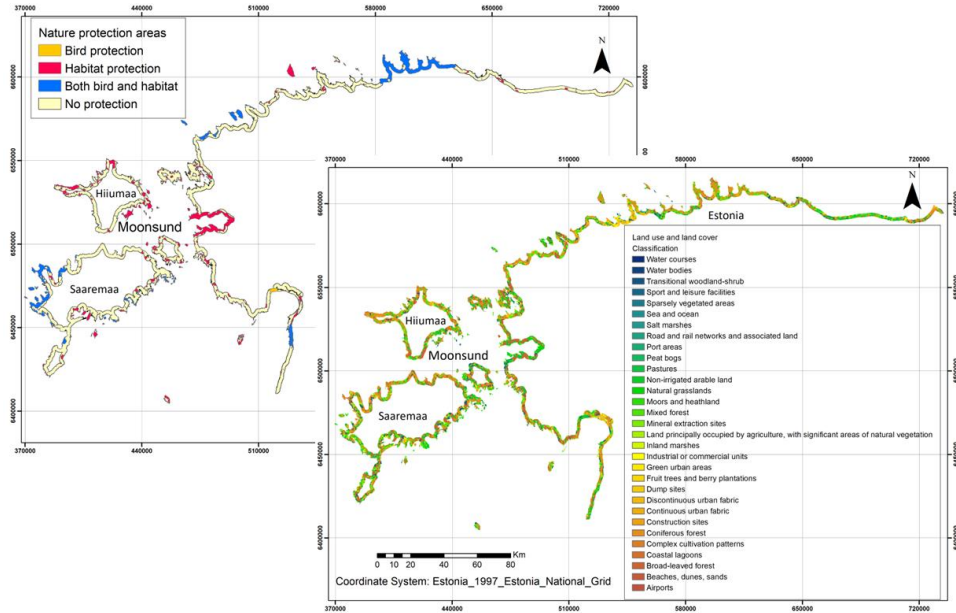

Figure 21. Nature protection areas (left) and land use and land cover (right). From   Paper III.
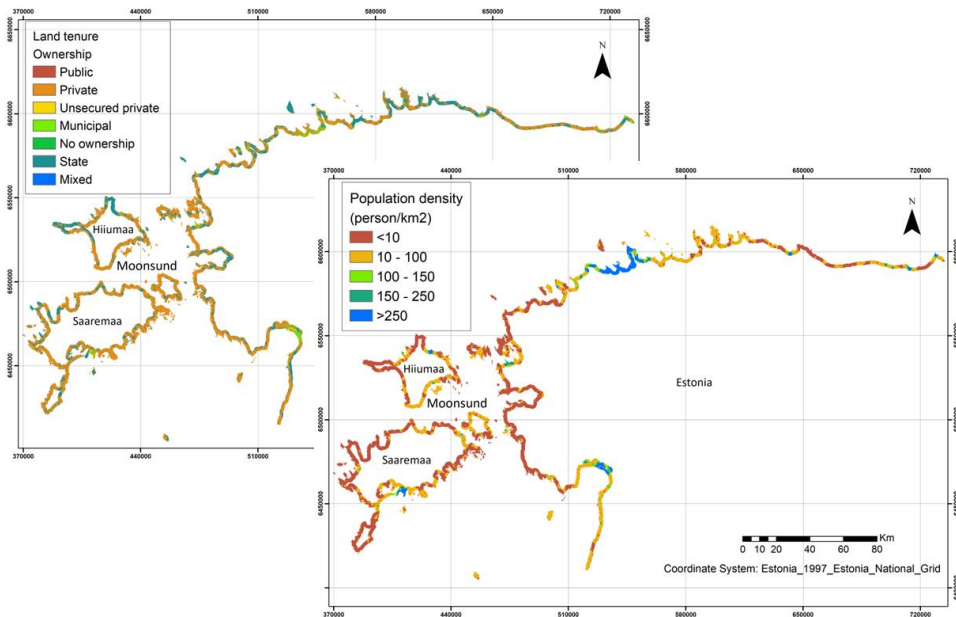

Figure 22. Land tenure (left) and population density (right). From Paper III.

In addition to traditional parameters like geomorphology and sediment, the analysis included the presence of protected natural areas, types of land use and cover, land tenure, and population density as two-dimensional sensitivity parameters to provide a more comprehensive view of inland vulnerability.

Resilience is the ability of a system to withstand or recover from physical, economic, and infrastructure damage caused by a hazard (Mullick et al., 2019). Resilience parameters (Figure 23) involve coastal protection structures and coastal setback. The resilience parameters are relatively few. To characterise shoreline conditions, the presence of coastal protection structures and measured the setback distance from the shoreline to the nearest infrastructure are used.

Following these ideas, the analysis in Paper III applied 16 parameters to the entire coastline of Estonia (Figure 15) in the multi-criteria decision analysis (MCDA) process (Section 1.2). The target was a 2 km wide nearshore zone from the 1 m elevation isoline relative to MSL (0 m contour). This approach effectively created a quasi-two-dimensional (2D) representation of parameters, which are essentially one-dimensional (1D) variables. The 1D parameters, which include beach slope, closure depth, extreme water level, geomorphology, maximum significant wave height, relative sea level rise, setback (the distance between the shoreline and the first infrastructure on the landward side), shoreline change, and underwater slope (Paper III), have distinct values at each specific coastal location and vary along the shoreline. Several other parameters are naturally two-dimensional, especially those associated with land features: land surface elevation, land tenure, land use and land cover, population density, the presence of nature protection areas, and sediment types (Paper III). Coastal protection structures are represented by specific locations (polygons) (Figure 23) for illustrative purposes but are accurately defined in the analysis. Thus, they are classified as "Not applicable" for both 1D and 2D categories in this context.

The data for GIS analysis were processed and prepared in ArcGIS Pro, using a spatial resolution of 10 × 10 m, based on the Estonia 1997 National Grid reference coordinate
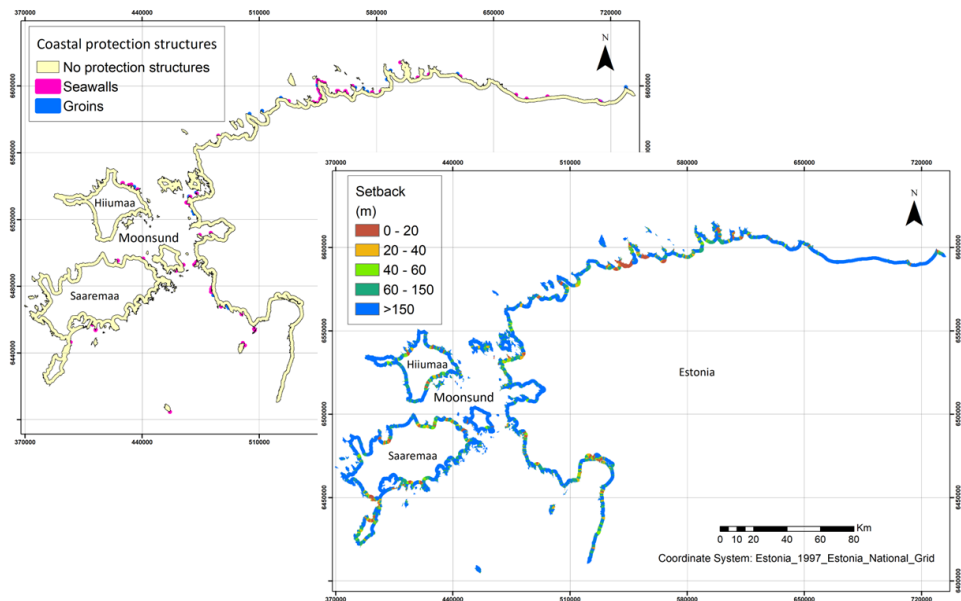

Figure 23. Coastal protection structures (left) and setback (right). From Paper III.

system. This resolution was applied to the entire Estonian shoreline, including areas selected for detailed analysis (Figure 15). Parameters initially available at a coarser resolution were interpolated to a 10 × 10 m raster using the inverse distance weighting method. Parameters that are inherently one-dimensional at the shoreline (e.g., closure depth) were extended to inland calculation cells perpendicular to the shoreline. The vertical datum system employed is the European Vertical Reference Frame 2007. The 0 m contour (Estonian Land Board, maaamet.ee) was used as an approximate mean sea level (MSL). In reality, MSL fluctuates between +19 cm and +27 cm relative to the datum (Estonian Land Board, 2023), largely due to the low (and spatially changing) salinity of the Baltic Sea waters (Ekman and Mäkinen, 1996).

The second step in the MCDA process (Figure 2 in Paper III) is to standardise the selected parameters using fuzzy logic standardisation (Section 1.2.1) so that they increase linearly between threshold values R_{min} and R_{max}, have zero value if the input is $< R_{min}$ and are equal to 1 if the input value is $> R_{max}$ (Eqs. (1), (2)). The input data (Table 2 in Paper III) include land surface elevation (digital terrain model from Estonian Land Board, maaamet.ee; threshold values $R_{min} = 2$ m and $R_{max} = 5$ m, decreasing function), beach slope (maaamet.ee; 1° and 7°, decreasing), underwater slope (maaamet.ee; 0.02° and 1°, increasing), shoreline change (EMODnet, emodnet-geology.eu; −1 m for erosion and 1 m for accretion, decreasing), closure depth (Soomere et al. (2013); 3 m and 6 m, increasing), extreme water level (Wolski et al. (2014); 1 m and 2.5 m, increasing), relative sea level rise (Madsen et al. (2019); −2 mm/yr and −1 mm/yr, decreasing), maximum significant wave height (Giudici et al. (2023); Najafzadeh et al. (2024); 0.3 m and 2.8 m, increasing). Information about geomorphology (0 for cliffs, 1 for artificial beach), sediments (0 for sand, 1 for gravel), nature protection areas (0 for no protection, 1 for nature protection areas with most vulnerable species and habitats), land use and land cover (0 for forests, marshes, water bodies, sea and ocean, 1 for industrial and commercial areas), land tenure (0 for public property, 1 for private property), population density (< 10 person/km^2 and > 250 person/km^2, increasing), coastal protection structures (0 for seawalls, 1 for no protection structures), and coastal setback (20 m and 150 m, decreasing) has been retrieved from various public sources.

The third step in the MCDA is implementing the Analytical Hierarchy Process (AHP), which relies on the personal assessments of experts regarding the relative importance of various parameters in coastal vulnerability assessment (Section 1.2.2). In the analysis performed in Paper III, the opinions of 10 experts were analysed to assess the significance of each parameter similar to the procedure described in Section 2.2.3. The geometric mean was used to calculate the relative weights of the parameters also here because it effectively accommodates the possibly diverging viewpoints of the experts (Table 3 in Paper III), providing a more balanced representation of their assessments (Mu and Pereyra-Rojas, 2018). These estimates were incorporated into a matrix to calculate their relative weights (importance) (Section 1.2.2). Finally, the weighted linear combination (WLC) technique was used to calculate the coastal vulnerability index (CVI) using all 16 parameters. The highest rank is set to 1 for the output map. As an additional step, vulnerability was re-evaluated across all raster points using only the three parameters with the highest weights from the AHP analysis: extreme water level, shoreline change, and geomorphology. The weights were renormalised to sum to 1 and applied in the Weighted Linear Combination (WLC) method to align with the map that reflects all 16 parameters. The CVI calculation was

performed at a 10×10 m spatial resolution by multiplying the standardised and weighted parameters to obtain a vulnerability score for each grid cell across the entire study area, including regions chosen for more detailed analysis.

The AHP analysis reveals that the most crucial parameters for a vulnerability assessment of the Estonian coast according to experts' opinions are extreme water levels, shoreline changes, and geomorphology. Closure depth, population density, and land tenure were the least significant parameters for coastal vulnerability assessment (Figure 24). Most experts provided weights in the range 1–5, not giving weights over the full scale from 1 to 9 (Table 3 of Paper III). This suggests that experts perceived only moderate differences in parameter importance. It is likely that they aimed to keep their evaluations consistent and dependable, using their professional judgment to avoid exaggerating the distinctions between parameter weights. Despite this feature of the opinions, the consistency ratio between experts' perspectives is $CR = 0.04$. As the method remains valid if the consistency ratio is ≤ 0.1 (Saaty and Tran, 2007), it is reasonable to use the retrieved weights of the parameters.

3.3 Coastal vulnerability index (CVI) analysis

The calculations performed in Paper III show that the CVI values range between 0.24 (very low vulnerability) and 0.72 (very high vulnerability). Therefore, the range of 0.48 which is almost half of the theoretically possible total range from 0 to 1 is covered by the calculated CVI index. It is therefore likely that the classic method of dividing CVI values for single locations equally into five linearly increasing classes provides a sensible representation of coastal vulnerability (Table 2).

Segments that have low or moderate vulnerability occur in almost the entire study area (Figure 25). The northern coast of Estonia has many segments with very low vulnerability dominantly comprising areas with stable limestone cliffs (Figure 25). The coastline of the interior water body of the West Estonian Archipelago, Moonsund, has also very low or low vulnerability along many its sections. This feature appears to
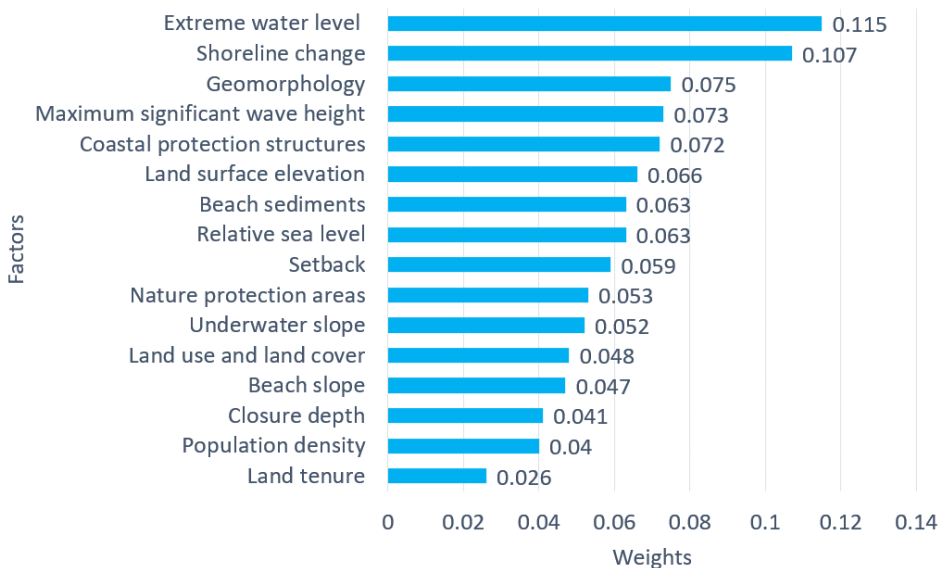

Figure 24. Relative weights assigned to the parameters using the AHP method. From Paper III.

53

Table 2. Coastal vulnerability analysis using MCDA and all 16 parameters. Areas are calculated for coastal land up to 2 km from MSL using equal interval classification method in ArcGIS Pro.

Vulnerability class	Area (km²)	Percent (%)	Main locations
Very low (0.24–0.34)	121	3.8	North-west
Low (0.34–0.44)	1496	47	North-west and north-east
Moderate (0.44–0.53)	1350	42.5	North-west, north-east, Pärnu Bay and western islands
High (0.53–0.63)	207	6.5	North-east, Pärnu Bay, and western islands
Very high (0.63–0.72)	6	0.2	Pärnu Bay and western islands

be a result of gradual uplift, moderate variations of water levels (Männikus and Soomere, 2023), and also because of limited wave heights.

There are a number of areas identified as the most vulnerable in the study area; mostly low-lying areas experiencing very high water level extremes. Additional factors contributing to the level of vulnerability are gradual erosion and the presence of various infrastructure located near the coast. The majority of areas with high and very high vulnerability are located on the western shore of Saaremaa and near Pärnu Bay. The main likely reasons for this classification are the possibility of high water levels (Suursaar and Sooäär, 2007; Eelsalu et al., 2014), shoreline erosion on the eastern shore of the Gulf of Riga (Tõnisson et al., 2013), and being open to storm events from the west (western coast of Saaremaa). However, the presented classification is to some extent counter-intuitive and does not always match the general perception of vulnerability. For example, problems and damage associated with high water levels, including major economic losses, are frequent in Pärnu (classified as having moderate vulnerability) but similar problems have not been reported for the western shore of Saaremaa, for which the MCDA analysis shows high vulnerability.

To shed more light on this issue, Paper III also presents another view of coastal
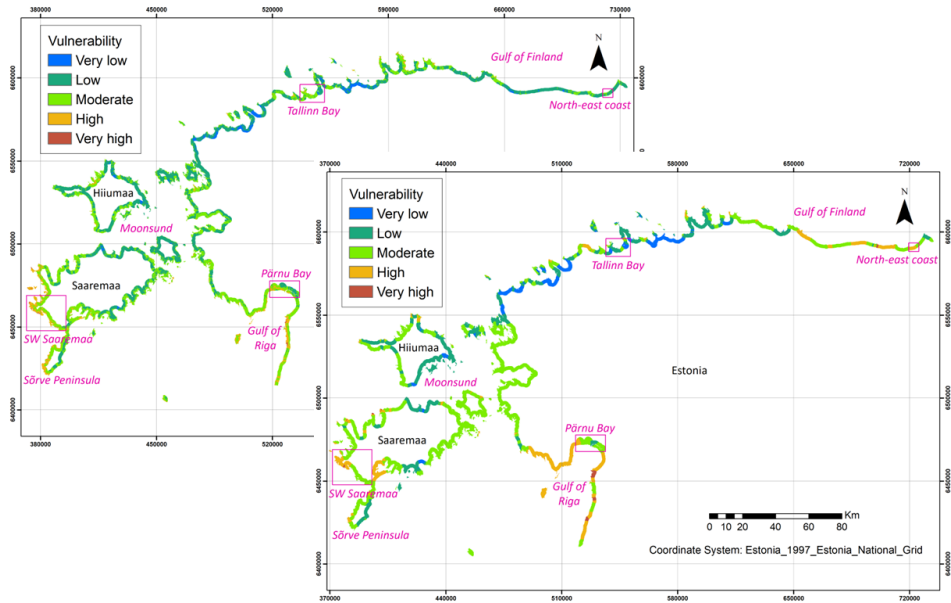

Figure 25. From left to right: Coastal vulnerability using the MCDA technique (all 16 parameters) and three most important parameters (extreme water level, shoreline change and geomorphology) based on the perception of experts. From Paper III. Pink boxes indicate sub-areas for which inland vulnerability is discussed below.

vulnerability that is evaluated as above but only the three parameters given the highest priority by experts (Figure 24) are considered (Figure 25). Namely, only extreme water levels, shoreline changes, and geomorphology are taken into account and all social or economic parameters are ignored. The results of both maps (the 16-parameter and three-parameter analyses) are qualitatively similar but show clear quantitative differences, highlighting differing levels of vulnerability in certain coastal segments. Experts did not prioritise some intuitively significant parameters, such as land elevation, coastal protection structures, and maximum wave height, as shown in the pairwise comparison matrix (Table 3, Paper III). Instead, they emphasised historical extreme water levels and specific physical characteristics (shoreline change and geomorphology). This reflects a limitation within the analytical hierarchy process (AHP), where expert preferences may diverge for parameters that straightforwardly support resilience, like high land elevation. This also emphasises the complexity of using expert judgments and the influence of contextual biases in decision-making, suggesting the value of incorporating perspectives outside traditional coastal science to enhance the focus on socio-economic parameters, possibly by asking experts to propose additional parameters and criteria to further strengthen the assessment.

The range of the CVI index with this approach is 0.64 (Table 3), which covers almost two-thirds of theoretically possible values. On the one hand, the resulting map contains a significantly smaller proportion of locations with low vulnerability than in Table 2. On the other hand, the proportion of locations with high vulnerability is clearly larger. Large segments of the south-western and north-eastern shores of Estonia have high vulnerability based on these three most important parameters. Consistently with the general perception, Pärnu Bay together with extended sections of the eastern coast of the Gulf of Riga has a generally high vulnerability to coastal hazards. This area is prone to high water levels during extreme events (Suursaar and Sooäär, 2007) and the coastal landscape contains many low-lying areas. It is likely that the frequent occurrence of particularly elevated water levels in the Gulf of Riga and severe wave events on the eastern shore of this gulf (Männikus and Soomere, 2023) contribute to the vulnerability of the eastern shores of the Gulf of Riga. This classification is still not perfect as several locations on the western shore of Saaremaa, areas of gravel and sandy beaches on the north-eastern coast of Estonia, and various locations on the eastern shore of Sõrve Peninsula are classified as high-vulnerability areas even though they are usually considered as stable being partially protected by boulders at the waterline.

The CVI range calculated using only three parameters (0.2244 to 0.8688) is considerably larger than the range obtained when all parameters are included (0.2441 to 0.7251). This outcome aligns with the general observation that adding more parameters tends to compress the range of CVI values under Baltic Sea conditions (Soomere et al., 2024). Furthermore, the standard deviation of CVI values with three

Table 3. Coastal vulnerability analysis using MCDA and three most important parameters according to the perception of experts. Areas are calculated for the coastal land up to 2 km from MSL using equal interval classification method in ArcGIS Pro.

Vulnerability class	Area (km²)	Percent (%)	Main locations
Very low (0.22–0.35)	247	7.7	North-west
Low (0.35–0.48)	807	25.4	North-west and north-east
Moderate (0.48–0.61)	1637	51.5	North-west, north-east, Pärnu Bay and western islands
High (0.61–0.74)	464	14.6	North-east, Pärnu Bay, and western islands
Very high (0.74–0.86)	25	0.8	Pärnu Bay and western islands

parameters (0.1015) is nearly twice as high as that derived from all parameters (0.0597). The point-to-point correlation between the two CVI datasets is 0.565, indicating a moderate relationship while reflecting significant differences in the information they contain. This result reinforces the main conclusion of Fig. 25: while the two measures share some spatial patterns and structural similarities, they are not perfectly aligned.

3.4 Extended vulnerability analysis

Paper III also explored options of extension of estimates of coastal vulnerability by up to 2 km inland, to emphasise vulnerability in low-lying areas where critical infrastructure may be located. For consistency, we present results using both all 16 parameters and the three most critical parameters identified by experts. A detailed quasi-two-dimensional coastal vulnerability index was developed to evaluate the spatial distribution of vulnerability within this coastal strip based on the classic CVI values on the shore and properties of this strip. Consistent with the above, Pärnu Bay (Figure 26), south-western Saaremaa (Figure 27) and Tallinn Bay (Figure 28) are among the areas with high vulnerability. The nearshore landscape of Estonia has generally relatively strong slope towards onshore. Thus, most of the described coastal strip area is elevated, with the exception of a few locations, such as Matsalu Bay directly to the east of Moonsund (Figure 15) or the vicinity of Haapsalu. Consequently, most inland areas of Estonia within 2 km from the waterline have very low vulnerability as the land elevation increases inland and this feature becomes dominant in the estimates (Figure 25). Only low-lying river valleys and other low-lying areas, such as former coastal lagoons, have high vulnerability.

The influence of various coastal parameters, such as wave height, creates a pattern of different vulnerability levels in inland areas if this type of approach is used. This pattern should be disregarded in management decisions. This recommendation becomes particularly evident when CVI maps are constructed using only three parameters (extreme water levels, shoreline changes, and geomorphology) (Figure 25, right panel; also Figures 26–28). Therefore these estimates can be applied only to a narrow coastal strip and cannot be applied further away from the coastline.

The estimated relatively high level of vulnerability of the south-western shore of Saaremaa (Figure 27) is determined by the specific characteristics of the coastal area. There are some locations that are highly vulnerable due to the openness of this area to strong westerly winds, which can result in very high local water levels (Eelsalu et al.,
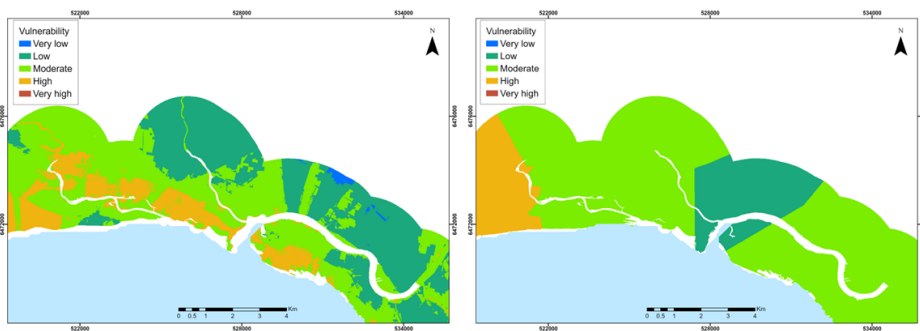

Figure 26. Coastal vulnerability map of the vicinity of Pärnu (see Figure 15) using MCDA based on all parameters (left), and three most important parameters (right). From Paper III.

2014) (Figure 27). The map based on the three most important parameters (Figure 27, right panel) has much less detail. However, unlike the case of Pärnu (Figure 26), this map offers a reasonable generalisation of the map based on 16 parameters.
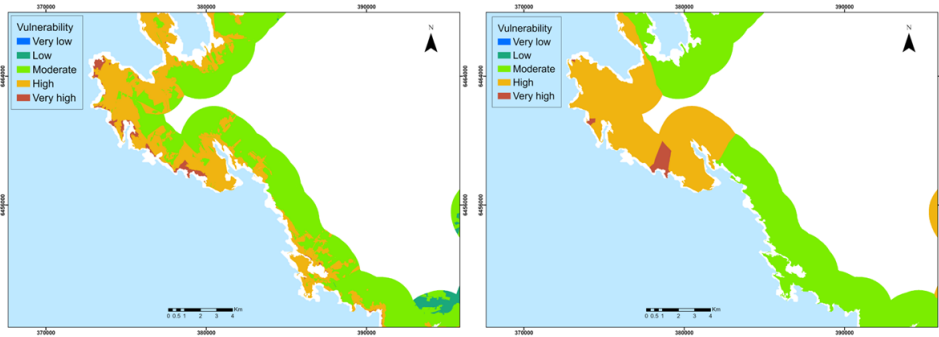

Figure 27. Coastal vulnerability map of western Saaremaa (see Figure 15) using MCDA based on all parameters (left), and three most important parameters (right). Pilguse is the birthplace of Fabian Gottlieb von Bellingshausen. From Paper III.

The estimated relatively high level of vulnerability of the south-western shore of Saaremaa (Figure 27) is determined by the specific characteristics of the coastal area. There are some locations that are highly vulnerable due to the openness of this area to strong westerly winds, which can result in very high local water levels (Eelsalu et al., 2014) (Figure 27). The map based on the three most important parameters (Figure 27, right panel) has much less detail. However, unlike the case of Pärnu, this map offers a reasonable generalisation of the map based on 16 parameters.

The geomorphology and coastal orientation make the northern coastline of Estonia along the Gulf of Finland less vulnerable. To the east of Tallinn, the historical coastal changes and the frequency and intensity of extreme events are lower (Suursaar and Sooäär, 2007). This region is characterised by cliffed coasts, extensive areas of pebbles, cobbles and boulders near the waterline, and areas with higher land surface elevation compared to the south and west of Estonia (Orviku, 2018). However, the vulnerability map of the Tallinn area (Figure 28) accurately identifies several well-known features, such as the low-lying areas on the Paljassaare Peninsula and the city centre around the Old Harbour. However, it does not accurately represent the significant variations in land elevations.
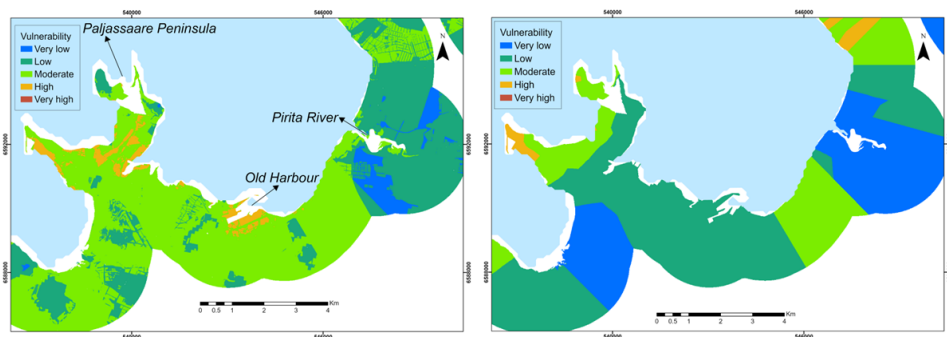

Figure 28. Coastal vulnerability map of the vicinity of Tallinn (see Figure 15) using MCDA based on all parameters (left), and three most important parameters (right). From Paper III.

Several areas near the mouth of the Pirita River are estimated as moderately vulnerable in Paper III, as their elevation is sufficient to mitigate marine hazards. Despite the presence of extensive infrastructure and high population density in Tallinn compared to Pärnu and the western coast of Saaremaa, many coastal areas near Tallinn have moderate and low vulnerability according to the presented estimates (Figure 28). This somewhat surprising outcome is likely due to the extensive coastal engineering and protection structures. It is likely that experts did not distinguish between low-lying natural sections and heavily engineered sub-areas. They also did not prioritise social and economic factors, which may be significant in some small regions.

The cliffs on the north-eastern coast of Estonia contribute to low to moderate coastal vulnerability (Figure 29). The low priority given to land surface elevation by the experts resulted in very high CVI values for this coastal segment in the metrics based on the three most important parameters (Figure 29).

In conclusion, it has become increasingly common to use decision support systems and systematic assessments of coastal vulnerability to inform coastal management decision-making (Wong-Parodi et al., 2020; Paper I). Even though Paper III and most of the other solutions presented in this thesis aim to assist coastal managers and stakeholders in identifying vulnerable areas for spatial planning and investment decisions, significant shortcomings have been identified from the critical consideration of the outcome.

First of all, issues arise from using a limited number of parameters or when experts prefer certain parameters over others. Numerous studies on coastal processes along the Estonian coast and nearby areas (Kovaleva et al., 2022) typically focus on small regions (Orviku et al., 2009; Tõnisson et al., 2018) or specific sets of related coastal processes (Kont et al., 2008; Tõnisson et al., 2011; Männikus and Soomere, 2023). These studies have identified specific vulnerabilities that can be compared to, but not always match, our findings. An exception is Tõnisson et al. (2013), which considers a country-wide approach but focuses specifically on coastal erosion.

The country-wide approach in Paper III takes into account a variety of coastal hazards affecting land, infrastructure, and inhabitants, rather than only focusing on coastal erosion, which is often regarded as the primary coastal hazard (Bagdanavičiūtė et al., 2015, 2019; Armenio et al., 2021). The extension of coastal vulnerability analysis also up to 2 km inland allows for the logical identification of interactions between land and sea environments, particularly in the lower reaches of rivers and estuaries.
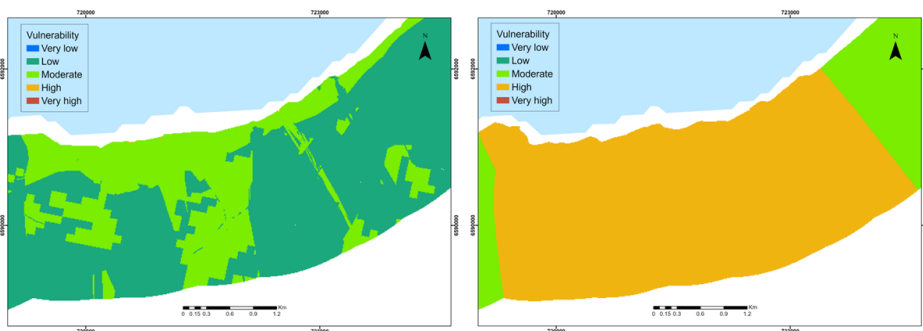

Figure 29. Coastal vulnerability map of the north-eastern coast of Estonia (see Figure 15) using MCDA based on all parameters (left), and three most important parameters (right). From Paper III.

However, this approach must be used cautiously, as some parameters are one-dimensional in nature.

This study also applies and expands MCDA and GIS methods to assess high-resolution coastal vulnerability in Estonia, filling gaps in prior studies by Kovaleva et al. (2022) in the eastern Gulf of Finland and Bagdanavičiūtė et al. (2019) in Lithuania by extending the analysis. Findings indicate that about 90% of Estonia's coast has low to moderate vulnerability, although some areas show high vulnerability, especially when focusing on three key parameters. Additional socio-economic and two-dimensional data are incorporated, revealing integration challenges between 1D and 2D data. The assessment spans 2 km inland, identifying areas of potential concern, such as regions behind dunes and along river valleys, offering valuable insights for coastal managers.

The response to a vulnerability assessment is a separate issue, which requires consideration of many factors, especially resource availability, environmental factors, and political considerations. Possible responses range from hard engineering solutions to do-nothing options (Masselink et al., 2011).

4 Conceptual and local applications

As discussed in the previous Chapters, coastal areas may be adversely affected by many marine-induced drivers, such as sea level rise and storm surges, causing flooding of low-lying areas (Nicholls et al., 2007), damage to infrastructure and human livelihoods (Tanner et al., 2014; Nicholls et al., 2019), or loss of ecosystem services, and disturbance to biodiversity (Myers et al., 2019). The coastal vulnerability index (CVI) is a commonly used tool for coastal vulnerability assessment. Decision support tools (DSTs) allow coastal vulnerability assessments to be integrated into adaptation planning (Gargiulo et al., 2020). Multi-criteria decision analysis (MCDA) combines spatial data with expert opinions to provide information for the decision-making process (Malczewski and Rinner, 2015). A geographical information system (GIS) is used for representing, analysing, and visualizing spatial data.

Many studies have analysed coastal vulnerability using variations of the described classic GIS-MCDA methods or various implementations of the CVI (Bagdanavičiūtė et al., 2019; Armenio et al., 2021; Ghosh and Mistri, 2022) as described in Paper I and Chapter 1. Several crucial limitations of these methods have been highlighted in Paper II and Paper III and reiterated in Sections 2.5 and 3.4. This Chapter includes two attempts to mitigate these limitations by means of implementation of machine learning technologies into coastal vulnerability assessment (Paper IV) and by incorporating advanced estimates of the properties of extreme water levels into the classic CVI estimates (Paper V). Finally, it is demonstrated that the techniques used in this thesis in marine and coastal context can also be applied to inland applications (Paper VI).

4.1 Integrating machine learning into coastal vulnerability assessment

The use of machine learning algorithms and geospatial techniques has gained popularity for mapping hazard susceptibility worldwide (Lei et al., 2020). A Random Forest model (RF) is a machine learning method that can process large datasets and model interactions between inputs (Wang et al., 2016). Machine learning techniques were used, e.g., by Ennouali et al. (2023) and Fannassi et al. (2023) in coastal vulnerability assessments in Morocco. There is, however, a lack of systematic comparison between the results of coastal vulnerability assessments from GIS-MCDA and machine learning methods.

The majority of the techniques described in the previous chapters work well along relatively straight shorelines where coastal vulnerability varies smoothly (e.g., Bagdanavičiūtė et al., 2015, 2019). Most studies in this field concentrate on small geographic regions (Ennouali et al., 2023; Fannassi et al., 2023) or specific coastal processes (Asiri et al., 2024). Hasan et al. (2023) took a broader approach by evaluating coastal vulnerability to flooding on a country-wide scale, with a primary focus on physical vulnerability parameters. A different situation exists in the eastern Baltic Sea, where complex geomorphology, geology, and coastal engineering structures are present (Kovaleva et al., 2022).

The analysis in Paper IV combines machine learning with GIS to assess coastal vulnerability using the RF technique. This assessment also incorporates less obvious and less studied parameters, such as nature conservation areas, land ownership, and setback, extending as in Paper III up to 2 km into inland from the long-term mean sea level (0 m in the EH2000 datum) (Figure 15) along the entire Estonian coastline.

4.1.1 Merging multi-criteria decision analysis (MCDA) with machine learning

The first steps of the analysis are the same as in Chapter 3 and Paper III. As described in Section 1.2, the MCDA method incorporates GIS, fuzzy logic standardisation, analytical hierarchy process (AHP), and weighted linear combination (WLC) to assess coastal vulnerability. The first step is to collect environmental and socioeconomic data, and to use the GIS environment for data quantification and raster analysis mapping.

The coastal vulnerability components are exposure, sensitivity, and resilience. Each of these components may be described by several parameters as detailed in Section 3.2. Larger values of some of these parameters (e.g., a higher value of extreme water level, sea level rise, maximum significant wave height, beach slope, or shoreline change) correspond to higher vulnerability, whereas a higher value of some other parameters (e.g., land elevation) indicates lower vulnerability. The numerical values of these parameters need to be standardised to take into consideration their different scales and meanings (Eastman, 2009). This is done using fuzzy standardisation algorithm that converts the input values into the range from 0 to 1 (Section 1.2.1, Eqs. (1) and (2)).

The AHP technique (Section 1.2.2) is employed next to determine the relative importance of each parameter using weights ranging from 1 to 9 according to Saaty and Tran (2007). The process is validated by a consistency ratio $CR \leq 0.1$. Finally, the WLC technique (Section 1.2.3) is used in the GIS environment to generate the final map by multiplying the relative weight of each parameter by its normalised value (Eq. (5)).

The main advancement in Paper IV is incorporation of one of the machine learning techniques, namely the RF algorithm, into the analysis of coastal vulnerability. In essence, the RF algorithm is a supervised machine learning technique that can be applied for classification or regression (Izquierdo-Horna et al., 2022). It is beneficial to specify the weight of parameters through investigating the relationship between independent and dependent variables (Gigović et al., 2019). The RF algorithm is a combination of numerous decision trees, each of which makes predictions. They are constructed using random samples from the original data through a technique known as bootstrapping and by taking into account the available predictors (Izquierdo-Horna et al., 2022). Each decision tree is developed after both the predictive and target variables are specified (Rihan et al., 2023).

To implement this technique, hazard and non-hazard locations (target variables) are specified and divided into two groups, which are used for training and testing the model. In the analysis performed in Paper IV, 1000 samples were selected randomly from the MCDA map to be used in the RF technique. From these, 700 points were used for training of the model and 300 points for testing. The coastal vulnerability parameters (predictive variables) were incorporated in the GIS environment and the training datasets were extracted for the hazard and non-hazard locations to proceed with the training process.

In the present work, the Receiver Operating Characteristic (ROC) curve was used as the primary method for validating the overall performance of the RF model. The ROC curve is widely recognised in the literature as an effective validation tool for probabilistic models, especially in natural hazard susceptibility assessments like floods and landslides (Gudiyangada Nachappa et al., 2020; Pradhan, 2013; Tien Bui et al., 2016). The ROC curve is generated by plotting the true positive rate (TPR), which represents the proportion of correctly identified vulnerable areas (sensitivity), against the false positive rate (FPR), which indicates the proportion of non-vulnerable areas that were incorrectly classified as vulnerable (specificity), across various threshold

values. This provides a clear representation of the model's ability to distinguish between vulnerable and non-vulnerable areas. The area under the curve (AUC) is then calculated to quantify the model's accuracy. Higher AUC values indicate stronger model performance, with an AUC of 1.0 representing a perfect model and an AUC of 0.5 representing a model that is not performing well.

4.1.2 Coastal vulnerability analysis based on MCDA and RF techniques

The comparative assessment of coastal vulnerability in the eastern Baltic Sea using multi-criteria decision analysis (MCDA, Paper III, Chapter 3) and RF techniques produced different outputs. In the MCDA framework, experts prioritised extreme water levels, shoreline change, and geomorphology (Section 3.2, Figure 24). A high consistency, characterised by small consistency ratio $CR = 0.04 \ll 0.1$ (Saaty and Tran, 2007) indicates strong agreement among experts (but not necessarily that the experts were right). The Coastal Vulnerability Index (CVI) map derived from MCDA (Figure 30) showed a high proportion of regions with low (47%) to moderate (42.5%) vulnerability (Table 2 in Section 3.3), with high-vulnerability areas concentrated along the western shoreline of Saaremaa and Pärnu Bay. This pattern is attributed to the frequent elevated water levels and shoreline erosion in the Gulf of Riga and susceptibility to westerly storm events on the western coast of Saaremaa (Section 3.3).

In contrast, the RF technique classified a larger proportion of areas (65.6%; Table 4) as having low vulnerability (Figure 31). The high vulnerability areas identified by RF are mainly located in the Gulf of Riga, including parts of Pärnu Bay. Despite some discrepancies in categorizing vulnerable locations, particularly in the Gulf of Riga, the western shore of Saaremaa, and Tallinn Bay, both techniques showed a degree of alignment in their spatial patterns with respect to high vulnerable areas in south of the country on the shores of the Gulf of Riga.
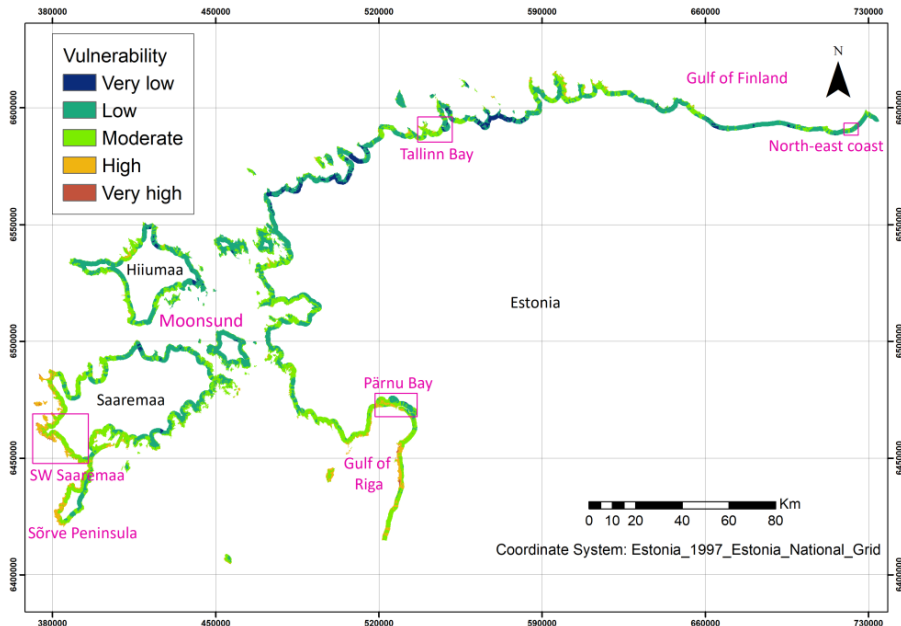

Figure 30. Coastal vulnerability analysis based on the MCDA technique. Originally presented in a slightly different form in Paper III. From Paper IV.

Table 4. Coastal vulnerability analysis using MCDA (left two columns) and RF (right two columns) techniques.

Vulnerability class	Area (km²) MCDA	% MCDA	Area (km²) RF	% RF
Very low	121	3.8	15	0.5
Low	1496	47	2086	65.6
Moderate	1350	42.5	793	24.9
High	207	6.5	236	7.4
Very High	6	0.2	50	1.6
Sum of classes	3180	100	3180	100

The RF analysis highlighted geomorphology, maximum significant wave height, and shoreline change as the most significant parameters. Table 4 compares the areas and percentages of vulnerability classifications between the MCDA and RF techniques, providing a comprehensive understanding of the spatial distribution of coastal vulnerability. The shores of the north-western region of Estonia show very low vulnerability, the north-east regions exhibit low vulnerability. Moderate vulnerability is characteristic in Tallinn Bay, some parts of Pärnu Bay, and the western islands. High and very high vulnerability levels are present to the south of Pärnu Bay and on some shores of the western islands.

The use of machine learning techniques, especially the RF approach, offers significant benefits for handling large datasets and identifying critical parameters through data-driven algorithms. However, the RF technique lacks the capability to incorporate expert opinions and site-specific knowledge, which are integral to MCDA techniques. The sequence of MCDA methods, such as fuzzy standardisation and logic, AHP, and WLC, provide flexibility in managing uncertainty and offer a detailed representation of vulnerability assessments. In this context it is likely that the integration of machine learning into coastal vulnerability assessment typically enhances the reliability of the outcomes compared to traditional methods.
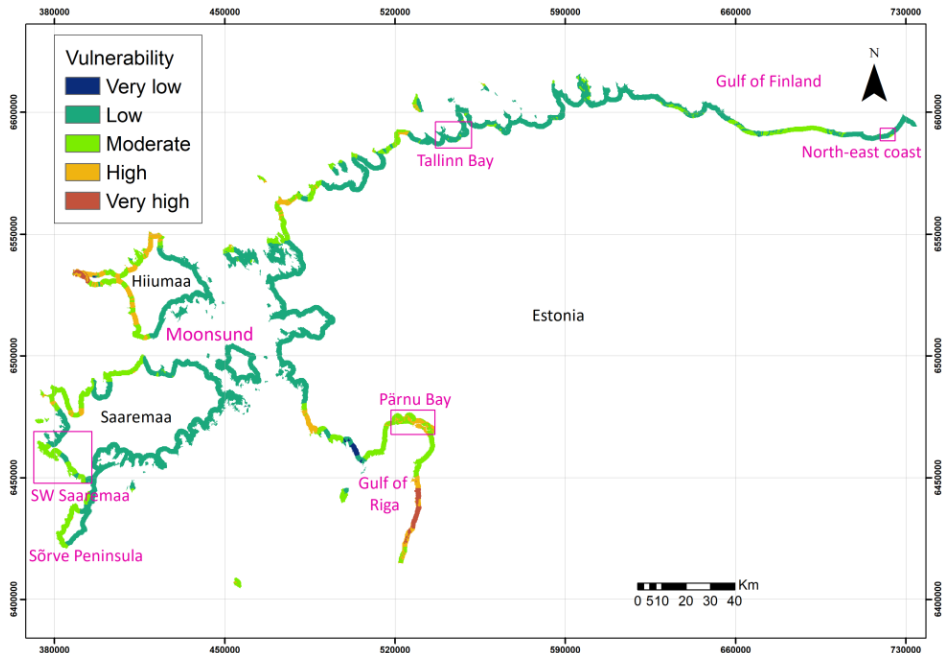

Figure 31. Coastal vulnerability analysis based on the Random Forest technique. From Paper IV.

For this study, the ROC curve was generated to assess the coastal vulnerability analysis validation using RF technique, and the results are illustrated in Figure 32, showing the trade-offs between sensitivity (TPR) and specificity (FPR) across different thresholds used in the analysis. The AUC (Area Under the Curve) for the Random Forest model was 0.94, which indicates that the model has a strong ability to distinguish between vulnerable and non-vulnerable coastal areas. An AUC of 0.94 suggests that the model performs significantly better than random guessing and demonstrates high accuracy in predicting coastal vulnerability. A model with this AUC value has a 94% chance of correctly ranking a randomly chosen vulnerable area higher than a non-vulnerable one.

The analysis in Paper III and Paper IV introduces a novel quasi-two-dimensional approach by examining a 2 km wide inland zone from the shoreline (0 m contour that represents the approximate long-term mean sea level), which facilitates the mapping of two-dimensional parameters. While both MCDA and RF methods have their strengths, challenges persist in integrating one-dimensional variables such as extreme water levels, shoreline change, coastal setback, etc., which naturally exist as line variables along the shoreline (Paper III, Chapter 3). Machine learning techniques like Random Forest can identify key parameters without explicitly modelling complex relationships. These algorithms automatically recognise patterns and correlations, which enable them to extract crucial parameters contributing to coastal vulnerability without relying on detailed prior knowledge or assumptions about the underlying relationships. This enhances the comprehensiveness and accuracy of a coastal vulnerability assessment. It is recommended that both techniques be applied in complex coastal environments to generate detailed vulnerability maps and support informed decision-making for sustainable coastal planning and management.
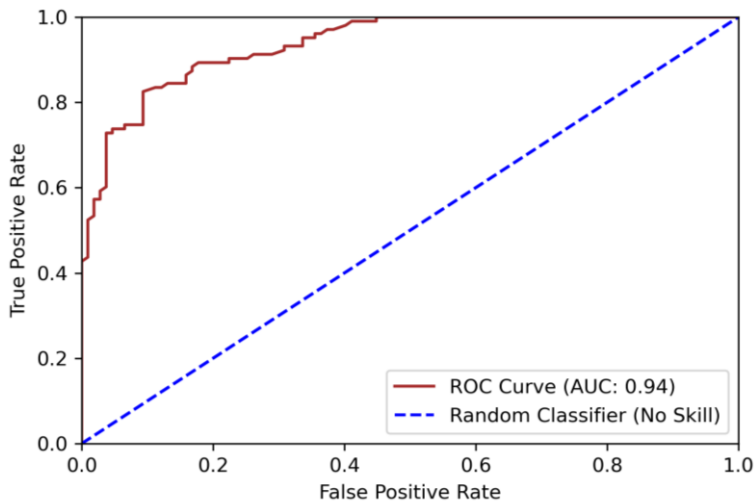

Figure 32. Receiver operating characteristic (ROC) curve for the coastal vulnerability analysis validation using the random forest algorithm. From Paper IV.

4.2 Incorporating water level variations into coastal vulnerability indexes in a microtidal sea

The geologically young and rapidly evolving shores of the Baltic Sea pose a major coastal management challenge due to spatial variability in climate change effects on coastal processes (Eelsalu et al., 2024; Soomere, 2024). This variability is largely driven by extremely intermittent wave impacts (Soomere and Eelsalu, 2014), loss of sea ice (Orviku et al., 2003; Ryabchuk et al., 2011), and probably most importantly by the dynamics of water level during severe wave storms (Weisse et al., 2021). Early efforts to quantify coastal vulnerability (Gornitz et al., 1991) included two parameters to describe water level variations: relative sea level change and tidal range. These parameters are inappropriate to describe alongshore variations in the vulnerability in the Baltic Sea. As described above, tidal range is only a few centimetres in this microtidal sea and relative sea level varies very slowly along the shore even on a country scale (Leppäranta and Myrberg, 2009).

The above has shown that implementation and interpretation of alongshore variations of different vulnerability parameters can be challenging. For instance, areas with large tidal ranges may be resilient to water level variations, whereas areas with smaller variations but mobile sediments might be more susceptible. Using traditional indicators can lead to contentious results, as seen in the vulnerability of the entire coastline of Estonia based on modelled extreme water level, shoreline change and geomorphology (Figure 33). Several shore segments that are considered vulnerable (such as Saaremaa) are protected by numerous rocks and/or resilient vegetation.
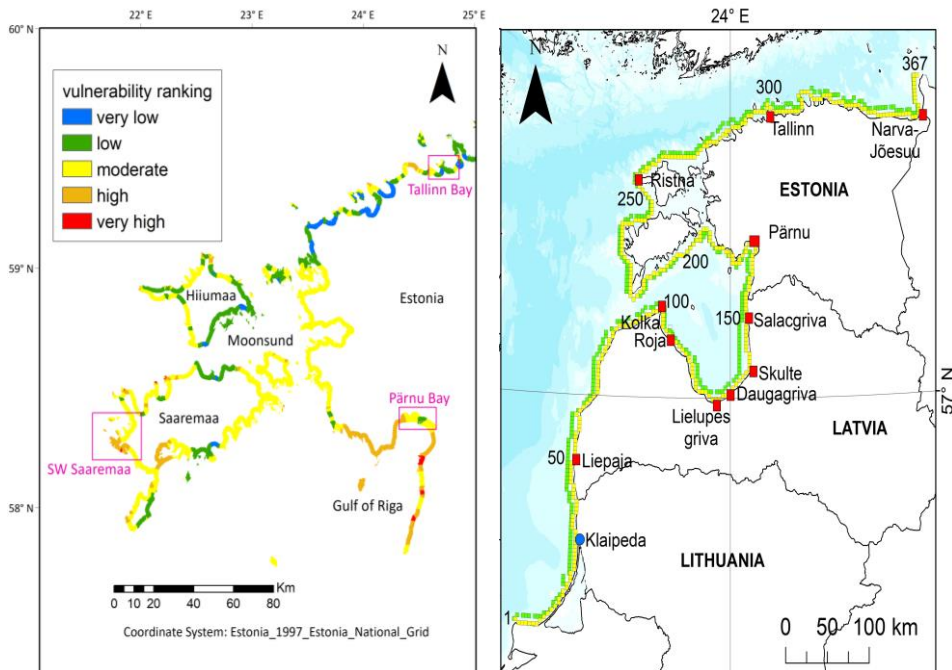

Figure 33. Left: Coastal vulnerability map of Estonia based on three most important parameters: extreme water level, shoreline change and geomorphology. See details in Chapter 3 and Paper III. Right: Circulation model calculation points for data. The blue box shows the area of evaluation of the CVI index in Figures 35 and 36. From Paper V.

However, moderate to low vulnerabilities can also be found in highly sensitive bayheads and beaches, such as the interior of Pärnu Bay (Section 3.3).

This situation motivates the search for parameters or variables that describe more comprehensibly the contribution of spatially varying (extreme) water levels into coastal vulnerability index. Recently several candidates for this purpose have emerged. Projections of extreme water levels with a 50-year return period are used in Paper III and Chapter 3 above. In many applications water levels with shorter return periods provide additional information for planning. All parameters of this kind represent past events. The scale parameter of the exponential distribution of local storm surges (Soomere et al., 2015) has a certain predictive power because the properties of storms vary slowly. The rate of increase in typical annual water level extremes (Soomere and Pindsoo, 2016; Pindsoo and Soomere, 2020) greatly varies along the eastern Baltic Sea shore. Finally, alongshore variations of the shape parameter of the generalised extreme value distribution along the eastern Baltic Sea (Viigand et al., 2024b) provide a proxy for estimates of the potential rate of increase of severity of extreme events.

The purpose of this Section is to present results of a pilot study (Paper V) of the potential uses of several parameters that characterise water level variations over a relatively short length of coast in estimating coastal vulnerability. More specifically, Paper V analyses how integration of various projections of extremely high and low water levels with different return periods affects the values of the classic CVI index.

4.2.1 Adapted coastal vulnerability index (CVI)

Paper V provides detailed analysis of the potential of inclusion information about extremely high and low water levels into the existing Coastal Vulnerability Index (CVI) framework to assess the susceptibility of the Lithuanian coast on the eastern shore of the microtidal Baltic Sea. The idea was to include, one by one, several variables that carry this information into the analysis performed by Bagdanavičiūtė et al. (2015, 2019). These works modify the approach originally developed by Gornitz et al. (1994) to reflect the unique characteristics of the study area. Specifically, the following factors were used to evaluate the CVI values: historical shoreline change rate, beach width, beach height, beach sediment type, underwater slope, number of sand bars, and significant wave height.

Data for these variables were gridded into 500 m long sections along the coastline of Lithuania and analysed using ArcGIS, as detailed in Bagdanavičiūtė et al. (2019). Each variable was assigned a vulnerability score ranging from 1 (very low) to 5 (very high). To ensure compatibility with earlier results, the study in Paper V used exactly the same procedures and dataset as Bagdanavičiūtė et al. (2019) and only adjusted the weights of individual parameters. Different from the analysis in all other parts of this thesis, the AHP and WLC techniques were not implemented and all criteria were considered to have an equal impact on coastal vulnerability. In other words, the CVI was calculated using the arithmetic mean of the scores. Similar to the above, the ranges of vulnerability for each parameter and the resulting CVI values were categorised into five equal classes, from very low to very high vulnerability.

4.2.2 Projections of extremely high and low water levels

The classic parameters such as projections of extreme water levels with 10 yr and 50 yr return periods were used to analyse the modifications of estimated vulnerability of coastal sectors of Lithuania. Unusually low water levels add vulnerability, e.g., in terms of safety of shipping in shallow waterways (Parker and Huff, 1998). The projections are based on two sets of modelled sea level time series for the Baltic Sea with a resolution of 2×2 nautical miles (Figure 33): the Rossby Centre Ocean (RCO) model data from 1961 to 2005 (Meier et al., 2003), which accurately replicates water levels in the eastern Baltic Sea (Soomere et al., 2015), and the RCA4-NEMO model data from 1961 to 2009 (Hordoir et al., 2013), which follows average and lower water levels closely (Viigand et al., 2024a). Projections for extreme sea levels at various return periods were made using an ensemble of reconstructions of parameters of extreme value distributions based on the block maxima method (Soomere et al., 2018; Viigand et al., 2024a). The projected sea level extremes significantly vary along the coasts of Lithuania, Latvia, and Estonia (Figure 34, Paper V). For example, the projected 50-year return period extreme sea level ranges from about 1.2 m in southern Lithuania to over 2 m in Pärnu Bay (Viigand et al., 2024a). Alongshore variations of projections of extremely low sea levels mirror those of extreme highs but with less pronounced spatial variation. Both extreme high and low sea levels exhibit about ±10% variation from their average values along the Lithuanian shore. This level of variations is expected to noticeably impact the CVI values.
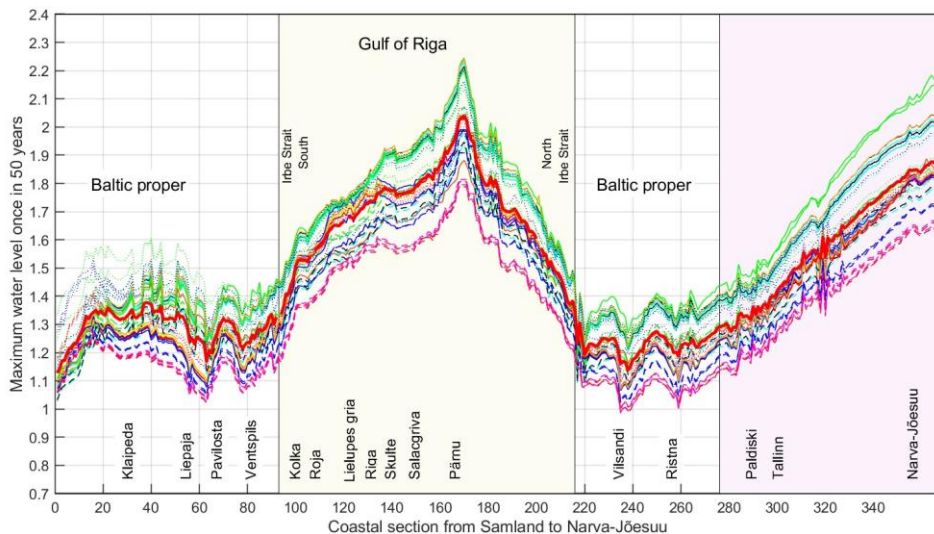
Figure 34. Projections of maximum sea levels for 50 yr return period along the coasts of Estonia, Latvia, and Lithuania. The bold red line represents the ensemble average used in Paper V. Graphics by Katri Viigand. For more details, see Viigand et al. (2024a). From Paper V.

4.2.3 Sea level maxima and minima once in 10 years

The analysis in Paper V reveals that contribution of sea level maxima with a 10-year return period to the CVI exhibits notable contrasts compared to the other seven constituents (Figure 35, Paper V). This parameter shows a distinct maximum for the northern Lithuanian shoreline, a minimum from Palanga to Klaipėda and for the northern Curonian Spit, and slightly above-average values for the southern Curonian

Spit. While its alongshore variation somewhat parallels other parameters, it apparently provides unique information. In contrast, the sea level minima with a 10-year return period provide different information, showing minimal vulnerability in the north where absolute values are smaller, and highest values in the south.

The impact of both parameters on the CVI is similar. Their inclusion results in minor changes to the minimum CVI value, increasing it from 1.71 to 1.75 for maxima and to 1.88 for minima (Table 1 of Paper V). The maximum CVI values change from 4.57 to 4.125 for maxima and to 4.25 for minima. The range of CVI values in different CVI estimates varied insignificantly, usually less than 10% compared to this range in the original work. Only if all four parameters were included, the range narrowed by about 20% (Table 1 in Paper V). Incorporating sea level maxima slightly increases CVI values in the north, while sea level minima do the same in the south. This indicates that both parameters provide different but equally important information for a reliable CVI. The patterns and magnitudes of spatial variations in extremely high and low sea levels once in 50 years follow those of the 10-year sea levels, suggesting similar contributions to the CVI. However, these variations are not identical.
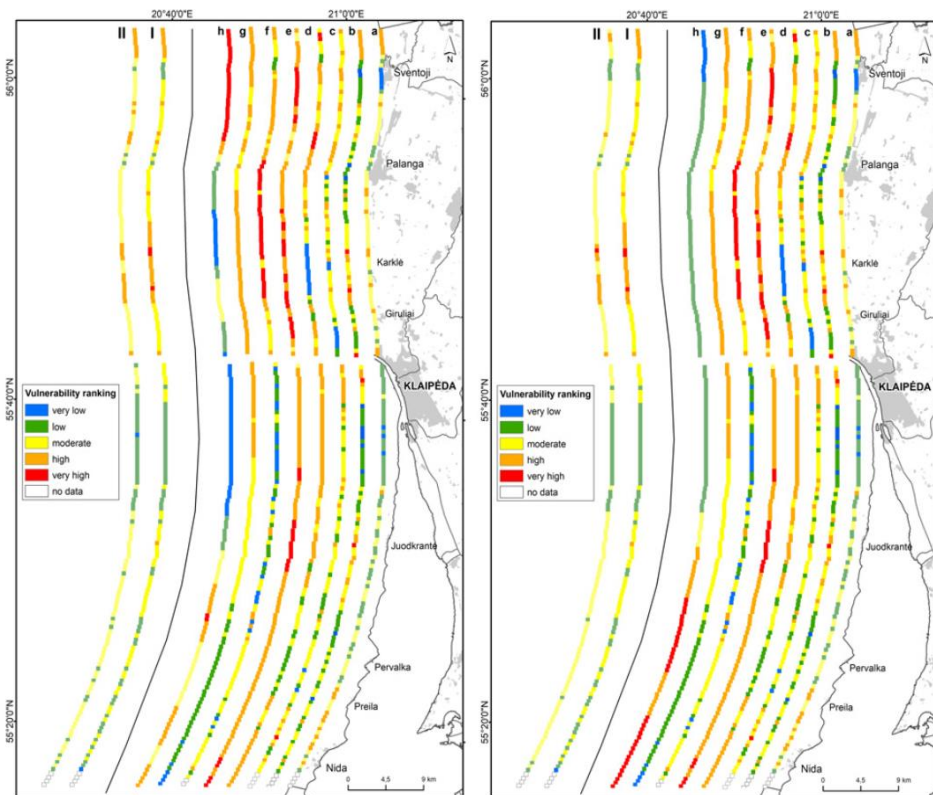
Figure 35. Relative coastal vulnerability evaluated based on: (a) historical shoreline change, (b) beach width, (c) beach height, (d) beach sediments, (e) underwater slope, (f) sandbars, (g) significant wave height, and (I) the Coastal Vulnerability Index (CVI) calculated from these factors using equal weights and an equal-interval classification from Bagdanavičiūtė et al. (2019). In panel (II), the CVI calculation includes the additional factor of (h) sea level extremes, specifically showing sea level maxima on the left and minima on the right, based on a 10-year return period. Note that the CVI in line (I) remains consistent for both panels.

All parameters agree that the central part of the study area, about 15 km north and south of Klaipėda, has low vulnerability to both high and low sea levels (Figure 36, Paper V). They also concur that the southernmost part is more vulnerable to sea level variations. Interestingly, the shore is less vulnerable to sea level extremes occurring once in 50 years compared to those occurring once in 10 years.

The four sea level variation parameters show disagreement in the northern part of the study area, which is highly vulnerable to sea level maxima but has very low vulnerability to sea level minima. Integrating each parameter and all considered parameters into the CVI using equal weights does not drastically change the alongshore variation of the CVI values but adds some nuances (Figure 36, Paper V). The length of segments with high and very high vulnerability decreases by 3–10%, while segments with moderate vulnerability increase by 9–21% (Figure 37).

Therefore, in Paper V, initial steps were taken to systematically include water level variations in estimating coastal vulnerability in microtidal water bodies using modelled
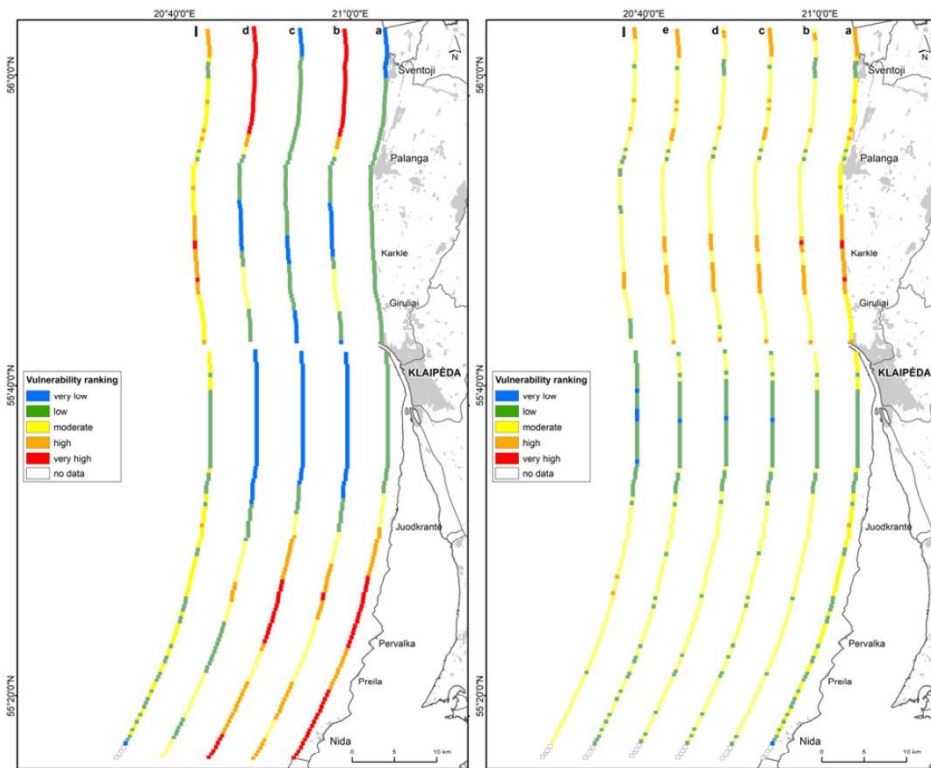
Figure 36. Left: Relative coastal vulnerability for (a) minimum sea level with a 10-year return period, (b) maximum sea level with a 10-year return period, (c) minimum sea level with a 50-year return period, and (d) maximum sea level with a 50-year return period, compared to (I) the CVI values based on the 7 criteria from Bagdanavičiūtė et al. (2019). Right: Relative coastal vulnerability for (a) the CVI values based on the 7 criteria from Bagdanavičiūtė et al. (2019) with equal weights and equal intervals classification, (b) CVI including minimum sea level with a 10-year return period, (c) CVI including maximum sea level with a 10-year return period, (d) CVI including minimum sea level with a 50-year return period, (e) CVI including maximum sea level with a 50-year return period, and (I) the CVI index based on 11 criteria with equal weights. Graphics by Ingrida Bagdanavičiūtė. From Paper V.
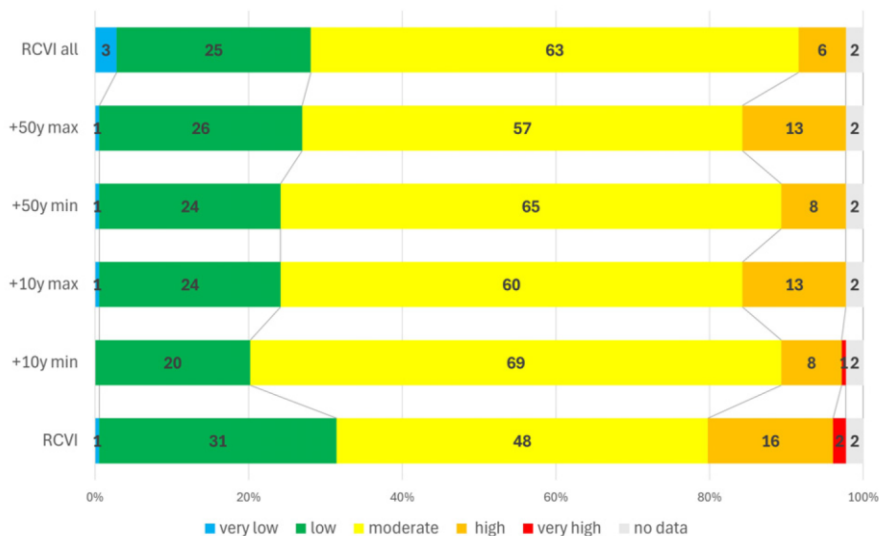
Figure 37. Distribution of CVI classes in coastal sections using different parameters of water level variations. From Paper V.

sea levels. The findings emphasise that extreme sea level projections for different return periods are crucial and stable parameters, complementing traditional geomorphological data. Both sea level minima and maxima provide unique insights, and incorporating these projections into the CVI reduces the range of CVI values due to the more diverse characterisation of vulnerability by different parameters.

In conclusion, it is safe to say that integration of projections of extreme water levels with various return periods provide important information about coastal vulnerability even along fairly featureless (in terms of the development of high and low water levels) coastal segments of Lithuania. This approach highlights the independent information provided by projected extreme sea levels with different return periods. A coastal vulnerability index based on these quantities is discussed in the context of local and regional variations.

4.3 Wind and solar farm site selection in inland area

Even though the described methods and techniques have been implemented in the context of marine and coastal tasks, they are fully usable, and sometimes in a more contrasted and clear manner in inland applications, where the role of interactions of different parameters, cumulative effects and long-range impacts are usually much smaller. To provide such an example that allows for identification of the necessary modifications in the process of preparation of evidence for decision-making, an examination of the methodologies and findings related to wind and solar farm site selection in the inland areas of Isfahan Province, Iran, is presented in this Section, following the analysis in Paper VI. Similar to the core task of Paper III in Chapter 3, the primary objective is to optimise renewable energy site selection using a combination of decision support tools (DSTs), ensuring environmental sustainability and economic viability.

To overcome the intermittency issues associated with relying on a single renewable energy resource, the performed analysis highlights the importance of considering wind

70

and solar energy. In earlier analyses, Díaz-Cuevas et al. (2019) found that weighted linear combination (WLC), analytical hierarchy process (AHP), and geographical information systems (GIS) (see Sections 1.1 and 1.2) are effective tools for ranking potential wind and solar farm sites. Further, Rekik and El Alimi (2023) demonstrated the effectiveness of using WLC, AHP, and GIS in their study on optimal wind and solar farm site selection. Their findings assisted policymakers in planning and implementing renewable energy infrastructure projects to meet national energy goals.

The study in Paper VI goes one step further. Namely, multi-criteria decision analysis (MCDA), including AHP and WLC techniques, is complemented in this analysis with fuzzy standardisation and logic to determine which locations in Isfahan Province, Iran (Figure 38), are most suitable for wind and solar farms. By integrating these techniques, a decision support system (DSS) is provided in Paper VI for identifying potential wind and solar farms, balancing environmental protection needs with socio-economic benefits for the human communities.

There have been numerous studies on renewable energy site selection that have primarily focused on a small number of tools and only one kind of renewable energy, solar or wind energy, for site suitability assessment (Uyan, 2017; Moradi et al., 2020; Xu et al., 2020; Ahadi et al., 2023). For this reason, another purpose of the study in Paper VI is to evaluate and compare several computer-based decision support systems (DSS) and how they can be used together. The background idea is that managers and decision-makers can use this integrated DSS to identify the most suitable inland sites for wind and solar farms.
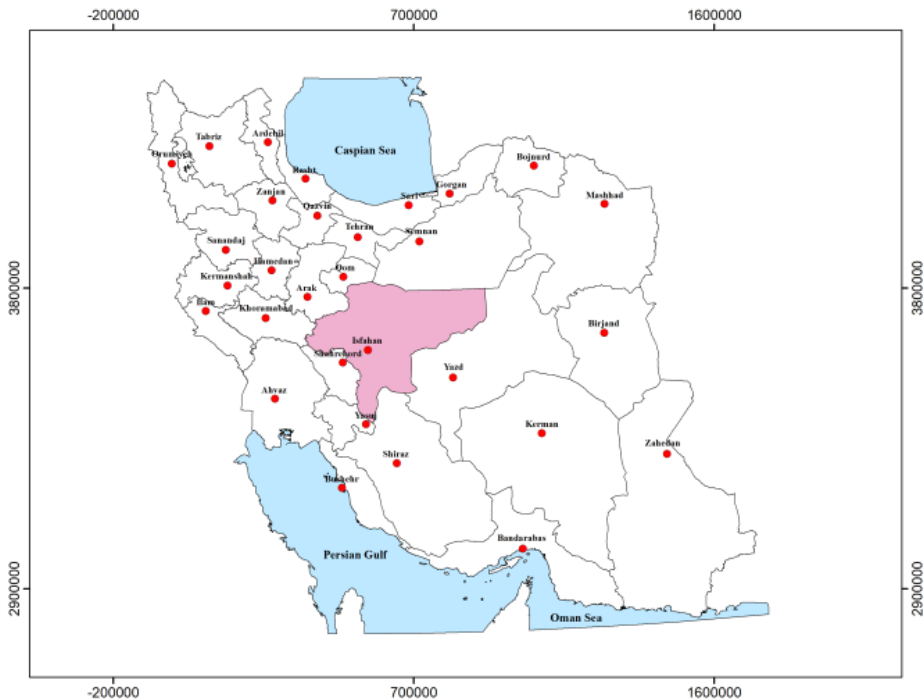

Figure 38. The location of Isfahan Province (in pink), Iran (Isfahan Province Management and Planning Organization, 2018). From Paper VI.

4.3.1 Study area

The Isfahan Province (Figure 38), located in central Iran, covers 107,017 km^2, which is more than two times the area of Estonia and roughly ¼ of the area of the Baltic Sea. Different from the Northern Europe, it has an arid to semi-arid climate. The province has a diverse physiographic region (Figure 39), densely populated cities, and numerous industrial centres, resulting in significant energy demand (Zoghi et al., 2015). During the selection of renewable energy sites, important ecological sites such as Ghomishloo National Park, Gavkhouni Wetland, Mouteh Wildlife Refuge, and Kolah Ghazi National Park must be protected. The high solar radiation and wind speeds in the region present significant potential for renewable energy development (Noorollahi et al., 2016b).

4.3.2 Data acquisition

In the initial phases of this study (Figure 3 in Paper VI), the most important parameters for evaluating wind and solar farm sites were determined. To do so, an extensive review of the literature along with regulations and standards relevant to renewable energy spatial planning was conducted first (Barzehkar et al., 2016; Yushchenko et al., 2018). It is crucial to select sites for solar and wind energy farms that have a high concentration of solar radiation and high wind speeds. The World Bank Group and Solargis (2019) provided long-term solar irradiance data, and the Iran Energy Efficiency Organization (2018) provided wind speed data, which was normalised to average annual wind speeds at 80 m above ground level. The evaluation of potential sites also considered slope, flood probability, distance from faults, soil texture, geological formations, and proximity to rivers (Table 1 in Paper VI). Similar to the analysis in
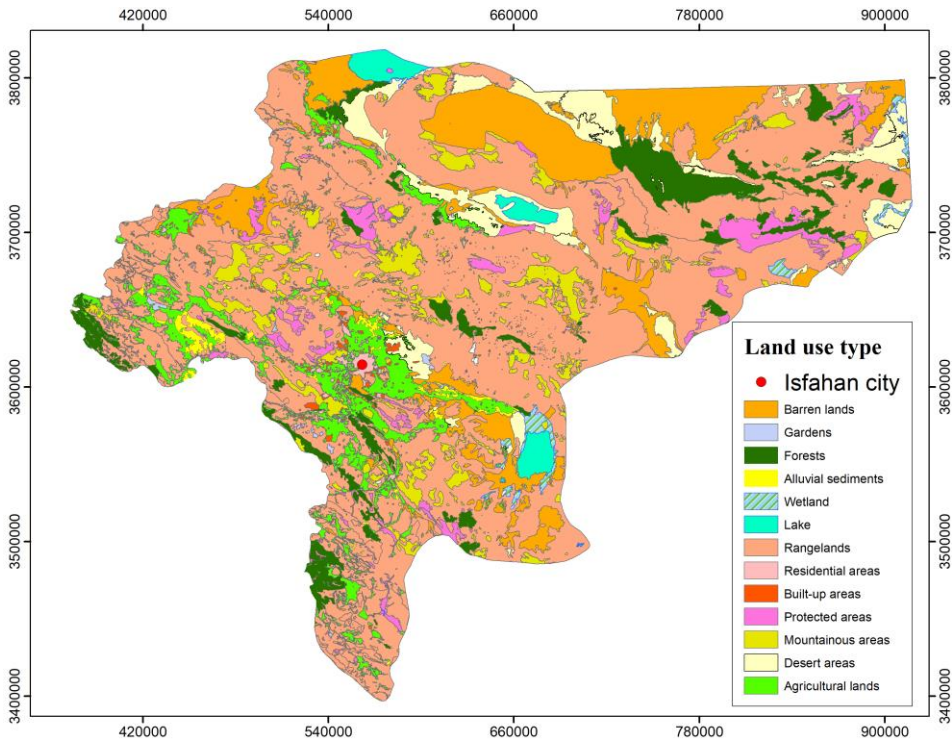

Figure 39. The land use map of Isfahan Province, Iran (Isfahan Province Management and Planning Organization, 2018). From Paper VI.

Section 2.5, the potential locations excluded areas with high biodiversity value, such as nature protection areas. Our analysis also included socioeconomic parameters such as proximity to power transmission lines, population centres, and land use/cover.

4.3.3 Steps of analysis

The parameters were first retrieved and quantified into raster layers on the extent of Isfahan province using ArcGIS 10.7 based on UTM Zone 39N coordinate system. The analysis in Paper VI starts from normalising raster layers. As explained in Section 1.2.1, it is necessary to standardise the numerical values characterising the factors before they can be combined because they are measured at different scales (Eastman, 2009). Piecewise linear fuzzy membership functions expressed by Eq. (1) and Eq. (2) were used to normalise raster layers on a scale from 0 to 1 and to convert increasing and decreasing functions into a united framework (Section 1.2.1). The 12 parameters employed in the analysis include slope (threshold values for fuzzy logic standardisation $R_{\min} = 3\%$ and $R_{\max} = 5\%$, decreasing function), solar radiation (1500 and 2000 KWh/m^2/year, increasing), wind speed (6 m/s and 7 m/s, increasing), distance from rivers (0.5 km and 1 km, increasing), flooding (0 for areas within the flood plain, 1 for areas outside the flood plain), distance from fault lines (0.5 km and 1 km, increasing), soil texture (0 for sandy, 1 for clay and silt clay textures), geological formations (0 unconsolidated deposits, 1 for igneous, metamorphic, and sedimentary rocks), distance from wetland and protected areas (0.5 km and 1 km, increasing), distance from population centres (0.5 km and 2 km, increasing), distance from roads (0.5 km and 2 km, decreasing), distance from transmission lines (0.5 km and 1 km, decreasing), and land use (0 for forests, water bodies, and wetlands, 1 for barren lands and areas with very low plant density) (Table 2 in Paper VI). These parameters are all measured in two-dimensional (2D) formats in inland areas of Isfahan Province.

The following step involved the application of the analytical hierarchy process (AHP) (Section 1.2.2). As common in applications of this technique, the significance of different parameters in wind and solar farm site selection is assessed by expert judgment. Different from marine and coastal applications where experts limited their estimates to minimum 1 and maximum 5 (Paper II, Paper III), most experts engaged into the study in Paper VI used the full scale from 1 to 9 proposed by (Saaty and Tran, 2007) (Table 3 in Paper VI). A pairwise comparison matrix was developed with input from twenty experts from Iran's Energy Efficiency Organization and the Iranian Department of Environment. Their opinions were complemented by five experts from academic institutions who are experienced in environmental planning and environmental impact assessment in the energy sector. The geometric mean of expert values assigned to each parameter for a pairwise comparison was calculated as explained in Section 1.2.2 and Papers I and II to determine its "priority" (Mu and Pereyra-Rojas, 2018). The relative weights (importance) of each parameter were evaluated using the Super Decisions software. The value of the Random Index for $N = 12$ is $RI = 1.535$ (Aguarón and Moreno-Jiménez, 2003). As the consistency ratio $CR = 0.09 < 0.1$, the comparisons are consistent (Saaty and Tran, 2007).

In the final step, raster maps were combined in GIS to create a map of the suitability of a site. In the GIS environment, weighted linear combination (WLC) is used to combine raster maps using map algebra technique following (Malczewski and Rinner, 2015) (Section 1.2.3).

4.3.4 Wind and solar farm site suitability

Based on the experts' perspectives (Figure 40), wind speed, solar radiation, and distance from power transmission lines were the most significant parameters for determining wind and solar farm site suitability in Isfahan Province. The distance from fault lines, soil texture, and geological formations were considered the least important parameters for site suitability analysis (Figure 40). Therefore, different from marine applications, experts prioritised energy generation parameters over distance-based parameters to protect the environment.
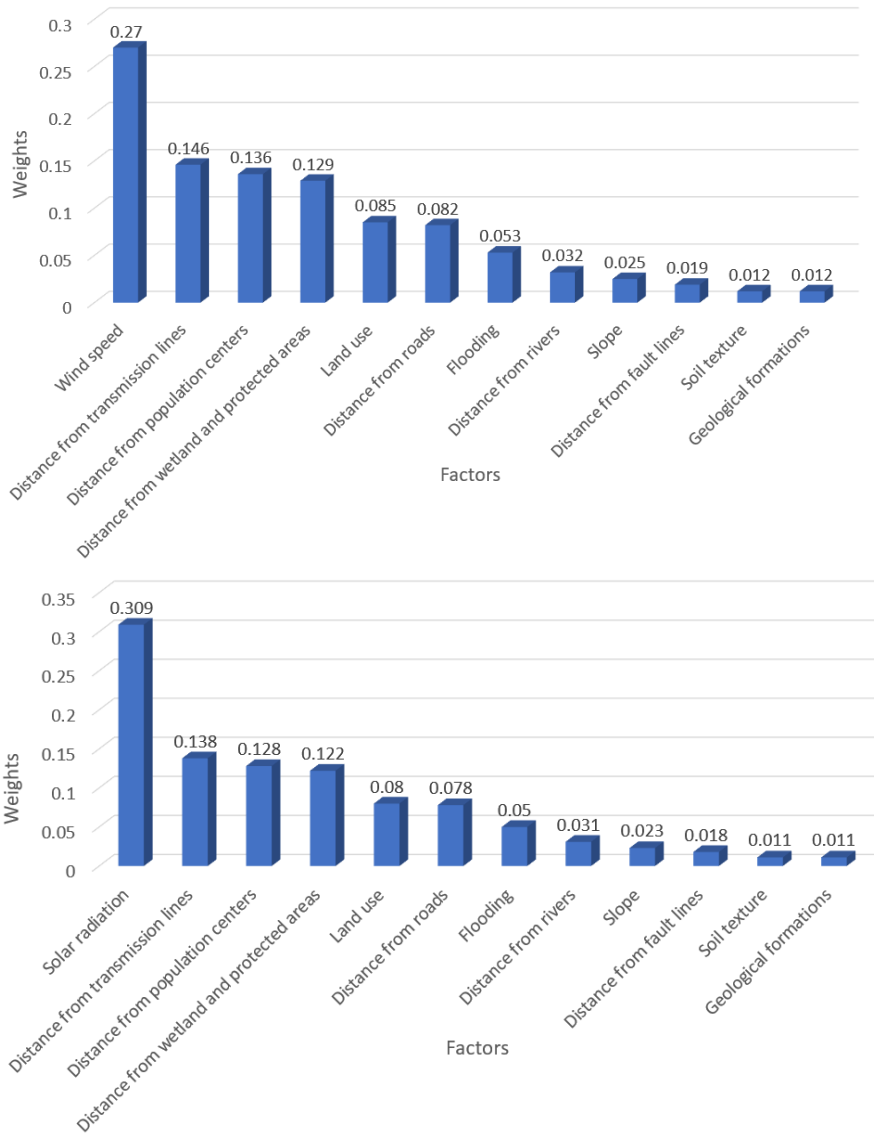

Figure 40. Relative weights assigned to parameters in wind farm site selection (above) and solar farm site selection (below) using the AHP method. From Paper VI.

The analysis demonstrated that 18% of the province is (highly) suitable for wind energy production whereas 26% is suitable for solar energy production (Table 5). The high suitability areas are characterised by low flooding probability, low permeable soil like clay, and large distances from wetlands, protected areas, fault lines, and rivers. The potential locations are also near cities, roads, and transmission lines, ensuring socioeconomic benefits to the community. Sites suitable for wind farms should have winds speeds of 6–7 m/s, while sites suitable for solar farms should have diffuse horizontal irradiance (DHI) of 1500–2000 KWh/m^2.

Table 5. Wind and solar farm site suitability analysis using GIS-MCDA.

Class of suitability	Wind farms		Solar farms	
	Area (km^2)	Percentage of area (%)	Area (km^2)	Percentage of area (%)
Very Low	15771	15	7656	7
Low	31494	29	26813	25
Moderate	40959	38	44929	42
High	18793	18	27619	26
Total	107017	100	107017	100

As shown in Figure 41, a higher suitability for wind farms is identified in the north and east of the province. These regions are associated with higher wind speeds. Likewise, the northern and eastern regions are better suited for solar energy (Figure 42) due to fewer cloudy days.

In conclusion, the study in Paper VI, additionally to the classic steps of MCDA, such as AHP and WLC, also used fuzzy logic to standardise raster maps on a scale from 0 to 1. On the one hand, by standardising pixel values in each raster layer, fuzzy logic reduces
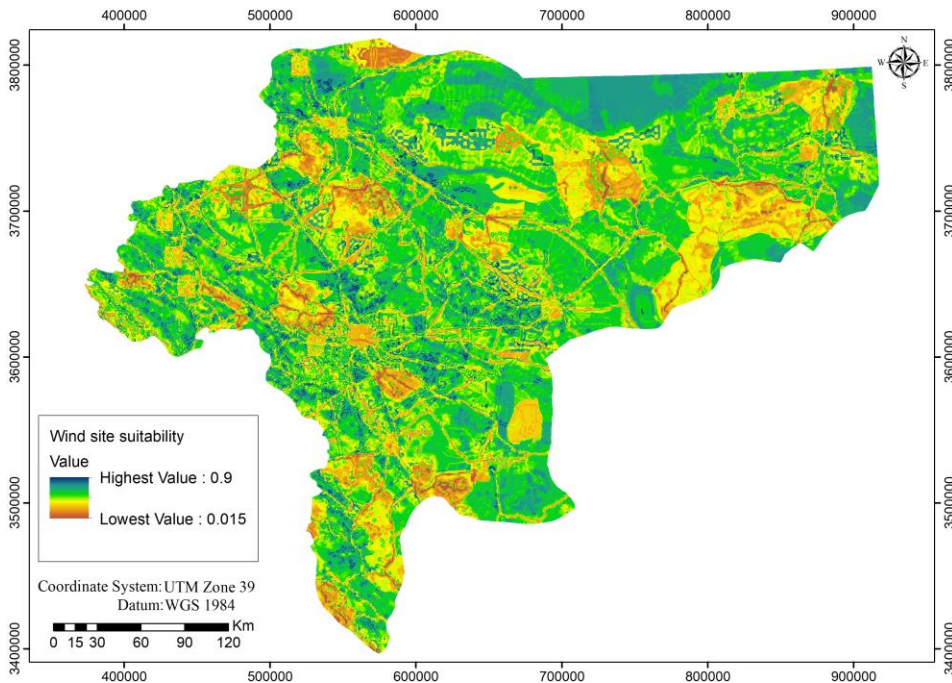
Figure 41. Wind farm site suitability map. From Paper VI.

uncertainty in site selection and thus eventually provides decision-makers and planners with better-informed options for site selection. On the other hand, the combination of fuzzy logic with AHP, WLC, and GIS offers a flexible approach to analyse land suitability for wind or solar energy development.

The results indicate that optimising the locations of wind and solar farms using a combination of GIS-MCDA techniques provides better outputs for environmental planning and sustainable development. This conjecture is built on a broad range of environmental and socioeconomic parameters that are considered in the study to ensure that renewable energy development aligns with environmental conservation and community energy needs. An important implication is that different areas of the province support better different renewable energy production. An implicit conjecture is that due to the variable climate conditions in Isfahan, neither wind nor solar energy alone could meet the energy needs. A hybrid approach is therefore required.

Figure 42. Solar farm site suitability map. From Paper VI.

Conclusions

Summary of the results

The studies presented in this thesis explore the development and application of decision support systems (DSSs) for offshore wind farm site selection, coastal vulnerability assessment, and inland renewable energy site selection, offering significant insights into the integration and effectiveness of various methodologies.

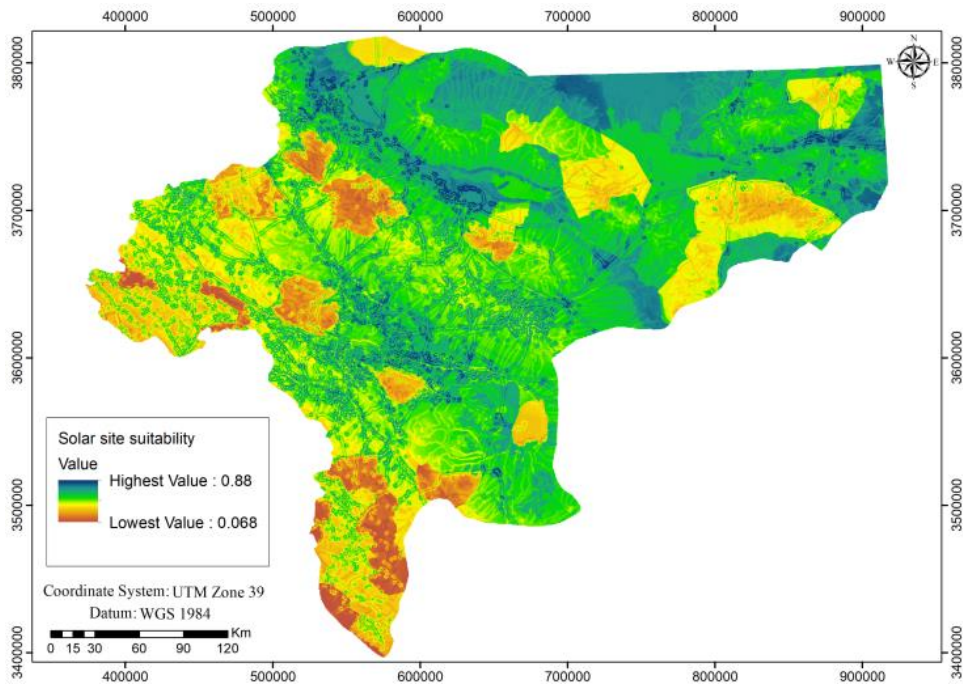A comprehensive overview of developments towards reliable integrated decision support systems for coastal planning and management is presented (Paper I). Such a system should be developed by combining various decision support tools such as GIS, multi-criteria decision analysis (MCDA), artificial neural networks (ANN), Google Earth Engine (GEE), and/or Bayesian networks. The integration of GIS and MCDA, especially with fuzzy standardisation and logic, Analytical Hierarchy Process (AHP), and weighted linear combination (WLC), was highlighted as being effective in creating robust DSS frameworks. The inclusion of ANN methods generally enhances the robustness of the DSS in terms of sensitivity and error analysis. Various environmental management challenges were addressed through the combination of these tools, including risk and hazard classification, site selection, land-use zoning, and resilience classification. Bayesian networks are effective at predicting environmental changes, but they are computationally complex and require high expertise.

The lessons from this analysis were implemented for the analysis of several challenges in the Baltic Sea region. A detailed consideration of site selection for offshore wind farms in the Baltic Sea (Paper II) highlighted the most suitable locations of wind power plants for grid electricity production in terms of the levelised cost of energy (LCOE) values. The analysis includes parameters such as wind speed, sediment on seabed, water depth, pipelines, shipping routes, military areas, and nature protection zones. The Danish waters are identified as most suitable locations due to the high wind speeds, large capacity factors, and shallow water depths. The GIS-MCDA analysis, incorporating AHP, fuzzy logic, and WLC techniques, supported these findings, emphasizing the suitability of nearshore areas with high wind speeds. The application of the technique for order of preference by similarity to ideal solution (TOPSIS) to rank the identified most suitable areas provided extra confidence in site suitability assessments. This integrated decision support framework contributes to the reduction of uncertainty of analysis, taking into consideration the standards of Danish Energy Agency DEA and European Maritime Spatial Planning platforms guidelines and expert knowledge.

The assessment of coastal vulnerability in Estonia using the Coastal Vulnerability Index (CVI) (Paper III) revealed a range of CVI values from 0.24 (very low vulnerability) to 0.72 (very high vulnerability), covering almost half of the possible range from 0 to 1. Segments with low or moderate vulnerability were identified along the northern coast with stable limestone cliffs and the West Estonian Archipelago with gradual land uplift. High vulnerability areas were mostly low-lying regions experiencing extreme water levels, erosion, and the presence of infrastructure near the coast, such as the western shore of Saaremaa and Pärnu Bay. The influence of the three most important parameters (extreme water level, shoreline change, and geomorphology) resulted in a CVI range of 0.64, highlighting more high-vulnerability locations than using 16 parameters for coastal vulnerability assessment. Extending the vulnerability assessment up to 2 km inland revealed that most inland areas had generally lower vulnerability due to higher elevation, with exceptions in low-lying river valleys and coastal lagoons. The study

emphasised the need for careful consideration of parameter selection and prioritisation of parameters in vulnerability assessment and the logical extension of coastal vulnerability analysis into inland areas.

A comparative assessment of coastal vulnerability in the eastern Baltic Sea using MCDA and Random Forest (RF) techniques (Paper IV) demonstrated that these methods produce different outputs. The MCDA framework identified coastal areas mainly with low to moderate vulnerability, while the RF technique classified a larger proportion of areas as having low vulnerability. High vulnerability areas identified by both techniques were primarily located in the Gulf of Riga, including Pärnu Bay. The RF analysis highlighted geomorphology, maximum significant wave height, and shoreline change as the most significant parameters. The MCDA approach provided a flexible method for managing uncertainty and incorporating expert opinions. The integration of machine learning into coastal vulnerability assessment enhances the reliability of outcomes compared to traditional methods by identifying patterns and correlations without requiring detailed prior knowledge or assumptions about the underlying relationships between parameters.

Incorporating sea level maxima and minima with 10-year and 50-year return periods into the CVI estimates (Paper V) provided some useful insights into vulnerability assessment along the Lithuanian shoreline. These parameters showed distinct maxima and minima patterns, contributing significantly to the CVI. The integration of these sea level projections reduced the range of CVI values due to more diverse characterisations of vulnerability by different parameters, emphasising the importance of including both sea level extremes and geomorphological data in coastal vulnerability assessments.

Finally, the thesis explored the similarity and differences of the use of the renewable site selection technologies in marine and inland conditions. For inland renewable energy site selection in Isfahan Province, Iran (Paper VI), experts prioritised wind speed, solar radiation, and distance from power transmission lines for determining site suitability assessment of wind or solar. The study showed that 18% of the province is highly suitable for wind energy production, and 26% is suitable for solar energy production. High suitability areas are characterised by low flooding probability, low permeable soil, and large distances from wetlands, protected areas, fault lines, and rivers. The combination of fuzzy logic with AHP, WLC, and GIS provided a flexible approach for analysing land suitability and optimising the locations for wind and solar farms. The results indicated that a hybrid approach, considering both wind and solar energy, is necessary to meet the energy needs of the province due to its variable climate conditions. Also, this study highlights the adaptability and effectiveness of the decision support tools in varying geographical contexts, reinforcing their applicability beyond coastal and offshore environments.

Overall, the studies highlight the critical role of integrating various decision support tools (DSTs) to improve coastal and renewable energy management. The findings highlight the importance of considering the different word views of experts, as exemplified by the discrepancy in expert priorities of environmental and economic parameters in different regions. European experts tended to emphasise environmental concerns more strongly than energy generation aspects, using only half of the available weighting scale (values from 1 to 5), while experts in Iran prioritised energy generation parameters, using the full weighting scale (values from 1 to 9). This discrepancy highlights the need for adaptable DSS that can accommodate varying priorities across different contexts, ensuring robust and informed decision-making processes.

Main conclusions proposed to defend

1. A comprehensive overview of the recent developments of decision support systems (DSS) demonstrates that integrating environmental and socioeconomic data is effective for coastal planning and management. The integration of GIS with other tools, such as multi-criteria decision analysis (MCDA), artificial neural networks (ANN), Google Earth Engine (GEE) or Bayesian network (BN) tools within the DSS framework enhances decision-making by addressing various environmental management challenges, including risk and hazard classification, site selection, land-use zoning, and resilience.

2. The analyses undertaken show that the combination of GIS and MCDA, especially when GIS is integrated with fuzzy logic, Analytical Hierarchy Process, and weighted linear combination, creates robust DSS frameworks that can handle large datasets. ANN methods improve sensitivity and error analysis, along with validation of the results. Bayesian networks are effective for predicting environmental changes, but require high expertise and are less community-friendly compared to more accessible tools like GIS and MCDA. The central conjecture is that integrated DSS is highly likely to provide better and effective outcomes for different environmental management challenges.

3. For offshore wind farm site selection in the Baltic Sea, parameters such as wind speed, capacity factor, water depth, and distance from nature protection areas are critical. The levelised cost of energy (LCOE) and the GIS-MCDA techniques treat these parameters differently. The LCOE values of 42–58 €/MWh cover 33% of the total sea area. The lowest LCOE values are generally near Danish shores. The Gulf of Bothnia, offshore areas of the Baltic proper far from Polish and German shores, and the central Gulf of Riga waters have higher LCOE values. The northern Baltic Sea is less suitable for wind farms due to a lower capacity factor.

4. The Coastal Vulnerability Index (CVI) significantly varies along the Estonian shores. High vulnerability areas are primarily located in low-lying regions exposed to very high water levels and coastal erosion. Extending the vulnerability assessment up to 2 km inland based on two-dimensional parameters for the entire Estonian coast highlighted the importance of considering land elevation, coastal infrastructure, population density, etc.

5. The multi-criteria decision analysis and Random Forest (RF) techniques provide different distributions of vulnerability of Estonian shores. The RF technique classified a larger proportion of areas than MCDA as having low vulnerability. The high vulnerability areas identified by RF are mainly located in the Gulf of Riga, including parts of Pärnu Bay.

6. Inclusion of sea level maxima and minima with different return periods in the CVI calculations contributes significantly to the vulnerability estimates for the Lithuanian shores. The information about extreme water level minima is an important constituent of CVI estimates.

7. For inland renewable energy site selection in Isfahan Province, experts prioritised wind speed, solar radiation, and proximity to power transmission lines. The integration of fuzzy logic with AHP, WLC, and GIS provided a flexible and reliable method for analysing land suitability and optimising renewable energy site selection.

8. The discrepancy in expert prioritisation of environmental and economic parameters between different regions and inland and marine environments highlights the need for adaptable DSS that can accommodate varying priorities. European experts emphasised environmental concerns strongly, while experts in Iran prioritised energy generation parameters.

Recommendations for future work

Several results presented in this thesis demonstrate the need to further enhance the effectiveness and applicability of decision support systems (DSS) for coastal and environmental management. While the current DSS frameworks effectively integrate environmental and socioeconomic data, incorporating more advanced analytical methods such as deep learning and other machine learning techniques, can improve their accuracy and predictive capabilities. These advancements can provide more dynamic and responsive decision-making capabilities, essential for managing complex coastal environments.

The methods of integration of diverse data sources into DSS frameworks should be expanded. Incorporating real-time data will eventually provide a more comprehensive and up-to-date dataset on many occasions, thus enhancing the effectiveness of coastal management strategies. This will promote accurate predictions and assessments. Another direction of future work should focus on refining the selection and weighting of parameters using more advanced approaches than AHP within DSS frameworks. A clear issue for further consideration is the use of only part of the scale in experts' opinions, particularly in marine applications and the ambiguity of interpretation of the contribution to vulnerability provided by different hydrometeorological phenomena. Developing reliable methods for obtaining, weighting and normalising expert opinions and incorporating stakeholder feedback will ensure that the most relevant and impactful parameters in coastal decision-making process are included.

Long-term monitoring programs are essential for validating the effectiveness of DSS frameworks in real-world applications. By tracking the outcomes of decisions made using DSS tools and comparing them with predicted outcomes, experts can identify areas for improvement and ensure that DSS tools remain accurate and reliable over time. Moreover, incorporating climate change projections into DSS frameworks will be crucial for adapting to long-term environmental changes and to ensure sustainable coastal planning and management.

Future studies on onshore and offshore renewable energy site selection should use the capabilities of machine learning approaches to improve site suitability assessment. Unlike traditional MCDA methods, which rely on predefined criteria and subjective weighting of experts, machine learning can analyse large datasets to specify patterns and correlations, providing a more adaptive and data-driven approach. Compared to LCOE, which focuses mainly on economic factors, machine learning can simultaneously consider environmental, technical, and economic parameters, contributing to a comprehensive and balanced site selection outcome.

For inland renewable energy site selection and similar problems in other fields of economy and environment, future studies should investigate the potential of hybrid solutions that combine multiple renewable energy sources, such as wind, solar, biomass, and geothermal. This approach can ensure a reliable and resilient energy supply, particularly in regions with diverse climatic conditions.

It would be helpful if the user-friendliness of DSS tools by developing more intuitive visualisation tools and interactive platforms, such as WebGIS, could be improved. This will increase their accessibility and usability among a wider range of stakeholders, including non-experts. Interactive maps for future assessments will allow stakeholders to engage with the data dynamically, improving the effectiveness of communication and decision-making processes.

It is important to encourage cross-disciplinary collaboration among scientists, engineers, policymakers, and stakeholders for the development and application of DSS frameworks. Such collaboration ensures that diverse perspectives and expertise are incorporated into the decision-making process.

Finally, public awareness and education about the capabilities and benefits of DSS tools should be increased. That can be achieved by implementing educational programs, workshops, and materials, which will assist stakeholders to better understand how DSS tools can support sustainable coastal management. This increased awareness and understanding will promote the wider application and effectiveness of DSS tools in various environmental situations.

List of figures

List of tables

References

Adger, W.N., Hughes, T.P., Folke, C., Carpenter, S.R., Rockström, J. 2005. Social-ecological resilience to coastal disasters. Science, 309(5737), 1036–1039, doi: 10.1126/science.1112122.

Adger, W.N. 2006. Vulnerability. Global Environmental Change, 16(3), 268–281, doi: 10.1016/j.gloenvcha.2006.02.006.

Adem Esmail, B., Geneletti, D. 2018. Multi-criteria decision analysis for nature conservation: A review of 20 years of applications. Methods in Ecology and Evolution, 9, 42–53, doi: 10.1111/2041-210X.12899.

Aghaloo, K., Ali, T., Chiu, Y.R., Sharifi, A. 2023. Optimal site selection for the solar-wind hybrid renewable energy systems in Bangladesh using an integrated GIS-based BWM-fuzzy logic method. Energy Conversion and Management, 283, 116899, doi: 10.1016/j.enconman.2023.116899.

Aguarón, J., Moreno-Jiménez, J.M. 2003. The geometric consistency index: Approximated thresholds. European Journal of Operational Research, 147(1), 137–145, doi: 10.1016/S0377-2217(02)00255-2.

Ahadi, P., Fakhrabadi, F., Pourshaghaghy, A., Kowsary, F. 2023. Optimal site selection for a solar power plant in Iran via the Analytic Hierarchy Process (AHP). Renewable Energy, 215, 118944, doi: 10.1016/j.renene.2023.118944.

Ahmadlou, M., Al-Fugara, A., Al-Shabeeb, A.R., Arora, A., Al-Adamat, R., Pham, Q.B., Al-Ansari, N., Linh, N.T.T., Sajedi, H. 2020. Flood susceptibility mapping and assessment using a novel deep learning model combining multilayer perceptron and autoencoder neural networks. Journal of Flood Risk Management, 14, 1–22. doi: 10.1111/jfr3.12683.

Ahmed, M.A., Sridharan, B., Saha, N., Sannasiraj, S.A., Kuiry, S.N. 2022. Assessment of coastal vulnerability for extreme events. International Journal of Disaster Risk Reduction, 82, 103341. doi: 10.1016/j.ijdrr.2022.103341.

Al-Masri, A.A., Shafi, K.M., Seyyed, H., Meo, S.A. 2023. Public perceptions: The role of individuals, societies, and states in managing the environmental challenges – cross-sectional study. Journal of King Saud University – Science, 35, 102581. doi: 10.1016/j.jksus.2023.102581.

Alsema, E.A. 2000. Energy pay-back time and CO_2 emissions of PV systems. Progress in Photovoltaics: Research and Applications, 8, 17–25. doi: 10.1002/(SICI)1099-159X(200001/02)8:1<17::AID-PIP295>3.0.CO;2-C.

Andrée, E., Su, J., Dahl Larsen, M. A., Drews, M., Stendel, M., Skovgaard Madsen, K. 2023. The role of preconditioning for extreme storm surges in the western Baltic Sea. Natural Hazards and Earth System Sciences, 23, 1817–1834, doi: 10.5194/nhess-23-1817-2023.

Ang, T.Z., Salem, M., Kamarol, M., Das, H.S., Nazari, M.A., Prabaharan, N. 2022. A comprehensive study of renewable energy sources: Classifications, challenges and suggestions. Energy Strategy Reviews, 43, 100939, doi: 10.1016/j.esr.2022.100939.

Annoni, A., Luzet, C., Gubler, E., Ihde, J. (Eds.) 2003. Map Projections for Europe. European Commission Joint Research Centre, reference EUR 20120 EN, http://mapref.org/LinkedDocuments/MapProjectionsForEurope-EUR-20120.pdf.

Aporta, C., Bishop, B., Choi, O., Wang, W. 2020. Knowledge and data: An exploration of the use of inuit knowledge in decision support systems in marine management. In: Chircop, A., Goerlandt, F., Aporta, C., Pelot, R. (Eds.), Governance of Arctic Shipping - Rethinking Risk, Human Impacts and Regulation. Springer, pp. 151–170, doi: 10.1007/978-3- 030-44975-9.

Armenio, E., Mossa, M., Petrillo, A.F. 2021. Coastal vulnerability analysis to support strategies for tackling COVID-19 infection. Ocean and Coastal Management, 211, 105731, doi: 10.1016/j.ocecoaman.2021.105731.

Arnett, E.B., Brown, W.K., Erickson, W.P., Fiedler, J.K., Hamilton, B.L., Henry, T.H., Jain, A., Johnson, G.D., Kerns, J., Koford, R.R., Nicholson, C.P., O'Connell, T.J., Piorkowski, M.D., Tankersley, R.D. Jr. 2008. Patterns of bat fatalities at wind energy facilities in North America. Journal of Wildlife Management, 72(1), 61-78, doi: 10.2193/2007-221.

Arrambide, I., Zubia, I., Madariaga, A. 2019. Critical review of offshore wind turbine energy production and site potential assessment. Electric Power Systems Research, 167, 39-47, doi: 10.1016/j.epsr.2018.10.016.

Arruda, V.L.S., Piontekowski, V.J., Alencar, A., Pereira, R.S., Matricardi, E.A.T., 2021. An alternative approach for mapping burn scars using Landsat imagery, Google Earth Engine, and Deep Learning in the Brazilian Savanna. Remote Sensing Applications: Society and Environment, 22, 100472, doi: 10.1016/j.rsase.2021.100472.

Araya-Munoz, D., Metzger, M.J., Stuart, N., Wilson, A.M.W., Carvajal, D. 2017. A spatial fuzzy logic approach to urban multi-hazard impact assessment in Concepcion, Chile. Science of The Total Environment, 576, 508–519, doi: 10.1016/j.scitotenv.2016.10.077.

Asante, W.A., Acheampong, E., Boateng, K., Adda, J. 2017. The implications of land tenure and ownership regimes on sustainable mangrove management and conservation in two Ramsar sites in Ghana. Forest Policy and Economics 85, 65–75, doi: 10.1016/j.forpol.2017.08.018.

Asiri, M.M., Aldehim, G., Alruwais, N., Allafi, R., Alzahrani, I., Nouri, A.M., Assiri, M., Abdelaziz Ahmed, N. 2024. Coastal flood risk assessment using ensemble multi-criteria decision-making with machine learning approaches. Environmental Research, 245, 118042, doi: 10.1016/j.envres.2023.118042.

Averkiev, A.S., Klevannyy, K.A. 2010. A case study of the impact of cyclonic trajectories on sea-level extremes in the Gulf of Finland. Continental Shelf Research, 30, 707–714, doi: 10.1016/j.csr.2009.10.010.

Aydin, N.Y., Kentel, E., Duzgun, S., 2010. GIS-based environmental assessment of wind energy systems for spatial planning: a case study from Western Turkey. Renewable and Sustainable Energy Reviews, 14(1), 364–373, doi: 10.1016/j.rser.2009.07.023.

Baban, S.M.J., Parry, T., 2001. Developing and applying a GIS-assisted approach to locating wind farms in the UK. Renewable Energy, 24 (1), 59–71, doi: 10.1016/S0960-1481(00)00169-5.

Bagdanavičiūtė, I., Kelpšaitė-Rimkienė, L., Galinienė, J., Soomere, T. 2019. Index based multi-criteria approach to coastal risk assessment. Journal of Coastal Conservation, 23(4), 785–800, doi: 10.1007/s11852-018-0638-5.

Bagdanavičiūtė, I., Kelpšaitė, L., Soomere, T. 2015. Multi-criteria evaluation approach to coastal vulnerability index development in micro-tidal low-lying areas. Ocean and Coastal Management, 104, 124–135, doi: 10.1016/j.ocecoaman.2014.12.011.

Barzehkar, M., Mobarghaee Dinan, N., Salemi, A. 2016. Environmental capability evaluation for nuclear power plant site selection: a case study of Sahar Khiz Region in Gilan Province, Iran. Environmental Earth Sciences, 75, 1016. doi: 10.1007/s12665-016-5825-9.

Bayat, M., Ghorbanpour, M., Zare, R., Jaafari, A., Pham, B.T. 2019. Application of artificial neural networks for predicting tree survival and mortality in the Hyrcanian forest of Iran. Computers and Electronics in Agriculture, 164, 104929, doi: 10.1016/j.compag.2019.104929.

Bell, M.L., Hobbs, B.F., Ellis, H. 2003. The use of multi-criteria decision-making methods in the integrated assessment of climate change: Implications for IA practitioners. Socio-Economic Planning Sciences, 37(4), 289–316, doi: 10.1016/S0038-0121(02)00047-2.

Ben-Gal., I. 2008. Bayesian networks. In: Ruggeri, F., Kenett, R.S., Faltin, F.W. (Eds.) Encyclopedia of Statistics in Quality and Reliability. Wiley, doi: 10.1002/9780470061572.eqr089.

Berk, R.A. 2006. An introduction to ensemble methods for data analysis. Sociological Methods & Research, 34(3), 263–295, doi: 10.1177/0049124105283119.

Bhattacharyya, S.C. 2012. Energy access programmes and sustainable development: A critical review and analysis. Energy for Sustainable Development, 16, 260–271, doi: 10.1016/j.esd.2012.05.002.

Bilgili, M., Sahin, B. 2009. Investigation of wind energy density in the southern and southwestern region of Turkey. Journal of Energy Engineering, 135(1), 12–20, doi: 10.1061/(ASCE)0733-9402(2009)135:1(12).

Bilgili, M., Yasar, A., Simsek, E. 2011. Offshore wind power development in Europe and its comparison with onshore counterpart. Renewable and Sustainable Energy Reviews, 15 (2), 905–915, doi: 10.1016/j.rser.2010.11.006.

Björkqvist, J.-V., Tuomi, L., Tollman, N., Kangas, A., Pettersson, H., Marjamaa, R., Jokinen, H., Fortelius, C. 2017. Brief communication: Characteristic properties of extreme wave events observed in the northern Baltic Proper, Baltic Sea. Natural Hazards and Earth System Sciences, 17, 1653–1658, https://doi.org/10.5194/nhess-17-1653-2017, 2017.

Björkqvist, J.-V., Rikka, S., Alari, V., Männik, A., Tuomi, L., Pettersson, H. 2020. Wave height return periods from combined measurement-model data: a Baltic Sea case study. Natural Hazards and Earth Systems Science, 20(12), 3593–3609, doi: 10.5194/nhess-20-3593-2020.

Björkqvist, J.V., Lukas, I., Alari, V., van Vledder, P.G., Hulst, S., Pettersson, H., Behrens, A., Männik A. 2018. Comparing a 41-year model hindcast with decades of wave measurements from the Baltic Sea. Ocean Engineering, 152, 57–71, doi: 10.1016/j.oceaneng.2018.01.048.

Bogdanov, D., Farfan, J., Sadovskaia, K., Aghahosseini, A., Child, M., Gulagi, A., Oyewo, A.S., Barbosa, L.D.N.S., Breyer, C. 2019. Radical transformation pathway towards sustainable electricity via evolutionary steps. Nature Communications, 10, 1077, doi: 10.1038/s41467-019-08855-1.

Booij, N., Ris, R.C., Holthuijsen, L.H., 1999. A third-generation wave model for coastal regions: 1. model description and validation. Journal of Geophysical Research-Oceans, 104(C4), 7649–7666, doi: 10.1029/98JC02622.

Brannstrom, C., Gorayeb, A., de Sousa Mendes. J., Loureiro, C., Meireles, A.J.d.A., Silva, E.V.d., Freitas, A.L.R.d., Oliveira, R.F.d. 2017. Is Brazilian wind power development sustainable? Insights from a review of conflicts in Ceará state. Renewable and Sustainable Energy Reviews, 67, 62–71, doi: 10.1016/j.rser.2016.08.047.

Caceoğlu, E., Yildiz, H.K., Öguz, E., Huvaj, N., Guerrero, J.M. 2022. Offshore wind ̆ power plant site selection using Analytical Hierarchy Process for Northwest Turkey. Ocean Engineering. 252, 111178, doi: 10.1016/j.oceaneng.2022.111178.

Cali, U., Kantar, E., Pamucar, D., Deveci, M., Taylor, P., Campos-Gaona, D., Anaya-Lara, O., Tande, J.O. 2024. Offshore wind farm site selection in Norway: Using a fuzzy trigonometric weighted assessment model. Journal of Cleaner Production, 436, 140530, doi: 10.1016/j.jclepro.2023.140530.

Cavazzi, S., Dutton, A.G., 2016. An Offshore Wind Energy Geographic Information System (OWE-GIS) for assessment of the UK's offshore wind energy potential. Renewable Energy, 87, 212–228, doi: 10.1016/j.renene.2015.09.021.

Chai, J., Liu, J.K.N., Ngai, E.W.T. 2013. Application of decision-making techniques in supplier selection: A systematic review of literature. Expert Systems with Applications 40 (10), 3872–3885, doi: 10.1016/j.eswa.2012.12.040.

Chaib, W., Guerfi, M., Hemdane, Y. 2020. Evaluation of coastal vulnerability and exposure to erosion and submersion risks in Bou Ismail Bay (Algeria) using the coastal risk index (CRI). Arabian Journal of Geosciences, 13, 420, doi: 10.1007/s12517-020- 05407-6.

Chang, L., Saydaliev, H.B., Meo, M.S., Mohsin, M. 2022. How renewable energy matter for environmental sustainability: Evidence from top-10 wind energy consumer countries of European Union. Sustainable Energy Grids & Networks, 32, 100716, doi: 10.1016/j.segan.2022.100716.

Chen, K.P., Jacobson, C., Blong, R. 2004. Artificial neural networks for risk decision support in natural hazards: A case study of assessing the probability of house survival from bushfires. Environmental Modeling & Assessment, 9(3), 189-199, doi: 10.1023/B:ENMO.0000049389.16864.b0.

Chen, W., Shirzadi, A., Shahabi, H., Ahmad, B.B., Zhang, S., Hong, H., Zhang, N. 2017. A novel hybrid artificial intelligence approach based on the rotation forest ensemble and naïve Bayes tree classifiers for a landslide susceptibility assessment in Langao County, China. Geomatics, Natural Hazards and Risk, 8(2), 1955–1977, doi: 10.1080/19475705.2017.1401560.

Cheng, Z., Zhang, Y., Wu, B., Soares, C.G. 2023. Traffic-conflict and fuzzy-logic-based collision risk assessment for constrained crossing scenarios of a ship. Ocean Engineering, 274, 114004, doi: 10.1016/j.oceaneng.2023.114004.

Chini, N., Stansby, P. 2015. Broad-scale hydrodynamic simulation, wave transformation and sediment pathways. In: Nicholls, R.J., Dawson, R.J., Day, S.A. (Eds.), Broad Scale Coastal Simulation. Advances in Global Change Research 49. Springer, Dordrecht, pp. 103–124, doi: 10.1007/978-94-007-5258-0_3.

Chu, L., Oloo, F., Sudmanns, M., Tiede, D., Hölbling, D., Blaschke, T., Teleoaca, I. 2020. Monitoring long-term shoreline dynamics and human activities in the Hangzhou Bay, China, combining daytime and nighttime EO data. Big Earth Data, 4(3), 242–264, doi: 10.1080/20964471.2020.1740491.

Coelho, C., Narra, P., Marinho, B., Lima, M., 2020. Coastal management software to support the decision-makers to mitigate coastal erosion. Journal of Marine Science and Engineering, 8, 37, doi: 10.3390/jmse8010037.

Danish Energy Agency (DEA) 2016. Technology Data - Energy Plants for Electricity and District heating generation. http://www.ens.dk/teknologikatalog.

Dao, D.V., Jaafari, A., Bayat, M., Mafi-Gholami, D., Qi, C., Moayedi, H., Phong, T.V., Bang Ly, H., Thinh Le, T., Trinh, P.T., Luu, C., Quoc, N.K., Thanh, B.N., Pham, B.T. 2020. A spatially explicit deep learning neural network model for the prediction of landslide susceptibility. Catena, 188, 104451, doi: 10.1016/j.catena.2019.104451.

Department for Energy Security and Net Zero 2022. National Policy Statement for Renewable Energy Infrastructure (EN-3). Retrieved from https://assets.publishing.service.gov.uk/media/64252f5f2fa848000cec0f52/NPS_EN-3.pdf.

De Serio, F., Armenio, E., Mossa, M., Petrillo, A.F. 2018. How to define priorities in coastal vulnerability assessment. Geosciences, 8(11), 415, doi: 10.3390/geosciences8110415.

Dhiman, R., Kalbar, P., Inamdar, A.B. 2019. Spatial planning of coastal urban areas in India: Current practice versus quantitative approach. Ocean and Coastal Management, 182, 104929, doi: 10.1016/j.ocecoaman.2019.104929.

Dhiman, R., Kalbar, P., Inamdar, A.B., 2018. GIS coupled multiple criteria decision making approach for classifying urban coastal areas in India. Habitat International, 71, 125–134, doi: 10.1016/j.habitatint.2017.12.002.

DHI, 2017. MIKE 21 Spectral Waves FM. Spectral Wave Module. User Guide.

Díaz-Cuevas, P., Domínguez-Bravo, J., Prieto-Campos, A. 2019. Integrating MCDM and GIS for renewable energy spatial models: assessing the individual and combined potential for wind, solar and biomass energy in Southern Spain. Clean Technologies and Environmental Policy, 21(9), 1855–1869, doi: 10.1007/s10098-019-01754-5.

Díaz, H., Guedes Soares, C. 2021. A multi-criteria approach to evaluate floating offshore wind farms siting in the Canary Islands (Spain). Energies, 14, 865, doi: 10.3390/en14040865.

Diaz-Cuevas, P., Prieto-Campos, A., Zujar, J.O., 2020. Developing a beach erosion sensitivity indicator using relational spatial databases and Analytic Hierarchy Process. Ocean and Coastal Management, 189, 105146, doi: 10.1016/j.ocecoaman.2020.105146.

Díaz, P. 2013. Renewable Energy and Territory: Potential for the Implementation of Wind Farms in Andalusia. Dissertation, University of Seville.

Easterling, D.R., Meehl, G.A., Parmesan, C., Changnon, S.A., Karl, T.R., Mearns, L.O. 2000. Climate extremes: Observations, modeling, and impacts. Science, 289(5487), 2068–2074, doi: 10.1126/science.289.5487.2068.

Eastman, J.R. 2009. IDRIS Taiga Guide to GIS and Image Processing. Clark Labs. Clark University, 1–342.

Edenhofer, O., Pichs-Madruga, R., Sokona, Y., Minx, J.C., Farahani, E., Kadner, S., Seyboth, K., Adler, A., Baum, I., Brunner, S., Eickemeier, P., Kriemann, B., Savolainen, J., Schlömer, S., Stechow, C.V., Zwickel, T. 2014. Contribution of Working Group III to the Fifth Assessment Report of the Intergovernmental Panel on Climate Change, Cambridge University Press, Cambridge.

Eelsalu, M., Soomere, T., Pindsoo, K., Lagemaa, P. 2014. Ensemble approach for projections of return periods of extreme water levels in Estonian waters. Continental Shelf Research, 91, 201–210, doi: 10.1016/j.csr.2014.09.012.

Eelsalu, M., Soomere, T., Parnell, K., Viška, M. 2024. Attribution of alterations in coastal processes in the southern and eastern Baltic Sea to climate change driven modifications of coastal drivers. Oceanologia, 66(3).

Ekman, M., Mäkinen, J. 1996. Mean sea surface topography in the Baltic Sea and its transition area to the North Sea: a geodetic solution and comparisons with oceanographic models. Journal of Geophysical Research–Oceans, 101(C5), 11993–11999, doi: 10.1029/96JC00318.

El-Shahat, S., El-Zafarany, A.M., El Seoud, T.A., Ghoniem, S.A. 2021. Vulnerability assessment of African coasts to sea level rise using GIS and remote sensing. Environment, Development and Sustainability, 23, 2827–2845, doi: 10.1007/s10668-020-00639-8.

Emeksiz, C., Demirci, B. 2019. The determination of offshore wind energy potential of Turkey by using novelty hybrid site selection method. Sustainable Energy Technologies and Assessments, 36, 100562, doi: 10.1016/j.seta.2019.100562.

Energinet, 2017. https://Energinet.dk, March 2017.

Ennouali, Z., Fannassi, Y., Lahssini, G., Benmohammadi, A., Masria, A. 2023. Mapping coastal vulnerability using machine learning algorithms: A case study at North coastline of Sebou estuary, Morocco. Regional Studies in Marine Science, 60, 102829, doi: 10.1016/j.rsma.2023.102829.

Estonian Land Board, 2023. Estonian Topographic Database. https://geoportaal.maaamet.ee.

European Commission, 2020. Recommendations for positive interactions between offshore wind farms and fisheries. pp. 26. https://maritime-spatial-planning.ec. europa.eu/sites/default/files/recommendations_for_positive_interactions_between_ offshore_wind_farms_and_fisheries.pdf.pdf.

European Commission, 2022. Proposal for a council regulation laying down a framework to accelerate the deployment of renewable energy. pp. 15. Retrieved from https://eur-lex.europa.eu/legal-content/EN/TXT/PDF/?uri=CELEX:52022PC0591&from=EN.

European MSP Platform, 2018a. Conflict fiche 8: Offshore wind and area-based marine conservation. 1–20. https://maritime-spatial-planning.ec.europa.eu/sites/default/ files/sector/pdf/8_offshore_wind_conservation.pdf.

European MSP Platform, 2018b. Maritime Spatial Planning (MSP) for Blue Growth. Final Tech. Study 1–307. https://doi.org/10.2826/04538.

European MSP Platform, 2018c. Sector Fiche: Cables and Pipelines. 1–11. https:// maritime-spatial-planning.ec.europa.eu/sites/default/files/sector/pdf/ mspforbluegrowth_sectorfiche_cablespipelines.pdf.

European MSP Platform, 2018d. Conflict fiche 7: Maritime transport and offshore wind. 1–22. https://maritime-spatial-planning.ec.europa.eu/sites/default/files/sector/pdf/7_transport_offshore_wind_kg.pdf.

European MSP Platform, 2018e. Conflict fiche 5: Offshore wind and commercial fisheries. 1–24. https://maritime-spatial-planning.ec.europa.eu/sites/default/files/sector/pdf/5_offshore_wind_fisheries.pdf.

European MSP Platform, 2019. Conflict fiche 3: Defence and other sea uses. 1–21. https://maritime-spatial planning.ec.europa.eu/sites/default/files/sector/pdf/3_ military.pdf.

Fannassi, Y., Ennouali, Z., Hakkou, M., Benmohammadi, A., Al-Mutiry, M., Elbisy, M.S., Masria, A. 2023. Prediction of coastal vulnerability with machine learning techniques, Mediterranean coast of Tangier-Tetouan, Morocco. Estuarine, Coastal and Shelf Science, 291, 108422, doi: 10.1016/j.ecss.2023.108422.

Feng, Q., An, C., Chen, Z., Owens, E., Niu, H., Wang, Z. 2021. Assessing the coastal sensitivity to oil spills from the perspective of ecosystem services: A case study for Canada's pacific coast. Journal of Environmental Management, 296, 113240, doi: 10.1016/j.jenvman.2021.113240.

Fernández-Guillamón, A., Das, K., Cutululis, N.A., Molina-García, A. 2019. Offshore wind power integration into future power systems: Overview and trends. Journal of Marine Science and Engineering, 7(11), 399, doi: 10.3390/jmse7110399.

Fetanat, A., Khorasaninejad, E. 2015. A novel hybrid MCDM approach for offshore wind farm site selection: A case study of Iran. Ocean and Coastal Management, 109, 17-28, doi: 10.1016/j.ocecoaman.2015.02.005.

Foroozesh, F., Monavari, S.M., Salmanmahiny, A., Robati, M., Rahimi, R. 2022. Assessment of sustainable urban development based on a hybrid decision-making approach: Group fuzzy BWM, AHP, and TOPSIS–GIS. Sustainable Cities and Society, 76, 103402, doi: 10.1016/j.scs.2021.103402.

Furlan, E., Dalla Pozza, P., Michetti, M., Torresan, S., Critto, A., Marcomini, A. 2021. Development of a Multi-Dimensional Coastal Vulnerability Index: assessing vulnerability to inundation scenarios in the Italian coast. Science of the Total Environment, 772, 144650, doi: 10.1016/j.scitotenv.2020.144650.

Gargiulo, C., Battarra, R., Tremiterra, M.R. 2020. Coastal areas and climate change: A decision support tool for implementing adaptation measures. Land Use Policy, 91, 104413, doi: 10.1016/j.landusepol.2019.104413.

Gašparović, I., Gašparović, M. 2019. Determining Optimal Solar Power Plant Locations Based on Remote Sensing and GIS Methods: A Case Study from Croatia. Remote Sensing, 11(12), 1481, doi: 10.3390/rs11121481.

Genç, M.S., Çelik, M., Karasu, I. 2012. A review on wind energy and wind-hydrogen production in Turkey: A case study of hydrogen production via electrolysis system supplied by wind energy conversion system in Central Anatolian Turkey. Renewable and Sustainable Energy Reviews, 16, 6631–6646, doi: 10.1016/j.rser.2012.08.011.

Genç, M.S., Karipoğlu, F., Koca, K., Azgın, S.T. 2021. Suitable site selection for offshore wind farms in Turkey's seas: GIS MCDM based approach. Earth Science Informatics, 14, 1213–1225, doi: 10.1007/s12145-021-00632-3.

Ghorbanzadeh, O., Blaschke, T., Gholamnia, K., Meena, S.R., Tiede, D., Aryal, J. 2019a. Evaluation of different machine learning methods and deep-learning convolutional neural networks for landslide detection. Remote Sensing, 11, 196, doi: 10.3390/rs11020196.

Ghorbanzadeh, O., Blaschke, T., Gholamnia, K., Aryal, J. 2019b. Forest fire susceptibility and risk mapping using social/infrastructural vulnerability and environmental variables. Fire 2(3), 50, doi: 10.3390/fire2030050.

Ghosh, P., Lepcha, K. 2019. Weighted linear combination method versus grid based overlay operation method – A study for potential soil erosion susceptibility analysis of Malda district (West Bengal) in India. The Egyptian Journal of Remote Sensing and Space Sciences, 22, 95–115, doi: 10.1016/j.ejrs.2018.07.002.

Ghosh, S., Mistri, B. 2022. Analyzing the multi-hazard coastal vulnerability of Matla–Bidya inter-estuarine area of Indian Sundarbans using analytical hierarchy process and geospatial techniques. Estuarine, Coastal and Shelf Science, 279, 108144, doi: 10.1016/j.ecss.2022.108144.

Giardino, A., Diamantidou, E., Pearson, S., Santinelli, G., Heijer, K.D. 2019. A regional application of Bayesian modeling for coastal erosion and sand nourishment management. Water, 11, 61, doi: 10.3390/w11010061.

Gielen, D., Boshell, F., Saygin, D., Bazilian, M.D., Wagner, N., Gorini, R. 2019. The role of renewable energy in the global energy transformation. Energy Strategy Reviews, 24, 38–50, doi: 10.1016/j.esr.2019.01.006.

Gigović, L., Pourghasemi, H.R., Drobnjak, S., Bai, S. 2019. Testing a new ensemble model based on SVM and Random Forest in forest fire susceptibility assessment and its mapping in Serbia's Tara National Park. Forests, 10(5), 408, doi: 10.3390/f10050408.

Gil-García, I.C., Ramos-Escudero, A., García-Cascales, M.S., Dagher, H., Molina-García, A. 2022. Fuzzy GIS-based MCDM solution for the optimal offshore wind site selection: The Gulf of Maine case. Renewable Energy, 183, 130–147, doi: 10.1016/j.renene.2021.10.058.

Giudici, A., Jankowski, M. Z., Männikus, R., Najafzadeh, F., Suursaar, Ü., Soomere, T. 2023. A comparison of Baltic Sea wave properties simulated using two modelled wind data sets. Estuarine, Coastal and Shelf Science, 290, 108401, doi: 10.1016/j.ecss.2023.108401.

Giupponi, C. 2007. Decision support systems for implementing the European Water Framework Directive: The MULINO approach. Environmental Modelling and Software, 22(2), 248–258, doi: 10.1016/j.envsoft.2005.07.024.

Gkeka-Serpetsidaki, P., Tsoutsos, T., 2022. A methodological framework for optimal siting of offshore wind farms: A case study on the island of Crete. Energy, 239, 122296, doi: 10.1016/j.energy.2021.122296.

Global Wind Atlas, 2022. Wind layers. https://globalwindatlas.info. (Accessed 15 February 2022).

Glover, D.M., Jenkins, W.J., Doney, S.C. 2011. Modeling Methods for Marine Science. Cambridge University Press.

Gokceoglu, C., Sonmez, H., Nefeslioglu, H.A., Duman, T.Y., Can, T. 2005. The 17 March 2005 Kuzulu landslide (Sivas, Turkey) and landslide-susceptibility map of its near vicinity. Engineering Geology, 81(1), 65–83, doi: 10.1016/j.enggeo.2005.07.011.

Goldstein, E.B., Coco, G., Plant, N.G. 2019. A review of machine learning applications to coastal sediment transport and morphodynamics. Earth-Science Reviews, 194, 97–108, doi: 10.1016/j.earscirev.2019.04.022.

Golestani, N., Arzaghi, E., Abbassi, R., Garaniya, V., Abdussamie, N., Yang, M. 2021. The Game of Guwarra: a game theory-based decision-making framework for site selection of offshore wind farms in Australia. Journal of Cleaner Production, 326, 129358, doi: 10.1016/j.jclepro.2021.129358.

González, A., Connell, P. 2022. Developing a renewable energy planning decision-support tool: Stakeholder input guiding strategic decisions. Applied Energy, 312, 118782, doi: 10.1016/j.apenergy.2022.118782.

González, A., Daly, G., Gleeson, J. 2016. Congested spaces, contested scales: a review of spatial planning for wind energy in Ireland. Landscape and Urban Planning, 145, 12–20, doi: 10.1016/j.landurbplan.2015.10.002.

Gornitz, V. 1991. Global coastal hazards from future sea level rise. Palaeogeography, Palaeoclimatology, Palaeoecology, 89, 379–398, doi: 10.1016/0031-0182(91)90173-O.

Gornitz, V.M., Daniels, R.C., White, T.W., Birdwell, K.R. 1994. The development of a coastal vulnerability assessment database, vulnerability to sea-level rise in the U.S. southeast. Journal of Coastal Research, 12, 327–338.

Guchhait, R., Sarkar, B. 2023. Increasing growth of renewable energy: A state of art. Energies, 16(6), 2665, doi: 10.3390/en16062665.

Gudiyangada Nachappa, T., Tavakkoli Piralilou, S., Gholamnia, K., Ghorbanzadeh, O., Rahmati, O., Blaschke, T. 2020. Flood susceptibility mapping with machine learning, multi-criteria decision analysis and ensemble using Dempster Shafer theory. Journal of Hydrology, 590, 125275, doi: 10.1016/j.jhydrol.2020.125275.

Guo, K., Zhang, X., Kuai, X., Wu, Z., Chen, Y., Liu, Y. 2020. A spatial Bayesian-network approach as a decision-making tool for ecological-risk prevention in land ecosystems. Ecological Modelling, 419, 108929, doi: 10.1016/j.ecolmodel.2019.108929.

Hadipour, V., Vafaie, F., Deilami, K. 2020a. Coastal flooding risk assessment using a GIS-based spatial multi-criteria decision analysis approach. Water, 12(9), 2379, doi: 10.3390/w12092379.

Hadipour, V., Vafaie, F., Kerle, N. 2020b. An indicator-based approach to assess social vulnerability of coastal areas to sea- level rise and flooding: A case study of Bandar Abbas city, Iran. Ocean and Coastal Management, 188, 105077, doi: 10.1016/j.ocecoaman.2019.105077.

Haapala, J.J., Ronkainen, I., Schmelzer, N., Sztobryn, M. 2015. Recent change - Sea ice. In: The BACC II Author Team, Second Assessment of Climate Change for the Baltic Sea Basin, Regional Climate Studies, Springer, Cham, 145–153, doi: 10.1007/978-3-319-16006-1_8.

Haque, A.N. 2016. Application of Multi-Criteria Analysis on Climate Adaptation Assessment in the Context of Least Developed Countries. Journal of Multi-Criteria Decision Analysis, 23, 210–224, doi: 10.1002/mcda.1571.

Harff, J., Furmańczyk, K., von Storch, H. 2017. Introduction. In: Harff, J., Furmańczyk, K., von Storch, H. (Eds). Coastline Changes of the Baltic Sea from South to East. Coastal Research Library, vol 19. Springer, Cham, pp. 363–386, doi: 10.1007/978-3-319-49894-2_1.

Hasager, C.B., Badger, M., Pena, A., Larsen, X.G., Bingol, F. 2011. SAR-based wind resource statistics in the Baltic Sea. Remote Sensing, 3(1), 117–144, doi:10.3390/rs3010117.

Hasan, M.H., Ahmed, A., Nafee, K.M., and Hossen, M.A. 2023. Use of machine learning algorithms to assess flood susceptibility in the coastal area of Bangladesh. Ocean and Coastal Management, 236, 106503, doi: 10.1016/j.ocecoaman.2023.106503.

Hernandez, R.R., Hoffacker, M.K., Murphy-Mariscal, M.L., Allen, M.F. 2015. Solar energy development impacts on land cover change and protected areas. Proceedings of the National Academy of Sciences, 112(44), 13579–13584, doi: 10.1073/pnas.1517656112.

Hersbach, H., Bell, B., Berrisford, P., Hirahara, S., Horanyi, A., Munoz-Sabater, J., Nicolas, J., Peubey, C., Radu, R., Schepers, D., Simmons, A., Soci, C., Abdalla, S., Abellan, X., Balsamo, G., Bechtold, P., Biavati, G., Bidlot, J., Bonavita, M., De Chiara, G., Dahlgren, P., Dee, D., Diamantakis, M., Dragani, R., Flemming, J., Forbes, R., Fuentes, M., Geer, A., Haimberger, L., Healy, S., Hogan, R.J., Holm, E., Janiskova, M., Keeley, S., Laloyaux, P., Lopez, P., Lupu, C., Radnoti, G., de Rosnay, P., Rozum, I., Vamborg, F., Villaume, S., Thepaut, J.N. 2020. The ERA5 global reanalysis. Quarterly Journal of the Royal Meteorological Society, 146(730), 1999–2049, doi: 10.1002/qj.3803.

Hordoir, R., An, B.W., Haapala, J., Dieterich, C., Schimanke, S., Höglund, A., Meier, H.E.M. 2013. BaltiX: A 3D Ocean Modelling Configuration for Baltic & North Sea Exchange Analysis. SMHI-Report, Oceanography, 48, 115 pp.

Hoque, M.A.A., Pradhan, B., Ahmed, N., Ahmed, B., M. Alamri, A. 2021. Cyclone vulnerability assessment of the western coast of Bangladesh. Geomatics, Natural Hazards and Risk, 12, 198–221, doi: 10.1080/19475705.2020.1867652.

Hoque, M.A.A., Ahmed, N., Pradhan, B., Roy, S. 2019. Assessment of coastal vulnerability to multi-hazardous events using geospatial techniques along the eastern coast of Bangladesh. Ocean and Coastal Management, 181, 104898, doi: 10.1016/j.ocecoaman.2019.104898.

Hünicke, B., Zorita, E., Soomere, T., Madsen, K.S., Johansson, M., Suursaar, Ü. 2015. Recent change - Sea level and wind waves. In: The BACC II Author Team, Second Assessment of Climate Change for the Baltic Sea Basin, Regional Climate Studies, Springer, pp. 155–185, doi: 10.1007/978-3-319-16006-1_9.

IPCC 2022. Climate Change 2022: Impacts, Adaptation, and Vulnerability. Contribution of Working Group II to the Sixth Assessment Report of the Intergovernmental Panel on Climate Change [Pörtner, H.-O., Roberts, D.C., Tignor, M., Poloczanska, E.S., Mintenbeck, K., Alegría, A., Craig, M., Langsdorf, S., Löschke, S., Möller, V., Okem, A., Rama, B. (Eds.)]. Cambridge University Press, Cambridge, UK and New York, NY, USA, 3056 pp, doi: 10.1017/9781009325844.

IPCC 2021. Climate Change 2021: The Physical Science Basis. Contribution of Working Group I to the Sixth Assessment Report of the Intergovernmental Panel on Climate Change. In Masson-Delmotte, V., Zhai, P., Pirani, A., Connors, S. L., Péan, C., Berger, S., Caud, N., Chen, Y., Goldfarb, L., Gomis, M. I., Huang, M., Leitzell, K., Lonnoy, E., Matthews, J.B.R., Maycock, T. K., Waterfield, T., Yelekçi, O., Yu, R., & Zhou, B. (Eds.). Cambridge University Press..

IPCC 2019. Special Report on the Ocean and Cryosphere in a Changing Climate. Cambridge University Press.

Iran Energy Efficiency Organization 2018. Average annual wind energy speed at a height of 100 meters. Atlas of the country's renewable and clean energy sources, 1st edn. Tehran, pp 80-85.

IRENA 2020. Renewable Power Generation Costs in 2019. International Renewable Energy Agency, Abu Dhabi.

Isfahan Province Management and Planning Organization 2018. Land use planning. http://www.mpo-es.ir/index.aspx?sub=11.

Ishtiaque, A., Eakin, H., Chhetri, N., Myint, S.W., Dewan, A., Kamruzzaman, M. 2019. Examination of coastal vulnerability framings at multiple levels of governance using spatial MCDA approach. Ocean and Coastal Management, 171, 66–79, doi: 10.1016/j.ocecoaman.2019.01.020.

Iyalomhe, F., Rizzi, J., Torresan, S., Gallina, V., Critto, A., Marcomini, A. 2013. Inventory of GIS-based decision support systems addressing climate change impacts on coastal waters and related inland watersheds. In: Singh, B.H. (Ed.), Climate Change – Realities, Impacts Over Ice Cap, Sea Level and Risks. InTech Open, Chapter 10, pp. 251–272, doi: 10.5772/51999.

Izquierdo-Horna, L., Zevallos, J., Yepez, Y. 2022. An integrated approach to seismic risk assessment using random forest and hierarchical analysis: Pisco, Peru. Heliyon, 8(10), e10926, doi: 10.1016/j.heliyon.2022.e10926

Jena, R., Pradhan, B., Beydoun, G., Ardiansyah, N., Sofyan, H., Affan, M. 2020. Integrated model for earthquake risk assessment using neural network and analytic hierarchy process: Aceh province, Indonesia. Geoscience Frontiers, 11, 613–634, doi: 10.1016/j.gsf.2019.07.006.

Johansson, M.M., Kahma, K.K. 2016. On the statistical relationship between the geostrophic wind and sea level variations in the Baltic Sea. Boreal Environment Research, 21(1–2), 25¬43. [no doi number assigned].

Johnston, B., Foley, A., Doran, J., Littler, T. 2020. Levelised cost of energy, A challenge for offshore wind. Renewable Energy, 160, 876–885, doi: 10.1016/j.renene.2020.06.030.

Kane, I.O., Vanderlinden, J.P., Baztan, J., Touili, N., Claus, S. 2014. Communicating risk through a DSS: A coastal risk centred empirical analysis. Coastal Engineering, 87, 240–248, doi: 10.1016/j.coastaleng.2014.01.007.

Kao, C., 2010. Fuzzy data standardization. IEEE Transactions on Fuzzy Systems, 18(4), 745–754. doi: 10.1109/TFUZZ.2010.2047948.

Khan, A., Seyedmahmoudian, M., Raza, A., Stojcevski, A. 2021. Analytical review on common and state-of-the-art FR strategies for VSC-MTDC integrated offshore wind power plants. Renewable and Sustainable Energy Reviews, 148, 111106, doi: 10.1016/j.rser.2021.111106.

Kim, M., You, S., Chon, J., Lee, J. 2017. Sustainable land-use planning to improve the coastal resilience of the social-ecological landscape. Sustainability, 9, 1086, doi: 10.3390/su9071086.

Klinge Jacobsen, H., Hevia-Koch, P., Wolter, C. 2019. Nearshore and offshore wind development: Costs and competitive advantage exemplified by nearshore wind in Denmark. Energy for Sustainable Development, 50, 91–100, doi: 10.1016/j.esd.2019.03.006.

Klutho, S., 2013. Mathematical decision making: An overview of the Analytic Hierarchy Process. 2–34, https://www.whitman.edu/Documents/Academics/Mathematics/Klutho.pdf (accessed 5 May 2021).

Komen, G.J., Cavaleri, L., Donelan, M., Hasselmann, K., Hasselmann, S., Janssen, P.A.E.M. 1994. Dynamics and Modelling of Ocean Waves. Cambridge University Press, doi: 10.1017/CBO9780511628955.

Konstantinos, I., Georgios, T., Garyfalos, A. 2019. A Decision Support System methodology for selecting wind farm installation locations using AHP and TOPSIS: Case study in Eastern Macedonia and Thrace region, Greece. Energy Policy, 132, 232–246, doi: 10.1016/j.enpol.2019.05.020.

Kontopoulos, C., Grammalidis, N., Kitsiou, D., Charalampopoulou, V., Tzepkenlis, A., Patera, A., Pataki, Z., Li, Z., Li, P., Guangxue, L., Lulu, Q., Dong, D. 2021. An integrated decision support system using satellite and in-situ data for coastal area hazard mitigation and resilience to natural disasters. EGU General Assembly 2021, EGU21-14674, doi: 10.5194/egusphere-egu21-14674.

Kont, A., Jaagus, J., Aunap, R. 2003. Climate change scenarios and the effect of sea-level rise for Estonia. Global and Planetary Change, 36, 1–15, doi: 10.1016/S0921-8181(02)00149-2.

Kont, A., Jaagus, J., Aunap, R., Ratas, U., Rivis, R. 2008. Implications of sea-level rise for Estonia. Journal of Coastal Research, 24, 423–431, doi: 10.2112/07A-0015.1.

Koroglu, A., Ranasinghe, R., Jimenez, J.A., Dastgheib, A. 2019. Comparison of Coastal Vulnerability Index applications for Barcelona Province. Ocean and Coastal Management, 178, 104799, doi: 10.1016/j.ocecoaman.2019.05.001.

Kovaleva, O., Sergeev, A., Ryabchuk, D. 2022. Coastal vulnerability index as a tool for current state assessment and anthropogenic activity planning for the Eastern Gulf of Finland coastal zone (the Baltic Sea). Applied Geography, 143, 102710, doi: 10.1016/j.apgeog.2022.102710.

Kuvlesky, Jr., W.P., Brennan, L.A., Morrison, M.L., Boydston, K.K., Ballard, B.M., Bryant, F.C., Hellgren, E.C. 2007. Wind energy development and wildlife conservation: challenges and opportunities. Journal of Wildlife Management, 71(8), 2487-2498, doi: 10.2193/2007-248.

Łabuz, T.A. 2015. Environmental impacts – Coastal erosion and coastline changes. In: The BACC II Author Team, Second Assessment of Climate Change for the Baltic Sea Basin, Regional Climate Studies, Springer, pp. 381–396, doi: 10.1007/978-3-319-16006-1_20.

Lamba, A., Cassey, P., Segaran, R.R., Koh, L.P. 2019. Deep learning for environmental conservation. Current Biology, 29(19), 977–982, doi: 10.1016/j.cub.2019.08.016.

Latinopoulos, D., Kechagia, K. 2015. A GIS-based Multi-criteria evaluation for wind farm site selection. A regional scale application in Greece. Renewable Energy, 78, 550–560, doi: 10.1016/j.renene.2015.01.041.

Lepäranta, M., Myrberg, K. 2009. Physical Oceanography of the Baltic Sea. Springer, Berlin, pp. 378, doi: 10.1007/978-3-540-79703-6.

Li, Z., Tian, G., El-Shafay, A.S. 2022. Statistical-analytical study on world development trend in offshore wind energy production capacity focusing on Great Britain with the aim of MCDA based offshore wind farm siting. Journal of Cleaner Production, 363, 132326, doi: 10.1016/j.jclepro.2022.132326.

Lovich, J.E., Ennen, J.R. 2011. Wildlife conservation and solar energy development in the desert southwest, United States. BioScience, 61(12), 982–992, doi: 10.1525/bio.2011.61.12.8.

Lorenz, M., Gräwe, U. 2023. Uncertainties and discrepancies in the representation of recent storm surges in a non-tidal semi-enclosed basin: a hind-cast ensemble for the Baltic Sea. Ocean Science, 19(6), 1753–1771, doi: 10.5194/os-19-1753-2023.

Luijendijk, A., Hagenaars, G., Ranasinghe, R., Baart, F., Donchyts, G., Aarninkhof, S. 2018. The state of the world's beaches. Scientific Reports, 8, 6641, doi: 10.1038/s41598-018-24630-6.

Maanan, M., Maanan, M., Rueff, H., Adouk, N., Zourarah, B., Rhinane, H. 2018. Assess the human and environmental vulnerability for coastal hazard by using a multi-criteria decision analysis. Human and Ecological Risk Assessment: An International Journal, 24, 6, doi: 10.1080/10807039.2017.1421452.

Madsen, K.S., Høyer, J.L., Suursaar, Ü., She, J., Knudsen, P. 2019. Sea level trends and variability of the Baltic Sea from 2D statistical reconstruction and altimetry. Frontiers in Earth Science, 7, 243, doi: 10.3389/feart.2019.00243.

Mafi-Gholami, D., Zenner, E.K., Jaafari, A., Riyahi Bakhtyari, H.R., Bui, D.T. 2019. Multi-hazards vulnerability assessment of southern coasts of Iran. Journal of Environmental Management, 252, 109628, doi: 10.1016/j.jenvman.2019.109628.

Mahdy, M., Bahaj, A.B.S. 2018. Multi criteria decision analysis for offshore wind energy potential in Egypt. Renewable Energy, 118, 278–289, doi: 10.1016/j.renene.2017.11.021.

Malczewski, J., Rinner, C. 2015. GIScience, spatial analysis, and decision support. In: Multicriteria Decision Analysis in Geographic Information Science, pp 3–21, Springer, doi: 10.1007/978-3-540-74757-4.

Malczewski, J. 2000. On the use of weighted linear combination method in GIS: Common and best practice approaches. Transactions in GIS, 4(1), 5–22, doi: 10.1111/1467-9671.00035.

Mani Murali R, Ankita, M., Vethamony, P. 2019. A new insight to vulnerability of Central Odisha coast, India using analytical hierarchical process (AHP) based approach. Journal of Coastal Conservation, 22, 799–819, doi: 10.1007/s11852-018-0610-4.

Männikus, R., Soomere, T. 2023. Directional variation of return periods of water level extremes in Moonsund and in the Gulf of Riga, Baltic Sea. Regional Studies in Marine Science, 57, 102741, doi: 10.1016/j.rsma.2022.102741.

Marsooli, R., Lin, N. 2018. Numerical modeling of historical storm tides and waves and their interactions along the U.S. East and Gulf coasts. Journal of Geophysical Research-Oceans, 123, 3844–3874, doi: 10.1029/2017JC013434.

Martinez, A., Iglesias, G. 2022. Mapping of the levelised cost of energy for floating offshore wind in the European Atlantic. Renewable and Sustainable Energy Reviews, 154, 111889, doi: 10.1016/J.RSER.2021.111889.

Masselink, G., Hughes, M., Knight, J., 2011. Introduction to Coastal Processes and Geomorphology, 2nd Ed, Routledge.

McLaughlin, S., Cooper, J.A.G. 2010. A multi-scale coastal vulnerability index: A tool for coastal managers?. Environmental Hazards, 9(3), 233–248, doi:10.3763/ehaz.2010.0052.

Mentaschi, L., Vousdoukas, MI., Pekel, JF., Voukouvalas, E., Feyen, L. 2018. Global long-term observations of coastal erosion and accretion. Scientific Reports, 8, 12876, doi: 10.1038/s41598-018-30904-w.

Meier, H.E.M. Döscher, R., Faxén, T. 2003. A multiprocessor coupled ice–ocean model for the Baltic Sea: applica¬tion to salt inflow. Journal of Geophysical Research–Oceans, 108(C8), 3273, doi: 10.1029/2000JC000521.

Moller, B., Hong, L., Lonsing, R., Hvelplund, F. 2012. Evaluation of offshore wind resources by scale of development. Energy, 48(1), 314–322, doi: 10.1016/j.energy.2012.01.029.

Moradi, S., Yousefi, H., Noorollahi, Y., Rosso, D. 2020. Multi-criteria decision support system for wind farm site selection and sensitivity analysis: Case study of Alborz Province, Iran. Energy Strategy Reviews, 29, 100478, doi: 10.1016/j.esr.2020.100478.

Morim, J., Erikson, L.H., Hemer, M., Young, I., Wang, X., Mori, N., Shimura, T., Stopa, J., Trenham, C., Mentaschi, L., Gulev, S., Sharmar, V.D., Bricheno, L., Wolf, J., Aarnes, O., Perez, J., Bidlot, J., Semedo, A., Reguero, B., Wahl, T. 2022. A global ensemble of ocean wave climate statistics from contemporary wave reanalysis and hindcasts. Scientific Data, 9(1), 358, doi: 10.1038/s41597-022-01459-3.

Moriarty, P., Honnery, D. 2012. What is the global potential for renewable energy? Renewable & Sustainable Energy Reviews, 16(1), 244–252, doi: 10.1016/j.rser.2011.07.151.

Mu, E., Pereyra-Rojas, M. 2018. Practical decision making using super decisions v3. An introduction to the Analytic Hierarchy Process. Chapter 3: Building AHP Models Using Super Decisions v3, pp. 23–42, doi: 10.1007/978-3-319-68369-0.

Mucerino, L., Albarella, M., Carpi, L., Besio, G., Benedetti, A., Corradi, N., Firpo, M., Ferrari, M. 2019. Coastal exposure assessment on Bonassola Bay. Ocean and Coastal Management, 167, 20–31, doi: 10.1016/j.ocecoaman.2018.09.015.

Mullick, Md. R.A., Tanim, A.H., Samiul Islam, S.M. 2019. Coastal vulnerability analysis of Bangladesh coast using fuzzy logic based geospatial techniques. Ocean and Coastal Management, 174, 154–169, doi: 10.1016/j.ocecoaman.2019.03.010.

Mytilinou, V., Lozano-Minguez, E., Kolios, A. 2018. A framework for the selection of optimum offshore wind farm locations for deployment. Energies, 11(7), 1855, doi: 10.3390/en11071855.

Myers, M.R., Barnard, P.L., Beighley, E., Cayan, D.R., Dugan, J.E., Feng, D., Hubbard, D.M., Iacobellis, S.F., Melack, J.M., Page, H.M. 2019. A multidisciplinary coastal vulnerability assessment for local government focused on ecosystems, Santa Barbara area, California. Ocean and Coastal Management, 182, 104921, doi: 10.1016/j.ocecoaman.2019.104921.

Mysiak, J., Giupponi, C., Rosato, P. 2005. Towards the development of a decision support system for water resource management. Environmental Modelling and Software, 20(2), 203–214, doi: 10.1016/j.envsoft.2003.12.019.

Najafzadeh, F., Jankowski, M.Z., Giudici, A., Männikus, R., Suursaar, Ü., Viška, M., Soomere, T. 2024. Spatiotemporal variability of wave climate in the Gulf of Riga. Oceanologia, 66(1), 56–77, doi: 10.1016/j.oceano.2023.11.001.

Nedjati, A., Yazdi, M., Abbassi, R. 2021. A sustainable perspective of optimal site selection of giant air-purifiers in large metropolitan areas. Environment, Development and Sustainability, 24, 8747–8778, doi: 10.1007/s10668-021-01807-0.

Nicholls, R.J., Wong, P.P., Burkett, V.R., Codignotto, J.O., Hay, J.E., McLean, R.F., Ragoonaden, S., Woodroffe, C.D. in: Parry, M.L., Canziani, O.F., Palutikof, J.P., van der Linden, P.J., Hanson C.E. (Eds.) 2007. Coastal systems and low-lying areas. In: Climate Change 2007: Impacts, Adaptation and Vulnerability. Contribution of Working Group II to the Fourth Assessment Report of the Intergovernmental Panel on Climate Change, Cambridge University Press, Cambridge, UK, pp. 315–356.

Ng, K., Borges, P., Philips, M.R., Medeiros, A., Calado, H. 2019. An integrated coastal vulnerability approach to small islands: The Azores case. Science of The Total Environment, 690, 1218–1227, doi: 10.1016/j.scitotenv.2019.07.013.

Nichols, C.R., Wright, L.D., Bainbridge, S.J., Cosby, A., Henaff, A., Loftis, J.D., Cocquempot, L., Katragadda, S., Mendez, G.R., Letortu, P., Le Dantec, N., Resio, D., Zarillo, G. 2019. Collaborative science to enhance coastal resilience and adaptation. Frontiers in Marine Science, 6, 404, doi: 10.3389/fmars.2019.00404.

Nicholls, R.J., Wong, P.P., Burkett, V.R., Codignotto, J.O., Hay, J.E., McLean, R.F., Ragoonaden, S., Woodroffe, C.D., in: Parry, M.L., Canziani, O.F., Palutikof, J.P., van der Linden, P.J., Hanson C.E. (Eds.) 2007. Coastal systems and low-lying areas. In: Climate Change 2007: Impacts, Adaptation and Vulnerability. Contribution of Working Group II to the Fourth Assessment Report of the Intergovernmental Panel on Climate Change, Cambridge University Press, Cambridge, UK, pp. 315–356.

Noorollahi, Y., Yousef, H., Mohammadi, M. 2016a. Multi-criteria decision support system for wind farm site selection using GIS. Sustainable Energy Technologies and Assessments, 13, 38–50, doi: 10.1016/j.seta.2015.11.007.

Noorollahi, E., Fadai, D., Akbarpour, Shirazi, M., Ghodsipour, S.H. 2016b. Land Suitability Analysis for Solar Farms Exploitation Using GIS and Fuzzy Analytic Hierarchy Process (FAHP)-A Case Study of Iran. Energies, 9, 643, doi: 10.3390/en9080643.

Noorollahi, Y., Senani, A.G., Fadaei, A., Simaee, M., Moltames, R. 2022. A framework for GIS-based site selection and technical potential evaluation of PV solar farm using Fuzzy-Boolean logic and AHP multi-criteria decision-making approach. Renewable Energy, 186, 89–104, doi: 10.1016/j.renene.2021.12.124.

Northrup, J.M., Wittemyer, G. 2013. Characterising the impacts of emerging energy development on wildlife, with an eye towards mitigation. Ecology Letters, 16(S1), 112–125, doi: 10.1111/ele.12009.

Nyberg, J., Zillen-Snowball, L., Stromstedt, E. 2022. Spatial characterization of seabed environmental conditions and geotechnical properties for the development of marine renewable energy in Sweden. Quarterly Journal of Engineering Geology and Hydrogeology, 55(4), 1–23, doi: 10.1144/qjegh2021-091.

Nursey-Bray, M.J., Vince, J., Scott, M., Haward, M., O'Toole, K., Smith, T., Harvey, N., Clarke, B. 2014. Science into policy? Discourse, coastal management and knowledge. Environmental Science and Policy, 38, 107–119, doi: 10.1016/j.envsci.2013.10.010.

Omer, A.M. 2008. Energy, Environment and Sustainable Development. Renewable and Sustainable Energy Reviews, 12(9), 2265-2300, doi: 10.1016/j.rser.2007.05.001.

Orhan, O. 2021. Land suitability determination for citrus cultivation using a GIS-based multi-criteria analysis in Mersin, Turkey. Computers and Electronics in Agriculture, 190, 106433, doi: 10.1016/j.compag.2021.106433.

Orviku, K., Jaagus, J., Kont, A., Ratas, U., Rivis, R. 2003. Increasing activity of coastal processes associated with climate change in Estonia. Journal of Coastal Research, 19(2), 364–375, https://www.jstor.org/stable/4299178.

Orviku, K., Suursaar, Ü., Tõnisson, H., Kullas, T., Rivis, R., and Kont, A. 2009. Coastal changes in Saaremaa Island, Estonia, caused by winter storms in 1999, 2001, 2005 and 2007. Journal of Coastal Research, Special Issue 56, 1651–1655.

Orviku, K. 2018. Rannad ja rannikud (Beaches and Coasts). Tallinn University Press, Tallinn [in Estonian].

Osman, A.I., Chen, L., Yang, M.Y., Msigwa, G., Farghali, M., Fawzy, S., Rooney, D.W., Yap, P.S. 2022. Cost, environmental impact, and resilience of renewable energy under a changing climate: a review. Environmental Chemistry Letters. 21, 741–764, doi: 10.1007/s10311-022-01532-8.

Pan, P.S.Y. 2005. Monitoring coastal environments using remote sensing and GIS, in: Bartlett, D., Smith, J. (Eds), GIS for Coastal Zone Management, US: CRC Press, pp. 61–75.

Parker, B.B. Huff, L.C. 1998. Modern under-keel clearance management. International Hydrographic Review, 75(2), 143–165.

Peponi, A., Morgado, P., Trindade, J. 2019. Combining artificial neural networks and GIS fundamentals for coastal erosion prediction modeling. Sustainability, 11, 975, doi: 10.3390/su11040975.

Pham, B.T., Luu, C., Dao, D.V., Phong, T.V., Nguyen, H.D., Le, H.V., Meding, J.V., Prakash, I. 2021. Flood risk assessment using deep learning integrated with multi-criteria decision analysis. Knowledge-Based Systems, 219, 106899, doi: 10.1016/j.knosys.2021.106899.

Pindsoo, K., Soomere, T. 2015. Contribution of wave set-up into the total water level in the Tallinn area. Proceedings of the Estonian Academy of Sciences, 64(3S), 338–348, doi: 10.3176/proc.2015.3S.03.

Pindsoo, K., Soomere, T. 2020. Basin-wide variations in trends in water level maxima in the Baltic Sea. Continental Shelf Research, 193, 104029, doi: 10.1016/j.csr.2019.104029.

Plomaritis, T.A., Costas, S., Ferreira, O. 2018. Use of a Bayesian Network for coastal hazards, impact and disaster risk reduction assessment at a coastal barrier (Ria Formosa, Portugal). Coastal Engineering, 134, 134–147, doi: 10.1016/j.coastaleng.2017.07.003.

Pourghasemi, H.R., Beheshtirad, M., Pradhan, B. 2016. A comparative assessment of prediction capabilities of modified analytical hierarchy process (m-AHP) and Mamdani fuzzy logic models using NETCAD-GIS for forest fire susceptibility mapping. Geomatics, Natural Hazards and Risk, 7, 861–885, doi: 10.1080/19475705.2014.984247.

Pradhan, B. 2013. A comparative study on the predictive ability of the decision tree, support vector machine and neuro-fuzzy models in landslide susceptibility mapping using GIS. Computers & Geosciences, 51, 350–365, doi: 10.1016/j.cageo.2012.08.023.

Ramieri, E., Hartley, A., Barbanti, A., Santos, F.D., Gomes, A., Hilden, M., Laihonen, P., Marinova, N., Santini, M. 2011. Methods for assessing coastal vulnerability to climate change. In: European Environment Agency. European Topic Centre on Climate Change Impacts, Vulnerability and Adaptation, pp. 1–93. Retrieved from http://cca.eionet.europa.eu/

Rangel-Buitrago, N., Neal, W.J., Bonetti, J., Anfuso, G., de Jonge, V.N. 2020a. Vulnerability assessments as a tool for the coastal and marine hazards management: An overview. Ocean and Coastal Management, 189, 105134, doi: 10.1016/j.ocecoaman.2020.105134.

Rangel-Buitrago, N., Gracia C. A., Anfuso, G., Bonetti, J. 2020b. GIS hazard assessments as the first step to climate change adaptation, in: Leal, W.F., Nagy, G., Borga, M., Chavez Muñoz, D., Magnuszewski, A. (Eds.), Climate Change, Hazards and Adaptation Options. Springer, pp. 135–146, doi: 10.1007/978-3-030-37425- 9_6.

Rangel-Buitrago, N.G., Anfuso, G., Williams, A., Bonetti, J., C. Adriana, G., Carlos Ortiz, J. 2017. Risk assessment to extreme eave events: The Barranquilla – Cienaga, Caribbean of Colombia case study, in: Botero, C.M., Cervantes, O., Finkl, C.W. (Eds.), Beach Management Tools - Concepts, Methodologies and Case Studies. Springer, pp. 469–496, doi: 10.1007/978-3-319-58304-4_23.

Rashidi, M., Ghodrat, M., Samali, B., Mohammadi, M. 2018. Decision Support Systems, in: Pomffyova, M. (Ed.), Management of Information Systems. InTech Open, Chapter 2, pp. 19–38, doi: 10.5772/intechopen.79390.

Reckermann, M., Omstedt, A., Soomere, T., Aigars, J., Akhtar, N., Bełdowska, M., Bełdowski, J., Cronin, T., Czub, M., Eero, M., Hyytiäinen, K.P., Jalkanen, J.P., Kiessling, A., Kjellström, E., Kuliński, K., Larsén, X.G., McCrackin, M., Meier, H.E.M., Oberbeckmann, S., Parnell, K., Pons-Seres De Brauwer, C., Poska, A., Saarinen, J., Szymczycha, B., Undeman, E., Wörman, A., Zorita, E. 2022. Human impacts and their interactions in the Baltic Sea region. Earth System Dynamics, 13, 1–80, doi: 10.5194/esd-13-1-2022.

Rehman, S., Jahangir, S., Azhoni, A. 2022. GIS based coastal vulnerability assessment and adaptation barriers to coastal regulations in Dakshina Kannada district, India. Regional Studies in Marine Science, 55, 102509, doi: 10.1016/j.rsma.2022.102509.

Rekik, S., El Alimi, S. 2023. Optimal wind-solar site selection using a GIS-AHP based approach: A case of Tunisia. Energy Conversion and Management: X, 18, 100355, doi: 10.1016/j.ecmx.2023.100355.

Rihan, M., Bindajam, A.A., Talukdar, S., Shahfahad; Naikoo, M.W., Mallick, J., Rahman, A. 2023. Forest fire susceptibility mapping with sensitivity and uncertainty analysis using machine learning and deep learning algorithms. Advances in Space Research, 72(2), 426–443, doi: 10.1016/j.asr.2023.03.026.

Rogers, J.C. 1997. North Atlantic storm track variability and its association to the north Atlantic oscillation and climate variability of northern Europe. Journal of Climate, 10(7), 1635–1647, doi: 10.1175/1520-0442(1997)010<1635:NASTVA>2.0.CO;2

Rosentau, A., Muru, M., Gauk, M., Oja, T., Liibusk, A., Kall, T., Karro, E., Roose, A., Sepp, M., Tammepuu, A., Tross, J., Uppin, M. 2017. Sea-level change and flood risks at Estonian coastal zone. In: Harff, J., Furmańczyk, K., von Storch, H. (Eds). Coastline Changes of the Baltic Sea from South to East. Coastal Research Library, vol 19. Springer, Cham, pp. 363–386, doi: 10.1007/978-3-319-49894-2_16.

Roy, R., Gain, A.K., Samat, N., Hurlbert, M., Tan, M.L., Chan, N.W. 2019. Resilience of coastal agricultural systems in Bangladesh: Assessment for agroecosystem stewardship strategies. Ecological Indicators, 106, 105525, doi: 10.1016/j.ecolind.2019.105525.

Rumson, A.G., Garcia, A.P., Hallett, S.H. 2020. The role of data within coastal resilience assessments: an East Anglia, UK, case study. Ocean and Coastal Management, 185, 105004, doi: 10.1016/j.ocecoaman.2019.105004.

Rusu, E. 2020. An evaluation of the wind energy dynamics in the Baltic Sea, past and future projections. Renewable Energy 160, 350–362, doi: 10.1016/j.renene.2020.06.152.

Rutgersson, A., Kjellström, E., Haapala, J., Stendel, M., Danilovich, I., Drews, M., Jylhä, K., Kujala, P., Larsén, X.G., Halsnæs, K., Lehtonen, I., Luomaranta, A., Nilsson, E., Olsson, T., Särkkä, J., Tuomi, L., Wasmund, N. 2022. Natural hazards and extreme events in the Baltic Sea region. Earth System Dynamics, 13, 251–301, doi: 10.5194/esd-13-251-2022.

Ryabchuk, D., Kolesov, A., Chubarenko, B., Spiridonov, M., Kurennoy, D., Soomere, T. 2011. Coastal erosion processes in the eastern Gulf of Finland and their links with geological and hydrometeorological factors. Boreal Environment Research, 16(Suppl. A), 117–137.

Saaty, T.L., 1980. The Analytic Hierarchy Process, McGraw-Hill, New York.

Saaty, T.L., Tran, L.T. 2007. On the invalidity of fuzzifying numerical judgments in the Analytic Hierarchy Process. Mathematical and Computer Modelling, 46, 962–975, doi: 10.1016/j.mcm.2007.03.022.

Sahin, O., Stewart, R.A., Faivre, G., Ware, D., Tomlinson, R., Mackey, B. 2019. Spatial Bayesian Network for predicting sea level rise induced coastal erosion in a small Pacific Island. Journal of Environmental Management, 238, 341–351, doi: 10.1016/j.jenvman.2019.03.008.

Sajjad, M., Chan, J.C.L., Kanwal, S. 2020. Integrating spatial statistics tools for coastal risk management: A case-study of typhoon risk in mainland China. Ocean and Coastal Management, 184, 105018, doi: 10.1016/j.ocecoaman.2019.105018.

Salvador, C.B., Arzaghi, E., Yazdi, M., Jahromi, H.A.F., Abbassi, R. 2022. A multi-criteria decision-making framework for site selection of offshore wind farms in Australia. Ocean and Coastal Management, 224, 106196, doi: 10.1016/j.ocecoaman.2022.106196.

Sanò, M., Jiménez, J.A., Medina, R., Stanica, A., Sanchez-Arcilla, A., Trumbic, I. 2011. The role of coastal setbacks in the context of coastal erosion and climate change. Ocean and Coastal Management, 54, 943–950, doi: 10.1016/j.ocecoaman.2011.06.008.

Santoro, F., Tonino, M., Torresan, S., Critto, A., Marcomini, A. 2013. Involve to improve: A participatory approach for a Decision Support System for coastal climate change impacts assessment. The North Adriatic case. Ocean and Coastal Management, 78, 101–111, doi: 10.1016/j.ocecoaman.2013.03.008.

Sarbayev, M., Yang, M., Wang, H., 2019. Risk assessment of process systems by mapping fault tree into artificial neural network. Journal of Loss Prevention in the Process Industries, 60, 203–212, doi: 10.1016/j.jlp.2019.05.006.

Scholten, D., Bosman, R. 2016. The geopolitics of renewables; exploring the political implications of renewable energy systems. Technological Forecasting and Social Change, 103, 273-283, doi: 10.1016/j.techfore.2015.10.014.

Schallenberg-Rodríguez, J., Montesdeoca, N.G. 2018. Spatial planning to estimate the offshore wind energy potential in coastal regions and islands. Practical case: The Canary Islands. Energy, 143, 91–103, doi: 10.1016/j. energy.2017.10.084.

Schumacher, J., Schernewski, G., Bielecka, M., Loizides, M.I., Loizidou, X.I. 2018. Methodologies to support coastal management - A stakeholder preference and planning tool and its application. Marine Policy, 94, 150–157, doi: 10.1016/j.marpol.2018.05.017.

Scolaro, M., Kittner, N. 2022. Optimizing hybrid offshore wind farms for cost-competitive hydrogen production in Germany. International Journal of Hydrogen Energy, 47, 6478–6493, doi: 10.1016/j.ijhydene.2021.12.062.

Sekovski, I., Del Rio, L., Armaroli, C. 2020. Development of a coastal vulnerability index using analytical hierarchy process and application to Ravenna province (Italy). Ocean and Coastal Management, 183, 104982, doi: 10.1016/j.ocecoaman.2019.104982.

Shafiee, M. 2022. Wind Energy Development Site Selection Using an Integrated Fuzzy ANP-TOPSIS Decision Model. Energies, 15, 4289, doi: 10.3390/en15124289.

Sindhu, S., Nehra, V., Luthra, S. 2017. Investigation of feasibility study of solar farms deployment using hybrid AHP-TOPSIS analysis: case study of India. Renewable and Sustainable Energy Reviews, 73, 496–511, doi: 10.1016/j.rser.2017.01.135.

Smallwood, K.S., Thelander, C. 2008. Bird mortality in the Altamont Pass Wind Resource Area, California. Journal of Wildlife Management, 72(1), 215-223, doi: 10.2193/2007-032.

Soomere, T. 2001. Extreme wind speeds and spatially uniform wind events in the Baltic Proper. Proceedings of the Estonian Academy of Sciences. Engineering, 7(3), 195–211, doi: 10.3176/eng.2001.3.01.

Soomere, T., Behrens, A., Tuomi, L., Nielsen, J.W. 2008. Wave conditions in the Baltic Proper and in the Gulf of Finland during windstorm Gudrun, Natural Hazards and Earth System Sciences, 8(1), 37–46, doi: 10.5194/nhess-8-37-2008.

Soomere, T., Viska, M., Eelsalu, M. 2013. Spatial variations of wave loads and closure depths along the coast of the eastern Baltic Sea. Estonian Journal of Engineering, 19(2), 93–109, doi: 10.3176/eng.2013.2.01.

Soomere, T., Eelsalu, M. 2014. On the wave energy potential along the eastern Baltic Sea coast. Renewable Energy, 71, 221–233, doi: 10.1016/j.renene.2014.05.025.

Soomere, T., Eelsalu, M., Kurkin, A., Rybin, A. 2015. Separation of the Baltic Sea water level into daily and multi-weekly components. Continental Shelf Research, 103, 23–32, doi: 10.1016/j.csr.2015.04.018.

Soomere, T., Pindsoo, K. 2016. Spatial variability in the trends in extreme storm surges and weekly-scale high water levels in the eastern Baltic Sea. Continental Shelf Research, 115, 53–64, doi: 10.1016/j.csr.2015.12.016.

Soomere, T., Eelsalu, M., Pindsoo, K. 2018. Variations in parameters of extreme value distributions of water level along the eastern Baltic Sea coast. Estuarine, Coastal and Shelf Science, 215, 59–68, doi: 10.1016/j.ecss.2018.10.010.

Soomere, T., Pindsoo, K., Kudryavtseva, N., Eelsalu, M. 2020. Variability of distributions of wave set-up heights along a shoreline with complicated geometry. Ocean Science, 16, 1047–1065, doi: 10.5194/os-16-1047-2020.

Soomere, T. 2024. Climate change and coastal processes in the Baltic Sea. Oxford Encyclopedia of Climate Science, doi: 10.1093/acrefore/9780190228620.013.897.

Steele, J. 1997. Sustainable architecture: Principles, paradigms, and case studies. McGraw-Hill.

Suuronen, A., Lensu, A., Kuitunen, M., Andrade-Alvear, R., Guajardo Celis, N., Miranda, M., Perez, M., Kukkonen, J.V.K. 2017. Optimization of photovoltaic solar power plant locations in northern Chile. Journal of Environmental Earth Science, 76, 824, doi: 10.1007/s12665-017-7170-z.

Suursaar, Ü., Jaagus, J. Tõnisson, H. 2015. How to quantify long-term changes in coastal sea storminess? Estuarine, Coastal and Shelf Science, 156, 31–41, doi: 10.1016/j.ecss.2014.08.001

Suursaar, Ü., Kullas, T., Otsmann, M., Saaremäe, I., Kuik, J., Merilain, M. 2006. Cyclone Gudrun in January 2005 and modelling its hydrodynamic consequences in the Estonian coastal waters. Boreal Environment Research, 11(2), 143–159.

Suursaar, Ü., Jaagus, J., Kont, A., Rivis, R., Tõnisson, H. 2008. Field observations on hydrodynamics and coastal geomorphic processes of Harilaid Peninsula (Baltic Sea) in winter and spring 2006-2007. Estuarine, Coastal and Shelf Science, 80, 31–41, doi: 10.1016/j.ecss.2008.07.007.

Suursaar, Ü., Sooäär, J. 2007. Decadal variations in mean and extreme sea level values along the Estonian coast of the Baltic Sea. Tellus, 59, 249–260, doi: 10.1111/j.1600-0870.2006.00220.x.

Tamiminia, H., Salehi, B., Mahdianpari, M., Quackenbush, L., Adeli, S., Brisco, B. 2020. Google Earth Engine for geo-big data applications: A meta-analysis and systematic review. ISPRS Journal of Photogrammetry and Remote Sensing, 164, 152–170, doi: 10.1016/j.isprsjprs.2020.04.001.

Tanner, T., Lewis, D., Wrathall, D., Bronen, R., Cradock-Henry, N., Huq, S., Lawless, C., Nawrotzki, R., Prasad, V., Rahman, M.A., Alaniz, R., King, K., McNamara, K., Nadiruzzaman, M., Henly-Shepard, S., Thomalla, F. 2014. Livelihood resilience in the face of climate change. Nature Climate Change, 5(1), 23–26, doi: 10.1038/NCLIMATE2431.

Tegou, L., Polatidis, H., Haralambopoulos, D.A. 2010. Environmental management framework for wind farm siting: methodology and case study. Journal of Environmental Management, 91, 2134–2147, doi: 10.1016/j.jenvman.2010.05.010.

Tercan, E., Tapkın, S., Latinopoulos, D., Dereli, M.A., Tsiropoulos, A., Ak, M.F. 2020. A GIS-based multi-criteria model for offshore wind energy power plants site selection in both sides of the Aegean Sea. Environmental Monitoring and Assessment, 192, 652, doi: 10.1007/s10661-020-08603-9.

Thirumurthy, S., Jayanthi, M., Samynathan, M., Duraisamy, M., Kabiraj, S., Anbazhahan, N. 2022. Multi-criteria coastal environmental vulnerability assessment using analytic hierarchy process based uncertainty analysis integrated into GIS. Journal of Environmental Management, 313, 114941, doi: 10.1016/j.jenvman.2022.114941.

Thi Ngo, P.T., Panahi, M., Khosravi, K., Ghorbanzadeh, O., Kariminejad, N., Cerda, A., Lee, S. 2021. Evaluation of deep learning algorithms for national scale landslide susceptibility mapping of Iran. Geoscience Frontiers, 12, 505–519, doi: 10.1016/j.gsf.2020.06.013.

Tien Bui, D., Tuan, T.A., Klempe, H., Pradhan, B., Revhaug, I. 2016. Spatial prediction models for shallow landslide hazards: a comparative assessment of the efficacy of support vector machines, artificial neural networks, kernel logistic regression, and logistic model tree. Landslides, 13(2), 361–378, doi: 10.1007/s10346-015-0557-6.

Tomlin, C.D. 1990. Geographic information systems and cartographic modeling. Englewood Cliffs, N.J., Prentice Hall.

Tõnisson, H., Kont, A., Orviku, K., Suursaar, Ü., Rivis, R., Palginõmm, V. 2018. Application of system approach framework for coastal zone management in Pärnu, SW Estonia. Journal of Coastal Conservation, 23, 931–942, doi: 10.1007/s11852-018-0637-6.

Tõnisson, H., Orviku, K., Lapinskis, J., Gulbinskas, S., Žaromskis, R. 2013. The Baltic States. In: Pranzini, E., Williams, A. (Eds). Coastal Erosion and Protection in Europe. Routledge, New York, pp. 111–130.

Tõnisson, H., Orviku, K., Lapinskis, J., Gulbinskas, S., Zaromskis, R. 2013. The Baltic States - Estonia, Latvia and Lithuania. In: Pranzini, E., Williams, A. (Eds.). Coastal erosion and protection in Europe, 47–80. Routledge, London.

Tõnisson, H., Suursaar, Ü., Orviku, K., Jaagus, J., Kont, A., Willis, D.A., Rivis, R. 2011. Changes in coastal processes in relation to changes in largescale atmospheric circulation, wave parameters and sea levels in Estonia. Journal Coastal Research, 64, 701–705.

Torresan, S., Critto, A., Valle, M.D., Harvey, N., Marcomini, A. 2008. Assessing coastal vulnerability to climate change: comparing segmentation at global and regional scales. Sustainability Science, 3, 45–65, doi: 10.1007/s11625-008-0045-1.

Torresan, S., Critto, A., Rizzi, J., Zabeo, A., Furlan, E., Marcomini, A. 2016. DESYCO: A decision support system for the regional risk assessment of climate change impacts in coastal zones. Ocean and Coastal Management, 120, 49–63, doi: 10.1016/j.ocecoaman.2015.11.003.

Townend, B.I.H., French, J.R., Nicholls, R.J., Brown, S., Carpenter, S., Haigh, I.D., Hill, C.T., Lazarus, E., Penning-Rowsell, E.C., Thompson, C.E.L., Tompkins, E.L. 2021. Operationalising coastal resilience to flood and erosion hazard: A demonstration for England. Science of The Total Environment, 783, 146880, doi: 10.1016/j.scitotenv.2021.146880.

Tsoutsos, T., Frantzeskakib, N., Gekasb, V. 2005. Environmental impacts from the solar energy technologies. Energy Policy, 33, 289–296, doi: 10.1016/S0301-4215(03)00241-6.

Turner II, B.L., Kasperson, R.E., Matson, P.A., McCarthy, J.J., Corell, R.W., Christensen, L., Eckley, N., Kasperson, J.X., Luers, A., Martello, M.L., Polsky, C., Pulsipher, A., Schiller, A. 2003. A framework for vulnerability analysis in sustainability science. Proceedings of the National Academy of Sciences, 100(14), 8074–8079, doi: 10.1073/pnas.1231335100.

Uhde, B., Andreas Hahn, W., Griess, V.C., Knoke, T. 2015. Hybrid MCDA methods to integrate multiple ecosystem services in forest management planning: A critical review. Environmental Management, 56, 373–388, doi: 10.1007/s00267-015-0503-3.

Uyan, M. 2017. Optimal site selection for solar power plants using multi-criteria evaluation: A case study from the Ayranci region in Karaman, Turkey. Clean Technologies and Environmental Policy, 19, 2231–2244, doi: 10.1007/s10098-017-1405-2.

Vagiona, D.G., Kamilakis, M. 2018. Sustainable site selection for offshore wind farms in the South Aegean — Greece. Sustainability, 10(3), 749, doi: 10.3390/su10030749.

Vagiona, D.G., Karanikolas, N.M. 2012. A multicriteria approach to evaluate offshore wind farms sitting in Greece. Global NEST Journal, 14, 235–243, doi: 10.30955/gnj.000868.

Vagiona, D.G., Tzekakis, G., Loukogeorgaki, E., Karanikolas, N. 2022. Site selection of offshore solar farm Deployment in the Aegean Sea, Greece. Journal of Marine Science and Engineering, 10(2), 224, doi: 10.3390/jmse10020224.

Vasileiou, M., Loukogeorgaki, E., Vagiona, D.G. 2017. GIS-based multi-criteria decision analysis for site selection of hybrid offshore wind and wave energy systems in Greece. Renewable and Sustainable Energy Reviews, 73, 745–757, doi: 10.1016/j.rser.2017.01.161.

Viigand, K., Eelsalu, M., Soomere, T. 2024a. Quantifying exposedness of the eastern Baltic Sea shores with respect to extremely high and low water levels. Coastal Engineering, in review.

Viigand, K., Eelsalu, M., Soomere, T. 2024b. Evaluating coastal vulnerability by temporal and spatial variation of parameters of the GEV distribution along the Baltic Sea coast. Journal of Coastal Research, Special Issue No. 113.

Virtanen, E.A., Lappalainen, J., Nurmi, M., Viitasalo, M., Tikanmäki, M., Heinonen, J., Atlaskin, E., Kallasvuo, M., Tikkanen, H. Moilanen, A. 2022. Balancing profitability of energy production, societal impacts and biodiversity in offshore wind farm design. Renewable and Sustainable Energy Reviews, 158, 112087, doi: 10.1016/j.rser.2022.112087.

Vos, K., Splinter, K.D., Harley, M.D., Simmons, J.A., Turner, I.L. 2019. CoastSat: A Google Earth Engine-enabled Python toolkit to extract shorelines from publicly available satellite imagery. Environmental Modelling and Software, 122, 104528, doi: 10.1016/j.envsoft.2019.104528.

Walling, E., Vaneeckhaute, C. 2020. Developing successful environmental decision support systems: Challenges and best practices. Journal of Environmental Management, 264, 110513, doi: 10.1016/j.jenvman.2020.110513.

Wang, Q., Qiu, H.N. 2009. Situation and outlook of solar energy utilization in Tibet, China. Renewable and Sustainable Energy Reviews, 13, 2181–2186, doi: 10.1016/j.rser.2009.03.011.

Wang, L., Zhou, X., Zhu, X., Dong, Z., Guo, W. 2016. Estimation of biomass in wheat using random forest regression algorithm and remote sensing data. The Crop Journal, 4(3), 212–219.

Weisse, R., Dailidiene, I., Hünicke, B., Kahma, K., Madsen, K., Omstedt, A., Parnell, K., Schöne, T., Soomere, T., Zhang, W., Zorita, E. 2021. Sea level dynamics and coastal Erosion in the Baltic Sea region. Earth System Dynamics, 12, 871–898, doi: 10.5194/esd-12-871-2021.

Wolski, T., Wiśniewski, B., Giza, A., Kowalewska-Kalkowska, H., Boman, H., Grabbi-Kaiv, S., Hammarklint, T., Holfort, J., Lydeikaite, Ž. 2014. Extreme sea levels at selected stations on the Baltic Sea coast. Oceanologia, 56, 259–290, doi: 10.5697/oc.56-2.259.

Wong-Parodi, G., Mach, K.J., Jagannathan, K., Sjostrom, K.D. 2020. Insights for developing effective decision support tools for environmental sustainability. Current Opinion in Environmental Sustainability, 42, 52–59, doi: 10.1016/j.cosust.2020.01.005.

Wu, B., Yip, T.L., Xie, L., Wang, Y. 2018. A fuzzy-MADM based approach for site selection of offshore wind farm in busy waterways in China. Ocean Engineering, 168, 121–132, doi: 10.1016/j.oceaneng.2018.08.065.

Wu, Z., Anping, H., Chun, C., Xiang, H., Duoqi, S., Zhifeng, W. 2014. Environmental impacts of large-scale CSP plants in North-Western China. Environmental Science: Processes & Impacts, 16, 2432–2441, doi: 10.1039/c4em00235k.

Xu, Y., Li, Y., Zheng, L., Cui, L., Li, S., Li, W., Cai, Y. 2020. Site selection of wind farms using GIS and multi-criteria decision making method in Wafangdian, China. Energy, 207, 118222, doi: 10.1016/j.energy.2020.118222.

Yariyan, P., Zabihi, H., Wolf, I.D., Karami, M., Amiriyan, S. 2020a. Earthquake risk assessment using an integrated Fuzzy Analytic Hierarchy Process with Artificial Neural Networks based on GIS: A case study of Sanandaj in Iran. International Journal of Disaster Risk Reduction, 50, 101705, doi: 10.1016/j.ijdrr.2020.101705.

Yariyan, P., Avand, M., Abbaspour, R.A., Karami, M., Tiefenbacher, J.P. 2020b. GIS-based spatial modeling of snow avalanches using four novel ensemble models. Science of The Total Environment, 745, 141008, doi: 10.1016/j.scitotenv.2020.141008.

Yun, Y., Ma, D., Yang, M. 2021. Human-computer interaction-based decision support system with applications in data mining. Future Generation Computer Systems, 114, 285–289, doi: 10.1016/j.future.2020.07.048.

Yushchenko, A., de Bono, A., Chatenoux, B., Kumar Patel, M., Ray, N. 2018. GIS-based assessment of photovoltaic (PV) and concentrated solar power (CSP) generation potential in West Africa. Renewable and Sustainable Energy Reviews, 81, 2088–2103, doi: 10.1016/j.rser.2017.06.021.

Zanuttigh, B., Simcic, D., Bagli, S., Bozzeda, F., Pietrantoni, L., Zagonari, F., Hoggart, S., Nicholls, R.J. 2014. THESEUS decision support system for coastal risk management. Coastal Engineering, 87, 218–239, doi: 10.1016/j.coastaleng.2013.11.013.

Zarin, R., Azmat, M., Naqvi, S.R., Saddique, Q., Ullah, S. 2021. Landfill site selection by integrating fuzzy logic, AHP, and WLC method based on multi-criteria decision analysis. Environmental Science and Pollution Research, 28 (16), 19726–19741, doi: 10.1007/s11356-020-11975-7.

Zhu, X., Linham, M. M., Nicholls, R.J. 2010. Technologies for climate change adaptation: Coastal erosion and flooding (Vol. 51). UNEP Risø Centre on Energy, Climate and Sustainable Development.

Ziemba, P. 2022. Uncertain Multi-Criteria analysis of offshore wind farms projects investments – Case study of the Polish Economic Zone of the Baltic Sea. Applied Energy, 309, 118232, doi: 10.1016/j.apenergy.2021.118232.

Zoghi, M., Ehsani, A.H., Sadat, M., Amiri, MJ. 2017. Optimization solar site selection by fuzzy logic model and weighted linear combination method in arid and semi-arid region: A case study Isfahan-IRAN. Renewable and Sustainable Energy Reviews, 68, 986–996, doi: 10.1016/j.rser.2015.07.014.

Acknowledgements

Abstract

Decision support tools for the management of eastern Baltic Sea coasts

This thesis addresses the development and application of decision support systems (DSS) for coastal vulnerability assessment, offshore wind farm site selection, and inland renewable energy site selection. The primary motivation is to promote environmental and socioeconomic planning and management through robust, data-driven frameworks in the context of climate change and growing energy demands. Existing Decision Support Tools (DSTs), such as Geographical Information Systems (GIS), Multi-Criteria Decision Analysis (MCDA), and Artificial Neural Networks (ANN), amongst others, are critically evaluated in the coastal context, offering a formal justification for tool selection and integration. Different hybrid combinations of such tools are evaluated for their effectiveness. It is demonstrated that combining various tools improves decision-making processes for coastal issues and promotes the creation of comprehensive DSS frameworks. These approaches are particularly useful for environmental risk classification, site selection, land-use zoning, and resilience classification.

The Baltic-wide analysis of offshore wind farm site selection is performed using parallel an integrated GIS-MCDA technique and a Levelised Cost of Energy (LCOE) model at high spatial resolution, considering various parameters such as wind speeds, seabed sediments, and distances from infrastructure and protected areas to balance environmental sustainability with economic feasibility. The LCOE and the GIS-MCDA techniques treat these parameters differently. The lowest LCOE values of 42–58 €/MWh cover 33% of the total sea area. The lowest LCOE values are near the Danish shores while the Gulf of Bothnia, offshore areas of the Baltic proper and the central Gulf of Riga waters have higher LCOE values. The northern Baltic Sea is less suitable for wind farms due to lower capacity factor.

The coastal vulnerability for the entire shoreline of Estonia is performed at high resolution for the coastline and is extended towards a quasi-two-dimensional analysis up to 2 km inland. The applied GIS-MCDA approach and a variation of the machine learning, Random Forest, technique treat differently diverse factors such as elevation, geomorphology, vulnerable infrastructure, population density, etc. Both approaches identify the western shores of Saaremaa and Pärnu Bay as the most vulnerable areas, which are prone to elevated water levels and coastal erosion. Various parameters characterising water level variations, most importantly high and low extreme sea levels for different return periods, provide independent information for the estimate of coastal vulnerability even on the relatively short and generally homogeneous Lithuanian shore, offering additional information for managing coastal hazards.

Several computer-based DSSs are applied, evaluated and compared to identify optimal sites for inland renewable energy site selection using the example of wind and solar farms in Isfahan Province, Iran, showing the suitablility of the discussed methods beyond coastal environments. By integrating GIS-MCDA techniques with fuzzy logic, suitable sites are identified for both types of renewable energy production that align with environmental conservation and community energy needs.

Overall, the presented results highlight the critical role of integrating diverse DSTs to enhance the effectiveness of DSS frameworks in coastal and inland planning and management.

Lühikokkuvõte

Läänemere idaranniku haldamise otsuste tugivahendid

Analüüsitakse rannikupiirkonna haldamise otsuste tugivahendite arendamise ja kasutamise võimalusi Eesti ranniku ja Läänemere kontekstis peamise eesmärgiga leida võimalused oluliste sotsiaal-majanduslike haldus- ja planeerimisülesannete lahendamiseks keskkonnasõbralikul moel kvaliteetsete andmete abil ka muutuva kliima ja suureneva energiatarbe tingimustes. Neid vahendeid rakendatakse Eesti ja Leedu rannikute tundlikkuse ja Läänemere meretuule kasutamise majanduslike aspektide hindamiseks.

Kriitiliselt vaadeldakse tugisüsteemide kesksete komponentide (geoinfosüsteemid, multimodaalne otsustusanalüüs, tehisnärvivõrgud jne) toimimist rannikute kontekstis ning põhjendusi üksikute meetodite ja nende kombinatsioonide valikuks. Kirjanduse alusel hinnatakse hübriidmeetodite sobivust ja efektiivsust. Näidatakse, et meetodite kombineerimine annab parema aluse informeeritud otsuste tegemiseks ning sobib süstemaatiliselt toimivate otsustustoesüsteemide arendamiseks. Kirjeldatud lähenemist rakendatakse keskkonnaohtude hindamiseks, oluliste objektide asukoha planeerimiseks, maakasutuse tsoneerimiseks ja säilenõtkuse klassifitseerimiseks.

Hinnatakse meretuuleparkidest toodetava elektri maksumust seadmete ja ühenduste kogu elukaare vältel lahutusvõimega 5 km kogu Läänemerel, rakendades kombineeritult geoinfosüsteeme ja multimodaalset otsustusanalüüsi ning tasakaalustades füüsikalistest, geograafilistest ja looduskaitselistest aspektidest (tuulekiirus, vee sügavus, merepõhja iseloom, tuugenite kaugus teistest taristutest jne) tulenevad aspektid majanduslike kaalutlustega. Toodetud elektri hinnanguline maksumus on 2020. a hindades 42–58 €/MWh ligikaudu ühel kolmandikul kogu merest, sh enamikus Eesti majandustsoonist. Elektri maksumus on madalaim Taani rannavetes, kuid kõrgem Liivi lahe keskosas ja Botnia merel ning suurim mere põhjaosas, kus tuul on ebapüsiv.

Kogu Eesti ranniku tundlikkust merelt lähtuvate ohtude suhtes on analüüsitud kõrglahutusega (10 m) andmestiku ja 16 parameetri alusel, alates maapinna digitaalsest mudelist, geomorfoloogia, lainetuse ja veetasemete omadustest kuni taristu omaduste ja asustustiheduseni. Uuenduslikult on analüüs laiendatud 2 km sügavusele sisemaale. Näidatakse, et geoinfosüsteemide ja multimodaalse otsustusanalüüsi kombinatsiooni ja masinõppe (nn juhusliku metsa) tehnoloogia rakendamine annab kohati oluliselt erinevad tulemused. Mõlemad lähenemised toovad esile, et Pärnu ümbrus ja Saaremaa läänerannik on kõige tundlikumad; eelkõige kõrge veetaseme ja ranna erosiooni tõttu. Selgub, et veetaseme muutlikkust peegeldavad suurused, nt eri korduvusperioodidele vastavad ülikõrged ja ülimadalad veetasemed, annavad sõltumatut informatsiooni eri rannapiirkondade tundlikkuse kohta isegi sellisel suhteliselt lühikesel ja vähevahelduval rannaosal nagu Leedu rannik.

Demonstreeritakse, et ranniku ja mere jaoks sobivad otsustustoesüsteemid, sh algoritm, mis sobib Läänemere tuugenite optimaalse asukoha leidmiseks, toimivad hästi ka sisemaa haldusülesannete puhul. Geoinfosüsteemi, multimodaalse otsustusanalüüsi ja hägusloogika kombinatsiooni abil on leitud parimad kohad päikeseenergia tootmiseks ja tuugenite paigutamiseks Isfahani provintsis Iraanis nii, et taastuvenergia vajaduse ja maksumuse kõrval on arvestatud keskkonnahoidu ja kohalike kogukondade seisukohti. Töö tulemused on seega universaalselt rakendatavad efektiivsete ja tasakaalustatud otsustustoe süsteemide loomiseks nii ranniku, mere kui ka sisemaa planeerimis- ja haldamisülesannete jaoks.

Appendix: Publications constituting the thesis

I

Publication I

Barzehkar, M., Parnell, K.E., Soomere, T., Dragovich, D., Engström, J. 2021. Decision support tools, systems and indices for sustainable coastal planning and management: A review. Ocean and Coastal Management, 212, 105813, doi: 10.1016/j.ocecoaman.2021.105813.

Decision support tools, systems and indices for sustainable coastal planning and management: A review

Mojtaba Barzehkar [a,*], Kevin E. Parnell [a,b], Tarmo Soomere [a,c], Deirdre Dragovich [d], Johanna Engström [e,f]

[a] *Department of Cybernetics, School of Science, Tallinn University of Technology, Tallinn, Estonia*
[b] *College of Science and Engineering, James Cook University, Townsville, Australia*
[c] *Estonian Academy of Sciences, 10130 Kohtu 6, Tallinn, Estonia*
[d] *School of Geosciences F09, The University of Sydney, NSW, 2006, Sydney, Australia*
[e] *Department of Geography, University of Florida, 3141 Turlington Hall, 330 Newell Dr., Gainesville, FL, 32611, USA*
[f] *Department of Applied Aviation Sciences, Embry-Riddle Aeronautical University, 1 Aerospace Boulevard, Daytona Beach, FL 32114, USA*

A B S T R A C T

Coasts worldwide are facing enormous challenges relating to extreme water levels, inundation and coastal erosion. These challenges need to be addressed with consideration given to the need for infrastructure such as for ports and other socio-economic developments, especially for coastal tourism. Choosing the optimal decision support tools (DSTs) for coastal vulnerability and resilience assessment is a major challenge for decision-makers and coastal planners. The robustness and flexibility of coastal decision-making can be improved by using effective DSTs, particularly for the management of coastal hazards. This study provides an overview of the construction and use of decision support systems (DSSs) as combinations of DSTs, such as the commonly used multi-criteria decision analysis (MCDA) methods and an artificial neural network (ANN), integrated with a geographical information system (GIS). The experience of many researchers is that the combination of MCDA techniques based on fuzzy logic, analytical hierarchy process (AHP) and weighted linear combination (WLC), with GIS, and possibly also incorporating ANN, provides decision-makers with a comprehensive tool for efficiently calculating decision support indices (DSIs). Hybrid tools are becoming more popular and relevant among experts due to their multiple functionalities that facilitate decision-making. An integration of DSTs in a DSS and further development of DSIs provides a path for the integration of quantitative and qualitative parameters into the decision-making process, and providing materials to be used in consultation processes. An integrated DSS is more likely to produce high-quality results for decision-makers, handle the uncertainty of analysis, and extend the long-term applicability of tools employed by coastal managers.

1. Introduction

Coastal communities are constantly subject to a wide range of hazards. Studies show that coastal areas are experiencing an increasing number of extreme events. Increases in the height and frequency of extreme sea levels, changes in the rate of sea level rise, the erosion rate, sea-ice cover, and wave height are all examples of changes that are almost certainly enhanced by climate change (Farquharson et al., 2018; Hünicke et al., 2015; Mioduszewski et al., 2018; Neves, 2020; Nerem et al., 2018; Palutikof et al., 2019; Reguero et al., 2019; Soomere et al., 2018; Vitousek et al., 2017a; 2017b; von Storch et al., 2015).

Vousdoukas et al. (2020) estimated that European countries alone spend 1.4 billion euros per year on coastal flood damage, an amount that is expected to increase significantly by the end of the century. Vitousek et al. (2017a) found that coastal flooding will become twice as frequent within the coming decades in the tropics, a region that is already socio-economically challenged. Various marine-driven hazards may cause damage to infrastructure and human livelihoods in populated coastal areas (Nichols et al., 2019; Tanner et al., 2014), and climate-influenced hazards may disrupt core ecological values such as biodiversity and marine and coastal ecosystem services (Myers et al., 2019). It is widely accepted that the world's coastal resources are under

pressure, and will be even more so given climate change projections (Nursey-Bray et al., 2014).

The physical, ecological, and socioeconomic environments of coastal areas are particularly susceptible to hazards triggered by extreme events (Easterling et al., 2000). Their impact depends on the coast's vulnerability and the exposure of human infrastructure to flooding (Maanan et al., 2018) and wave impact. Human activities such as dredging (Vitousek et al., 2017b) or building of coastal structures can be a major element in increasing the likelihood of coastal erosion (Bagdanavičiūtė et al., 2019; Mentaschi et al., 2018). Managing the coast effectively is thus crucial, from both social and ecological perspectives (Nursey-Bray et al., 2014).

Despite having been described for many years (Poch et al., 2004), the use of decision support systems (DSSs) has become increasingly prevalent in recent years (Walling and Vaneeckhaute, 2020; Wong-Parodi et al., 2020). A DSS is the combination of computer-based decision support tools (DSTs) designed to assist in decision-making, applied to such matters as the management of environmental problems and long-term planning (Wong-Parodi et al., 2020). Relying on only individual DSTs may not guarantee effective planning and management decisions when they are compared with combinations of DSTs (Barzehkar et al., 2020). A DSS is a set of problem-solving approaches to assist in achieving both environmental sustainability and development goals in coastal areas (Wong-Parodi et al., 2020). The incorporation of DSSs into the planning process (Zanuttigh et al., 2014) will help decision-makers to efficiently assess risk levels and appropriately prioritize areas where mitigation and adaptation measures are urgently needed (Torresan et al., 2016).

The effectiveness of a DSS can be increased if accurate data at a small grid-cell scale is incorporated into a vulnerability analysis (Mullick et al., 2019), as experts are then more likely to accurately identify the spatial distribution of vulnerability at the local level (Mullick et al., 2019). In other words, the determination of the spatial extent and distribution of the vulnerable locations with high accuracy is the initial phase in determining satisfactory management options (Arabameri et al., 2021). For example, a DSS might allow decision-makers to better understand the options for coastal management by mapping or modeling the relationships between hazards and exposures, enabling the identification of suitable buffer zones for coastal protection and infrastructure development (Wong-Parodi et al., 2020). A DSS is primarily a data-based and model-based approach to help managers organize and analyze a large amount of pertinent spatial information assisted by analytical or predictive models (Abdel-Fattah et al., 2021). The use of a DSS, a set of tools employing realist rationality (Rousseau, 2020), does not negate the need to incorporate other considerations such as the values, preferences, and experiences of decision-makers, communities, and other stakeholders (Ibrahim, 2018).

The application of a DSS supports the development of decision support indices (DSIs) relating to measures of coastal vulnerability to assist decision-makers undertaking tasks such as coastal adaptation planning (Gargiulo et al., 2020). DSIs are index-based approaches allowing the combination of multiple environmental and socioeconomic dimensions of vulnerability, risk, and resilience (Furlan et al., 2021). The outputs of DSSs (such as classification maps or predictive models) relating to coastal vulnerability, can assist in management actions relating to mitigation measures applied to coastal hazards (Torresan et al., 2016; Zanuttigh et al., 2014). A DSS may include a number of tools including geographical information systems (GIS), multi-criteria decision analysis (MCDA), artificial neural network (ANN) techniques, Google Earth Engine (GEE), and model-driven approaches such as Bayesian network (BN) and numerical methods (Yariyan et al., 2020a).

The recent literature has many examples of the application of DSSs, combining various DSTs, in environmental management. Arabameri et al. (2021) applied GIS-based MCDA and artificial intelligence models for zoning land-subsidence susceptibility in Iran. Pham et al. (2021) used GIS, MCDA based on the analytical hierarchy process (AHP), and an

Artificial Neural Network (ANN) for flood risk assessment in Vietnam. Jena et al. (2020) applied GIS, ANN-AHP for earthquake risk mapping in Indonesia. Yariyan et al. (2020a) undertook earthquake risk mapping using Fuzzy-AHP based on GIS and ANN in Iran. Hadipour et al. (2020a) employed an integrated approach using GIS-MCDA to classify coastal risk in Iran. Tercan et al. (2020) applied the integration of GIS and MCDA methods for offshore wind energy infrastructure site selection in the Aegean Sea. Mullick et al. (2019) incorporated fuzzy logic and GIS into the coastal decision support framework in Bangladesh. Bagdanavičiūtė et al. (2019) used GIS, AHP, and weighted linear combination (WLC) for risk classification of the Lithuanian coast of the Baltic Sea. Peponi et al. (2019) utilized GIS-ANN to predict the coastal erosion changes in Portugal. Dao et al. (2020) analyzed and mapped the susceptibility of the landslide in Vietnam by combining GIS and ANN. Arruda et al. (2021) used GEE and ANN for mapping and classifying forest fires in Brazil. Vos et al. (2019) employed GEE and ANN to examine shoreline changes in Australia. Sahin et al. (2019) predicted the extent of coastal erosion based on rising sea levels by the integration of GIS and a Bayesian Network (BN). Furlan et al. (2020) applied GIS-BN to provide scenarios for hazard probability distributions and probabilistic maps for marine spatial planning in the Adriatic Sea. A review of recent literature across environmental management applications indicates that a combination of GIS with MCDA and ANN is becoming increasingly common and flexible approaches to vulnerability assessments (Pham et al., 2021; Yariyan et al., 2020a).

Even though many studies use DSTs in coastal management, a formal consideration of why a particular tool or a combination of tools has been chosen for a particular problem is lacking. A DSS framework is needed, for example, to support the decision-making process in the context of coastal adaptation strategies based on socio-ecologic system evaluation (Palutikof et al., 2019). The available literature indicates that coastal vulnerability, risk, and resilience assessments are often performed using individual tools. However, the advantages of using a combination of DSTs in a DSS have not been systematically considered for the management of coastal areas. The main aim of this overview is to provide information about the use of various DSTs and DSSs in different applications for coastal science, management, and assessment. Based on recent research literature, we discuss the usefulness and efficacy of combinations of DSTs and DSSs that are adapted specifically to assist decision-makers working on coastal risk and resilience.

The applicability of various DSTs and DSSs reported in the coastal management literature to a particular problem can be confusing. For this reason, we focus on three important and interrelated objectives applicable to coastal areas. First, we review and characterize different DSTs and DSSs that have been applied to the management of coastal regions. Second, we attempt to identify DSSs that can take into account several elements including coastal sustainability, social needs, and economic considerations throughout the management process. Third, we attempt to characterize, mostly qualitatively, which DSTs and DSSs can be best applied to the development of DSIs for coastal hazard mitigation and the implementation of adaptation measures. The outcome is intended to assist coastal managers and decision-makers to determine which tools would be most appropriate to address a particular problem.

2. DSSs for coastal planning and management

Coastal managers are usually confronted with making multi-objective decisions that have significant environmental, social, and economic implications (Uhde et al., 2015; Westmacott, 2001). Such decisions can be complex and they often cannot be generalized due to the interconnectedness of human activities within an ecosystem, ecosystem dynamics (Garmendia et al., 2010), and the complexity of the response of a particular environment (such as a water body) to a changing climate (Pindsoo and Soomere, 2020). Computer-based decision support tools use the capabilities of interactive software to assist decision-makers to gain useful information from a combination of raw

data sets by employing a logical scientific framework (Marto et al., 2019). The quality of the decision-making process can be markedly improved by considering different DSTs along with up-to-date and accurate information (Wong-Parodi et al., 2020). An integrated DSS may be an appropriate method to prioritize coastal segments based on the levels of vulnerability, risk, and resilience (Bagdanavičiūtė et al., 2019; Sajjad et al., 2020).

DSSs can provide a quantitative approach to decisions in situations where coastal issues are normally expressed in qualitative terms (Sajjad et al., 2020). Integrating and dealing with diverse data types is one of the advantages of DSSs (Rodela et al., 2017). DSSs can assist in minimizing costs and delays by assisting managers and decision-makers to make rapid decisions (Kitsios and Kamariotou, 2018), encouraging coastal adaptation strategies to be implemented rather than being indefinitely delayed (Gargiulo et al., 2020). An additional advantage is that the maps that may be generated by DSSs provide information in a form that can be helpful for raising public awareness of the process and decisions, such as the socio-ecological benefits of identifying and applying coastal buffer zones (Povak et al., 2020). They can be used as community engagement tools that engage with the ideas and experiences of local people, thereby reinforcing participatory coastal management (Aporta et al., 2020). Fig. 1 shows the advantages of DSSs for coastal planning and management.

3. Computer-based decision support tools (DSTs)

3.1. Google Earth Engine (GEE)

Google Earth Engine (GEE) (not to be confused with Google Earth) has been widely used in the geospatial big data processing. GEE is a web-based (cloud computing) platform built on algorithms written in JavaScript and Python environments that enable an analysis of regional and planetary-scale geospatial data (Tamiminia et al., 2020; Vos et al., 2019). It provides wide access to a series of satellite images and affords global scale analysis capabilities, which enables practitioners to undertake geospatial analyses (Arruda et al., 2021). The application of GEE using Landsat-8 and Sentinel-2 satellite images is a useful DST to analyze changes in shoreline position information using satellite altimetry, and land use (Chu et al., 2020). CoastSat, based on Python, is an example of GEE that enables managers to generate a time-series of available satellite images for classifying coastline changes over the last 30 years (Vos et al., 2019). This classification may identify the vulnerability of coastal segments in any region in the world based on shoreline changes, at least for locations where the change has been significant (Vos et al., 2019).

3.2. Geographical information system (GIS)

GIS is a powerful DST for storing, displaying, and analyzing spatial data (Iyalomhe et al., 2013), including large amounts of coastal data (Rangel-Buitrago et al., 2020a) from different sources. GIS is, in essence, a technology for effective representation, analysis, and visualization of geographical data. Its flexibility for controlling spatial data has made it a cost-effective technique for long-term planning of coastal adaptation (Pan, 2005). Its usefulness in decision-making can be further enhanced by the integration of MCDA methods into the mathematical operations

for determining priorities by allocating values and weights to maps (Malczewski and Rinner, 2015). It can be used to map vulnerable coastal areas by combining map layers to calculate a Coastal Vulnerability Index (CVI) (Hoque et al., 2019). It is also an effective tool for the analysis of coastal resilience, integrating and then mapping resilience parameters and calculating a Coastal Resilience Index (CoRI) (Gargiulo et al., 2020). GIS can be used as an engagement tool by providing output maps accessible to both coastal managers and nonspecialists (Aporta et al., 2020; Iyalomhe et al., 2013). Digital maps can be visualized and interpreted to identify the location of susceptible coastal areas. This knowledge ultimately will support the decision-making (Rangel-Buitrago et al., 2017, 2020b).

In particular, DESYCO software is a DST based on GIS, which has been specifically developed as an engagement tool to raise public awareness about the effects of sea level rise and coastal erosion on human assets and ecosystems (Torresan et al., 2016). It reinforces the concept of adaptation planning and builds a pathway for decision-makers to determine the most suitable adaptation strategies (Santoro et al., 2013). DESYCO is a flexible tool that provides updatable risk assessments, which are accessible to the public via communication and training (Torresan et al., 2016). THESEUS is another GIS-based software tool, which is used to assess coastal risks and the implications of various mitigation options for flooding and erosion (Zanuttigh et al., 2014). It is used to assess mitigation options such as engineering defense, environmentally-based solutions, and socioeconomic mitigation based on a balance between analytical models and experts' opinions (Kane et al., 2014).

3.3. Multi-criteria decision analysis (MCDA) methods

The MCDA approach integrates tools such as the analytical hierarchy process (AHP), fuzzy logic, and weighted linear combination (WLC) methods (Malczewski and Rinner, 2015). It has been widely used for incorporating the preferences and expertise of specialists into the coastal decision-making process (Adem Esmail and Geneletti, 2018; Haque, 2016). It specifies and prioritizes vulnerable locations and risk areas based on multiple criteria (Johnston et al., 2014) and is one of the most productive tools to facilitate complex coastal management decisions (Uhde et al., 2015). Environmental and socioeconomic parameters (Townend et al., 2021) that are aligned with goals are identified and then weighted and ranked (Mafi-Gholami et al., 2019).

3.3.1. Analytical hierarchy process (AHP)

AHP is one of the MCDA approaches used to rank the priorities set by decision-makers for coastal vulnerability, risk, and resilience assessments (Hadipour et al., 2020b). It is based on a pairwise comparison matrix for ranking the importance of each factor compared to others based on an assessment by experts (Sekovski et al., 2020), with different values being assigned to the variables of coastal risk and resilience (Serafim et al., 2019). A set of questionnaires reflecting the vulnerability and resilience of coastal areas are given to relevant experts for the ranking of each parameter based on its relative weight (significance) (Ishtiaque et al., 2019). Normally, a scale from 1 to 9 is used, where rank 1 represents a very low influence of a given parameter, and rank 9 indicates a very high influence (De Serio et al., 2018). This kind of
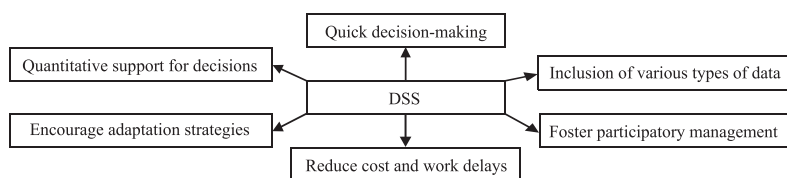
Fig. 1. The advantages of DSS for planning and management.

categorization makes it possible to provide quantitative information about the importance of parameters that influence the total CVI, Coastal Risk Index (CRI), and CoRI (Mani Murali et al., 2018). The final stage of an AHP is the comparison between the individual experts' perspectives. The outcome is the consistency ratio CR (Gargiulo et al., 2020)

$$CR = \frac{CI}{RI},\tag{1}$$

where CI is the consistency index of the pairwise comparison matrix, and RI is the average consistency index calculated from a large number of randomly generated reciprocal matrices (Diaz-Cuevas et al., 2020). The consistency index (Ahmed et al., 2021) is evaluated as

$$CI = \frac{\lambda_{max} - n}{n - 1},\tag{2}$$

where λ_{max} is the largest eigenvalue of the pairwise comparison matrix, and n is the order of the comparisons. The index RI can be calculated by the randomly generated average consistency index of size n, where $\overline{\lambda}_{max}$ is the average value of λ_{max} for a large number of $n \times n$ matrices (Klutho, 2013):

$$RI = \frac{\overline{\lambda}_{max} - n}{n - 1}.\tag{3}$$

The AHP analysis is acceptable if CR is less than or equal to 0.10 (Diaz-Cuevas et al., 2020).

3.3.2. Fuzzy logic

The pixels (cells) of raster map data layers (such as elevation, land use, etc.) are often not standardized and are measured in different units (Barzehkar et al., 2016). Fuzzy logic is an approach to standardize the pixels of raster maps in a range between 0 and 1 (Araya-Munoz et al., 2017), where the endpoints represent very low or very high vulnerability. Within this range, vulnerability is usually considered on a 5-step scale, as low, low/moderate, moderate, moderate/high, and high (Hoque et al., 2021). Other parameters (such as resilience) can be handled similarly. There are different ways for normalization of raster layers, applying minimum and maximum values (Barzehkar et al., 2016). The most common approach is to use a linear scale. This approximation may require reversing the sequence of these five steps depending on whether the particular variable contributes to a decrease or increase in vulnerability (Barzehkar et al., 2020). For example, the number assigned decreases for elevation, coastal slope, the rate of shoreline change, cyclone track density, or population density and increases for sea level rise rate, significant wave height, flooding, or beach sediment size.

The fuzzy standardization of parameters is based on the following normalizations:

$$X_1(i) = \frac{R_i - R_{min}}{R_{max} - R_{min}},\tag{4}$$

$$X_2(i) = \frac{R_{max} - R_i}{R_{max} - R_{min}},\tag{5}$$

where Eq. (4) is used for increasing and Eq. (5) for decreasing, functions. Here $X_1(i)$ and $X_2(i)$ are the fuzzy membership functions, R_i is the input raster value of each parameter, R_{min} is the minimum threshold and R_{max} is the maximum threshold of this parameter (Kao, 2010).

3.3.3. Weighted linear combination (WLC)

The prioritization and zoning of coastal vulnerability and resilience are of vital importance (Şeker et al., 2016). WLC is a widely used method in MCDA for the integration of various environmental and socioeconomic data to calculate DSIs for coastal management, to rank vulnerability and risk in different parts of the system (Hadipour et al., 2020a, 2020b). In this context, GIS based on the Map Algebra tool is effective in developing zones for generating maps for WLC assessment (Malczewski, 2000). The WLC approach is implemented by applying the following expression:

$$WLC = \sum_{j=1}^{n} a_{ij}w_j,\tag{6}$$

where a_{ij} is the i-th rank of the j-th attribute and w_j is the weight of the j-th attribute (Ghosh and Lepcha, 2019). Attributes can be, e.g., elevation, slope, geology, shoreline change rate, land use, etc. Numerous researchers have utilized this method for coastal vulnerability assessment, including Bagdanavičiūtė et al. (2019), Hadipour et al. (2020a, 2020b), and Simões Vieira et al. (2017).

3.4. Artificial neural network (ANN)

Machine learning techniques using ANN are mathematical, algorithmic, and software models influenced primarily by biological artificial neural networks (Hill et al., 1994). They are data-based methods that can mathematically express nonlinear features of environmental hazard built on previously collected data without the need to completely understand all the fundamental physical processes involved (Gudiyangada Nachappa et al., 2020). ANN methods are popular for classifying images and maps to detect features of vulnerable coastal ecosystems (Rumson et al., 2020). Interactions between the layers of a network are determined through neurons such that the output of the first layer (input layer) is considered as the input to the next layer (hidden layer) (Ahmadlou et al., 2020).

The most widely used ANN in coastal change classification is a multi-layer perceptron (MLP) based on supervised classification, which is influenced by several layers showing an input layer, one or more hidden layers, and an output layer (Goldstein et al., 2019). In supervised classification, both the input and output data are recognizable and each feature is labeled as compatible with latent relationships of data to predict the labels of unseen data after training the model (Panahi et al., 2021). An ANN based on MLP has to be trained with a backpropagation algorithm (BPA), which is the most prevalent algorithm for training ANN (Ghorbanzadeh et al., 2019). The number of hidden layer units of any MLP depends on the complexity of the problem. The initial weights of input parameters are randomly selected by the BPA. The difference between the output values and expected values are obtained across all observations until the mean-square error stabilizes at an adequately low level (Ghorbanzadeh et al., 2019).

The MLP is used for studying nonlinear dynamic systems and for approximation problems (Ghorbanzadeh et al., 2019). Samples in MLP are randomly chosen, which represent hazard and non-hazard locations so that the output is predicted (Dao et al., 2020). For example, Yariyan et al. (2020b) samples 101 hazard and 101 non-hazard locations. Hazard locations are divided into two groups based on a ratio, for example 70:30, 71 points for training of the model and 30 points for testing of the model. The same process for non-hazard locations is implemented. The number of samples and the ratio depends on the study area extent and the desired output accuracy. More data lead to a more accurate prediction (Thi Ngo et al., 2021).

3.5. Bayesian Network (BN)

BN models are graphical representations of the probability distribution of changes based on predictive modeling that processes multi-type data and can work in a poor data-collection environment (Guo et al., 2020). BN is becoming a popular DST for modeling vulnerability and risk assessments of coastal areas where there is considerable uncertainty (Sahin et al., 2019). The outcome of a BN is a graphical display of the probability distribution of a hazard (Sahin et al., 2019). One common application of a BN is to forecast erosion and accretion rates in relation to sea level rise (Sahin et al., 2019). The BN contains nodes

showing factors such as coastal response, boundary conditions, location, hazards, and wave properties (usually period and height) which are connected with arrows indicating connections between nodes (Plomaritis et al., 2018). The resulting directed acyclic graph (DAG) represents causative connections between two parameters related to coastal hazards (Giardino et al., 2019). In essence, a BN often serves as an appropriate substitute for numerical modeling of coastal hazards and for calculating hazard impact on infrastructure and the ecosystem (Plomaritis et al., 2018).

As this DST integrates information from multiple variables, it likely provides robust data-driven or model-driven forecasts (Giardino et al., 2019). The formula for a BN is (Giardino et al., 2019):

$$p(F_i|O_j) = \frac{p(O_j|F_i)p(F_i)}{p(O_j)}, \tag{7}$$

where the left-hand side of Eq. (7) is the updated conditional probability (posterior probability) of a forecast F_i based on a particular set of observations O_j. The first term of the numerator on the right-hand side is the likelihood of observations O_j based on the forecast F_i. The second term of the numerator on the right is the prior probability distribution of F_i (the probability of a given forecast based on the entire training dataset, in the absence of any additional observations). The denominator contains the prior probability distribution of O_j (Giardino et al., 2019).

3.6. Numerical methods and satellite measurements

Numerical models have increasingly become an important DST to simulate drivers such as wind, waves, and other physical processes in coastal areas (Coelho et al., 2020). They can model the spatio-temporal variations of wave properties (Hünicke et al., 2015), estimate alongshore sediment transport (DHI, 2017), and model shoreline change including sediment budgets (Coelho et al., 2020) at local and regional scales. Numerical methods such as the Simulating WAves Nearshore model (SWAN) (Booij et al., 1999), WAve Model (WAM) (Komen et al., 1994), MIKE 21 software by the Danish Hydraulic Institute, and others, are widely used to simulate the generation and propagation of wind-generated waves, estimating wave parameters (such as significant wave height SWH) and distributions over periods of time based on measured or modelled wind datasets (DHI, 2017). However, the use of process-based numerical models is time-consuming, due to the simulation of all coastal processes simultaneously, and they can be computationally time-intensive (Chini and Stansby, 2015). Coastal numerical models can provide information about storm surge levels, and when combined with wave models, about wave setup and runup (Marsooli and Lin, 2018). Generic difficulties with numerical models are how to specify the correct boundary conditions, how to deal with tide or swell waves generated outside of the model's domain, and how to handle energy dissipation within the model (Masselink et al., 2011). Some numerical models (e.g., MIKE 21) have extensions that can be used for estimates of sediment transport and development of coastal morphology (DHI, 2017).

Satellite altimetry may be an alternative for measuring some variables such as water level (Alsdorf et al., 2007) or SWH (Gallego Perez and Selvaraj, 2019). Its applications in coastal areas and semi-enclosed and seasonally ice-covered seas require special care to avoid distortion of land and ice cover and to compensate for missing values of low wave heights (Kudryavtseva and Soomere, 2017). The CFOSAT, Sentinel-3B, and 3A satellite images provide instantaneous and extensive spatial coverage and time-series data for measuring SWH (Gallego Perez and Selvaraj, 2019).

3.7. Relationship between DSTs and an integrated DSS for coastal management

Due to the complexity of coastal decisions and significant spatio-temporal variations of coastal processes, the most suitable decision support method, or a combination of methods, must be considered for particular problems (Uhde et al., 2015). Hybrid methods can be developed using an integration of DSTs to improve functionality in the decision-making process (Uhde et al., 2015). AHP and fuzzy logic, for example, can contribute to determining the relative weights and ranking of the parameters involved in coastal management (Hadipour et al., 2020b), and GIS for visualizing and communicating interactive maps to the community (Assumma et al., 2021). Hybrid tools are effective in tackling complicated problems related to climate change effects and human activities in coastal areas (Maanan et al., 2018), where the combined expertise of many stakeholders is needed to plan for the long-term consequences of coastal hazards (Molino et al., 2020).

The provided analysis suggests that integration of combinations of GIS (possibly with GEE), ANN, and MCDA methods, along with BN and numerical models is appropriate and satisfactory for quantifying the dual objectives of community resilience and environmental sustainability for most problems. The integrated approach enhances decision-makers' choices to classify vulnerable areas based on their vulnerability and resilience ranking and criteria weighting. The output maps derived from this approach are effective in identifying areas where coastal changes, such as shoreline movements and sea level rise, are likely to affect communities and ecosystems. Table 1 shows the contribution of various computer-based DSTs in strengthening the process of coastal management planning. The 'Sources' column provides a selection of resources including illustrative examples of the use of the tools.

4. Decision support indices (DSIs) for coastal planning and management

4.1. Coastal Vulnerability Index (CVI)

CVI provides a quantitative analysis for vulnerability ranking of coastal segments to identify the susceptible areas requiring protection measures for community resilience (Hoque et al., 2019; Bagdanavičiūtė et al., 2015; Koroglu et al., 2019). Vulnerability is the degree to which a system is susceptible to, and is unable to cope with, adverse effects (Adger, 2006). CVI has several sub-indices that can be used in combination (Mullick et al., 2019). The coastal characteristics vulnerability index (CCVI) is used for parameters such as slope, elevation, and the rate of shoreline change (Mullick et al., 2019). The coastal forcing vulnerability index (CFVI) incorporates factors such as sea level rise, cyclone track density, and significant wave height into the CVI (Mullick et al., 2019). The socioeconomic vulnerability index (SEVI) considers population density, infrastructure, cultural heritage, land use, and land cover (McLaughlin et al., 2010; Mullick et al., 2019; Ng et al., 2019).

4.2. Coastal exposure index (CEI)

The CEI evaluates the likelihood of socioeconomically valuable features such as infrastructure and urban areas to be negatively affected by a hazard, such as flooding (Bagdanavičiūtė et al., 2019). Coastal flooding can be either land-derived (e.g., river/estuarine flooding when combined with high tides) or marine-driven (e.g., storm surge, tsunami, attack by unusually high waves). Flood maps are an important proxy in determining the CEI, which is often developed from hydrodynamic models based on the maximum water level (Bagdanavičiūtė et al., 2019). The exposure map provides information to understand extreme water

Table 1
The contribution of various computer-based DSTs in strengthening coastal management planning.

Decision Support Tools (DSTs)		Characteristics	Contribution	Other Considerations	Sources
GEE		Uses regional-scale satellite imagery; high-speed processing; a library of application programming interfaces.	Monitoring long-term shoreline changes; analyzing coastal land-use changes.	Time-series mapping; easy download of satellite images from GEE.	Vos et al. (2019); Tamiminia et al. (2020)
GIS		Spatial data analysis and visualization; handling large data; a long-term digital database.	Provides digital maps for coastal managers; producing spatial information with respect to stakeholder preferences and coastal conditions.	Used for zoning of coastal vulnerable areas; applying knowledge-based decision making; an engagement tool to offer visualized outputs to the community.	Gargiulo et al. (2020); Pan (2005)
MCDA	AHP	A participatory tool; hierarchy creation between criteria and sub-criteria; pairwise comparisons; consistency investigation; provides for/requires the input of experts.	Combination of priorities of decision-makers and multiple criteria; development of a strategy with analytical support for coastal managers.	Aggregation of coastal data with information from interviews to create management zones; ranking the importance of parameters relevant to coastal vulnerability.	Malczewski and Rinner (2015); De Serio et al. (2018)
	Fuzzy logic	Designed for complex problems; flexibility in the standardization of maps to address data variability and imprecision.	Normalization of pixels in raster maps to create a comparable assessment for the evaluation of the variability of coastal vulnerability.	Handles effectively the uncertainty of large-scale vulnerability.	Mullick et al. (2019); Barzehkar et al. (2020)
	WLC	Integration of multiple data to create output maps for vulnerability and resilience analysis.	A logical approach for classifying and ranking coastal vulnerability and resilience.	Defines a set of alternatives for coastal decision-making.	Malczewski and Rinner (2015); Tercan et al. (2020)
ANN		Integration of data; solving complex spatial problems.	Shoreline detection; identification of vulnerability changes; feature exploration; able to be used for future prediction of environmental changes.	Classifying the map or image; properly demarcates an area into different classes of environmental hazard susceptibility with respect to the historical extreme events; determination of error in the weighting of parameters by sensitivity analysis.	Goldstein et al. (2019); Peponi et al. (2019); Yarriyan et al. (2020a)
BN		A single probabilistic model; causal dependencies between parts of a system; graphically represents expert's knowledge.	Forecast long-term shoreline change associated with sea level rise; Interactive probabilistic predictions for coastal erosion.	High flexibility to integrate with GIS for generating probabilistic predictionmaps; an approach to model dealing with uncertainties.	Giardino et al. (2019); Sahin et al. (2019)
Numerical models		Simulation of hazards and time-series analysis; modeling the distribution of hazards.	Model wave parameters; sediment transport modelling.	Capacity to simulate wave parameters in 2D or 3D; predict patterns of storm surge, setup, and runup.	Coelho et al. (2020); DHI (2017)

level return periods, acknowledging that there can be changes to estimates of these return periods over time (Mucerino et al., 2019). The exposure criteria are normally assessed on the low probability of events such as 10-year or longer return periods (Bagdanavičiūtė et al., 2019).

4.3. Coastal risk index (CRI)

The CRI is an approach that can be used for identifying the most vulnerable locations associated with climate change effects (Bagdanavičiūtė et al., 2019). For the calculation of the CRI, an exposure map of infrastructure and a community's exposure to flooding is used (Chaib et al., 2020). The CRI is derived from the CVI and CEI to identify the coastal sectors that are affected by natural hazards and to quantify those hazards (Bagdanavičiūtė et al., 2019). Not only does this approach facilitate the strategies for promoting the resilience of infrastructure, it can also assist with the creation of plans for coastal protection against climatic-caused hazards (Chaib et al., 2020). This means that the CRI can be used to help quantify the impacts of combined high anthropogenic pressure and climate change on coastal areas (Bagdanavičiūtė et al., 2019). The results of CRI analysis can be used as a basis of an engagement strategy for stakeholders (Bagdanavičiūtė et al., 2019). This index is useful for determining which protective measures may help to prevent a problem, such as loss of land (Bagdanavičiūtė et al., 2019).

4.4. Coastal area index (CAI)

The CAI is used in land-use planning strategies to determine the priority areas for coastal protection in regions subject to development activities (Dhiman et al., 2019). Using a quantitative analysis based on CAI will allow decision-makers to classify the coastal areas according to their sensitivity to infrastructure development (Dhiman et al., 2019). Factors such as elevation, coastal slope, rate of shoreline change,

geological formation, soil texture, vegetation, land use, and land cover are parameters for the calculation of CAI (Dhiman et al., 2018). This decision index emphasizes the scientific basis for sustainable management of coastal areas rather than the interest of stakeholders (Dhiman et al., 2018). It strengthens decision-making for the classification of coastal areas, which could contribute to the creation of a trade-off between conservation and sustainable development (Dhiman et al., 2019).

4.5. Coastal Resilience Index (CoRI)

The CoRI is used to measure the capacity of the coastal area to respond to (e.g., climate-induced) hazards in such a way that the impacts of hazards will be reduced (Gargiulo et al., 2020). This provides input for flexible adaptation strategies to changes triggered by climate change (Gargiulo et al., 2020). Many factors influence coastal resilience, but the three most important elements are the distance from the coastline, elevation, and human activities, as the populated low-lying regions that are close to the shoreline, are the most susceptible (and thus the least resilient) to storm surge and flooding (Gargiulo et al., 2020), and to sea level rise (Roy et al., 2019). Human actions such as tourism or urban development might also contribute to land-use changes and declining the resilience of coastal areas (Kim et al., 2017). The assessment emphasizes sustainable development objectives and synthesizes potential solutions (Sajjad et al., 2020). Resilience can be better framed by incorporating economic, environmental, and social aspects into coastal planning and integrating the knowledge of professionals and local people (Townend et al., 2021).

4.6. Contributions of DSIs for coastal management

The use of indices can help to identify vulnerable coastal zones (Chaib et al., 2020), and their use have become popular in a drive to

meet the coastal management goals (Bagdanavičiūtė et al., 2019). The presented analysis indicates that depending solely on the most common index (the CVI) does not necessarily guarantee the success of long-term planning for coastal sustainability and the safety of people and infrastructure. The integration of environmental sustainability and social welfare goals in coastal regions is more likely to be captured when multiple DSIs are incorporated into the coastal management process. The inclusion of CRI, CoRI, and CAI into coastal management strategies can create a pathway to identify the locations under the largest pressure by, e.g., sea level rise and shoreline change. Such an integrated approach based on a quantitative analysis could contribute substantially to proactive mitigation and adaptation. Not only would this strengthen the adaptive capacity of coastal ecosystems to climate change, but it would also advance risk assessment procedures. Managers need to employ tools that can be utilized to enhance both risk mitigation measures and the potential capacity of coastal areas. This is more likely to be achieved by a mix of several DSIs to satisfy the socioeconomic needs (human livelihoods and safety) of people in the community and combating climate change-induced hazards. Table 2 shows the characteristics and contributions of various DSIs to improve coastal planning and management.

5. Methodology of hybrid methods and tools for coastal decision-making

An appropriate methodology may be to combine DSTs into a DSS, and then calculate DSIs. An example of a methodology combining DSTs into a DSS is standardizing and prioritizing environmental and socio-economic raster layers using fuzzy logic and AHP, aggregating them using a WLC approach in GIS, and either classifying or validating the results using an ANN model (Pham et al., 2021; Yariyan et al., 2020a). Determining the proper combination of methods is a strategic step, allowing the development of an inclusive plan for fostering hazard mitigation, coastal adaptation planning, and resilience initiatives (Kontopoulos et al., 2021).

Until relatively recently, the combination of MCDA tools and GIS has been the most common and preferred DSS approach (Hadipour et al.,

Table 2
The characteristics of DSIs and their contributions to improve coastal management planning.

DSIs	Functionalities	Contributions	Sources
CVI	Multi-scale vulnerability analysis; map representation; statistical distribution of vulnerabilities; vulnerability scenarios.	A suitable index to calculate coastal vulnerability; and provides an effective management approach for tackling climate-induced hazards.	Bagdanavičiūtė et al. (2015); McLaughlin et al. (2010)
CEI	Coastal inundation analysis; inundation scenarios; map representation.	Identify better prevention measures for coastal flooding to plan for population and infrastructure safety.	Bagdanavičiūtė et al. (2019); Chaib et al. (2020)
CRI	Coastal risk analysis; risk mitigation scenarios; map representation.	Facilitate coastal risk mitigation measures; consideration of socio-economic needs and environmental protection.	Bagdanavičiūtė et al. (2019); Chaib et al. (2020)
CoRI	Coastal resilience analysis; resilience scenarios; map representation.	Foster coastal adaptation strategies; taking into account human safety and coastal sustainability.	Gargiulo et al. (2020); Townend et al. (2021)
CAI	Coastal protection analysis; sensitivity scenarios; map representation.	Minimize the effects of human activities on sensitive coastal areas; long-term planning for protecting susceptible regions.	Dhiman et al. (2018); Dhiman et al. (2019)

2020a; Tercan et al., 2020). For many problems, this combination may still be adequate and realistic (Bagdanavičiūtė et al., 2019; Masoudi et al., 2021; Tercan et al., 2020). However, recently there has been increased recognition of the value of including the use of ANN methods for problems including the classification and ranking of environmental hazards (Pham et al., 2021; Yariyan et al., 2020a). ANN requires large data sets (which may not be available) and the computation time may restrict its value when working with big datasets from wide areas. If a big dataset is used, graphical processing units or cloud computing services are required (Dao et al., 2020).

The application of MCDA and GIS, and perhaps also including ANN, enables environmental, social, and economic data to be used in coastal risk and resilience assessments (Rumson et al., 2020), which includes ranking coastal segments and prioritizing them for interventions. Using a combination of DSTs can assist in the production of suitable maps to plan effectively for coastal protection measures such as establishing an adequate setback zone for erosion and coastal inundation control. The combined application can contribute to decision-making for common coastal planning problems such as the determination of an appropriate width of a buffer zone, the setback for infrastructure development at a particular location, or a management plan for (e.g. port) construction. Similarly, it is possible to determine the required floor level heights for buildings, and identify the parts of the shoreline that need specific measures such as seawalls or beach nourishment to control erosion. Some examples of the combined application of tools in a DSS for coastal problems can be found in Bagdanavičiūtė et al. (2019), Mullick et al. (2019), and Hadipour et al. (2020a).

An integrated approach aims to promote the quality of analysis for coastal vulnerability and resilience evaluations while allowing for ongoing monitoring. Monitoring permits the evaluation of previous decisions or interventions, particularly for identifying any unplanned or inadvertent outcomes. This knowledge is useful to understand whether unplanned effects arise from an inexact description of a single hazard (which may lead to another problem being created) or are related to the overall course of events, that may need a completely different approach. An integrated approach, may provide better information than using single tools and has led to sound environmental planning decisions (Pham et al., 2021; Yariyan et al., 2020a).

Sea level rise and increase in extreme water levels combined with anthropogenic activities have affected many coastal areas and their joint impact is continuing to grow (Sahin et al., 2019). Some individual tools for coastal management have strong functionality to help mitigate these problems, however their functions usually do not go beyond the lifetime of a particular project (Schumacher et al., 2018). The long-term applicability of DSTs for coastal planning is important to protect coastal ecosystems and to promote the livelihoods of local people. Furthermore, most coastal hazards are localized in small segments of the shore. The mitigation thus needs to be addressed at a local scale that considers the specific characteristics of the coast (Mullick et al., 2019). Analyzing such hazards at a local scale is often extremely complicated because of the lack of high-resolution data. Coastal management thus requires the flexibility of DSTs to handle the variability of various hazards in different locations. The integration of DSTs creates a new pathway to consider the spatial changes of coastal vulnerability, risk, and resilience at finer scales (down to the pixel level in models), which can realistically determine the rates of change at appropriate scales.

An assessment of error or uncertainty is important and is incorporated in MCDA tools based on fuzzy logic and in ANN algorithms implemented in MLP (Yariyan et al., 2020a). The effective communication of uncertainty is crucially important for the community. If fuzzy logic and ANN methods are integrated into the decision support framework, errors or uncertainties that occur in a single technique will likely be identified and removed using other methods so that uncertainty is minimized (Yariyan et al., 2020a). ANN methods are particularly useful in analyzing uncertainty. The advantage of ANN to the MCDA based on AHP is related to the determination of uncertainty for the

weighting of parameters (Gudiyangada Nachappa et al., 2020). A sensitivity analysis for weighting of parameters implemented in ANN shows the importance, or usefulness, of the various input variables in a specific neural network. Sensitivity analysis also finds the variables that can be neglected in the analyses and the variables that need to be maintained (Peponi et al., 2019). By implementing a sensitivity analysis, the network error is determined by comparing the observed values of each variable input with the estimated values of outputs (Bayat et al., 2019). This comparison is continued until the mean-square error (MSE) reaches a very low level and the coefficient of determination (R^2) is high so that the ANN model is appropriately fitted to reality, and suits the purpose of the investigation (Yariyan et al., 2020a).

Using single methods (e.g., AHP) could increase the possibility of variable rankings, depending on the allocation of weights to a particular criterion. An increased number of inputs from different tools may lead to variable rankings (Walling and Vaneeckhaute, 2020). However, an integrated DSS, when appropriately considered by professionals, is more likely to produce consistent results than single methods (Barzehkar et al., 2020), which may individually make too many assumptions, using data sets that have considerable noise or uncertainty. Using DSS can reduce the production of inconsistent outcomes by taking into account expert knowledge for calibration and validation of methods. Thus, by using a range of techniques, different tools can be assessed in terms of their consistency (or divergence) so that the best decision is the one that matches the results of most tools. This approach has conceptual similarity to ensemble methods in statistics and machine learning (Berk, 2006).

Human-machine interaction is becoming increasingly important in the use of DSTs and the development of DSS (Yun et al., 2021). The operator has to ensure that correct input data are incorporated and that the outputs are a reasonable and reliable reflection of reality. Good expert knowledge is required for the interpretation of the input data for managing coastal hazards (Rumson et al., 2020). Only then will coastal managers benefit from the decision-making process. However, a DSS is not capable of facilitating the analysis of complex decisions (Rashidi et al., 2018). It is the expert who must structure complex decisions into smaller comprehensible segments e.g., creating buffer zones on output maps.

Fig. 2 shows the steps for applying a particular combination of DSTs in coastal planning and management with an example workflow for steps 2 and 3 shown in Fig. 3. Fig. 4 summarizes the potential benefits of using a DSS for coastal planning and management.

6. Discussion

The aim of the overview of DSTs is to provide a rational framework that incorporates environmental and socioeconomic data to assist in coastal planning and management. Many coastal problems may benefit from a combination of DSTs to strengthen the effectiveness of the decision-making process. Previous studies (Arruda et al., 2021; Guo
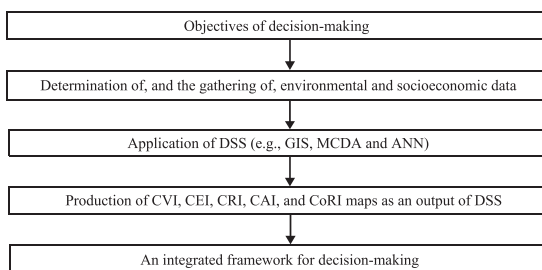
et al., 2020, Hadipour et al., 2020a; Peponi et al., 2019; Yariyan et al., 2020a, and many others) use a combination of GIS-MCDA, GIS-ANN, GEE-ANN, GIS-MCDA-ANN, or GIS-BN for prioritizing and ranking a variety of environmental hazards. While many studies have successfully combined GIS and MCDA into a DSS (Bagdanavičiūtė et al., 2019; Hadipour et al., 2020a; Masoudi et al., 2021; Tercan et al., 2020), recent literature suggests the addition of ANN adds significantly, particularly concerning sensitivity and error analysis. Based on the existing literature (Jena et al., 2020; Pham et al., 2021; Yariyan et al., 2020a), we can conclude that the combination of GIS and MCDA (using AHP, fuzzy logic, and WLC approaches), with the additional application of ANN tools, is the most effective DSS for most coastal applications. Importantly, these combinations use tools, particularly those available in GIS to produce products, that can visually aid interpretation for the public, raise public awareness of coastal sustainability, and provide the basis for discussion among experts for knowledge-based decision-making.

Even though one cannot derive any strict conclusions from the presented comparison of different approaches, the analyzed material, in our opinion, still makes it possible to identify several practical implications. As can be seen from Table 3, combinations of methods effectively address different problems in environmental management, such as environmental risk classification, infrastructure site selection, land-use zoning, and environmental resilience classification.

An important advantage of a combination including MCDA is that it easily allows the incorporation of environmental, social, and economic objectives into decision-making (Masoudi et al., 2021; Tercan et al., 2020). Another advantage of this method is the involvement of scientists and other stakeholders, who can provide input based on their knowledge, experience (particularly related to community expectations), and values, thereby overcoming some of the issues associated with using a realist, quantitative approach to a problem that has many dimensions (Uhde et al., 2015). This aspect is particularly important for coastal management planning, which may require the simultaneous consideration of several disparate hazards. It can be important for reinforcing a positive public perception of the decision-making process. The use of ANN better meets the need for the validation of results and consideration of future conditions and changes, as well as present conditions (Peponi et al., 2019), and it enables improved determinations of environmental hazards particularly in areas where large datasets are available (Lamba et al., 2019; Yariyan et al., 2020a). Combinations including only ANN methods without MCDA do not generally integrate the knowledge of experts in determining the relationships between input and output data for weighting of parameters (Sarbayev et al., 2019). BN methods are similarly effective in predicting environmental changes (Sahin et al., 2019), however they are computationally complex and require even more expertise and experience to implement and interpret (Sahin et al., 2019). Moreover, they provide outputs that are less user-friendly for community engagement (Guo et al., 2020). They are incapable of demonstrating the dynamic relationships and feedbacks between parameters (Guo et al., 2020). GEE is useful to access and analyze large publicly available satellite datasets and can be used in combination with ANN as an alternative combination when appropriate data sets are available (Arruda et al., 2021). This combination requires specialist skills to apply.

GIS and MCDA tools are widely available in most organizations, and the combination is already employed by many practitioners, due to the wide accessibility of its components and ease with which the methods can be used and applied (Malczewski and Rinner, 2015). ANN methods require more training and are therefore less accessible. However, this is changing with ANN skills now being taught across more fields including for environmental practitioners (Lamba et al., 2019; Pham et al., 2021). GIS-MCDA or GIS-MCDA-ANN combinations will generate outputs for managers, decision-makers, and governmental authorities, that are easily understandable to others within the decision-making communities and other stakeholders (Yariyan et al., 2020a). As GIS-MCDA methods are conceptually simple, accessible, and produce outputs

Fig. 2. Systematic steps for applying an integrated DSS in coastal planning and management.
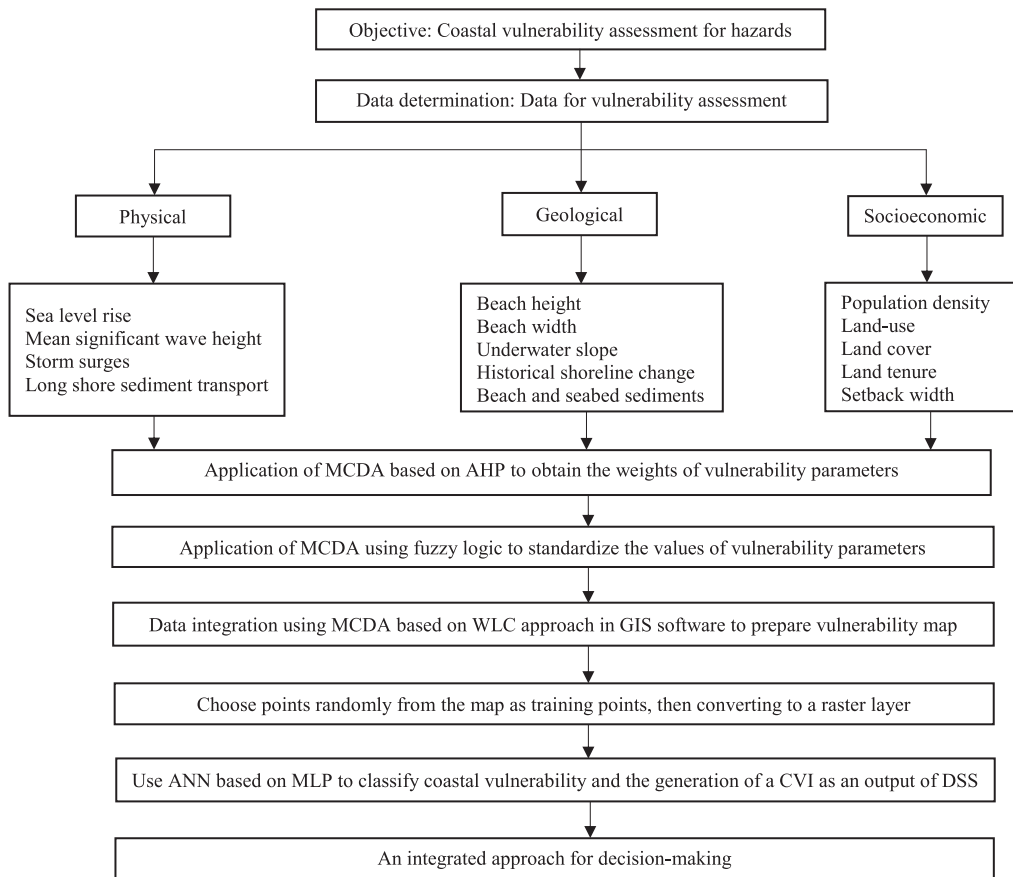
Fig. 3. An integrated DSS workflow for a coastal vulnerability assessment using GIS-MCDA-ANN.
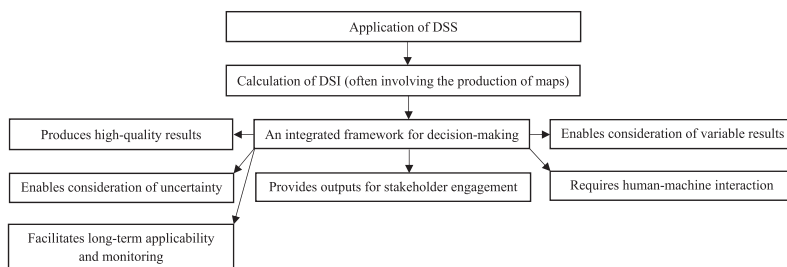
Fig. 4. Effectiveness of using a DSS for coastal planning and management.

readily able to be used in consultation, this combination has been very widely used (Malczewski, 2006). However, the advantages of incorporating ANN are now recognized (Yariyan et al., 2020a). The GIS-MCDA-ANN combination is likely to become the standard for investigations that require the use of a DSS. Although this integrated DSS is appropriate where large input data are available for the important parameters, it may not be appropriate where sufficient input data are not available or able to be produced (Jena et al., 2020).

Best practice understanding of coastal risk and resilience is important for coastal protection and infrastructure development, and human

safety. The use of an appropriate DSS in planning and management is becoming widespread. This process can appropriately incorporate the consideration of economic and social parameters alongside environmental parameters. However, a DSS remains a support tool using realist rationality (Rousseau, 2020), essentially a normative and descriptive process (Jankelová and Puhovichová, 2020), which is data-based or model-based (Abdel-Fattah et al., 2021) and broadly aligned with science-based decision-making. Such an approach can be dismissive of both local interests and the preferences of stakeholders (Dhiman et al., 2018). While some DSTs allow for expert input, particularly for the

Table 3

Characteristics of various combinations of DSTs in a DSS. In the references, * indicates a coastal application, and ˆ indicates other applications.

DSS	References	Advantages	Limitations	Accessibility	Most commonly addressed problems
GIS MCDA	Bagdanavičiūtė et al. (2019)* [coastal risk assessment]; Hadipour et al. (2020a)* [coastal flooding risk assessment]; Tercan et al. (2020)* [offshore wind energy site selection]; Masoudi et al. (2021)ˆ [sustainable land-use planning]; Assumma et al. (2021)ˆ [land resilience assessment]	Provides for the contribution of experts and specialists. Provides outputs easily explained to communities (particularly maps) that can be used for consultation.	Access to a group of experts with knowledge across a range of fields is required. The method does not assess future changes. Unable to incorporate a very large dataset into the decision-making process.	GIS is widely used by environmental management professionals, and is available in most organizations. It is easy for practioners to access and learn the methods.	Environmental risk classification. Appropriate infrastructure site selection. Appropriate land-use zoning. Environmental resilience classification.
GIS ANN	Peponi et al. (2019)* [coastal erosion modelling]; Dao et al. (2020)ˆ [the prediction of landslide susceptibility]	Excellent ability to work with noisy data in difficult, non-ideal contexts. Provides prediction of future environmental changes.	Does not provide the contribution of experts and specialists. Requires extensive training. Computationally expensive.	GIS is readily available in most organizations. ANN is difficult for practioners to access and learn the methods due to the need for special skills to develop the model.	Classification of environmental changes. Future environmental changes. Environmental hazards classification.
GEE ANN	Arruda et al. (2021)ˆ [forest fires assessment]; Vos et al. (2019)* [shoreline change assessment]	Access, manipulate, and analyze large amounts of data. The integration of various datasets. Uses freely available data sets (e.g. satellite images).	Requires high-end computer with large memory and storage for the maps and images. Does not integrate experts' knowledge into decision-making. Requires extensive training. Computationally expensive.	GEE is easily available to practioners and it is easy to learn how to use the tools. Spatial data and images are readily available, with coverage continually improving. Statistical and computing skills are required for advanced functionality. ANN is difficult for practioners to access and learn the methods.	Ranking and classifying environmental changes. Environmental hazards classification
GIS BN	Sahin et al. (2019)* [sea level rise and coastal erosion]; Furlan et al. (2020)* [maritime spatial planning]; Guo et al. (2020)ˆ [ecological risk prevention assessment]	Convenient for locations where either data is unavailable or difficult to collect, or local conditions are challenging for physical data collection.	Computational complexity. Not able to show the dynamic relationships and feedbacks between parameters.	GIS is extremely available to the public. BN is less accessible to practitioners due to unfamiliarity with software.	Probability modelling of environmental changes. Prediction of environmental hazards
GIS MCDA ANN	Jena et al. (2020)ˆ [earthquake risk assessment]; Pham et al. (2021)ˆ [flood risk assessment]; Yariyan et al. (2020a)ˆ [earthquake risk assessment]	Possibility for the contribution of experts and specialists. Provides outputs with good accuracies that can be used for community consultation. Validation of results. Sensitivity analysis and error determination in weighting of parameters.	Requires large datasets. Advanced computing skills are required.	GIS and MCDA allow the incorporation of practioners local knowledge. ANN is difficult for practioners to access and learn the methods.	Environmental risk classification.

weight given to certain parameters, a DSS as described above does not allow for the direct application of less quantifiable values, emotions, preferences, motivations, intuitions, traditions, and experiences of decision-makers, professionals, stakeholders, and community members, all of which must be taken into account for optimal decision making (Hahn et al., 2018). The use of a DSS must therefore only be regarded as a part of the final decision-making process and does not abrogate the responsibility of decision-makers to incorporate the less quantifiable factors (Ibrahim, 2018).

7. Conclusions

Based on the review of recent literature, we conclude that the integration of GIS, multi-criteria decision analysis (MCDA), and artificial neural network (ANN) is a useful combination of decision support tools (DSTs) to apply to many coastal problems. The resulting decision support system (DSS) can assist coastal managers and stakeholders mitigate current coastal hazards and help predict future coastal changes. Outputs

may include resources, such as maps, that can be used for the communication of management options for mitigation and adaptation.

A DSS serves to assist decision-makers, consultants, and governmental authorities to determine appropriate coastal buffer zones and vulnerable coastal areas requiring protection, identify where development may occur in areas with high resilience, and prioritize areas with high risk or high resilience to inform investment decisions. The outputs of DSSs, including decision support indices (DSI), can be used to engage with managers, stakeholders, community and governmental organizations for a better understanding of the options for environmental hazard management and adaptation.

While not neglecting the requirement to consider less tangible parameters such as values, traditions, and preferences, the use of evidence-based management tools based on high-quality data and analysis is vital for a prosperous society and a sustainable coastal environment. An integrated decision support framework can assist with the planning of appropriate mitigation and adaptation measures, providing for human safety and protection of infrastructure and the coastal environment

sustainability in the long term.

Ethical statement

We declare that this manuscript has not been previously published and is not under consideration for publication elsewhere; that its publication is approved by all authors. All authors have contributed sufficiently to the paper to be included as authors.

Declaration of competing interest

The authors declare that they have no known competing financial interests or personal relationships that could have appeared to influence the work reported in this paper.

Acknowledgments

References

Abdel-Fattah, D., Trainor, S., Hood, E., Hock, R., Kienholz, C., 2021. User engagement in developing use-inspired glacial lake outburst flood decision support tools in Juneau and the Kenai Peninsula, Alaska. Front. Earth Sci. 9, 635163. https://doi.org/10.3389/feart.2021.635163.

Adem Esmail, B., Geneletti, D., 2018. Multi-criteria decision analysis for nature conservation: a review of 20 years of applications. Methods Ecol. Evol. 9, 42–53. https://doi.org/10.1111/2041-210X.12899.

Adger, W.N., 2006. Vulnerability. Glob. Environ. Change 16 (3), 268–281. https://doi.org/10.1016/j.gloenvcha.2006.02.006.

Ahmadlou, M., Al-Fugara, A., Al-Shabeeb, A.R., Arora, A., Al-Adamat, R., Pham, Q.B., Al-Ansari, N., Linh, N.T.T., Sajedi, H., 2020. Flood susceptibility mapping and assessment using a novel deep learning model combining multilayer perceptron and autoencoder neural networks. J. Flood Risk Manag. 14, 1–22. https://doi.org/10.1111/jfr3.12683.

Ahmed, N., Howlader, N., Al-Amin Hoque, M., Pradhan, B., 2021. Coastal erosion vulnerability assessment along the eastern coast of Bangladesh using geospatial techniques. Ocean Coast Manag. 199, 105408. https://doi.org/10.1016/j.ocecoaman.2020.105408.

Alsdorf, D.E., Rodriguez, E., Lettenmaier, D.P., 2007. Measuring surface water from space. Rev. Geophys. 45 (2), RG2002. https://doi.org/10.1029/2006RG000197.

Aporta, C., Bishop, B., Choi, O., Wang, W., 2020. Knowledge and data: an exploration of the use of inuit knowledge in decision support systems in marine management. In: Chircop, A., Goerlandt, F., Aporta, C., Pelot, R. (Eds.), Governance of Arctic Shipping - Rethinking Risk, Human Impacts and Regulation. Springer, pp. 151–170. https://doi.org/10.1007/978-3-030-44975-9.

Arabameri, A., Chandra Pal, S., Rezaie, F., Chakrabortty, R., Chowdhuri, I., Blaschke, T., Thao Thi Ngo, P., 2021. Comparison of multi-criteria and artificial intelligence models for land-subsidence susceptibility zonation. J. Environ. Manag. 284, 112067. https://doi.org/10.1016/j.jenvman.2021.112067.

Araya-Munoz, D., Metzger, M.J., Stuart, N., Wilson, A.M.W., Carvajal, D., 2017. A spatial fuzzy logic approach to urban multi-hazard impact assessment in Concepcion, Chile. Sci. Total Environ. 576, 508–519. https://doi.org/10.1016/j.scitotenv.2016.10.077.

Arruda, V.L.S., Piontekowski, V.J., Alencar, A., Pereira, R.S., Matricardi, E.A.T., 2021. An alternative approach for mapping burn scars using Landsat imagery, Google Earth Engine, and Deep Learning in the Brazilian Savanna. Rem. Sens. Appl. Soc. Environ. 22, 100472. https://doi.org/10.1016/j.rsase.2021.100472.

Assumma, V., Bottero, M., De Angelis, E., Lourenco, J.M., Monaco, R., Soares, A.J., 2021. A decision support system for territorial resilience assessment and planning: an application to the Douro Valley (Portugal). Sci. Total Environ. 756, 143806. https://doi.org/10.1016/j.scitotenv.2020.143806.

Bagdanavičiūtė, I., Kelpšaitė-Rimkienė, L., Galinienė, J., Soomere, T., 2019. Index based multi-criteria approach to coastal risk assessment. J. Coast Conserv. 23 (4), 785–800. https://doi.org/10.1007/s11852-018-0638-5.

Bagdanavičiūtė, I., Kelpšaitė, L., Soomere, T., 2015. Multi-criteria evaluation approach to coastal vulnerability index development in micro-tidal low-lying areas. Ocean Coast Manag. 104, 124–135. https://doi.org/10.1016/j.ocecoaman.2014.12.011.

Barzehkar, M., Parnell, K.E., Mobarghaee Dinan, N., Brodie, G., 2020. Decision support tools for wind and solar farm site selection in Isfahan Province, Iran. Clean Technol. Environ. Policy. https://doi.org/10.1007/s10098-020-01978-w.

Barzehkar, M., Mobarghaee Dinan, N., Salemi, A., 2016. Environmental capability evaluation for nuclear power plant site selection: a case study of Sahar Khiz Region

in Gilan Province, Iran. Environ. Earth Sci. 75, 1016. https://doi.org/10.1007/s12665-016-5825-9.

Bayat, M., Ghorbanpour, M., Zare, R., Jaafari, A., Pham, B.T., 2019. Application of artificial neural networks for predicting tree survival and mortality in the Hyrcanian forest of Iran. Comput. Electron. Agric. 164, 104929. https://doi.org/10.1016/j.compag.2019.104929.

Berk, R.A., 2006. An introduction to ensemble methods for data analysis. Socio. Methods Res. 34 (3), 263–295. https://doi.org/10.1177/0049124105283119.

Booij, N., Ris, R.C., Holthuijsen, L.H., 1999. A third-generation wave model for coastal regions: 1. model description and validation. J. Geophys. Res. Oceans 104 (C4), 7649–7666. https://doi.org/10.1029/98JC02622.

Chaib, W., Guerfi, M., Hemdane, Y., 2020. Evaluation of coastal vulnerability and exposure to erosion and submersion risks in Bou Ismail Bay (Algeria) using the coastal risk index (CRI). Arab. J. Geosci. 13, 420. https://doi.org/10.1007/s12517-020-05407-6.

Chini, N., Stansby, P., 2015. Broad-scale hydrodynamic simulation, wave transformation and sediment pathways. In: Nicholls, R.J., Dawson, R.J., Day, S.A. (Eds.), Broad Scale Coastal Simulation. Advances in Global Change Research 49. Springer, Dordrecht, pp. 103–124. https://doi.org/10.1007/978-94-007-5258-0_3.

Chu, L., Oloo, F., Sudmanns, M., Tiede, D., Hölbling, D., Blaschke, T., Teleoaca, I., 2020. Monitoring long-term shoreline dynamics and human activities in the Hangzhou Bay, China, combining daytime and nighttime EO data. Big Earth Data 4 (3), 242–264. https://doi.org/10.1080/20964471.2020.1740491.

Coelho, C., Narra, P., Marinho, B., Lima, M., 2020. Coastal management software to support the decision-makers to mitigate coastal erosion. J. Mar. Sci. Eng. 8, 37. https://doi.org/10.3390/jmse8010037.

Dao, D.V., Jaafari, A., Bayat, M., Mafi-Gholami, D., Qi, C., Moayedi, H., Phong, T.V., Bang Ly, H., Thinh Le, T., Trinh, P.T., Luu, C., Quoc, N.K., Thanh, B.N., Pham, B.T., 2020. A spatially explicit deep learning neural network model for the prediction of landslide susceptibility. Catena 188, 104451. https://doi.org/10.1016/j.catena.2019.104451.

De Serio, F., Armenio, E., Mossa, M., Petrillo, A.F., 2018. How to define priorities in coastal vulnerability assessment. Geosci. 8 (11), 415. https://doi.org/10.3390/geosciences8110415.

Dhiman, R., Kalbar, P., Inamdar, A.B., 2019. Spatial planning of coastal urban areas in India: current practice versus quantitative approach. Ocean Coast Manag. 182, 104929. https://doi.org/10.1016/j.ocecoaman.2019.104929.

Dhiman, R., Kalbar, P., Inamdar, A.B., 2018. GIS coupled multiple criteria decision making approach for classifying urban coastal areas in India. Habitat Int. 71, 125–134. https://doi.org/10.1016/j.habitatint.2017.12.002.

DHI, 2017. MIKE 21 Spectral Waves FM. Spectral Wave Module. User Guide.

Diaz-Cuevas, P., Prieto-Campos, A., Zujar, J.O., 2020. Developing a beach erosion sensitivity indicator using relational spatial databases and Analytic Hierarchy Process. Ocean Coast Manag. 189, 105146. https://doi.org/10.1016/j.ocecoaman.2020.105146.

Easterling, D.R., Meehl, G.A., Parmesan, C., Changnon, S.A., Karl, T.R., Mearns, L.O., 2000. Climate extremes: observations, modeling, and impacts. Science 289 (5487), 2068–2074. https://doi.org/10.1126/science.289.5487.2068.

Farquharson, L.M., Mann, D.H., Swanson, D.K., Jones, B.M., Buzard, R.M., Jordan, J.W., 2018. Temporal and spatial variability in coastline response to declining sea-ice in northwest Alaska. Mar. Geol. 404, 71–83. https://doi.org/10.1016/j.margeo.2018.07.007.

Furlan, E., Dalla Pozza, P., Michetti, M., Torresan, S., Critto, A., Marcomini, A., 2021. Development of a Multi-Dimensional Coastal Vulnerability Index: assessing vulnerability to inundation scenarios in the Italian coast. Sci. Total Environ. 144650 https://doi.org/10.1016/j.scitotenv.2020.144650.

Furlan, E., Slanzi, D., Torresan, S., Critto, A., Marcomini, A., 2020. Multi-scenario analysis in the Adriatic Sea: a GIS-based Bayesian network to support maritime spatial planning. Sci. Total Environ. 703, 134972. https://doi.org/10.1016/j.scitotenv.2019.134972.

Gallego Perez, B.E., Selvaraj, J.J., 2019. Evaluation of coastal vulnerability for the District of Buenaventura, Colombia: a geospatial approach. Rem. Sens. Appl.: Soc. Environ. 16, 100263. https://doi.org/10.1016/j.rsase.2019.100263.

Gargiulo, C., Battarra, R., Tremiterra, M.R., 2020. Coastal areas and climate change: a decision support tool for implementing adaptation measures. Land Use Pol. 91, 104413. https://doi.org/10.1016/j.landusepol.2019.104413.

Garmendia, E., Gamboa, G., Franco, J., Garmendia, J.M., Liria, P., Olazabal, M., 2010. Social multi-criteria evaluation as a decision support tool for integrated coastal zone management. Ocean Coast Manag. 53, 385–403. https://doi.org/10.1016/j.ocecoaman.2010.05.001.

Ghorbanzadeh, O., Blaschke, T., Gholamnia, K., Meena, S.R., Tiede, D., Aryal, J., 2019. Evaluation of different machine learning methods and deep-learning convolutional neural networks for landslide detection. Rem. Sens. 11, 196. https://doi.org/10.3390/rs11020196.

Ghosh, P., Lepcha, K., 2019. Weighted linear combination method versus grid based overlay operation method – a study for potential soil erosion susceptibility analysis of Malda district (West Bengal) in India. Egypt. J. Rem. Sens. Space Sci. 22, 95–115. https://doi.org/10.1016/j.ejrs.2018.07.002.

Giardino, A., Diamantidou, E., Pearson, S., Santinelli, G., Heijer, K.D., 2019. A regional application of Bayesian modeling for coastal erosion and sand nourishment management. Water 11, 61. https://doi.org/10.3390/w11010061.

Goldstein, E.B., Coco, G., Plant, N.G., 2019. A review of machine learning applications to coastal sediment transport and morphodynamics. Earth Sci. Rev. 194, 97–108. https://doi.org/10.1016/j.earscirev.2019.04.022.

Gudiyangada Nachappa, T., Tavakkoli Piralilou, S., Gholamnia, K., Ghorbanzadeh, O., Rahmati, O., Blaschke, T., 2020. Flood susceptibility mapping with machine

learning, multi-criteria decision analysis and ensemble using Dempster Shafer theory. J. Hydrol. 590, 125275. https://doi.org/10.1016/j.jhydrol.2020.125275.

Guo, K., Zhang, X., Kuai, X., Wu, Z., Chen, Y., Liu, Y., 2020. A spatial Bayesian-network approach as a decision-making tool for ecological-risk prevention in land ecosystems. Ecol. Model. 419, 108929. https://doi.org/10.1016/j.ecolmodel.2019.108929.

Hadipour, V., Vafaie, F., Deilami, K., 2020a. Coastal flooding risk assessment using a GIS-based spatial multi-criteria decision analysis approach. Water 12 (9), 2379. https://doi.org/10.3390/w12092379.

Hadipour, V., Vafaie, F., Kerle, N., 2020b. An indicator-based approach to assess social vulnerability of coastal areas to sea: level rise and flooding: a case study of Bandar Abbas city, Iran. Ocean Coast Manag. 188, 105077. https://doi.org/10.1016/j.ocecoaman.2019.105077.

Hahn, T., Figge, F., Pinkse, J., Preuss, L., 2018. A paradox perspective on corporate sustainability: descriptive, instrumental, and normative aspects. J. Bus. Ethics 148, 235–248. https://doi.org/10.1007/s10551-017-3587-2.

Haque, A.N., 2016. Application of multi-criteria analysis on climate adaptation assessment in the context of least developed countries. J. Multi-Criteria Decis. Anal. 23, 210–224. https://doi.org/10.1002/mcda.1571.

Hill, T., Marquez, L., O'Connor, M., Remus, W., 1994. Artificial neural network models for forecasting and decision making. Int. J. Forecast. 10 (1), 5–15. https://doi.org/10.1016/0169-2070(94)90045-0.

Hoque, M.A.A., Pradhan, B., Ahmed, N., Ahmed, B., Alamri, A.M., 2021. Cyclone vulnerability assessment of the western coast of Bangladesh. Geomatics, Nat. Hazards Risk 12, 198–221. https://doi.org/10.1080/19475705.2020.1867652.

Hoque, M.A.A., Ahmed, N., Pradhan, B., Roy, S., 2019. Assessment of coastal vulnerability to multi-hazardous events using geospatial techniques along the eastern coast of Bangladesh. Ocean Coast Manag. 181, 104898. https://doi.org/10.1016/j.ocecoaman.2019.104898.

Hünicke, B., Zorita, E., Soomere, T., Madsen, K.S., Johansson, M., Suursaar, Ü., 2015. Recent change - sea level and wind waves. In: The BACC II Author Team, Second Assessment of Climate Change for the Baltic Sea Basin, Regional Climate Studies. Springer, pp. 155–185. https://doi:10.1007/978-3-319-16006-1_9.

Ibrahim, O., 2018. Design and Investigation of a Decision Support System for Public Policy Formulation. Academic Dissertation for the Degree of Doctor of Philosophy. Computer and Systems Sciences. Stockholm University, p. 102.

Ishtiaque, A., Eakin, H., Chhetri, N., Myint, S.W., Dewan, A., Kamruzzaman, M., 2019. Examination of coastal vulnerability framings at multiple levels of governance using spatial MCDA approach. Ocean Coast Manag. 171, 66–79. https://doi.org/10.1016/j.ocecoaman.2019.01.020.

Iyalomhe, F., Rizzi, J., Torresan, S., Gallina, V., Critto, A., Marcomini, A., 2013. Inventory of GIS-based decision support systems addressing climate change impacts on coastal waters and related inland watersheds. In: Singh, B.H. (Ed.), Climate Change – Realities, Impacts over Ice Cap, Sea Level and Risks. InTech Open, pp. 251–272. https://doi.org/10.5772/51999 (Chapter 10).

Jankelová, N., Puhovichová, D., 2020. Normative and descriptive perception of strategic decision making. SHS Web Conf 83, 01027. https://doi.org/10.1051/shsconf/20208301027.

Jena, R., Pradhan, B., Beydoun, G., Ardiansyah, N., Sofyan, H., Affan, M., 2020. Integrated model for earthquake risk assessment using neural network and analytic hierarchy process: aceh province, Indonesia. Geosci. Front. 11, 613–634. https://doi.org/10.1016/j.gsf.2019.07.006.

Johnston, A., Slovinsky, P., Yates, K.L., 2014. Assessing the vulnerability of coastal infrastructure to sea level rise using multi- criteria analysis in Scarborough, Maine (USA). Ocean Coast Manag. 95, 176–188. https://doi.org/10.1016/j.ocecoaman.2014.04.016.

Kane, I.O., Vanderlinden, J.P., Baztan, J., Touili, N., Claus, S., 2014. Communicating risk through a DSS: a coastal risk centred empirical analysis. Coast. Eng. 87, 240–248. https://doi.org/10.1016/j.coastaleng.2014.01.007.

Kao, C., 2010. Fuzzy data standardization. IEEE Trans. Fuzzy Syst. 18 (4), 745–754. https://doi.org/10.1109/TFUZZ.2010.2047948.

Kim, M., You, S., Chon, J., Lee, J., 2017. Sustainable land-use planning to improve the coastal resilience of the social-ecological landscape. Sustainability 9, 1086. https://doi.org/10.3390/su9071086.

Kitsios, F., Kamariotou, M., 2018. Decision support systems and strategic planning: information technology and SMEs' performance. Int. J. Decis. Support Syst. 3, 53–70. https://doi.org/10.1504/IJDSS.2018.094260.

Klutho, S., 2013. Mathematical Decision Making: an Overview of the Analytic Hierarchy Process. Whitman College. https://www.whitman.edu/Documents/Academics/Mathematics/Klutho.pdf. (Accessed 5 May 2021).

Komen, G.J., Cavaleri, L., Donelan, M., Hasselmann, K., Hasselmann, S., Janssen, P.A.E. M., 1994. Dynamics and Modelling of Ocean Waves. Cambridge University Press. https://doi.org/10.1017/CBO9780511628955.

Kontopoulos, C., Grammalidis, N., Kitsiou, D., Charalampopoulou, V., Tzepkenlis, A., Patera, A., Pataki, Z., Li, Z., Li, P., Guangxue, L., Lulu, Q., Dong, D., 2021. An integrated decision support system using satellite and in-situ data for coastal area hazard mitigation and resilience to natural disasters. In: EGU General Assembly 2021. https://doi.org/10.5194/egusphere-egu21-14674. EGU21-14674.

Koroglu, A., Ranasinghe, R., Jimenez, J.A., Dastgheib, A., 2019. Comparison of coastal vulnerability index applications for Barcelona province. Ocean Coast Manag. 178, 104799. https://doi.org/10.1016/j.ocecoaman.2019.05.001.

Kudryavtseva, N.A., Soomere, T., 2017. Satellite altimetry reveals spatial patterns of variations in the Baltic Sea wave climate. Earth Syst. Dyn. 8, 697–706. https://doi.org/10.5194/esd-8-697-2017.

Lamba, A., Cassey, P., Segaran, R.R., Koh, L.P., 2019. Deep learning for environmental conservation. Curr. Biol. 29 (19), 977–982. https://doi.org/10.1016/j.cub.2019.08.016.

Maanan, M., Maanan, M., Rueff, H., Adouk, N., Zourarah, B., Rhinane, H., 2018. Assess the human and environmental vulnerability for coastal hazard by using a multi-criteria decision analysis. Hum. Ecol. Risk Assess. 24, 6. https://doi.org/10.1080/10807039.2017.1421452.

Mafi-Gholami, D., Zenner, E.K., Jaafari, A., Riyahi Bakhtyari, H.R., Bui, D.T., 2019. Multi-hazards vulnerability assessment of southern coasts of Iran. J. Environ. Manag. 252, 109628. https://doi.org/10.1016/j.jenvman.2019.109628.

Malczewski, J., Rinner, C., 2015. GIScience, spatial analysis, and decision support. In: Malczewski, J., Rinner, C. (Eds.), Multicriteria Decision Analysis in Geographic Information Science. Springer, New York, pp. 3–21. https://doi.org/10.1007/978-3-540-74757-4.

Malczewski, J., 2006. GIS-based multicriteria decision analysis: a survey of the literature. Int. J. Geogr. Inf. Syst. 20 (7), 703–726. https://doi.org/10.1080/13658810600661508.

Malczewski, J., 2000. On the use of weighted linear combination method in GIS: common and best practice approaches. Trans. GIS 4 (1), 5–22. https://doi.org/10.1111/1467-9671.00035.

Mani Murali, R., Ankita, M., Vethamony, P., 2018. A new insight to vulnerability of Central Odisha coast, India using analytical hierarchical process (AHP) based approach. J. Coast Conserv. 22, 799–819. https://doi.org/10.1007/s11852-018-0610-4.

Marsooli, R., Lin, N., 2018. Numerical modeling of historical storm tides and waves and their interactions along the U.S. East and Gulf coasts. J. Geophys. Res. Oceans. 123, 3844–3874. https://doi.org/10.1029/2017JC013434.

Marto, M., Reynolds, K.M., Borges, J.G., Bushenkov, V.A., Marques, S., Marques, M., Barreiro, S., Botequim, B., Tomé, M., 2019. Web-based forest resources management decision support system. Forests 10, 1079. https://doi.org/10.3390/f10121079.

Masoudi, M., Centeri, C., Jakab, G., Nel, L., Mojtahedi, M., 2021. GIS-based multi-criteria and multi-objective evaluation for sustainable land-use planning (Case study: Qaleh Ganj county, Iran) "Landuse Planning Using MCE and Mola". Int. J. Environ. Res. 15, 1–18. https://doi.org/10.1007/s41742-021-00326-0.

Masselink, G., Hughes, M., Knight, J., 2011. Introduction to Coastal Processes and Geomorphology, second ed. Routledge.

McLaughlin, S., Cooper, J., Andrew, G., 2010. A multi-scale coastal vulnerability index: a tool for coastal managers? Environ. Hazards 9, 233–248. https://doi.org/10.3763/ehaz.2010.0052.

Mentaschi, L., Vousdoukas, M.I., Pekel, J.F., Voukouvalas, E., Feyen, L., 2018. Global long-term observations of coastal erosion and accretion. Sci. Rep. 8, 12876. https://doi.org/10.1038/s41598-018-30904-w.

Mioduszewski, J., Vavrus, S., Wang, M.Y., 2018. Diminishing Arctic sea ice promotes stronger surface wind. J. Clim. 31, 8101–8119. https://doi.org/10.1175/JCLI-D-18-0109.1.

Molino, G.D., Kenney, M.A., Sutton-Grier, A.E., 2020. Stakeholder-defined scientific needs for coastal resilience decisions in the Northeast. U.S. Mar. Pol. 118, 103987. https://doi.org/10.1016/j.marpol.2020.103987.

Mucerino, L., Albarella, M., Carpi, L., Besio, G., Benedetti, A., Corradi, N., Firpo, M., Ferrari, M., 2019. Coastal exposure assessment on Bonassola Bay. Ocean Coast Manag. 167, 20–31. https://doi.org/10.1016/j.ocecoaman.2018.09.015.

Mullick, M.R.A., Tanim, A.H., Samiul Islam, S.M., 2019. Coastal vulnerability analysis of Bangladesh coast using fuzzy logic based geospatial techniques. Ocean Coast Manag. 174, 154–169. https://doi.org/10.1016/j.ocecoaman.2019.03.010.

Myers, M.R., Barnard, P.L., Beighley, E., Cayan, D.R., Dugan, J.E., Feng, D., Hubbard, D.M., Iacobellis, S.F., Melack, J.M., Page, H.M., 2019. A multidisciplinary coastal vulnerability assessment for local government focused on ecosystems, Santa Barbara area, California. Ocean Coast Manag. 182, 104921. https://doi.org/10.1016/j.ocecoaman.2019.104921.

Nerem, R.S., Beckley, B.D., Fasullo, J.T., Hamlington, B.D., Masters, D., Mitchum, G.T., 2018. Climate-change-driven accelerated sea-level rise detected in the altimeter era. Proc. Natl. Acad. Sci. U. S. A. 115 (9), 2022–2025. https://doi.org/10.1073/pnas.1717312115.

Neves, C.F., 2020. A letter to my climate change skeptical neighbor: some thoughts about the coastal zone. Geo Mar. Lett. 40, 829–833. https://doi.org/10.1007/s00367-019-00586-y.

Ng, K., Borges, P., Philips, M.R., Medeiros, A., Calado, H., 2019. An integrated coastal vulnerability approach to small islands: the Azores case. Sci. Total Environ. 690, 1218–1227. https://doi.org/10.1016/j.scitotenv.2019.07.013.

Nichols, C.R., Wright, L.D., Bainbridge, S.J., Cosby, A., Henaff, A., Loftis, J.D., Cocquempot, L., Katragadda, S., Mendez, G.R., Letortu, P., Le Dantec, N., Resio, D., Zarillo, G., 2019. Collaborative science to enhance coastal resilience and adaptation. Front. Mar. Sci. 6, 404. https://doi.org/10.3389/fmars.2019.00404.

Nursey-Bray, M.J., Vince, J., Scott, M., Haward, M., O'Toole, K., Smith, T., Harvey, N., Clarke, B., 2014. Science into policy? Discourse, coastal management and knowledge. Environ. Sci. Pol. 38, 107–119. https://doi.org/10.1016/j.envsci.2013.10.010.

Palutikof, J.P., Rissik, D., Webb, S., Tonmoy, F.N., Boulter, S.L., Leitch, A.M., Perez Vidaurre, A.C., Campbell, M.J., 2019. CoastAdapt: an adaptation decision support framework for Australia's coastal managers. Climatic Change 153, 491–507. https://doi.org/10.1007/s10584-018-2200-8.

Panahi, M., Jaafari, A., Shirzadi, A., Shahabi, H., Rahmati, O., Omidvar, E., Lee, S., Bui, D.T., 2021. Deep learning neural networks for spatially explicit prediction of flash flood probability. Geosci. Front. 12 (3), 101076. https://doi.org/10.1016/j.gsf.2020.09.007.

Pan, P.S.Y., 2005. Monitoring coastal environments using remote sensing and GIS. In: Bartlett, D., Smith, J. (Eds.), GIS for Coastal Zone Management. CRC Press, US, pp. 61–75.

Peponi, A., Morgado, P., Trindade, J., 2019. Combining artificial neural networks and GIS fundamentals for coastal erosion prediction modeling. Sustainability 11, 975. https://doi.org/10.3390/su11040975.

Pham, B.T., Luu, C., Dao, D.V., Phong, T.V., Nguyen, H.D., Le, H.V., Meding, J.V., Prakash, I., 2021. Flood risk assessment using deep learning integrated with multi-criteria decision analysis. Knowl-Based Syst. 219, 106899. https://doi.org/10.1016/j.knosys.2021.106899.

Pindsoo, K., Soomere, T., 2020. Basin-wide variations in trends in water level maxima in the Baltic Sea. Continent. Shelf Res. 193, 104029. https://doi.org/10.1016/j.csr.2019.104029.

Plomaritis, T.A., Costas, S., Ferreira, O., 2018. Use of a Bayesian Network for coastal hazards, impact and disaster risk reduction assessment at a coastal barrier (Ria Formosa, Portugal). Coast. Eng. 134, 134–147. https://doi.org/10.1016/j.coastaleng.2017.07.003.

Poch, M., Comas, J., Rodríguez-Roda, I., Sànchez-Marrè, M., Cortés, U., 2004. Designing and building real environmental decision support systems. Environ. Model. Software 19, 857–873. https://doi.org/10.1016/j.envsoft.2003.03.007.

Povak, N.A., Giardina, C.P., Hessburg, P.F., Reynolds, K.M., Brion Salter, R., Heider, C., Salminen, E., MacKenzie, I., 2020. A decision support tool for the conservation of tropical forest and nearshore environments on Babeldaob Island, Palau. For. Ecol. Manage. 476, 118480. https://doi.org/10.1016/j.foreco.2020.118480.

Rangel-Buitrago, N., Neal, W.J., De Jonge, V.N., 2020a. Risk assessment as tool for coastal erosion management. Ocean Coast Manag. 186, 105099. https://doi.org/10.1016/j.ocecoaman.2020.105099.

Rangel-Buitrago, N., Gracia, C.A., Anfuso, G., Bonetti, J., 2020b. GIS hazard assessments as the first step to climate change adaptation. In: Leal, W.F., Nagy, G., Borga, M., Chavez Muñoz, D., Magnuszewski, A. (Eds.), Climate Change, Hazards and Adaptation Options. Springer, pp. 135–146. https://doi.org/10.1007/978-3-030-37425-9_6.

Rangel-Buitrago, N.G., Anfuso, G., Williams, A., Bonetti, J., Adriana, G.C., Carlos Ortiz, J., 2017. Risk assessment to extreme eave events: the Barranquilla – Cienaga, Caribbean of Colombia case study. In: Botero, C.M., Cervantes, O., Finkl, C.W. (Eds.), Beach Management Tools - Concepts, Methodologies and Case Studies. Springer, pp. 469–496. https://doi.org/10.1007/978-3-319-58304-4_23.

Rashidi, M., Ghodrat, M., Samali, B., Mohammadi, M., 2018. Decision support systems. In: Pomffyova, M. (Ed.), Management of Information Systems. InTech Open, pp. 19–38. https://doi.org/10.5772/intechopen.79390 (Chapter 2).

Reguero, B.G., Losada, I.J., Mendez, F.J., 2019. A recent increase in global wave power as a consequence of oceanic warming. Nat. Commun. 10, 205. https://doi.org/10.1038/s41467-018-08066-0.

Rodela, R., Bregt, A.K., Ligtenberg, A., Pérez-Soba, M., Verweij, P., 2017. The social side of spatial decision support systems: investigating knowledge integration and learning. Environ. Sci. Pol. 76, 177–184. https://doi.org/10.1016/j.envsci.2017.06.015.

Rousseau, D.M., 2020. The realist rationality of evidence-based management. Acad. Manag. Learn. Educ. 19 (3), 415–424. https://doi.org/10.5465/amle.2020.0050.

Roy, R., Gain, A.K., Samat, N., Hurlbert, M., Tan, M.L., Chan, N.W., 2019. Resilience of coastal agricultural systems in Bangladesh: assessment for agroecosystem stewardship strategies. Ecol. Indicat. 106, 105525. https://doi.org/10.1016/j.ecolind.2019.105525.

Rumson, A.G., Garcia, A.P., Hallett, S.H., 2020. The role of data within coastal resilience assessments: an East Anglia, UK, case study. Ocean Coast Manag. 185, 105004. https://doi.org/10.1016/j.ocecoaman.2019.105004.

Sahin, O., Stewart, R.A., Faivre, G., Ware, D., Tomlinson, R., Mackey, B., 2019. Spatial Bayesian Network for predicting sea level rise induced coastal erosion in a small Pacific Island. J. Environ. Manag. 238, 341–351. https://doi.org/10.1016/j.jenvman.2019.03.008.

Sajjad, M., Chan, J.C.L., Kanwal, S., 2020. Integrating spatial statistics tools for coastal risk management: a case-study of typhoon risk in mainland China. Ocean Coast Manag. 184, 105018. https://doi.org/10.1016/j.ocecoaman.2019.105018.

Santoro, F., Tonino, M., Torresan, S., Critto, A., Marcomini, A., 2013. Involve to improve: a participatory approach for a Decision Support System for coastal climate change impacts assessment. The North Adriatic case. Ocean Coast Manag. 78, 101–111. https://doi.org/10.1016/j.ocecoaman.2013.03.008.

Sarbayev, M., Yang, M., Wang, H., 2019. Risk assessment of process systems by mapping fault tree into artificial neural network. J. Loss Prev. Process. Ind. 60, 203–212. https://doi.org/10.1016/j.jlp.2019.05.006.

Schumacher, J., Schernewski, G., Bielecka, M., Loizides, M.I., Loizidou, X.I., 2018. Methodologies to support coastal management - a stakeholder preference and planning tool and its application. Mar. Pol. 94, 150–157. https://doi.org/10.1016/j.marpol.2018.05.017.

Şeker, D.Z., Tanık, A., Çitil, E., Öztürk, I., Övez, S., Baycan, T., 2016. Importance and vulnerability analyses for functional zoning in a coastal district of Turkey. Int. J. Environ. Geo. 3 (3), 76–91. https://doi.org/10.30897/ijegeo.306484.

Sekovski, I., Del Rio, L., Armaroli, C., 2020. Development of a coastal vulnerability index using analytical hierarchy process and application to Ravenna province (Italy). Ocean Coast Manag. 183, 104982. https://doi.org/10.1016/j.ocecoaman.2019.104982.

Serafim, M.B., Siegle, E., Cristina Corsi, A., Bonetti, J., 2019. Coastal vulnerability to wave impacts using a multi-criteria index: Santa Catarina (Brazil). J. Environ. Manag. 230, 21–32. https://doi.org/10.1016/j.jenvman.2018.09.052.

Simões Vieira, J.G.M., Salgueiro, J., Maia Soares, A.M.V.D., Azeiteiro, U., Morgado, F., 2017. An integrated approach to assess the vulnerability to erosion in mangroves using GIS models in a tropical coastal protected area. Int. J. Clim. Chang. Strateg. Manag. 11 (2), 289–307. https://doi.org/10.1108/IJCCSM-05-2017-0110.

Soomere, T., Eelsalu, M., Pindsoo, K., 2018. Variations in parameters of extreme value distributions of water level along the eastern Baltic Sea coast. Estuar. Coast Shelf Sci. 215, 59–68. https://doi.org/10.1016/j.ecss.2018.10.010.

Tamiminia, H., Salehi, B., Mahdianpari, M., Quackenbush, L., Adeli, S., Brisco, B., 2020. Google Earth Engine for geo-big data applications: a meta-analysis and systematic review. ISPRS J. Photogrammetry Remote Sens. 164, 152–170. https://doi.org/10.1016/j.isprsjprs.2020.04.001.

Tanner, T., Lewis, D., Wrathall, D., Bronen, R., Cradock-Henry, N., Huq, S., Lawless, C., Nawrotzki, R., Prasad, V., Rahman, M.A., Alaniz, R., King, K., McNamara, K., Nadiruzzaman, M., Henly-Shepard, S., Thomalla, F., 2014. Livelihood resilience in the face of climate change. Nat. Clim. Change 5 (1), 23–26. https://doi.org/10.1038/NCLIMATE2431.

Tercan, E., Tapkın, S., Latinopoulos, D., Dereli, M.A., Tsiropoulos, A., Ak, M.F., 2020. A GIS-based multi-criteria model for offshore wind energy power plants site selection in both sides of the Aegean Sea. Environ. Monit. Assess. 192, 652. https://doi.org/10.1007/s10661-020-08603-9.

Thi Ngo, P.T., Panahi, M., Khosravi, K., Ghorbanzadeh, O., Kariminejad, N., Cerda, A., Lee, S., 2021. Evaluation of deep learning algorithms for national scale landslide susceptibility mapping of Iran. Geosci. Front. 12, 505–519. https://doi.org/10.1016/j.gsf.2020.06.013.

Torresan, S., Critto, A., Rizzi, J., Zabeo, A., Furlan, E., Marcomini, A., 2016. DESYCO: a decision support system for the regional risk assessment of climate change impacts in coastal zones. Ocean Coast Manag. 120, 49–63. https://doi.org/10.1016/j.ocecoaman.2015.11.003.

Townend, B.I.H., French, J.R., Nicholls, R.J., Brown, S., Carpenter, S., Haigh, I.D., Hill, C. T., Lazarus, E., Penning-Rowsell, E.C., Thompson, C.E.L., Tompkins, E.L., 2021. Operationalising coastal resilience to flood and erosion hazard: a demonstration for England. Sci. Total Environ. 783, 146880. https://doi.org/10.1016/j.scitotenv.2021.146880.

Uhde, B., Andreas Hahn, W., Griess, V.C., Knoke, T., 2015. Hybrid MCDA methods to integrate multiple ecosystem services in forest management planning: a critical review. J. Environ. Manag. 56, 373–388. https://doi.org/10.1007/s00267-015-0503-3.

Vitousek, S., Barnard, P.L., Fletcher, C.H., Frazer, N., Erikson, L., Storlazzi, C.D., 2017a. Doubling of coastal flooding frequency within decades due to sea-level rise. Sci. Rep. 7 (1), 1399. https://doi.org/10.1038/s41598-017-01362-7.

Vitousek, S., Barnard, P.L., Limber, P., 2017b. Can beaches survive climate change? J. Geophys. Res. Earth. Surf. 122 (4), 1060. https://doi.org/10.1002/2017JF004308.

von Storch, H., Omstedt, A., Pawlak, J., Reckermann, M., 2015. Introduction and summary. In: The BACC II Author Team, Second Assessment of Climate Change for the Baltic Sea Basin, Regional Climate Studies. Springer, Cham, pp. 1–22. https://doi.org/10.1007/978-3-319-16006-1_1.

Vos, K., Splinter, K.D., Harley, M.D., Simmons, J.A., Turner, I.L., 2019. CoastSat: a Google Earth Engine-enabled Python toolkit to extract shorelines from publicly available satellite imagery. Environ. Model. Software 122, 104528. https://doi.org/10.1016/j.envsoft.2019.104528.

Vousdoukas, M.I., Mentaschi, L., Hinkel, J., Ward, P.J., Mongelli, I., Ciscar, J.C., Feyen, L., 2020. Economic motivation for raising coastal flood defenses in Europe. Nat. Commun. 11 (1), 1–11. https://doi.org/10.1038/s41467-020-15665-3.

Walling, E., Vaneeckhaute, C., 2020. Developing successful environmental decision support systems: challenges and best practices. J. Environ. Manag. 264, 110513. https://doi.org/10.1016/j.jenvman.2020.110513.

Westmacott, S., 2001. Developing decision support systems for integrated coastal management in the tropics: is the ICM decision-making environment too complex for the development of a useable and useful DSS? J. Environ. Manag. 62, 55–74. https://doi.org/10.1006/jema.2001.0420.

Wong-Parodi, G., Mach, K.J., Jagannathan, K., Sjostrom, K.D., 2020. Insights for developing effective decision support tools for environmental sustainability. Curr. Opin. Environ. Sustain. 42, 52–59. https://doi.org/10.1016/j.cosust.2020.01.005.

Yariyan, P., Zabihi, H., Wolf, I.D., Karami, M., Amiriyan, S., 2020a. Earthquake risk assessment using an integrated fuzzy analytic hierarchy process with artificial neural networks based on GIS: a case study of Sanandaj in Iran. Int. J. Disast. Risk. Re. 50, 101705. https://doi.org/10.1016/j.ijdrr.2020.101705.

Yariyan, P., Avand, M., Abbaspour, R.A., Karami, M., Tiefenbacher, J.P., 2020b. GIS-based spatial modeling of snow avalanches using four novel ensemble models. Sci. Total Environ. 745, 141008. https://doi.org/10.1016/j.scitotenv.2020.141008.

Yun, Y., Ma, D., Yang, M., 2021. Human-computer interaction-based decision support system with applications in data mining. Future Generat. Comput. Syst. 114, 285–289. https://doi.org/10.1016/j.future.2020.07.048.

Zanuttigh, B., Simcic, D., Bagli, S., Bozzeda, F., Pietrantoni, L., Zagonari, F., Hoggart, S., Nicholls, R.J., 2014. THESEUS decision support system for coastal risk management. Coast. Eng. 87, 218–239. https://doi.org/10.1016/j.coastaleng.2013.11.013.

II

Publication II

Barzehkar, M., Parnell, K., Soomere, T., Koivisto, M. 2024. Offshore wind power plant site selection in the Baltic Sea. Regional Studies in Marine Science, 73, 103469, doi: 10.1016/j.rsma.2024.103469.
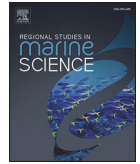
Offshore wind power plant site selection in the Baltic Sea

Mojtaba Barzehkar [a],[*], Kevin Parnell [a], Tarmo Soomere [a],[b], Matti Koivisto [c]

[a] *Department of Cybernetics, School of Science, Tallinn University of Technology, Tallinn, Estonia*
[b] *Estonian Academy of Sciences, 10130 Kohtu 6, Tallinn, Estonia*
[c] *Department of Wind and Energy Systems, Technical University of Denmark, Frederiksborgvej 399, Roskilde 4000, Denmark*

ARTICLE INFO

ABSTRACT

The selection of suitable sites for offshore wind power plants is an important marine spatial planning problem in the Baltic Sea. The application of multiple and different decision support tools (DSTs) can facilitate site selection. This study employs a geographical information system (GIS) integrated with the levelized cost of energy (LCOE) model, and GIS with multi-criteria decision analysis (MCDA) using an analytical hierarch process (AHP), fuzzy logic, weighted linear combination (WLC), and the technique for order of preference by similarity to ideal solution (TOPSIS) as an extension of MCDA. The core novelty of the study is the use of several concurrent state-of-the art techniques to quantify the detailed spatial pattern of suitability of different sea areas for offshore wind power plant installations for the entire Baltic Sea at an unprecedented, for such a large sea area, resolution. Important parameters were identified and data from the Global Wind Atlas, HELCOM, and EMODnet portals were used. The most appropriate areas exhibit LCOE values between 42 and 58 €/MWh, MCDA values in the range of 0.78–0.92, and capacity factor values from 0.52 to 0.55. The areas identified as the least appropriate were characterized by LCOE values ranging from 107 to 210 €/MWh, MCDA values between 0.34 and 0.59, and capacity factor values within the range of 0.30–0.43. The outcomes using both methodologies were similar. The decision preferred are mostly locations close to shore in shallow water and with a high capacity factor. The largest suitable areas are in the south-west Baltic Sea whereas some suitable locations are identified further to the north and east.

1. Introduction

The increasing demand for renewable energy worldwide mirrors the reduction in the use of fossil fuels, coupled with industrial development and population growth (Emeksiz and Demirci, 2019). Renewable energy technologies for the generation of electricity are being used and favoured worldwide (Akarsu and Genç, 2022), in large part as a response to climate change (Genç and Gökçek, 2009). Renewable energy can supply two-thirds of the total global energy demand by 2050 (Gielen et al., 2019).

One of the most important renewable energy resources is wind (Noorollahi et al., 2016; Gielen et al., 2019), which is a cost-effective, safe, and an environmentally preferred source for producing electricity (Baban and Parry, 2001; Latinopoulos and Kechagia, 2015). The use of wind energy has risen substantially in recent decades (Guchhait and Sarkar, 2023), primarily attributed to a reduction in the costs of generation (Osman et al., 2022). Wind energy also has the potential to produce power in the vicinity of load centers, mitigating transmission

losses and facilitating power distribution in remote regions (Genç, 2011).

The development of offshore wind power plants has the potential to generate more energy and reduce considerably aesthetic and noise effects compared to onshore wind farms (Bilgili et al., 2011; Wu et al., 2018). Greater economic benefits for offshore installations mostly stem from higher wind speeds in marine areas and more flexibility for the installation of devices. The expenses relating to foundation construction and cable connection depend primarily on the water depth and distance to shore (Khan et al., 2021) and the availability of suitable ports. On the one hand, more expensive foundations and/or longer cables are required when plant is located in deeper water or farther offshore. On the other hand, locations further from the shore may provide better wind conditions and thus a higher capacity factor. However, the construction of offshore wind power plants can conflict with human activities such as marine space for shipping, tourism, commercial fishing, and seabed resource exploitation (Virtanen et al., 2022).

Selecting an appropriate location for offshore wind power plants

requires a complex planning process that is based on diverse environmental, social, and economic factors (Tercan et al., 2020). There are conflicting objectives in the site selection process, which encompass reducing the rate of environmental disruption and maximizing economic profits (Golestani et al., 2021; Nedjati et al., 2021). Site selection for wind power plants has a major impact on energy production and installation costs (Shafiee, 2022). This kind of analysis is surprisingly scarce in the literature for the Baltic Sea region, an area that is considered as one of the best locations for production of offshore wind energy (Hasager et al., 2011, 2020; Shipkovs et al., 2013; Rusu, 2020). It has only addressed seabed characteristics (Nyberg et al., 2022). This study makes an attempt to systematically fill this gap based on contemporary decision support tools (DSTs).

It is well known that the application of DSTs can assist in selecting optimal locations for the establishment of renewable energy infrastructure (González and Connell, 2022). Several DSTs have been used for offshore wind power plant site selection. They commonly incorporate the use of Geographical Information Systems (GIS) and are popular for both onshore and offshore wind power plant site selection (Aydin et al., 2010; Emeksiz and Demirci, 2019; Vagiona and Karanikolas, 2012; Tegou et al., 2010).

The advantage of using a GIS is that it provides a systematic framework for analysis, processing, and management of spatial data that makes it possible to include various parameters together with specific applications for their analysis (Díaz-Cuevas et al., 2019). Multi-criteria decision analysis (MCDA) is a widely used method for ranking and prioritizing different locations, and for the integration of qualitative and quantitative attributes in the decision-making process (Mytilinou et al., 2018). GIS combined with MCDA methods is often used to address holistically the renewable energy site selection issues (Vagiona et al., 2022). A GIS-based MCDA is a methodology that integrates geographical information (input maps) and the priorities of experts into an output (Malczewski and Rinner, 2015). There have been numerous studies using GIS with MCDA (Gil-García et al., 2022; Genç et al., 2021; Li et al., 2022). MCDA methods are highly suitable for large-scale marine spatial planning (Tercan et al., 2020) and are now well established for site-selection studies.

Spyridonidou and Vagiona (2020) added the technique for order of preference by similarity to ideal solution (TOPSIS) to their analysis. Vagiona and Kamilakis (2018) concluded that the combined application of GIS with analytical hierarch process (AHP) and TOPSIS methods is useful to rank suitable areas in hierarchical order. There is still discussion as to whether the TOPSIS method provides significant added value to the analysis, as noted, e.g., by Gil-García et al. (2022) in a study of wind power plant site selection in the Gulf of Maine, USA. In our study, we address this issue in the context of the Baltic Sea, in a greatly different context and wind climate.

Another approach to the problem of site selection is the levelized cost of energy (LCOE) technique applied to a similar problem by Martinez and Iglesias (2022). This approach has been extensively used for single (sets of) mainland locations (Genç et al., 2012a; 2012b; Gökçek and Genç, 2009, among many others). However, it has been usually applied only for sea areas of fairly limited size, such as sea areas surrounding Denmark (Möller et al., 2012), the UK renewable energy zone (Cavazzi and Dutton, 2016), Canarian waters (Schallenberg-Rodríguez and Montesdeoca, 2018), Turkey's seas (Genç et al., 2021), or the Gulf of Maine (Gil-García et al., 2022).

While the use of DSTs to assist with wind energy generation site selection is now commonplace, this study makes three particular contributions and innovations.

Firstly, we extend this type of analysis from looking at a few single locations or limited sea areas, to the construction of a Baltic-wide holistic view of spatial variations in the suitability of different areas for installing wind power plants, across many national borders and covering effectively about 400,000 km^2 of the region favorable for wind energy generation. To do so, our analyses use both LCOE and MCDA
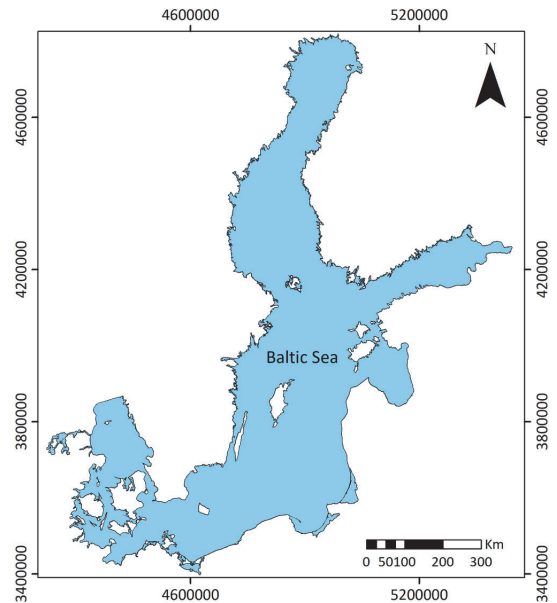
Fig. 1. The Baltic Sea.

methodologies within a GIS framework to easily enable consideration of large areas, such as the entire Baltic Sea. We benefit from the extensive coverage of the Baltic Sea for the necessary data.

Secondly, given the scale of the addressed region, we perform the analysis with a very high resolution (about 5 km) that resolves the properties of the marine environment and uses of marine space with unprecedented accuracy, comparable to the examples of this analysis for relatively small mainland regions (Karipoğlu et al., 2021).

Thirdly, the LCOE model analysis has been applied in an integrated GIS environment in combination with more conventional MCDA (plus TOPSIS) methods to provide extra confidence in the results.

Finally, we provide detailed consideration of a large number of parameters, some of which have been overlooked in earlier studies, in conjunction with existing wind farm sites, and with suggestions for new wind farm locations.

This approach eventually can foster international cooperation in the field and ultimately, better use of resources. In addition, application in a GIS framework provides tools for easy dissemination of results to a range of audiences, stakeholders and decision-makers. The results can be immediately applied to specify the optimal location of new wind power plants that are being currently considered (Danish Energy Agency DEA, 2022) in the Baltic Sea.

Our analysis focuses on large offshore wind turbines that are commonly used or are planned to be used in the Baltic Sea and reflected in the Danish Energy Agency (DEA) guidelines. Extension of our results to other types of devices and different systems, including those considered in (Genç et al., 2012a, 2012b; Gökçek and Genç, 2009), is basically straightforward as for doing so it is only needed to replace the relevant parameters that are constant for the entire study area. However, the resulting pattern is generally not invariant with respect to a change in the device type.

The composition of the paper follows the classic scheme. Section 2 introduces the study area and describes the used material, the variety of employed data sets and applied methods, and presents the flowchart of their use. Section 3 provides an overview of spatial patterns of suitability of sea areas as wind farm locations from different viewpoints and portrays differences of this pattern obtained using different methods and/or

external restrictions. The discussion in Section 4 attempts to relate some specific features of environmental and sea space use data with the resulting maps while the core conclusions are formulated in Section 6.

2. Materials and methods

2.1. The study area

The study area, the Baltic Sea (Fig. 1), is a semi-enclosed sea in Northern Europe. It is surrounded by Finland, Estonia, Lithuania, Latvia, Denmark, Sweden, Germany, Poland and Russia, with an area of 392,978 km^2, an average water depth of 54 m and brackish water ecosystem (Leppäranta and Myrberg, 2009).

The Baltic Sea is subjected to a variety of human pressures including fisheries, offshore wind power plants, shipping, and tourism (Reckermann et al., 2022). Interest in wind power generation in the Baltic Sea (particularly in the south) has significantly increased, with a lot of research on technical aspects (Klinge Jacobsen et al., 2019; Scolaro and Kittner, 2022; Ziemba, 2022) while recognizing that these developments have effects on marine ecosystems, shipping routes, coastal tourism, fisheries, and socioeconomic aspects (Reckermann et al., 2022). Thus, the evaluation of optimal locations for offshore wind power plants incorporating technical and socio-economic and environmental variables is urgent, to reduce environmental concerns and boost energy production (Tercan et al., 2020). Increased production capacity has become even more urgent with the significant reduction of energy supplied from the Russian Federation (European Commission, 2022).

2.2. Methodology

2.2.1. Levelized cost of energy (LCOE) model

In the energy sector, the levelized cost of energy (LCOE; or levelized cost of electricity when relating to the electricity market specifically) is the most common way of calculating and discussing the cost of electricity (Johnston et al., 2020) and other carriers of energy, such as hydrogen (Genç et al., 2012a). This is the reason why this quantity is commonly used in estimates of economic feasibility of energy production at a particular site. The numerical values of LCOE represent the ratio of the costs of energy production to the energy generation over the total lifetime of a project. These costs are usually split into the initial (nonrecurring investment) costs (from setup and planning, feasibility studies, permits and legal costs over investments into development and build etc., until decommission) and recurring operational costs (maintenance, fuel, and similar). The LCOE is thus the average cost per unit of output over the lifetime of the project or wind turbine. The principal expression for the LCOE values is (Johnston et al., 2020)

$$LCOE = \frac{\widehat{C}}{\widehat{E}} = \frac{\sum_{t=0}^{t=\mathrm{LT}} C}{\sum_{t=0}^{t=\mathrm{LT}} E}. \tag{1}$$

Here, $\widehat{C}$ is the total cost over the entire lifetime (with a dimension of some currency) and $\widehat{E}$ is the total output (e.g., MWh for electricity or kg for hydrogen) from the launch of the project at some time instant $t = 0$ to the end of life at some (usually much later) time instant $t = $ LT, after full decommissioning and eventually environmental rehabilitation of the site.

The quantities $\widehat{C}$ and $\widehat{E}$ may involve a multitude of constituents C and E that appear in the cost list during different time periods and may have different expected service times and/or discount rates, and may be modulated by different escalation rates (e.g., Genç et al., 2012a). In the energy sector, the constituents and discount rates are usually expressed as annual values. The total cost is traditionally split into the investment cost I_t in a specific year t, operations and maintenance expenditures M_t and fuel cost F_t. For the constant discount rate $r\%$ and LT years of

lifetime, the constituents of the right hand side of Eq. (1) read (Johnston et al., 2020):

$$\widehat{C} = \sum_{t=1}^{t=\mathrm{LT}} \frac{I_t + M_t + F_t}{(1 + r)^t}, \quad \widehat{E} = \sum_{t=1}^{t=\mathrm{LT}} \frac{E_t}{(1 + r)^t}. \tag{2}$$

For marine wind turbines, fuel costs are evidently zero except for maintenance-related fuel. For more complicated systems (e.g., including battery bank) and processes with different properties Eq. (2) can be expanded to explicitly embrace, e.g., the capital cost of each component (wind turbine, battery bank, civil works, inverter, miscellaneous) as well as an option to adjust for escalation (Genç et al., 2012a) as kindly but strongly suggested by one anonymous referee. In such a case Eq. (1) obtains a more complicated appearance:

$$LCOE = \frac{\sum_{i=1}^{n} (C_i \times CRF_i) + C_{om}}{E_p}, \tag{3}$$

where C_i

$$C_i = I_{we} \times P_r. \tag{4}$$

represents the capital cost of each component (e.g., wind turbine, battery bank, civil works, inverter, miscellaneous expenses), expressed as the product of the specific cost I_{we} of each component and the rated power P_r (maximum power output that a wind turbine can generate under optimal conditions), and E_p is the total output expressed similar to Eq. (2). In essence, it is the potential maximum output multiplied by so-called capacity factor. This representation encounters the situation where capital recovery factors CRF_i of single components may have different discount rate r and lifetime T_i (Genç et al., 2012a):

$$CRF_i = \frac{(1 + r)^{T_i} \times r}{(1 + r)^{T_i} - 1}. \tag{5}$$

The method developed in Genç et al. (2012a) makes it possible to take into account escalation of operation and maintenance costs M_t [€/year] adjusted for escalation and calculated (Genç et al., 2012a):

$$\widehat{M}_t = C_{om-esc} = \frac{C_{om}}{r - e_{om}} \left[1 - \frac{(1 + e_{om})^{T_i}}{(1 + r)^{T_i}} \right], \tag{6}$$

where $C_{om} = M_1$ is the initial operation and maintenance cost for the first year, and e_{om} is the escalation ratio of operation and maintenance costs. The escalation ratio from 2015 to 2020 is approximately 0.986, indicating a 0.986% decrease in operational and maintenance costs over this period. On top of that, the model is expanded in Genç et al. (2012a) to incorporate situations when a wind turbine or farm is being sold or bought.

2.2.2. LCOE model for the Baltic Sea

The model described in the previous subsection can be used for many purposes, from estimates of feasibility of a few wind generators to estimates of the cost of electricity and subsequent hydrogen production reportedly reaching the accuracy of several valid significant digits (Genç, 2010; Akarsu and Genç, 2022) when all details are taken into account. As we focus on the quantification of different sea areas in terms of their suitability for wind farms, such exact estimates and exact representation of possible changes (escalation ratios) of operation and maintenance costs are not necessary. Instead, we aim at solutions that express the spatial pattern of LCOE generated by the variety of environmental conditions and assuming that all other aspects (e.g., the start of the project) are equal for any location.

This focus leads to several natural simplifications of the model expressed in Eqs. (3–6). First of all, the resulting pattern is invariant with respect to presence or absence of additional features (e.g., battery banks, hydrogen production, etc.). It is evident from the structure of Eq. (3) that
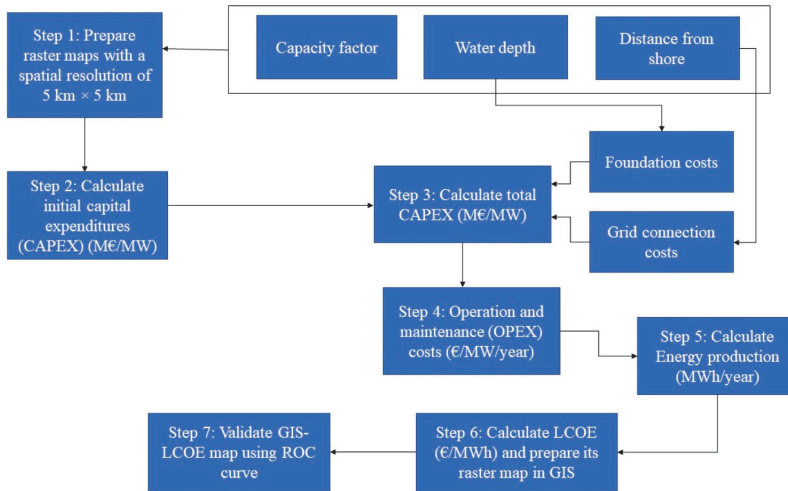
Fig. 2. Flowchart for offshore wind farm site selection methodology using GIS-LCOE.

accommodation of such features will only add a constant to the map of LCOE values and these features can be left out. Further, any escalation rate works uniformly for the entire study area. We focus on the task of highlighting the spatial pattern of LCOE under a fixed start instant of activity. For simplicity, we also assume that the capital recovery factor is the same for all non-recurring and recurring costs. In this framework, the expression for LCOE is essentially Eq. (2) with $F_t = 0$.

To maintain a visual link between the names and content of the used variables, we use the abbreviation $CAPEX(t) = I_t$ for the whole capital expense at time t, $OPEX(t) = M_t$ for the operation and maintenance expenses at time t, and $E(t) = E_t$ for the energy generation at time t. The numerical values of LCOE represent the ratio of the costs of energy production to the energy generation over the lifetime LT of a project:

$$LCOE = \frac{\sum_{t=1}^{LT} \frac{CAPEX(t) + OPEX(t)}{(1+r)^t}}{\sum_{t=1}^{LT} \frac{E(t)}{(1+r)^t}}, \qquad (7)$$

where, now, summation is performed over full years from 1 to LT. The specific cost of the wind farm related to wind turbines, civil works, inverter, miscellaneous, etc., were incorporated in initial $CAPEX(1)$ as the sum of the expenses for equipment and installation in the first year 2020. The rated power in our study is the generation capacity for one unit (MW). In our study, $C_{om} = M_1$ refers to $OPEX(1)$, which corresponds to the 2020 cost based on the Danish Energy Agency data catalogue (Danish Energy Agency DEA, 2016).

2.2.3. Flow chart of calculations

A flow chart of the application of the LCOE model in a GIS environment is shown in Fig. 2. The first step is to prepare raster layers and extract values for essential parameters used in LCOE calculation, namely capacity factor (defined as the annual power production divided by the maximum potential annual production; Danish Energy Agency DEA, 2016), water depth, and distance to shore. The whole Baltic Sea was divided into pixels with dimensions of 5000 × 5000 m (Fig. 2) for standardizing data and for quantitative analysis as recommended in Díaz and Guedes Soares (2020). For every pixel, water depth, distance to shore, and capacity factor were calculated using ArcGIS software and appropriate datasets.

Many older analyses of LCOE (Bilgili and Sahin, 2009; Genç, 2010, 2011, Genç and Gökçek, 2009; Genç et al., 2012a, 2012b, among others)

rely on actually measured wind data at the standard height of 10 m above surface. In these sources, the recorded data are projected to the wind generator height using a log law and approximated by a 2-dimensional Weibull distribution. Main parameters of the wind climate are optionally translated to the location of the generator using the WAsP software. Finally, the capacity factor is evaluated using the scale parameter of the Weibull distribution for the local wind climate.

This approach cannot be directly applied for marine conditions. A state of the art solution is provided by the Global Wind Atlas (2022) (GWA). The properties of marine wind climate are reconstructed from atmospheric re-analysis data. The existing resource is based on the ERA5 dataset (Hersbach et al., 2020) from the European Centre for Medium-Range Weather Forecasts (ECMWF) for the time period of 2008–2017 with a spatial resolution of approximately 30 km. A higher resolution wind climate with a resolution of 3 km is evaluated using the Weather Research and Forecasting (WRF) mesoscale model (Global Wind Atlas, 2022). This information is further detailed via a WAsP calculation of local wind climates for every 250 m at 10; 50; 100; 150 and 200 m height. This calculation includes evaluation of the capacity factor with the same spatial and vertical resolution. The capacity factor data come from the Global Wind Atlas (2022) using capacity factor class I. The use of this class matches the importance of the suitability of high specific power turbines for very high wind locations in terms of LCOE optimization (Swisher et al., 2022). This selection also ensures that our cost considerations align with offshore wind industry standards, providing a robust foundation for our analysis. The water depth is also taken from the Global Wind Atlas (2022). The shoreline data are taken from the HELCOM portal (HELCOM, 2022b).

The LCOE values for offshore wind power plant in every pixel were calculated using Eq. (7). The costs were specified in terms of total capital expenditures (CAPEX), and operational and maintenance expenditures (OPEX). The total CAPEX depends on water depth (foundation costs), the distance to shore (grid connection costs), and initial CAPEX (Martinez and Iglesias, 2022). Initial CAPEX is the cost associated with the installation, development, equipment, and materials above the sea surface for the first year of the project, which is fixed for the total CAPEX calculation.

In step 2, the initial CAPEX was calculated including cost of wind turbine, in particular, by incorporating rotor diameter (m), hub height of wind turbine (m), size of wind turbine in terms of generating capacity for one unit (MW), specific power (W/m^2), and area coverage (MW/

Table 1

Offshore wind turbine costs in 2020 for the base case 20 m water depth and 30 km distance to shore (Danish Energy Agency DEA, 2016).

Technical/financial data	Large offshore wind turbines	
	Year of final investment decision	
	2015	2020
Generation capacity for one unit (MW)	8	10
Average annual full-load hours (MWh)	4400	4500
Technical lifetime (years)	25	27
Rotor diameter (m)	164	190
Hub height (m)	103	115
Specific power (W/m^2)	379	353
Specific area coverage (MW/km^2)	5.4	4.5
Nominal investment (M€/MW)	2.86	2.13
- of which equipment	1.11	0.79
- of which installation	1.35	0.96
- of which grid connection	0.40	0.38
Fixed operation and maintenance (€/MW/year)	57,300	40,059
Variable operation and maintenance (€/MWh)	4.3	3.0

Table 2

Foundation costs for different water depths (Danish Energy Agency DEA, 2016).

Water depth (m)	Foundation costs (M€/MW)	
	2007 study	2014 study
10	0.48	Not specified
20 (base case)	0.74	0.42
30	1.18	0.67
40	1.88	0.84
50	Not specified	1.05

Table 3

Grid connection costs for different distances to shore (Danish Energy Agency DEA, 2016).

Distance to shore (km)	Total grid connection costs (M€/MW)
10	0.35
20	0.37
30 (base case)	0.40
40	0.43
50	0.45
60	0.48
70	0.51
80	0.53

km^2) (Table 1). The information shows the parameters of turbines that have been commonly used in the Baltic Sea based on the DEA guidelines (Table 1). We do not address in this analysis turbines and systems that are not commonly used or considered for use for the Baltic Sea wind power plants.

The fixed part of operation and maintenance (OPEX) costs result from maintaining the wind turbines and associated infrastructure (Martinez and Iglesias, 2022). The variable part of OPEX costs depend on energy generation over any period of interest and vary with energy production (California ISO, 2018). As the LCOE is calculated over many years into the future, the future years need to be discounted to their present values using a discount rate. It indicates the market value of equity and debt (Myhr et al., 2014).

The foundation costs (costs for wind turbine structures below sea surface) for corresponding water depths with respect to the "base case" 20 m water depth (Table 2) were derived based on the DEA Technology Data Catalogue (Danish Energy Agency DEA, 2016). This source reports studies made in 2007 and 2014. We have used the 2014 study because it is based on a more recent price forecast for Siemens wind power turbines and is the only available data set of good quality for Baltic Sea conditions. We only consider bottom-fixed foundations at water depths <50 m. Grid connection costs depend on sea cable cost per km and on

Table 4

Total grid connection costs for offshore wind turbines for the base case (2015 prices) (Danish Energy Agency DEA, 2016).

Grid connection costs (2015 prices)	(M€/MW)
Total grid connection costs	0.40
Offshore platform	0.16
Project management and environmental assessment	0.027
Transformer station onshore (M€/MW)	0.067
Sea cable costs per km (M€/km/MW)	0.00269
Land cable costs per km (M€/km/MW)	0.00134
Base case cable lengths	km
Sea cable	30
Land cable	50

the distance to shore (Tables 3 and 4) (Danish Energy Agency DEA, 2016).

The grid connection costs for plants in each pixel to shore based on the estimated values for the 30 km distance to shore (Table 3) were calculated using (Danish Energy Agency DEA, 2016) (Table 4). Grid connection data (Table 4) are based on the Energinet (Energinet, 2017) which provides the costs of connecting the latest four projects in the Baltic Sea (HR2, Rødsand 2, Anholt and HR3). The estimated grid connection costs are 0.4 M€/MW for offshore wind power plants with the transformer station located on the offshore platform, power plants of 400–600 MW, and plants located about 30 km from the shore (Tables 3 and 4) (Danish Energy Agency DEA, 2016). It is assumed that the grid connection costs are 0.3 M€/MW for near-shore wind power plants that are connected to onshore transformer stations, power plants of 50–200 MW, and located 4–10 km from the shore (Danish Energy Agency DEA, 2016). The grid connection costs in 2020 have been calculated by 1% cost reduction per year until 2020. We assume a minimum distance of 4 km for the LCOE calculations because we validate the model against existing locations, some of which are very close to shore. New large offshore wind power plants are likely to be built much further from shore (Danish Energy Agency DEA, 2016).

A relationship between water depth and foundation costs (Table 2), and distance to shore and grid connection costs (Table 3) were calculated from Danish Energy Agency DEA (2016). They were used to evaluate the foundation and grid connection cost difference between the base case and other water depth and distance to shore values.

Total costs for grid connection presented in Table 4 were calculated for each pixel by multiplying and summing land cable length with land cable costs per km, and sea cable length with sea cable costs per km, along with the sum of the costs for the offshore platform, project management and environmental assessment, and the transformer station onshore. Most of these costs were assumed to be fixed for all pixels. Only sea cable and land cable length were evaluated for each pixel (Table 4).

The offshore wind turbine cost in 2020 (Table 1) was used to calculate the LCOE based on Eq. (3). Calculations of total offshore investment costs (CAPEX) (M€/MW) were performed using values for the above-described base case (20 m water depth and 30 km distance to shore) (Danish Energy Agency DEA, 2016). The deployment plans for offshore wind power plants in the Baltic Sea were expected to reduce the nominal investment costs (CAPEX), and operation and maintenance costs (OPEX) (costs drop by 1% per year) alongside increasing capacity of turbines from 2015 to 2020 through increased output power in building wind power plants (Danish Energy Agency DEA, 2016). In reality, there is ongoing technological improvement towards larger-capacity turbines with higher hubs, bigger rotors, and longer blades to capture more wind energy and produce more electricity and to reduce the capital and operation costs per unit of installed capacity (IRENA, 2019). There is also an increase in annual power production (MWh) per installed power (MW) (average annual full-load hours) from 2015 to 2020 but this depends on the location of the plant, technological features of the individual turbines, and wake losses (Table 1) (Danish Energy Agency DEA, 2016).
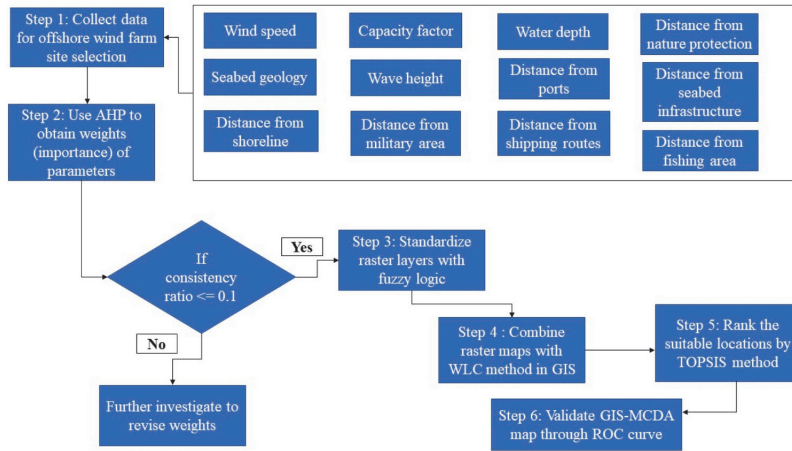
Fig. 3. Flowchart for offshore wind farm site selection methodology using GIS-MCDA.

In step 3, the total CAPEX was calculated as the sum of the expenses for equipment and installation in the first year 2020 (initial CAPEX which was held constant for the total CAPEX calculation), foundation costs (dependent on water depth) and grid connection costs (dependent on distance to shore) in million euros (M€). The costs for each pixel were evaluated based on the difference in the water depth and distance to shore from those of the base case. For each 1 m depth difference from the base case 30 m, the foundation costs were changed by 0.0206 M€. For each 1 km difference in the distance to shore from the base case (30 km), the sea cable cost was changed by 0.00269 M€/km/MW.

In step 4, the fixed and variable OPEX were calculated for 2020 using (Danish Energy Agency DEA, 2016) (Table 1). The total OPEX is the sum of fixed and variable components, covering the whole expected lifetime of the project. The OPEX values do not depend on water depth and distance to shore. All CAPEX and OPEX values refer to the 2020 cost data projections in Danish Energy Agency DEA (2016).

In step 5, the energy production of the offshore wind power plant (LCOE) was calculated by multiplying the capacity factor by 8760 h/yr to acquire the annual energy production of the farm, assuming an installed capacity of 1000 MW. In large offshore wind farms, energy losses caused by turbine wakes are expected to be 10–20% of total power output. This is a contributing consideration for investments (Barthelmie et al., 2007). For every year from 2020 to 2047 (assumed lifetime 27 yr; Danish Energy Agency DEA, 2016), energy production was calculated by taking into consideration power losses of about 10%. In the final stage, the LCOE was calculated for every pixel using Eq. (3) by dividing the sum of costs by the sum of energy generation for 27 years, using a discount rate of 8% (Freyman and Tran, 2018).

2.2.4. GIS-multi-criteria decision analysis (MCDA)

2.2.4.1. Data collection.
The first step of the MCDA is to specify the constraints and potential locations for the development of offshore wind power plants from a review of the literature and national regulations (Fig. 3). The process for the identification of the most important parameters for plant site selection is based on previous works (Wu et al., 2018). The layers for GIS analysis were created for 5000 × 5000 m pixels in ArcGIS with the ETRS_1989_LAEA reference coordinate system (Annoni et al., 2003).

The parameters are determined based on the DEA standards (Danish Energy Agency DEA, 2016), the European Maritime Spatial Planning (MSP) platform (European MSP Platform, 2018a,b,c,d,e, 2019) and other literature (Chaouachi et al., 2017; Deveci et al., 2020; Emeksiz and

Demirci, 2019; Genç et al., 2021; Gil-García et al., 2022; Spyridonidou and Vagiona, 2020; Tercan et al., 2020), the data source, and the parameter descriptions. (Danish Energy Agency DEA, 2016) is the only available set of standards for water depth and distance from shore, that determine how these parameters affect the cost and location of wind farms. A variety of parameters were used in this study (Table 5): wind speed, capacity factor, water depth, distance from nature protection area, seabed geology, wave height, distance from ports, distance from seabed infrastructure, distance from shoreline, distance from military area, distance from shipping routes, and distance from fishing area.

2.2.4.2. Analytical Hierarchy Process (AHP).
The second step in the MCDA design is to specify the contribution of the different parameters to wind farm site suitability. The AHP is, in essence, a pairwise comparison exercise in which each factor (parameter) is weighted against other factors to determine its relative significance (Mu and Pereyra-Rojas, 2018). If larger values are "better", the weights of parameters range from 1 to 9 as recommended in the classic work (Saaty and Tran, 2007). Class 9 corresponds to an extremely prioritized situation, class 7 to very strongly prioritized, class 5 to strongly prioritized, class 3 to moderately prioritized and class 1 to equally prioritized (neutral) situation. Experts asked to evaluate priorities may also use intermediate values 2, 4, 6, 8 between the classes. If smaller values are better, the weights are decreasing (e.g., 1/3, 1/5, 1/7, 1/9, Saaty and Tran, 2007).

One way to obtain the relative weights of factors is to use super decisions software (Mu and Pereyra-Rojas, 2018) by comparing the importance of factors to each other. It is part of the AHP methodology that expert opinions are collected to determine appropriate weightings for parameters, using a pairwise comparison matrix. For this study, 10 experts in various academic institutes and governmental agencies with backgrounds in renewable energy and coastal sciences were interviewed (Table 6). In this study, the geometric mean was employed for aggregating judgments in AHP due to its ability to capture the reciprocal nature of experts' opinions (Mu and Pereyra-Rojas, 2018).

The calculation of the weight for each criterion used the geometric mean of the values (Mu and Pereyra-Rojas, 2018) provided by experts for each pair of comparisons (Table 7). Then pairwise comparison matrix of these values was normalized by dividing the value in each cell by the sum of values over all cells in the relevant column. The sum of the rows of the normalized matrix leads to a new one-column matrix. The entries of this matrix can be eventually normalized by dividing the values in each cell by the number of criteria (average) to calculate weights (relative importance of parameters) (Mahdy and Bahaj, 2018;

Table 5

The most important parameters, their data source and description, for offshore wind power plant site selection in the Baltic Sea.

Criteria	Sub-criteria	Data source	Description
Wind resource	Wind speed	Global Wind Atlas (2022)	Wind speed is the crucial parameter for the energy production of wind power plants and investment returns (Tercan et al., 2020). The average wind speed is estimated at 100 m above the sea surface, which is the normal height of a turbine hub. An average wind speed of 7.0 m/s is generally regarded as a minimum wind speed for offshore wind power plant sites (Genç et al., 2021; Vinhoza and Schaeffer, 2021). According to (Danish Energy Agency DEA, 2016), the maximum annual average wind speed at 100 m height is 10 m/s in the Baltic Sea. The highest power generation is reached at ~ 12 m/s and at ~25 m/s the power generation is reduced Between 12 and 25 m/s the maximum power generation remains stable (Danish Energy Agency DEA, 2016).
Physical	Capacity factor	Global Wind Atlas (2022)	The capacity factor is the annual power production divided by the maximum potential annual production (Danish Energy Agency DEA, 2016). This parameter has a major impact on the anticipated investment returns (Chaouachi et al., 2017). The average capacity factor for offshore wind power plants worldwide was 33% in 2018 and new offshore wind turbines are planned to have a capacity factor between 40–50% (IEA, 2019). The capacity factor in coastal locations of the Baltic Sea is over 31% (Tonderski and Jędrzejewski, 2013).
	Water depth	Global Wind Atlas (2022) derived from GEBCO Bathymetric Compilation Group (2020)	Water depth influences the foundation costs of offshore wind power plants. Water depths >50 m are not considered as potential locations of offshore wind power plants in (Danish Energy Agency DEA, 2016). Most offshore wind turbines have been installed at sites with water depths of less than 50 m (Spyridonidou and Vagiona, 2020). Between the water depths of 0 – 50 m, lower values are better. There may be a scour issue in shallow water depths caused by the effects of waves and currents on the seabed causing negative impacts on the wind power plant. This problem requires scour protection if it exists (Thor Ugelvig, 2014).
	Distance from nature protection area	HELCOM (2022a)	Protected areas including NATURA 2000 areas, marine protected areas, wetlands, and RAMSAR areas must be considered. The environmental impacts of wind power plants are related to bird collisions and changes to fauna and flora habitats (Bailey et al., 2014; Wang and Wang, 2015). The construction process impacts are noise and habitat degradation, along with the increased ship traffic, and the wind power plant operational impacts are noise, movement of marine animals from their normal habitats, and collisions (European MSP Platform, 2018a). This source specifies a minimum 2 km distance from marine protected to avoid disturbance of seabirds. Above 2 km distance, bigger distances are better.
	Seabed geology	EMODnet (2022a)	The costs of offshore wind power plant installation increase if the seabed is rocky (Emeksiz and Demirci, 2019). A muddy substrate is more suitable for offshore wind power plant construction than sandy sediments (Rambøll, 2014). A muddy substrate has very high suitability, muddy sand/sandy mud substrates have high suitability, sand substrates have moderate suitability, coarse substrates have low suitability and mixed coarse sediments have very low suitability for the location of offshore wind power plants (Gkeka-Serpetsidaki and Tsoutsos, 2022). According to (European MSP Platform, 2018b), sediments comprised of (finer) sediments are suitable for the establishment of wind turbine foundations.
	Wave height	Copernicus Marine Service (2020)	Wave height affects the offshore wind power plant design (Wu et al., 2018). Large waves influence construction, operation, and maintenance costs due to access issues (Deveci et al., 2020; Eelsalu et al., 2024), and in small water depths large waves may jeopardize the offshore wind turbine foundations. A maximum single wave height >10 m is not suitable for offshore wind power plant locations (Gil-García et al., 2022). Maximum single wave height H_{max} is approximately 1.6–2 times significant wave height (SWH) H_S (Satish et al., 2019), that is approximately equal to the average height of the highest one-third of waves (Díaz and Guedes Soares, 2020). The maximum measured SWH in the Baltic Sea is 8.2 m and maximum SWH up to 10 m may occur in contemporary climate (Björkqvist et al., 2018). The maximum SWH between 1993-2020 based on Copernicus dataset was approximately 3.9 m in the vicinity of selected locations of offshore power plants in Fig. 8. However, maximum SWH>4 m are rare in the Baltic Sea, so wave height is unlikely to be a problem in this water body.
Socioeconomic	Distance from ports	EMODnet (2022b)	A short distance from ports is vital to minimize the costs of installation and maintenance of offshore wind power plants (Gil-García et al., 2022). A distance of between 10–80 km from ports is suitable. Within this range, the lower values are better. Areas more than 80 km from ports are generally considered unsuitable (Spyridonidou and Vagiona, 2020). Evaluation of the minimum distance from a port includes an analysis of the distance from the shoreline (see below).
	Distance from seabed infrastructure	EMODnet (2022b)	Seabed infrastructure may be present for the transport of gas, oil, water, or electricity. Existing infrastructure should not be adversely affected by wind power plants (Emeksiz and Demirci, 2019). It is also a potential obstacle during the installation of plants (Tercan et al., 2020). A minimum distance of 500 m from seabed infrastructure is used in this study (Vinhoza and Schaeffer, 2021). Above 500 m, larger distances are better. The International Cable Protection Committee (ICPC) suggests an exclusion zone of 500 m from existing cables in shallower waters (up to a depth of 75 m) (European MSP Platform, 2018c).
	Distance from shoreline	HELCOM (2022b)	Distance from the shoreline is an important constituent of the installation and maintenance costs. DEA (2016) does not consider wind power plants located less than 10 km from shore. The Estonian Maritime Spatial Plan (2019) specified a 10 km distance from the shore to reduce visual disturbance by offshore wind power plants and to assure that plants do not interfere with surfing and sports activities in marine areas. A

Table 5 (*continued*)

Criteria	Sub-criteria	Data source	Description
			wind power plant close to the shoreline might create visual and noise impacts (Zhou et al., 2022) or influence human activities, so marine areas with proximity to the shoreline should be excluded from analysis (Díaz and Guedes Soares, 2020).
	Distance from military area	EMODnet (2022b)	Offshore wind power plants can interfere with areas used for military activities and these areas need to be free of offshore wind turbine developments (European MSP Platform, 2019). Marine areas used for military purposes, particularly for military exercises and training, are excluded from the offshore wind power plant site selection (Zhou et al., 2022). The European MSP Platform (2019) determined a 500 m distance from military areas as a buffer zone for the safety of these areas. Above 500 m distance from military areas, the greater distances are better.
	Distance from shipping routes	EMODnet (2022b)	Shipping routes are significant because the construction of wind power plants in areas with busy shipping routes can increase the potential for accidents (Deveci et al., 2020). The safety of a wind power plant is better in marine areas with lower ship traffic. The EMODnet's shipping density map is used for this study, which shows the time spent by all ship types in hours per month per km^2 (EMODnet, 2019). The high traffic routes are extracted visually in ArcGIS from the shipping density map. The European MSP Platform (2018d) recommends a minimum distance of 2 nautical miles (approximately 3.7 km) between the outside borders of the offshore wind power plant and the shipping route for safety purposes.
	Distance from fishing area	EMODnet (2022b)	The installation and operation of a wind power plant may also contribute to the displacement or disturbance of fish caused by noise and lead to the reduction of fish production (European MSP Platform, 2018e). Maintaining distance from a fishing area reduces conflicts (Tercan et al., 2020) and offshore wind farms should avoid areas of particularly intense fishing activity. Fishing activities, particularly trawling which is the most common fishing method in Europe, are not allowed within the locality of offshore wind power plants and their cables (European Commission, 2020). According to the United Nations Convention on the Law of the Sea (UNCLOS), a buffer zone of 500 m around offshore wind power plants is established. Fishing activities in Europe in the North Sea may be (and are by several countries) excluded within a 500 m distance of offshore wind power plants and their cables (European Commission, 2020).

Vasileiou et al., 2017).

To validate the results of the weighting by AHP, a consistency ratio *CI* must be estimated (Mu and Pereyra-Rojas, 2018). This quantity is the ratio between the consistency index

$$CI = \frac{\lambda_{\max} - N}{N - 1} \qquad (8)$$

of the pairwise comparison matrix and the Random Index *RI* of Saaty and Tran (2007). Here, $\lambda_{\max}$ is the largest eigenvalue of the pairwise comparison matrix and *N* is the size of this matrix. The values of *RI* are calculated (Saaty and Tran, 2007) from the analysis of the *N*-by-*N* matrix of random decisions. In each such matrix the entries above the main diagonal are filled at random from the 17 values {1/9, 1/8,. 1/2, 1, 2,..., 8, 9}. The entries below the diagonal are filled with their reciprocals (e. g. 9→1/9) whereas ones are put on the main diagonal. The *RI* is the average consistency index of such *n*-by-*n* matrices (Saaty and Tran, 2007). The values of *RI* rapidly increase to about 1.5 when *N* increases from 1 to 10 and then level off around 1.6 (Aguarón and Moreno-Jiménez, 2003). The size of the matrix *N* = 12 in this study and the associated *RI* is 1.54. The AHP result for the weighting of parameters is consistent if the (consistency) ratio of the consistency index *CI* and *RI* is below 0.1 (Saaty and Tran, 2007):

$$CR = \frac{CI}{RI} \leq 0.1. \qquad (9)$$

2.2.4.3. Fuzzy logic. The third step is to standardize the values of raster layers to make a quantitative assessment of site suitability (Fig. 3). As factors are measured on different scales, it is important to standardize (normalize) their numerical values before combining them (Eastman, 2009). The fuzzy logic technique involves normalizing the values of estimates of various factors or parameters in single pixels of raster maps between 0 and 1 (see Barzehkar et al., 2021 for an overview of various implementations of fuzzy logic into DSTs). Fuzzy logic is based on the principle that binary (Boolean) logic does not have the ability to express some transitional conditions between true (1) and false (0) values (Zarin et al., 2021). To apply this approach, the data were reclassified to normalize the values in the different layers (Gil-García et al., 2022). After reclassification, lower and upper threshold values for factors were specified. A lower threshold value (minimum) represents the least appropriate value. The larger the estimate, the better is the suitability according to this parameter. All values over an upper threshold (maximum) are optimal (Latinopoulos and Kechagia, 2015). In other words, the result at each pixel in the fuzzy map indicates its suitability in relation to a given parameter (Noorollahi et al., 2022). Table 8 shows threshold values and the associated types of fuzzy membership functions to standardize different raster layers in ArcGIS software.

The fuzzy standardization of parameters was made, for example, as follows. If the minimum acceptable distance from nature protection area, "a", is 2 km, then all locations less than 2 km from the nature protection area are not appropriate and assigned the value zero. The value "b" is 5 km. Thus, the relevant parameter was assigned the value 1 whenever the distance is >5 km as all these locations are well suitable. On the contrary, for water depth, "a" is 10 m. This means that water

Table 6
Details of the experts used for weighting of parameters.

Demography of experts	Governmental organizations	Academic institutions
Male/Female (number)	2/2	3/3
Age range (years)	37–58	40–60
Education (degree)	MSc or PhD	MSc or PhD
Field of expertise	Offshore wind farm development; Renewable energy	Coastal geomorphology; Coastal processes and oceanography; Offshore renewable energy

Table 7
Pairwise comparison matrix of parameters for offshore wind power plant site selection.

Parameters for offshore wind farm site selection	Pairwise comparison matrix											
	Wind speed	Capacity factor	Water depth	Distance from ports	Distance from seabed infrastructure	Distance from shore	Distance from military area	Distance from shipping routes	Distance from nature protection area	Seabed geology	Wave height	Distance from fishing area
Wind speed	1	2	4	3	4	4	3	3	3	3	3	3
Capacity factor	1/2	1	3	4	3	4	3	3	2	3	3	3
Water depth	1/4	1/3	1	3	3	2	3	3	2	2	1	2
Distance from ports	1/3	1/4	1/3	1	1	1	1	1	1/3	1	1	2
Distance from seabed infrastructure	1/4	1/3	1/3	1	1	2	1	1/3	1/4	1	1	2
Distance from shore	1/4	1/4	1/2	1	1/2	1	1	1	1/3	2	1	2
Distance from military area	1/3	1/3	1/3	1	1	1	1	1	1/2	1	1/2	2
Distance from shipping route	1/3	1/3	1/3	1	3	1	1	1	1/3	1	1/2	2
Distance from nature protection area	1/3	1/2	1/2	3	4	3	2	3	1	1	1	4
Seabed geology	1/3	1/3	1/2	1	1	1/2	1	1	1	1	1	2
Wave height	1/3	1/3	1	1	1	1	1	2	1	1	1	2
Distance from fishing area	1/3	1/3	1/2	1/2	1/2	1/2	1/2	1/2	1/4	1/2	1/2	1

depth less than 10 m is always suitable (the value 1) and between 10–50 m the lower numbers are better. The number "b" for water depth is 50 m. All locations with this and larger water depths were also given the value zero indicating unsuitability of such locations. Finally, the fuzzy membership functions $X1(i)$ and $X2(i)$ are generated:

$$X1(i) = \frac{R_i - R_{\min}}{R_{\max} - R_{\min}}, \tag{10}$$

$$X2(i) = \frac{R_{\max} - R_i}{R_{\max} - R_{\min}}. \tag{11}$$

Eq. (10) was used for increasing functions and Eq. (11) was applied for decreasing functions, R_i is the input raster value of each parameter, $R_{\min}$ is the minimum threshold and $R_{\max}$ is the maximum threshold of this parameter from Table 8 (Kao, 2010).

2.2.4.4. Weighted linear combination (WLC). The fourth step is to combine raster maps in GIS to prepare a map of site suitability (Fig. 3). The WLC method is applied in the GIS environment using map algebra techniques to combine raster maps (Malczewski and Rinner, 2015). This approach was used to calculate site suitability (Díaz-Cuevas et al., 2019), by multiplying the relative weight W_i of the factor and the normalized (fuzzy standardized) value X_i of the factor, where N is the number of criteria (Díaz-Cuevas et al., 2019).

$$S = \sum_{i=1}^{N} W_i X_i \tag{12}$$

To complete the WLC method, all cells on the output layer were ranked with respect to their overall rating. The cell with the rank of 1 is the most suitable option (Malczewski, 2000).

2.2.4.5. Technique for Order of Preference by Similarity to Ideal Solution (TOPSIS). A fifth step, used to provide confidence in the results, is to rank the suitable locations using a complementary method, order of preference by similarity to ideal solution (TOPSIS). TOPSIS is a simple and effective MCDA approach for choosing the most appropriate solution from a series of alternatives (Vagiona et al., 2022). The TOPSIS methodology is based on the concept that the best alternative must have the shortest geometric distance from the positive ideal solution and the longest geometric distance from the negative ideal solution (Sindhu et al., 2017). The highest benefit is contained in the positive-ideal solution and the lowest benefit is represented by the negative-ideal solution (Díaz and Guedes Soares, 2021). This method was used in the final step of the assessment for ranking the sites with the highest site suitability derived from the Fuzzy-AHP-WLC method. First, a decision matrix was created with $J = 15$ alternatives (locations A1 to A15 in Fig. 8) and the above-described $N = 12$ criteria based on the integration of each criterion i and alternative j given as x_{ij}. Second, the decision matrix was normalized (Konstantinos et al., 2019):

$$r_{ij} = \frac{x_{ij}}{\sqrt{\sum_{j=1}^{J} x_{ij}^2}}, \tag{13}$$

The third step encompasses the calculation of the weighted normalized values v_{ij} (Vagiona et al., 2022):

$$v_{ij} = w_j r_{ij}, \quad i = 1, 2, \ldots, N; \quad j = 1, 2, \ldots, J. \tag{14}$$

In the fourth step, the positive ideal solution V_j^+ and negative ideal solution V_j^- were determined:

$$A^+ = \left\{ V_1^+, \ldots, V_N^+ \right\}, \quad V_j^+ = \left\{ (\max(v_{ij}), j \in J'), \; (\min(v_{ij}), j \in J'') \right\}. \tag{15}$$

$$A^- = \left\{ V_1^-, \ldots, V_N^- \right\}, \quad V_j^- = \left\{ (\min(v_{ij}), j \in J'), \; (\max(v_{ij}), j \in J'') \right\}. \tag{16}$$

Here, J' denotes the set of indices from $1, 2, \ldots, J$ that correspond to benefit criteria and J'' denotes the similar set that corresponds to the cost

Table 8
Threshold values and fuzzy membership function to standardize raster layers in fuzzy logic for offshore wind power plant site selection.

Criteria	Sub-criteria	Reference	Threshold values		Type of the Fuzzy membership function
			Minimum threshold a	Maximum threshold b	
Wind resource	Wind speed	Danish Energy Agency DEA (2016)	7 m/s	10 m/s	Increasing
Physical	Capacity factor	Wind Europe (2019)	35%	55%	Increasing
	Water depth	Danish Energy Agency DEA (2016)	10 m	50 m	Decreasing
	Distance from nature protection area	European MSP Platform (2018a)	2 km	5 km	Increasing
	Seabed geology	European MSP Platform (2018b)	0 (Rocks and boulders)	1 (Muddy)	User-defined based on expert judgement and literature
	Wave height	Gil-García et al. (2022)	< 10 m	> 10 m	Decreasing
Socioeconomic	Distance from ports	Based on the distance to shore (see below)	10 km	80 km	Decreasing
	Distance from seabed infrastructure	European MSP Platform (2018c)	500 m	5000 m	Increasing
	Distance from shoreline	Danish Energy Agency DEA (2016) Spyridonidou and Vagiona (2020)	10 km	80 km	Decreasing
	Distance from military area	European MSP Platform (2019)	500 m	5000 m	Increasing
	Distance from shipping routes	European MSP Platform (2018d)	3.7 km	5 km	Increasing
	Distance from fishing area	European Commission (2020)	500 m	5000 m	Increasing
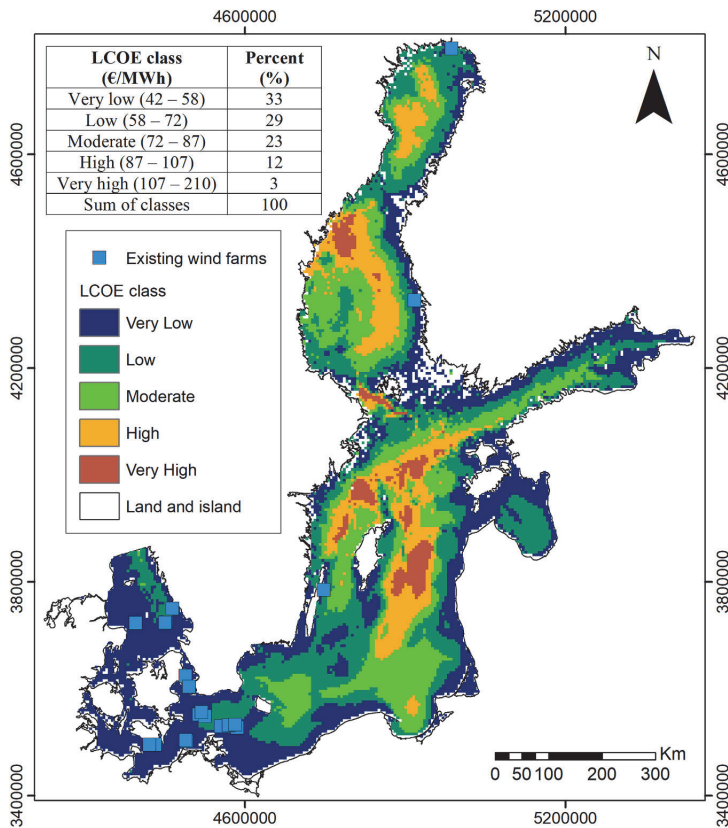
Fig. 4. Offshore wind power plant site suitability based on the GIS-LCOE (low value is better).
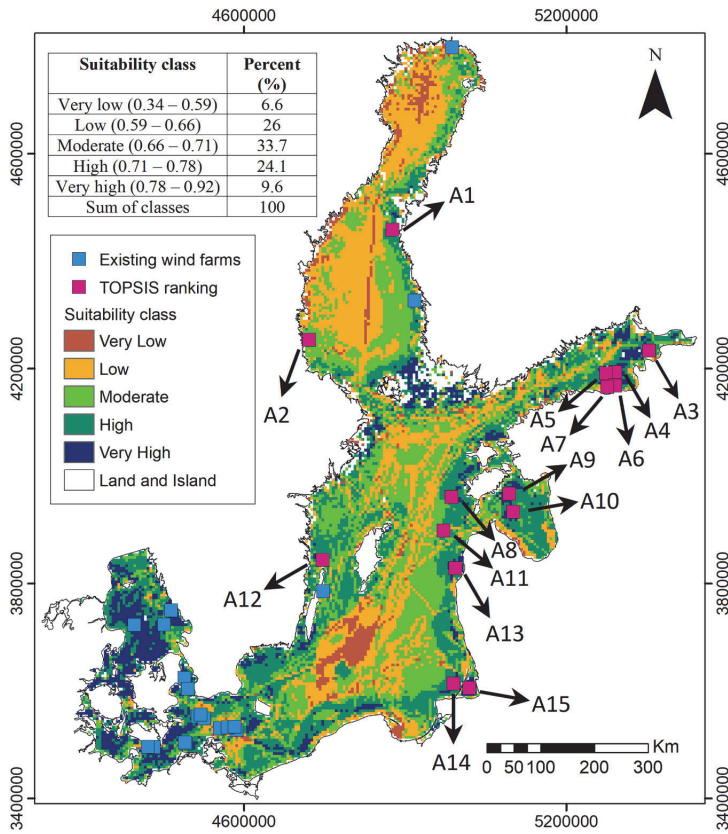
Fig. 5. Offshore wind power plant site suitability based on the GIS-MCDA (high value is better).

criteria (Vagiona et al., 2022). In our case, the criteria identified for evaluation were inherently benefit-oriented, focusing on positive impacts and improvements rather than negative aspects. Therefore, in our analysis $J' = \{1, 2, ..., J\}$ and $J'' = \emptyset$. Then the differences of the alternatives from the positive S_i^+ and negative S_i^- ideal solutions were calculated (Foroozesh et al., 2022):

$$S_j^+ = \sqrt{\sum_{i=1}^{N}\left(v_{ij} - V_j^+\right)^2}, \; j = 1, 2, ..., J,$$ (17)

$$S_j^- = \sqrt{\sum_{i=1}^{N}\left(v_{ij} - V_j^-\right)^2}, \; j = 1, 2, ..., J.$$ (18)

In the final step, the calculation of the relative closeness to the positive ideal solution for site selection was calculated (Vagiona and Kamilakis, 2018).

$$C_j^+ = \frac{S_j^-}{S_j^+ + S_j^-}, \; j = 1, 2, ..., J$$ (19)

to determine how far from the ideal the realistic locations are. Fig. 3 shows the steps for offshore wind power plant site selection using the GIS-MCDA methodology.

2.2.4.6. Validation. The sixth step is to validate the outputs of models. We use the receiver operating characteristic (ROC) curve, a common method for verifying a model's prediction (Ghorbanzadeh et al., 2019).

The method was applied to both GIS-LCOE and GIS-MCDA. The ROC curve is a measure of sensitivity as a function of the false-positive rate (specificity), where the *x*-axis shows the cumulative distribution function of the false positive rate, and the *y*-axis is the sensitivity (Chen et al., 2018). It is generated by plotting the false positive rate on the *x*-axis and the true positive rate on the *y*-axis (Pourghasemi et al., 2016).

In this study, we used existing wind power plants as indicative of the true positive rate and the chosen locations from GIS-LCOE and GIS-MCDA maps as the false positive rate because there is not, in reality, a wind power plant in these locations. The value for the area under the curve (AUC) was used in the accuracy analysis of the suitability map, where the value of 1 shows that the model is perfect and 0.5 represents a model that is not performing well (Orhan, 2021). In this study, sensitivity, specificity, and accuracy were used to assess the performance of the model as follows (Chen et al., 2017; Tien Bui et al., 2016):

$$Sensitivity = \frac{TP}{TP + FN}, \; Specifity = \frac{TN}{FP + TN},$$

$$Accuracy = \frac{TP + TN}{TP + FP + TN + FN}.$$ (20)

Here false positive (*FP*) and false negative (*FN*) are the number of pixels that are incorrectly classified, true positive (*TP*) and true negative (*TN*) are the number of pixels that are correctly classified.
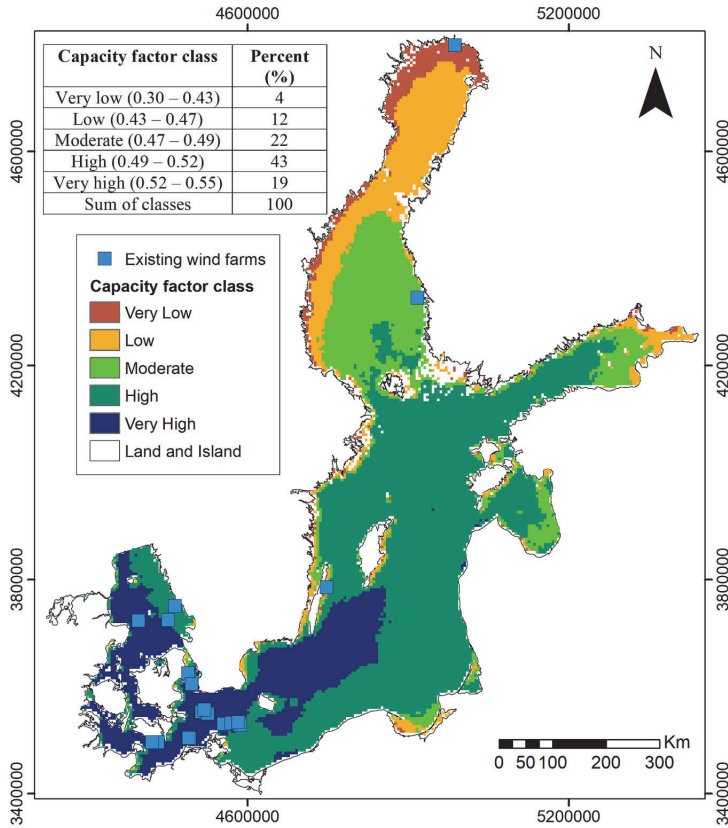
Fig. 6. Capacity factor for offshore wind power plant site suitability.

3. Results

3.1. Mapping based on LCOE, MCDA and capacity factor

The outputs derived from the GIS-LCOE model (Fig. 4), and GIS-MCDA (Fig. 5) for offshore wind locations in the Baltic Sea have broad similarity. It is thus likely that both techniques are capable of identifying suitable locations in the Baltic Sea where the wind speed is high and the cost of energy is low based on the DEA and European MSP platform guidelines and regulations.

The most appropriate offshore wind power plant locations based on GIS-LCOE analysis have low LCOE values (lower values are better for wind site suitability). Such areas are close to the shores (especially Danish shores) with high wind speeds and shallow water depths (Fig. 4). These are areas with likely lower capital expenditures that require shorter electric cables for grid connection and lower construction costs. Locations far from the shore with lower wind speeds and deep water received higher LCOE values. These locations are mainly in the Gulf of Bothnia, the Gulf of Riga, and areas far from German and Polish shores (Fig. 4).

The application of GIS-MCDA using AHP, fuzzy logic, and WLC (Fig. 5) indicates a similar pattern of the most suitable locations for the installation of offshore wind power plants as large values of the output of this technique. These were prioritized by European MSP platform guidelines and expert' perspectives as those with close proximity to shore, shallow water depths, areas with high wind speeds, far from nature protection areas, reasonably separated from seabed

infrastructure (pipelines, cables), military areas, shipping routes, fishing areas, and have finer bottom sediments and lower wave heights. The higher values of this map (Fig. 5) are better. The locations with low site suitability do not have these characteristics.

Another view on the suitability of wind power plants can be inferred from the spatial pattern of the capacity factor (Fig. 6). This projection does not take into account environmental and socioeconomic factors. In this view, a significant proportion of annual energy outputs (i.e., capacity factors of over 50%) are in the south of the Baltic Sea. These areas for wind farm installation have the potential to meet the energy demands of southern Baltic countries, especially Denmark, Sweden, Germany and Poland.

The most suitable areas have LCOE values in the range of about 42–58 €/MWh (about 33% of the total sea area) (Fig. 4), MCDA values of 0.78–0.92 (9.6% of the total sea area) (Fig. 5), and capacity factor values of 0.52–0.55 (19% of the total sea area) (Fig. 6). The least suitable areas have LCOE values from 107 to 210 €/MWh (3% of the sea area), MCDA values 0.34–0.59 (6.6%), and capacity factor values of 0.30–0.43 (4%).

The north of the Baltic Sea is less favorable for wind farm development as the capacity factor is generally less than 50% in this region. However, when all the environmental and socioeconomic parameters are taken into account, a few locations in northern Baltic Sea, particularly close to the Finnish coasts, could also serve as suitable locations for wind power generation because of small distance from shoreline, proximity to ports, etc. (Fig. 5). In the south and east of the Baltic Sea, the most suitable areas generally follow spatial distributions of other parameters, such as (high) wind speeds, seabed consisting of fine

Table 9

Matrix assessment of the most suitable sites identified by the TOPSIS method. Locations A1 to A15 are shown in Fig. 8.

Sites	Wind Speed (m/s)	Capacity factor (%)	Water depth (m)	Distance from ports (km)	Distance from seabed infrastructure (km)	Distance from shoreline (km)	Distance from military area (km)	Distance from shipping route (km)	Distance from nature protection area (km)	Seabed geology	Maximum significant wave height (m) between 1993-2020	Distance from fishing area (km)
A1	8.96	53	6.00	48.49	17.68	12.10	276.91	33.99	9.71	0.2 (Mixed sediment)	2.12	279.39
A2	8.55	52	15.00	14.58	156.45	12.77	245.73	54.03	10.86	0.2 (Mixed sediment)	1.76	420.27
A3	8.76	53	16.00	41.48	21.92	15.58	92.67	4.88	26.38	0.6 (Sand)	1.41	505.77
A4	8.87	53	28.00	44.69	19.51	33.00	38.30	26.15	29.25	0.8 (Mud to muddy sand)	1.62	429.61
A5	8.95	54	15.00	52.45	28.59	34.69	24.52	21.71	35.34	0.8 (Mud to muddy sand)	1.74	416.03
A6	8.80	53	40.00	30.73	43.90	10.41	29.25	9.75	38.31	1 (Mud)	1.27	412.06
A7	8.86	54	39.00	44.09	51.09	12.34	14.62	24.91	29.60	1 (Mud)	1.35	398.19
A8	9.37	56	18.00	45.10	28.34	26.71	70.02	10.88	26.31	0.6 (Sand)	3.38	78.58
A9	9.15	55	26.00	34.51	91.36	21.94	79.08	34.51	13.74	0.8 (Mud to muddy sand)	1.95	128.03
A10	9.11	55	5.00	55.40	108.60	36.78	114.68	20.76	6.87	0.2 (Mixed sediment)	1.77	113.69
A11	9.44	57	19.00	48.62	17.63	48.29	134.47	9.75	15.44	0.6 (Sand)	3.42	28.36
A12	9.10	56	26.00	34.10	107.20	15.01	229.25	6.88	20.10	0.2 (Mixed sediment)	2.09	10.92
A13	9.38	57	27.00	41.73	34.13	15.79	162.55	39.33	17.63	0.8 (Mud to muddy sand)	3.20	24.89
A14	9.17	56	13.00	67.96	98.60	14.86	26.28	47.93	15.41	0.4 (Coarse sediment)	3.19	96.94
A15	8.97	55	1.00	73.22	108.12	11.38	37.06	59.59	13.77	0.2 (Mixed sediment)	1.05	115.79

Table 10

Geometric distance of sites from the negative and positive ideal solution and final ranking using the TOPSIS method. Locations A1 to A15 are shown in Fig. 8.

Sites	S_i^-	S_i^+	C_i^+	Site suitability ranking
A1	0.0280	0.0243	0.5351	11
A2	0.0300	0.0216	0.5820	3
A3	0.0279	0.0228	0.5504	8
A4	0.0280	0.0205	0.5777	4
A5	0.0327	0.0190	0.6332	1
A6	0.0296	0.0235	0.5566	7
A7	0.0262	0.0222	0.5413	10
A8	0.0282	0.0216	0.5668	6
A9	0.0241	0.0228	0.5142	15
A10	0.0274	0.0252	0.5214	13
A11	0.0259	0.0242	0.5171	14
A12	0.0256	0.0222	0.5347	12
A13	0.0255	0.0215	0.5434	9
A14	0.0288	0.0214	0.5742	5
A15	0.0315	0.0224	0.5844	2

sediments (muddy and sandy), shallow water depths, reasonable distance from pipelines and military areas, etc. It is also clear that distance from shipping routes and pipelines, distance from nature protection areas, and distance from shoreline largely affect the suitability of potential wind farm locations in the entire Baltic Sea basin (Fig. 5).

3.2. Application of the TOPSIS technique

As a final step, the most suitable areas determined using GIS-MCDA (with the ranking of suitability) for offshore wind power plants were prioritized and ranked (sites A1 to A15) based on the TOPSIS method (Fig. 5). The initial assessment matrix to implement the TOPSIS approach (Table 9) shows the numerical values for parameters for the most appropriate sites. Then, the geometric distance of the sites (A1 to A15) from the positive and negative ideal solutions was calculated (Table 10). It is clear that the distance from a military area contributes significantly to the higher ranking of A1 and A2, and the distance from a fishing area is important in the higher ranking of A3 and A4. Both the distance from a nature protection area and the seabed geology influence the ranking of A5, A6, and A7 (Table 9).

Wind speed and capacity factor are the contributing parameters that give the higher ranking to A11, A13, and A8 sites. Distance from seabed infrastructure and proximity to ports have impacted the A10 and A15 rankings. The TOPSIS methodology ranking is mainly influenced by the highest value of the factor (distance from the negative ideal solution) or the lowest value of the factor (distance from the positive ideal solution) (Azadeh et al., 2011). The TOPSIS ranking (Fig. 5 and Table 9) was affected significantly by the highest distance from the negative ideal solution including a nature protection area, military area, seabed infrastructure, etc. This means that the highest distance from these objects is better for wind site suitability, while the GIS-Fuzzy-AHP-WLC

Fig. 7. Offshore wind power plant site suitability based on the GIS-LCOE, with all areas of restrictions highlighted.

required only a buffer based on the national guidelines and standards for site selection. The presented feature suggests that GIS integrated with fuzzy logic, AHP and WLC provides a more consistent and balanced approach than TOPSIS for standardization, weighting, and combining factors based on the European MSP platform standards and experts' perspectives. However, the TOPSIS analysis may be worth performing to provide extra confidence in the results.

Site suitability maps constructed based on GIS-LCOE (Fig. 7) and GIS-MCDA (Fig. 8) techniques were produced by excluding marine protected areas, areas less than 4 km from shore, and areas with water depth >50 m (bold brown color). The classification boundaries in Figs. 7 and 8 were chosen by taking into account these limitations for offshore wind farm site selection. The map of final capacity factor (Fig. 9) was produced incorporating the restrictions, and by including 10% energy losses for large offshore wind turbines. The locations with high capacity factors are in areas where LCOE values are low. This means that the costs of electricity production per year would be lower in locations where wind turbines have greater capacity factors.

Experts consulted for this study advised that the most important parameters that influence the offshore wind power plant site suitability evaluation in the Baltic Sea were wind speed, capacity factor, and water depth. The distance from nature protection areas, wave height, seabed geology and distance from shipping routes had somewhat lower weights (Fig. 10). The distance from a fishing area had the lowest priority. The consistency ratio (Eq. (9)) between experts' opinions was 0.03, which is much less than 0.1.

Only a few experts in this study used full range of 1–9. Most experts used half the range of 1–5 for weighting of parameters. Wind speed and capacity factor received higher weights (importance) from experts in comparison to other parameters. A majority of experts have preferenced distance-based parameters over wind power generation parameters.

This may reflect different 'world views' of experts. However, the small consistency ratio signals that this feature did not undermine the validity of the results of the AHP method.

The resulting site suitability maps were validated using the ROC curve (Fig. 11). The AUC value for both maps is slightly over 92% (92.2% for the GIS-LCOE map and 92.6% for the GIS-Fuzzy-AHP-WLC map). This indicates that the chosen locations closely align with the actual locations of existing wind farms. Thus, there is a high correlation between current sites of wind power plants and the high suitability sites identified by GIS-LCOE and GIS-MCDA. In other words, the classifier of the ROC method is highly capable of distinguishing between pixel classes of actual and chosen locations. The AUC value for the TOPSIS model is 82%, which is lower than the other two models.

4. Discussion

There are clearly distinguishable line features in Fig. 4 (GIS-LCOE) and Fig. 5 (GIS-MCDA) that match the vicinity of shipping routes and pipelines as unsuitable for wind power plants. Nature protection areas in the Swedish, Latvian, Polish and German nearshore are also clearly identifiable. Areas close to shore are preferred for offshore wind power plant location. If marine protection areas, locations closer than 4 km to shore, and areas with water depths >50 m are excluded (bold brown colors in Figs. 6 and 7), the two methods produce similar results.

The application of different and multiple techniques provides additional confidence that the outcome of our research properly reflects the suitability in question, given that the MCDA and LCOE methods use quite different data. Application of the AHP approach to the results derived using the MCDA technique adds opinions of experts, reflected in the weights of the parameters (Chaouachi et al., 2017), providing even more confidence in the results that, in general, should lead to better
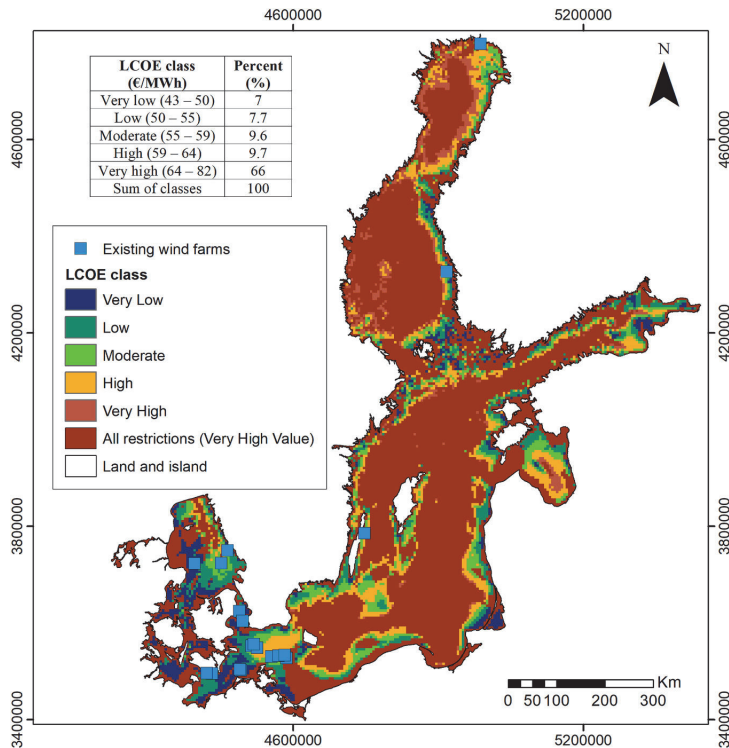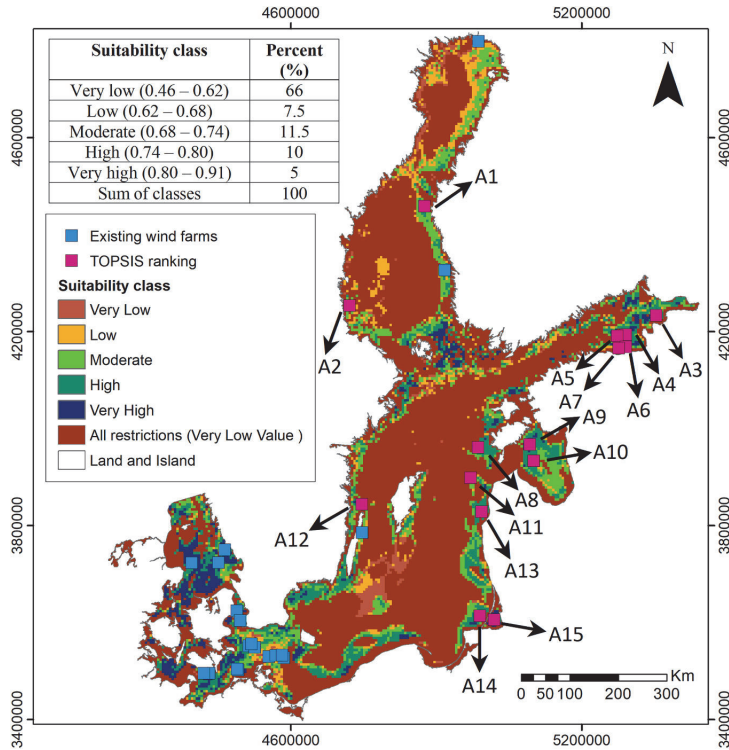
Fig. 8. Offshore wind power plant site suitability based on the GIS-MCDA, with all areas of restrictions highlighted.

spatial planning and decision making. Notably, the existing wind power plants are located in areas with low LCOE and high MCDA values.

The analysis also highlights large variations in the relative importance of variables in different part of the study area. For example, the northern parts of the Baltic Sea have high wind speeds, but other factors such as proximity to the shore and to ports, dominate the results. Martinez and Iglesias (2022) suggested this was primarily influenced by the distance to grid connection points. The importance of suitable seabed substrate influenced suitable areas located near the Danish, German, and Polish shores.

Although the use of LCOE methods for wind farm site selection is well established (Martinez and Iglesias, 2022), its implementation in a GIS framework for site selection, as has been done in this study, has not previously been reported. The benefits of this approach include the ability to easily incorporate buffer and exclusion zones, and the ease with which the results can be compared with those using other methodologies such as MCDA.

This study considered a wider variety of parameters than earlier studies (Caceoğlu et al., 2022; Gil-García et al., 2022; Gkeka-Serpetsidaki and Tsoutsos, 2022; Salvador et al., 2022, among others) for wind farm site suitability at the scale of the Baltic Sea. This exercise is the first basin-scale suitability assessment of its kind in the region. It also incorporates state-of-the-art industrial (Danish Energy Agency) standards and high-level environmental policy guidelines, such as European Maritime Spatial Planning Platform guidelines. The use of three different techniques, and multiple datasets provide confidence in the adequacy (and timeliness) of the outcome. The use of various environmental and socioeconomic parameters encourages managers and decision-makers to rely on this type of evidence-based considerations when planning future wind farm installations in the Baltic Sea.

The consideration of various MCDA methods in this study based on

fuzzy logic-AHP-WLC and the TOPSIS integrated with GIS and comparison with LCOE provided better outputs than studies based on a single technique (Caceoğlu et al., 2022; Gil-García et al., 2022; Martinez and Iglesias, 2022; Sánchez-Lozano et al. 2022). This approach makes it possible to choose suitable locations not only from the environmental perspective but also from an economic viewpoint. These considerations assist managers and decision-makers to create a balance between both environmental and economic objectives for wind farm development and to facilitate wind turbines investments and environmental protection in the long-term. Even though Vagiona and Kamilakis (2018) concluded that the combined application of GIS with AHP and TOPSIS methods is useful to rank the suitable areas in hierarchical order, our analysis suggests that the TOPSIS method does not necessarily add significant value to the analysis, similar to a conjecture by Gil-García et al. (2022) in the context of the Gulf of Maine, USA.

In this study, experts presented diverse worldviews, but they did not utilize the full weighting scale for making pairwise comparisons. This variation in utilization depends on the individual preferences of experts. Most experts favored environmental parameters over wind power generation parameters. In a study for renewable energy site selection in Iran (Barzehkar et al., 2020), most experts allocated higher priorities to energy generation parameters over those of parameters that are distance-based to protect the environment. This may indicate that experts in Europe prioritize environmental concerns more strongly than economic considerations when it comes to renewable power generation issues.

A limitation of the present study is the lack of data relating to potential grid connection points. This information may considerably affect wind farm site selection process in the Baltic Sea. The areas closer to grid connection points will be preferred over other sites due to lower cost for transferring power to the grid.
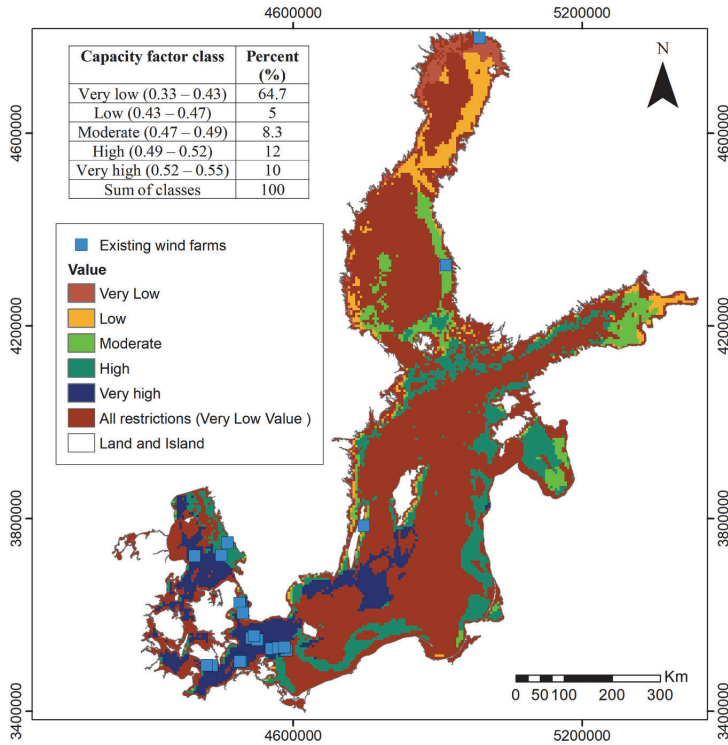
Fig. 9. Capacity factor for offshore wind power plant site suitability, with all areas of restrictions highlighted.
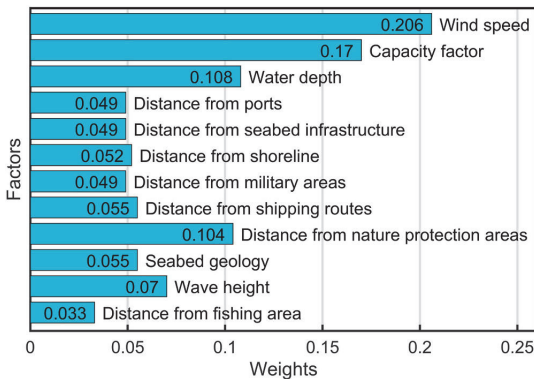
Fig. 10. Final weights assigned to the factors using the AHP method.

Fig. 11. Validation of results using the ROC model.

5. Conclusions

This study has been undertaken using multiple parameters, and a range of methods, considering the locations of existing wind farms, to suggest new sites for wind farms. This analysis helps experts to improve the accuracy of modelling and evaluation processes for wind farm site selection at a large scale (the Baltic Sea).

The study employed two well established techniques, the levelized cost of energy (LCOE) and multi-criteria decision analysis (MCDA) approach based on an analytical hierarch process (AHP), fuzzy logic, and weighted linear combination (WLC), with the technique for order of preference by similarity to ideal solution (TOPSIS) as an extension of the
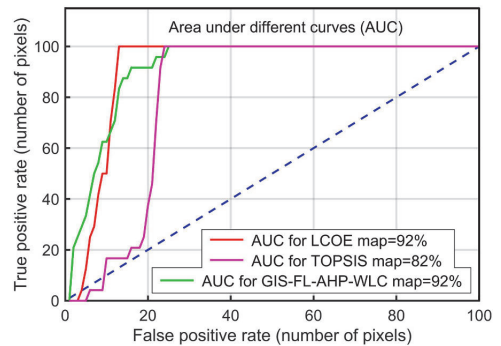
MCDA analysis, to analyze and map suitability for offshore wind farms locations.

The methods were applied within the framework of a GIS. The GIS technologies enable easy exclusion or buffering of areas based on important factors (such as the presence of marine protected areas). The use of both GIS-LCOE and GIS-MCDA provides a sound basis for spatial planners and decision makers to identify, rank, and optimize the locations of offshore wind farm at a large regional scale, in this case the entire Baltic Sea.

The use of different methodologies and different data types enables a comparison which supports confidence in the results. The two main techniques gave quite similar results that also match the already made decisions about the location of wind farms in the study area. It is thus

likely that both are suitable for application at the Baltic Sea scale when suitable input data are available. We used the guidelines of the Danish Energy Agency and the European Maritime Spatial Planning Platform, as well as publicly available scientific datasets. The addition of the TOPSIS technique did not add significantly to the study.

The most important factors determining site suitability in the Baltic Sea were wind speed, capacity factor, and water depth. Distance to nature protection area was also very significant. Some areas were specifically excluded (marine protection areas, sites too close to the shore, water depths >50 m). Some other areas require buffers (military areas, fishing areas, shipping lanes). While the most suitable areas for wind farms are in the south-west Baltic Sea, several suitable locations are identified further to the north and east.

CRediT authorship contribution statement

Kevin Parnell: Funding acquisition, Supervision, Writing – review & editing. **Mojtaba Barzehkar:** Conceptualization, Formal analysis, Investigation, Methodology, Writing – original draft. **Tarmo Soomere:** Writing – review & editing. **Matti Koivisto:** Methodology, Supervision, Writing – review & editing.

Declaration of competing interest

The authors declare that they have no known competing financial interests or personal relationships that could have appeared to influence the work reported in this paper.

Data availability

Data will be made available on request.

Acknowledgments

References

Aguarón, J., Moreno-Jiménez, J.M., 2003. The geometric consistency index: Approximated thresholds. Eur. J. Oper. Res. 147 (1), 137–145. https://doi.org/10.1016/S0377-2217(02)00255-2.

Akarsu, B., Genç, M.S., 2022. Optimization of electricity and hydrogen production with hybrid renewable energy systems. Fuel 324, 124465. https://doi.org/10.1016/j.fuel.2022.124465.

Annoni, A., Luzet, C., Gubler, E., Ihde, J. (eds.), 2003. Map Projections for Europe. European Commission Joint Research Centre, reference EUR 20120 EN, http://mapref.org/LinkedDocuments/MapProjectionsForEurope-EUR-20120.pdf.

Azadeh, A., Kor, H., Hatefi, S.M., 2011. A hybrid genetic algorithm-TOPSIS-computer simulation approach for optimum operator assignment in cellular manufacturing systems. J. Chin. Inst. Eng. 34 (1), 57–74. https://doi.org/10.1080/02533839.2011.552966.

Aydin, N.Y., Kentel, E., Duzgun, S., 2010. GIS-based environmental assessment of wind energy systems for spatial planning: a case study from Western Turkey. Renew. Sustain. Energy Rev. 14 (1), 364–373. https://doi.org/10.1016/j.rser.2009.07.023.

Baban, S.M.J., Parry, T., 2001. Developing and applying a GIS-assisted approach to locating wind farms in the UK. Renew. Energy 24 (1), 59–71. https://doi.org/10.1016/S0960-1481(00)00169-5.

Barthelmie, R.J., Frandsen, S.T., Nielsen, M.N., Pryor, S.C., Rethore, P.E., Jørgensen, H. E., 2007. Modelling and measurements of power losses and turbulence intensity in wind turbine wakes at Middelgrunden offshore wind farm. Wind Energy 10 (6), 517–528. https://doi.org/10.1002/we.238.

Bailey, H., Brookes, K.L., Thompson, P.M., 2014. Assessing environmental impacts of offshore wind farms: Lessons learned and recommendations for the future. Aquat. Biosyst. 10 (1), 8. https://doi.org/10.1186/2046-9063-10-8.

Barzehkar, M., Parnell, K.E., Mobarghaee Dinan, N., Brodie, G., 2020. Decision support tools for wind and solar farm site selection in Isfahan Province, Iran. Clean. Environ. Policy 23 (4), 1179–1195. https://doi.org/10.1007/s10098-020-01978-w.

Barzehkar, M., Parnell, K.E., Soomere, T., Dragovich, D., Engström, J., 2021. Decision support tools, systems and indices for sustainable coastal planning and management: A review. Ocean Coast. Manag. 212, 105813 https://doi.org/10.1016/j.ocecoaman.2021.105813.

Bilgili, M., Sahin, B., 2009. Investigation of wind energy density in the southern and southwestern region of Turkey. J. Energy Eng. 135 (1), 12–20. https://doi.org/10.1061/(ASCE)0733-9402(2009)135:1(12).

Bilgili, M., Yasar, A., Simsek, E., 2011. Offshore wind power development in Europe and its comparison with onshore counterpart. Renew. Sustain. Energy Rev. 15 (2), 905–915. https://doi.org/10.1016/j.rser.2010.11.006.

Björkqvist, J.V., Lukas, I., Alari, V., van Vledder, P.G., Hulst, S., Pettersson, H., Behrens, A., Männik, A., 2018. Comparing a 41-year model hindcast with decades of wave measurements from the Baltic Sea. Ocean Eng. 152, 57–71. https://doi.org/10.1016/j.oceaneng.2018.01.048.

Caceoğlu, E., Yildiz, H.K., Oğuz, E., Huvaj, N., Guerrero, J.M., 2022. Offshore wind power plant site selection using Analytical Hierarchy Process for Northwest Turkey. Ocean Eng. 252, 111178 https://doi.org/10.1016/j.oceaneng.2022.111178.

California ISO, 2018. Variable Operations and Maintenance Cost. Externally-authored report, pp. 21. https://www.caiso.com.

Cavazzi, S., Dutton, A.G., 2016. An Offshore Wind Energy Geographic Information System (OWE-GIS) for assessment of the UK's offshore wind energy potential. Renew. Energy 87, 212–228. https://doi.org/10.1016/j.renene.2015.09.021.

Chaouachi, A., Covrig, C.F., Ardelean, M., 2017. Multi-criteria selection of offshore wind farms: Case study for the Baltic States. Energy Policy 103, 179–192. https://doi.org/10.1016/j.enpol.2017.01.018.

Chen, W., Peng, J., Hong, H., Shahabi, H., Pradhan, B., Liu, J., Zhu, A.X., Pei, X., Duan, Z., 2018. Landslide susceptibility modelling using GIS-based machine learning techniques for Chongren County, Jiangxi Province, China. Sci. Total Environ. 626, 1121–1135. https://doi.org/10.1016/j.scitotenv.2018.01.124.

Chen, W., Shirzadi, A., Shahabi, H., Ahmad, B.B., Zhang, S., Hong, H., Zhang, N., 2017. A novel hybrid artificial intelligence approach based on the rotation forest ensemble and naïve Bayes tree classifiers for a landslide susceptibility assessment in Langao County, China. Geomat., Nat. Hazards Risk 8 (2), 1955–1977. https://doi.org/10.1080/19475705.2017.1401560.

Copernicus Marine Service, 2020. Baltic Sea Wave Hindcast. https://resources.marine.copernicus.eu/product-detail/BALTICSEA_REANALYSIS_WAV_003_015/INFORMATION. (Accessed 28 February 2022).

Danish Energy Agency (DEA), 2016. Technology Data - Energy Plants for Electricity and District heating generation. http://www.ens.dk/teknologikatalog.

Danish Energy Agency (DEA), 2022. Offshore Wind Development. https://ens.dk/sites/ens.dk.

Deveci, M., Özcan, E., John, R., Covrig, C.F., Pamucar, D., 2020. A study on offshore wind farm siting criteria using a novel interval-valued fuzzy-rough based Delphi method. J. Environ. Manag. 270, 110916 https://doi.org/10.1016/j.jenvman.2020.110916.

Díaz-Cuevas, P., Domínguez-Bravo, J., Prieto-Campos, A., 2019. Integrating MCDM and GIS for renewable energy spatial models: assessing the individual and combined potential for wind, solar and biomass energy in Southern Spain. Clean. Technol. Environ. Policy 21 (9), 1855–1869. https://doi.org/10.1007/s10098-019-01754-5.

Díaz, H., Guedes Soares, C., 2020. An integrated GIS approach for site selection of floating offshore wind farms in the Atlantic continental European coastline. Renew. Sustain. Energy Rev. 134, 110328 https://doi.org/10.1016/j.rser.2020.110328.

Díaz, H., Guedes Soares, C., 2021. A multi-criteria approach to evaluate floating offshore wind farms siting in the Canary Islands (Spain). Energies 14, 865. https://doi.org/10.3390/en14040865.

Eastman, J.R., 2009. IDRIS Taiga Guide to GIS and Image Processing. Clark Labs Clark Univ. 1–342.

Eelsalu, M., Aramburo, D., Montoy, R.D., Osorio, A.F., Soomere, T., 2024. Spatial and temporal variability of wave energy resource in eastern Pacific from Panama to the Drake Passage. Renewable Energy 224, 120180. https://doi.org/10.1016/j.renene.2024.120180.

Emeksiz, C., Demirci, B., 2019. The determination of offshore wind energy potential of Turkey by using novelty hybrid site selection method. Sustain. Energy Technol. Assess. 36, 100562 https://doi.org/10.1016/j.seta.2019.100562.

EMODnet, 2022a. Seabed substrates. https://www.emodnet-geology.eu/ma p-viewer/?p=seabed_substrate. (Accessed 22 February 2022).

EMODnet, 2022b. Human activities. https://www.emodnet-humanactivities.eu/search-results.php?dataname=Ship+Wrecks. (Accessed 15 February 2022).

EMODnet, 2019. EU Vessel density map Detailed method. Human activities making use of our oceans. pp. 36. https://www.emodnet-humanactivities.eu.

Energinet, 2017. https://Energinet.dk, March 2017.

Estonian Maritime Spatial Plan, 2019. The draft of the MSP. pp. 42. http://mereala.hendrikson.ee/dokumendid/Eskiis/Estonian_MSP_draft_plan_ENG.pdf.

European Commission, 2020. Recommendations for positive interactions between offshore wind farms and fisheries. pp. 26. https://maritime-spatial-planning.ec.europa.eu/sites/default/files/recommendations_for_positive_interactions_between_offshore_wind_farms_and_fisheries.pdf.pdf.

European Commission, 2022. Proposal for a council regulation laying down a framework to accelerate the deployment of renewable energy. pp. 15. https://eur-lex.europa.eu/legal-content/EN/TXT/PDF/?uri=CELEX:52022PC0591&from=EN.

European MSP Platform, 2018a. Conflict fiche 8: Offshore wind and area-based marine conservation. 1 – 20. https://maritime-spatial-planning.ec.europa.eu/sites/default/files/sector/pdf/8_offshore_wind_conservation.pdf.

European MSP Platform, 2018b. Maritime Spatial Planning (MSP) for Blue Growth. Final Tech. Study 1–307. https://doi.org/10.2826/04538.

European MSP Platform, 2018c. Sector Fiche: Cables and Pipelines. 1–11. https://maritime-spatial-planning.ec.europa.eu/sites/default/files/sector/pdf/mspforbluegrowth_sectorfiche_cablespipelines.pdf.

European MSP Platform, 2018d. Conflict fiche 7: Maritime transport and offshore wind. 1 – 22. https://maritime-spatial-planning.ec.europa.eu/sites/default/files/sector/pdf/7_transport_offshore_wind_kg.pdf.

European MSP Platform, 2018e. Conflict fiche 5: Offshore wind and commercial fisheries. 1 – 24. https://maritime-spatial-planning.ec.europa.eu/sites/default/files/sector/pdf/5_offshore_wind_fisheries.pdf.

European MSP Platform, 2019. Conflict fiche 3: Defence and other sea uses. 1–21. https://maritime-spatial planning.ec.europa.eu/sites/default/files/sector/pdf/3_military.pdf.

Freyman, T., Tran, T., 2018. Grant Thornton: Renewable energy discount rate survey results – 2017. A Grant Thornton and Clean Energy Pipeline initiative. https://www.grantthornton.co.uk/insights/renewable-energy-discount-rate-survey/.

Foroozesh, F., Monavari, S.M., Salmanmahiny, A., Robati, M., Rahimi, R., 2022. Assessment of sustainable urban development based on a hybrid decision-making approach: Group fuzzy BWM, AHP, and TOPSIS–GIS. Sustain. Cities Soc. 76, 103402 https://doi.org/10.1016/j.scs.2021.103402.

GEBCO Bathymetric Compilation Group, 2020. The GEBCO_2020 Grid - a continuous terrain model of the global oceans and land. British Oceanographic Data Centre. National Oceanography Centre,, NERC, UK. https://doi.org/10.5285/a29c5465-b138-234d-e053-6c86abc040b9.

Genç, M.S., 2010. Economic analysis of large-scale wind energy conversion systems in Central Anatolian Turkey. In: Eguchi, K. (ed). Clean Energy Systems and Experiences. Intech-Sciyo, 131–154. https://doi.org/10.5772/intechopen.83968.

Genç, M.S., 2011. Economic viability of water pumping systems supplied by wind energy conversion and diesel generator systems in North Central Anatolia, Turkey. J. Energy Eng. -ASCE 137 (1), 21–35. https://doi.org/10.1061/(ASCE)EY.1943-7897.0000033.

Genç, M.S., Gökçek, M., 2009. Evaluation of wind characteristics and energy potential in Kayseri, Turkey. J. Energy Eng. -ASCE 135 (2), 33–43. https://doi.org/10.1061/(ASCE)0733-9402(2009)135:2(33).

Genç, M.S., Çelik, M., Karasu, İ., 2012a. A review on wind energy and wind–hydrogen production in Turkey: A case study of hydrogen production via electrolysis system supplied by wind energy conversion system in Central Anatolian Turkey. Renew. Sustain. Energy Rev. 16, 6631–6646. https://doi.org/10.1016/j.rser.2012.08.011.

Genç, G., Çelik, M., Genç, M.S., 2012b. Cost analysis of wind-electrolyzer-fuel cell system for energy demand in Pınarbaşı-Kayseri. Int. J. Hydrog. Energy 37 (17), 12158–12166. https://doi.org/10.1016/j.ijhydene.2012.05.058.

Genç, M.S., Karipoğlu, F., Koca, K., Azgın, S.T., 2021. Suitable site selection for offshore wind farms in Turkey's seas: GIS MCDM based approach. Earth Sci. Inform. 14, 1213–1225. https://doi.org/10.1007/s12145-021-00632-3.

Ghorbanzadeh, O., Blaschke, T., Gholamnia, K., Aryal, J., 2019. Forest fire susceptibility and risk mapping using social/infrastructural vulnerability and environmental variables. Fire 2 (3), 50. https://doi.org/10.3390/fire2030050.

Gielen, D., Boshell, F., Saygin, D., Bazilian, M.D., Wagner, N., Gorini, R., 2019. The role of renewable energy in the global energy transformation. Energy Strategy Rev. 24, 38–50. https://doi.org/10.1016/j.esr.2019.01.006.

Gil-García, I.C., Ramos-Escudero, A., García-Cascales, M.S., Dagher, H., Molina-García, A., 2022. Fuzzy GIS-based MCDM solution for the optimal offshore wind site selection: The Gulf of Maine case. Renew. Energy 183, 130–147. https://doi.org/10.1016/j.renene.2021.10.058.

Global Wind Atlas, 2022. Wind layers. https://globalwindatlas.info. (Accessed 15 February 2022).

Gkeka-Serpetsidaki, P., Tsoutsos, T., 2022. A methodological framework for optimal siting of offshore wind farms: A case study on the island of Crete. Energy 239, 122296. https://doi.org/10.1016/j.energy.2021.122296.

Gökçek, M., Genç, M.S., 2009. Evaluation of electricity generation and energy cost of wind energy conversion systems (WECSs) in Central Turkey. Appl. Energy 86 (12), 2731–2739. https://doi.org/10.1016/j.apenergy.2009.03.025.

Golestani, N., Arzaghi, E., Abbassi, R., Garaniya, V., Abdussamie, N., Yang, M., 2021. The Game of Guwarra: a game theory-based decision-making framework for site selection of offshore wind farms in Australia. J. Clean. Prod. 326, 129358 https://doi.org/10.1016/j.jclepro.2021.129358.

González, A., Connell, P., 2022. Developing a renewable energy planning decision-support tool: Stakeholder input guiding strategic decisions. Appl. Energy 312, 118782. https://doi.org/10.1016/j.apenergy.2022.118782.

Guchhait, R., Sarkar, B., 2023. Increasing growth of renewable energy: A state of art. Energies 16 (6), 2665. https://doi.org/10.3390/en16062665.

Hasager, C.B., Badger, M., Pena, A., Larsen, X.G., Bingol, F., 2011. SAR-based wind resource statistics in the Baltic Sea. Remote Sens. 3 (1), 117–144. https://doi.org/10.3390/rs3010117.

Hasager, C.B., Hahmann, A.N., Ahsbahs, T., Karagali, I., Sile, T., Badger, M., Mann, J., 2020. Europe's offshore winds assessed with synthetic aperture radar, ASCAT and WRF. Wind Energy Sci. 5 (1), 375–390. https://doi.org/10.5194/wes-5-375-2020.

HELCOM, 2022a. Protected areas. https://maps.helcom.fi/website/mapservice/index.html. (Accessed 15 February 2022).

HELCOM, 2022b. Coastline. https://maps.helcom.fi/website/mapservice/index.html. (Accessed 15 February 2022).

Hersbach, H., Bell, B., Berrisford, P., Hirahara, S., Horanyi, A., Munoz-Sabater, J., Nicolas, J., Peubey, C., Radu, R., Schepers, D., Simmons, A., Soci, C., Abdalla, S., Abellan, X., Balsamo, G., Bechtold, P., Biavati, G., Bidlot, J., Bonavita, M., De Chiara, G., Dahlgren, P., Dee, D., Diamantakis, M., Dragani, R., Flemming, J.,

Forbes, R., Fuentes, M., Geer, A., Haimberger, L., Healy, S., Hogan, R.J., Holm, E., Janiskova, M., Keeley, S., Laloyaux, P., Lopez, P., Lupu, C., Radnoti, G., de Rosnay, P., Rozum, I., Vamborg, F., Villaume, S., Thepaut, J.N., 2020. The ERA5 global reanalysis. Q. J. R. Meteorol. Soc. 146 (730), 1999–2049. https://doi.org/10.1002/qj.3803.

IEA, 2019. Offshore Wind Outlook. International Energy Agency, pp. 96. https://www.iea.org/corrections/www.oecd.org/about/ publishing/corrigenda.htm.

IRENA, 2019. Future of wind deployment, investment, technology, grid integration and socio-economic aspects (A Global Energy Transformation paper). International Renewable Energy Agency, Abu Dhabi, pp. 83. https://www.irena.org/-/media/files/irena/agency/publication/2019/oct/irena_future_of_wind_2019.pdf.

Johnston, B., Foley, A., Doran, J., Littler, T., 2020. Levelised cost of energy, A challenge for offshore wind. Renew. Energy 160, 876–885. https://doi.org/10.1016/j.renene.2020.06.030.

Kao, C., 2010. Fuzzy data standardization. IEEE Trans. Fuzzy Syst. 18, 745–754. https://doi.org/10.1109/TFUZZ.2010.2047948.

Karipoğlu, F., Genç, M.S., Koca, K., 2021. Determination of the most appropriate site selection of wind power plants based Geographic Information System and Multi-Criteria Decision-Making approach in Develi. Turk. Int. J. Sustain. Energy Plan. Manag. 30, 97–114. https://doi.org/10.5278/ijsepm.6242.

Khan, A., Seyedmahmoudian, M., Raza, A., Stojcevski, A., 2021. Analytical review on common and state-of-the-art FR strategies for VSC-MTDC integrated offshore wind power plants. Renew. Sustain. Energy Rev. 148, 111106 https://doi.org/10.1016/j.rser.2021.111106.

Klinge Jacobsen, H., Hevia-Koch, P., Wolter, C., 2019. Nearshore and offshore wind development: Costs and competitive advantage exemplified by nearshore wind in Denmark. Energy Sustain. Dev. 50, 91–100. https://doi.org/10.1016/j.esd.2019.03.006.

Konstantinos, I., Georgios, T., Garyfalos, A., 2019. A Decision Support System methodology for selecting wind farm installation locations using AHP and TOPSIS: Case study in Eastern Macedonia and Thrace region, Greece. Energy Policy 132, 232–246. https://doi.org/10.1016/j.enpol.2019.05.020.

Latinopoulos, D., Kechagia, K., 2015. A GIS-based multi-criteria evaluation for wind farm site selection. A regional scale application in Greece. Renew. Energy 78, 550–560. https://doi.org/10.1016/j.renene.2015.01.041.

Leppäranta, M., Myrberg, K., 2009. Physical Oceanography of the Baltic Sea. Springer,, Berlin, p. 378. https://doi.org/10.1007/978-3-540-79703-6.

Li, Z., Tian, G., El-Shafay, A.S., 2022. Statistical-analytical study on world development trend in offshore wind energy production capacity focusing on Great Britain with the aim of MCDA based offshore wind farm siting. J. Clean. Prod. 363, 132326 https://doi.org/10.1016/j.jclepro.2022.132326.

Malczewski, J., Rinner, C., 2015. GIScience, Spatial Analysis, and Decision Support. Multicriteria Decision Analysis in Geographic Information Science. Springer, pp. 3–21. https://doi.org/10.1007/978-3-540-74757-4.

Malczewski, J., 2000. On the use of weighted linear combination method in GIS: common and best practice approaches. Trans. GIS 4 (1), 5–22. https://doi.org/10.1111/1467-9671.00035.

Mahdy, M., Bahaj, A.B.S., 2018. Multi criteria decision analysis for offshore wind energy potential in Egypt. Renew. Energy 118, 278–289. https://doi.org/10.1016/j.renene.2017.11.021.

Martinez, A., Iglesias, G., 2022. Mapping of the levelised cost of energy for floating offshore wind in the European Atlantic. Renew. Sustain. Energy Rev. 154, 111889 https://doi.org/10.1016/J.RSER.2021.111889.

Martinez, A., Iglesias, G., 2022. Site selection of floating offshore wind through the levelised cost of energy: A case study in Ireland. Energy Convers. Manag. 266, 115802 https://doi.org/10.1016/j.enconman.2022.115802.

Möller, B., Hong, L., Lonsing, R., Hvelplund, F., 2012. Evaluation of offshore wind resources by scale of development. Energy 48 (1), 314–322. https://doi.org/10.1016/j.energy.2012.01.029.

Mu, E., Pereyra-Rojas, M., 2018. Practical Decision Making using Super Decisions v3. An Introduction to The Analytic Hierarchy Process. Chapter 3: Build. AHP Models Using Super. Decis. v3 23–42. https://doi.org/10.1007/978-3-319-68369-0.

Myhr, A., Bjerkseter, C., Ågotnes, A., Nygaard, T.A., 2014. Levelised cost of energy for offshore floating wind turbines in a life cycle perspective. Renew. Energy 66, 714–728. https://doi.org/10.1016/j.renene.2014.01.017.

Mytilinou, V., Lozano-Minguez, E., Kolios, A., 2018. A framework for the selection of optimum offshore wind farm locations for deployment. Energies 11 (7), 1855. https://doi.org/10.3390/en11071855.

Nedjati, A., Yazdi, M., Abbassi, R., 2021. A sustainable perspective of optimal site selection of giant air-purifiers in large metropolitan areas. Environ., Dev. Sustain. 24, 8747–8778. https://doi.org/10.1007/s10668-021-01807-0.

Noorollahi, Y., Senani, A.G., Fadaei, A., Simaee, M., Moltames, R., 2022. A framework for GIS-based site selection and technical potential evaluation of PV solar farm using Fuzzy-Boolean logic and AHP multi-criteria decision-making approach. Renew. Energy 186, 89–104. https://doi.org/10.1016/j.renene.2021.12.124.

Noorollahi, Y., Yousefi, H., Mohammadi, M., 2016. Multi-criteria decision support system for wind farm site selection using GIS. Sustain. Energy Technol. Assess. 13, 38–50. https://doi.org/10.1016/j.seta.2015.11.007.

Nyberg, J., Zillen-Snowball, L., Stromstedt, E., 2022. Spatial characterization of seabed environmental conditions and geotechnical properties for the development of marine renewable energy in Sweden. Quartely J. Eng. Gecology Hydrogeol. 55 (4), 1–23. DOI10.1144/qjegh2021-091.

Orhan, O., 2021. Land suitability determination for citrus cultivation using a GIS-based multi-criteria analysis in Mersin, Turkey. Comput. Electron. Agric. 190, 106433 https://doi.org/10.1016/j.compag.2021.106433.

Pourghasemi, H.R., Beheshtirad, M., Pradhan, B., 2016. A comparative assessment of prediction capabilities of modified analytical hierarchy process (m-AHP) and Mamdani fuzzy logic models using NETCAD-GIS for forest fire susceptibility mapping. Geomat., Nat. Hazards Risk 7, 861–885. https://doi.org/10.1080/19475705.2014.984247.

Osman, A.I., Chen, L., Yang, M.Y., Msigwa, G., Farghali, M., Fawzy, S., Rooney, D.W., Yap, P.S., 2022. Cost, environmental impact, and resilience of renewable energy under a changing climate: a review. Environ. Chem. Lett. 21, 741–764. https://doi.org/10.1007/s10311-022-01532-8.

Rambøll, 2014. Sejerø Bugt Offshore Wind Farm Fish. https://ramboll.com/energy.

Reckermann, M., Omstedt, A., Soomere, T., Aigars, J., Akhtar, N., Bełdowska, M., Bełdowski, J., Cronin, T., Czub, M., Eero, M., Hyytiäinen, K.P., Jalkanen, J.P., Kiessling, A., Kjellström, E., Kuliński, K., Larsén, X.G., McCrackin, M., Meier, H.E.M., Oberbeckmann, S., Parnell, K., Pons-Seres De Brauwer, C., Poska, A., Saarinen, J., Szymczycha, B., Undeman, E., Wörman, A., Zorita, E., 2022. Human impacts and their interactions in the Baltic Sea region. Earth Syst. Dyn. 13, 1–80. https://doi.org/10.5194/esd-13-1-2022.

Rusu, E., 2020. An evaluation of the wind energy dynamics in the Baltic Sea, past and future projections. Renew. Energy 160, 350–362. https://doi.org/10.1016/j.renene.2020.06.152.

Saaty, T.L., Tran, L.T., 2007. On the invalidity of fuzzifying numerical judgments in the Analytic Hierarchy Process. Math. Comput. Model. 46, 962–975. https://doi.org/10.1016/j.mcm.2007.03.022.

Salvador, C.B., Arzaghi, E., Yazdi, M., Jahromi, H.A.F., Abbassi, R., 2022. A multi-criteria decision-making framework for site selection of offshore wind farms in Australia. Ocean Coast. Manag. 224, 106196 https://doi.org/10.1016/j.ocecoaman.2022.106196.

Sánchez-Lozano, J.M., Ramos-Escudero, A., Gil-García, I.C., García-Cascales, M.S., Molina-García, A., 2022. A GIS-based offshore wind site selection model using fuzzy multi-criteria decision-making with application to the case of the Gulf of Maine. Expert Syst. Appl. 210, 118371 https://doi.org/10.1016/j.eswa.2022.118371.

Satish, S., Sannasiraj, S.A., Sundar, V., 2019. Estimation and analysis of extreme maximum wave heights. In: K. Murali et al. (Ed.). Proceedings of the Fourth International Conference in Ocean Engineering (ICOE2018), 22, 723–732. https://doi.org/10.1007/978-981-13-3119-0_47.

Schallenberg-Rodríguez, J., Montesdeoca, N.G., 2018. Spatial planning to estimate the offshore wind energy potential in coastal regions and islands. Practical case: The Canary Islands. Energy 143, 91–103. https://doi.org/10.1016/j.energy.2017.10.084.

Scolaro, M., Kittner, N., 2022. Optimizing hybrid offshore wind farms for cost-competitive hydrogen production in Germany. Int. J. Hydrog. Energy 47, 6478–6493. https://doi.org/10.1016/j.ijhydene.2021.12.062.

Shafiee, M., 2022. Wind energy development site selection using an Integrated Fuzzy ANP-TOPSIS Decision Model. Energies 15, 4289. https://doi.org/10.3390/en15124289.

Shipkovs, P., Bezrukov, V., Pugachev, V., Bezrukovs, V., Silutins, V., 2013. Research of the wind energy resource distribution in the Baltic region. Renew. Energy 49, 119–123. https://doi.org/10.1016/j.renene.2012.01.050.

Sindhu, S., Nehra, V., Luthra, S., 2017. Investigation of feasibility study of solar farms deployment using hybrid AHP-TOPSIS analysis: case study of India. Renew. Renew. Sustain. Energy Rev. 73, 496–511. https://doi.org/10.1016/j.rser.2017.01.135.

Spyridonidou, S., Vagiona, D.G., 2020. Spatial energy planning of offshore wind farms in Greece using GIS and a hybrid MCDM methodological approach. Eur. -Mediterr. J. Environ. Integr. 5, 24. https://doi.org/10.1007/s41207-020-00161-3.

Swisher, P., Leon, J.P.M., Gea-Bermúdez, J., Koivisto, M., Madsen, H.A., Münster, M., 2022. Competitiveness of a low specific power, low cut-out wind speed wind turbine in North and Central Europe towards 2050. Appl. Energy 306, 118043. https://doi.org/10.1016/j.apenergy.2021.118043.

Tegou, L., Polatidis, H., Haralambopoulos, D.A., 2010. Environmental management framework for wind farm siting: methodology and case study. J. Environ. Manag. 91, 2134–2147. https://doi.org/10.1016/j.jenvman.2010.05.010.

Tercan, E., Tapkın, S., Latinopoulos, D., Dereli, M.A., Tsiropoulos, A., Ak, M.F., 2020. A GIS-based multi-criteria model for offshore wind energy power plants site selection in both sides of the Aegean Sea. Environ. Monit. Assess. 192, 652. https://doi.org/10.1007/s10661-020-08603-9.

Thor Ugelvig, P., 2014. Scour around Offshore Wind Turbine Foundations. Ph.D. thesis. Section. In: for Fluid Mechanics, Coastal and Maritime Engineering. Department of Mechanical Engineering. Technical University of Denmark, Kgs. Lyngby, Denmark.

Tien Bui, D., Tuan, T.A., Klempe, H., Pradhan, B., Revhaug, I., 2016. Spatial prediction models for shallow landslide hazards: a comparative assessment of the efficacy of support vector machines, artificial neural networks, kernel logistic regression, and logistic model tree. Landslides 13 (2), 361–378. https://doi.org/10.1007/s10346-015-0557-6.

Tonderski, A., Jędrzejewski, A. (eds.), 2013. Offshore wind energy in the South Baltic region - Challenges & opportunities. https://backend.orbit.dtu.dk/ws/portalfiles/portal/155566673/South_Baltic_OFFER.pdf.

Vagiona, D.G., Kamilakis, M., 2018. Sustainable site selection for offshore wind farms in the South Aegean — Greece. Sustainability 10 (3), 749. https://doi.org/10.3390/su10030749.

Vagiona, D.G., Karanikolas, N.M., 2012. A multicriteria approach to evaluate offshore wind farms sitting in Greece. Glob. NEST J. 14, 235–243. https://doi.org/10.30955/gnj.000868.

Vagiona, D.G., Tzekakis, G., Loukogeorgaki, E., Karanikolas, N., 2022. Site selection of offshore solar farm Deployment in the Aegean Sea, Greece. J. Mar. Sci. Eng. 10 (2), 224. https://doi.org/10.3390/jmse10020224.

Vasileiou, M., Loukogeorgaki, E., Vagiona, D.G., 2017. GIS-based multi-criteria decision analysis for site selection of hybrid offshore wind and wave energy systems in Greece. Renew. Sustain. Energy Rev. 73, 745–757. https://doi.org/10.1016/j.rser.2017.01.161.

Vinhoza, A., Schaeffer, R., 2021. Brazil's offshore wind energy potential assessment based on a Spatial Multi-Criteria Decision Analysis. Renew. Sustain. Energy Rev. 146, 111185 https://doi.org/10.1016/j.rser.2021.111185.

Virtanen, E.A., Lappalainen, J., Nurmi, M., Viitasalo, M., Tikanmäki, M., Heinonen, J., Atlaskin, E., Kallasvuo, M., Tikkanen, H., Moilanen, A., 2022. Balancing profitability of energy production, societal impacts and biodiversity in offshore wind farm design. Renew. Sustain. Energy Rev. 158, 112087 https://doi.org/10.1016/j.rser.2022.112087.

Wang, S., Wang, S., 2015. Impacts of wind energy on environment: A review. Renew. Sustain. Energy Rev. 49, 437–443. https://doi.org/10.1016/j.rser.2015.04.137.

Wind Europe. Wind energy in Europe in 2019. Trends and statistics. https://windeurope.org/wp-content/uploads/files/about-wind/statistics/WindEurope-Annual-Statistics-2019.pdf.

Wu, B., Yip, T.L., Xie, L., Wang, Y., 2018. A fuzzy-MADM based approach for site selection of offshore wind farm in busy waterways in China. Ocean Eng. 168, 121–132. https://doi.org/10.1016/j.oceaneng.2018.08.065.

Zarin, R., Azmat, M., Naqvi, S.R., Saddique, Q., Ullah, S., 2021. Landfill site selection by integrating fuzzy logic, AHP, and WLC method based on multi-criteria decision analysis. Environ. Sci. Pollut. Res. 28 (16), 19726–19741. https://doi.org/10.1007/s11356-020-11975-7.

Zhou, X., Huang, Z., Wang, H., Yin, G., Bao, Y., Dong, Q., Liu, Y., 2022. Site selection for hybrid offshore wind and wave power plants using a four-stage framework: A case study in Hainan, China. Ocean Coast. Manag. 218, 106035 https://doi.org/10.1016/j.ocecoaman.2022.106035.

Ziemba, P., 2022. Uncertain Multi-Criteria analysis of offshore wind farms projects investments – Case study of the Polish Economic Zone of the Baltic Sea. Appl. Energy 309, 118232. https://doi.org/10.1016/j.apenergy.2021.118232.

III

Publication III

Barzehkar, M., Parnell, K., Soomere, T. 2024. Extending multi-criteria coastal vulnerability assessment to low-lying inland areas: examples from Estonia, eastern Baltic Sea. Estuarine, Coastal and Shelf Science, 311, 109014, doi: 10.1016/j.ecss.2024.109014.

Extending multi-criteria coastal vulnerability assessment to low-lying inland areas: Examples from Estonia, eastern Baltic Sea

Mojtaba Barzehkar [a,*], Kevin Parnell [a], Tarmo Soomere [a,b]

[a] Department of Cybernetics, School of Science, Tallinn University of Technology, Tallinn, Estonia
[b] Estonian Academy of Sciences, 10130, Kohtu 6, Tallinn, Estonia

A R T I C L E   I N F O

A B S T R A C T

The assessment of vulnerability to coastal hazards is a significant coastal management problem in regions with complicated shoreline, such as Estonia. This study implements the vulnerability assessment based on the multi-criteria decision analysis using fuzzy logic, analytical hierarchy process, and weighted linear combination (including input from experts) integrated with a geographical information system, to map the coastal vulnerability index (CVI) of the Estonian coasts at high resolution based on 16 parameters. The novelty of our approach is that we expand this assessment to a 2 km wide inland area that is an intrinsic but often overlooked part of coastal vulnerability estimates. The Estonian shores have mostly low and moderate vulnerability. Short segments with high vulnerability are impacted by severe waves and highly elevated water levels. The CVI also characterizes low-lying areas, such as large river valleys, reasonably well. Estimates of coastal vulnerability based on the three most important parameters according to experts' judgements provide a reasonable approximation of the 16-parameter CVI in mostly homogeneous coastal regions, but less so elsewhere where its value is questioned. The results show that the application of the developed integrated decision support system, applied to a 2 km wide coastal strip, provides more information than single tools to assist coastal managers and stakeholders in planning, preparing for and responding to hazards.

1. Introduction

Coastal areas worldwide are susceptible to climate change induced hazards (IPCC et al., 2022; Torresan et al., 2008; WMO, 2021; Tokunaga et al., 2021). Coastal regions can be adversely affected by sea level changes, storm surges, and resulting inundation of low-lying areas (Torresan et al., 2008; Nicholls et al., 2007). Coastal hazards can cause damage to the physical environment and may lead to loss of land (Wong et al., 2014). They can also negatively affect infrastructure and human livelihoods (Nichols et al., 2019; Tanner et al., 2014), along with loss of ecosystem services and biodiversity in marine and coastal ecosystems (Myers et al., 2019).

The identification of causes and effects of marine-driven threats (Rutgersson et al., 2022) assists a community to deal effectively with the hazards, to improve social well-being and reduce economic damage. An appropriate strategy for coastal protection and management should specifically identify climatic hazards, the exposure of people and assets to the hazards, and the susceptibility of human and natural systems to damage (IPCC et al., 2014). Coastal vulnerability describes the

characteristics and circumstances of an asset, community, or system that make it susceptible to the harmful effects of coastal hazards (Rangel-Buitrago et al., 2020). One planning strategy is vulnerability assessment, which has become increasingly used by scientists and managers to help coastal communities become resilient to hazards (Adger et al., 2005). It assists coastal managers and planners to comprehend the impacts of natural elements and to determine the vulnerability of locations in terms of planning environmental management strategies (Thirumurthy et al., 2022). Not only is it important to incorporate climate change-induced hazards into coastal vulnerability assessments, but also human-induced environmental changes and socio-economic developments, and their interactions (Ramieri et al., 2011).

Coastal vulnerability indicators are parameters or values derived from environmental parameters that describe some aspect of the state of a coastal system. They may represent a moment in time, or if appropriately measured, may show changes or trends. A coastal vulnerability assessment may be based on indicators alone, as analysed or reviewed by relevant experts. Indicators can be characterized, and then by

aggregation and/or weighting, be the basis of an index (Mclaughlin and Cooper, 2010), sometimes referred to as a 'composite indicator' (Hinkel, 2011). For some problems consideration of indicators alone may be sufficient, but for others, including for comparison and decision support, indexes may be more useful.

Although the weighting and ranking of variables involves some subjectivity, with well-defined criteria, the resulting index becomes a valuable tool for decision-makers. Its simplified format enhances its utility as a practical management tool (Ramieri et al., 2011) Although other indices have been proposed (Mullick et al., 2019; Alcántara-Carrió et al., 2024), the coastal vulnerability index (CVI) (Gornitz et al., 1994) remains the most used method to calculate coastal vulnerability (Rangel-Buitrago et al., 2020). It is a numerical method for prioritizing the vulnerability of coastal segments considering the contribution of different parameters describing geophysical (Bagdanavičiūtė et al., 2015; Koroglu et al., 2019) and socio-economic (Serafim et al., 2019; Tanim et al., 2022; Sethuraman et al., 2024) conditions. This flexibility is one of the reasons why we decided to employ this quantity for our analysis.

The application of decision support tools (DSTs) assists the estimates of coastal vulnerability to incorporate into coastal adaptation planning strategies (Gargiulo et al., 2020). Geographical Information Systems (GIS) have been widely used in many studies of coastal vulnerability (Ahmed et al., 2022; Armenio et al., 2021; Hoque et al., 2019; Rehman et al., 2022). The use of GIS allows spatial information to be represented, analyzed, and visualized effectively (Barzehkar et al., 2021), and makes combining different parameters in a vulnerability assessment possible (Thirumurthy et al., 2022).

Multi-criteria decision analysis (MCDA) is a methodology for specifying and allocating values to the evaluation parameters according to the decision situation. The integration of GIS and MCDA provides a set of tools that transform and combine spatial data and expert priorities to generate information for the decision-making process (Malczewski and Rinner, 2015). MCDA provides a way to better understand the outputs incorporating the opinions of experts and enables trade-offs among decision goals (Bell et al., 2003).

The application of GIS and MCDA based on the analytical hierarchy process (AHP) has been used in many studies for coastal vulnerability assessment (Armenio et al., 2021; Bagdanavičiūtė et al., 2015; Ghosh and Mistri, 2022; Sekovski et al., 2020). Mullick et al. (2019) undertook a coastal vulnerability analysis by integrating GIS and fuzzy logic in Bangladesh. This exercise was revisited using principal component analysis to map climate vulnerability of the coastal region of Bangladesh (Uddin et al., 2019). Bagdanavičiūtė et al. (2019) employed GIS, AHP, and weighted linear combination (WLC) for coastal vulnerability and exposure assessment of the Lithuanian coast of the Baltic Sea. Kovaleva et al. (2022) employ both the classic CVI estimates based on the approach of Gornitz (1991) and its weighted version for the eastern Gulf of Finland in the Baltic Sea. A further of extension of this kind of analysis is addressed by (Fannassi et al., 2023) who made an attempt to integrate machine learning models in this technique.

All these techniques and approaches work well along relatively straight shores where the parameters that govern coastal vulnerability vary smoothly. The situation is much more complicated in regions with complex geometry, morphology and geology, and even more in locations that have various coastal engineering structures, such as in the vicinity of major cities in the eastern Baltic Sea (Kovaleva et al., 2022).

While different approaches to assess coastal vulnerability could be used, in this study we choose to apply and develop the most widely used method, the CVI, to make three specific contributions to fill gaps in the existing literature, while also providing an assessment of the coastal vulnerability for Estonia, eastern Baltic Sea (Fig. 1), in this sense serving as a major extension of the analysis of Kovaleva et al. (2022) undertaken for the eastern end of the Gulf of Finland in a similar intricate situation.

The three objectives of this study are: (1) in the context of the CVI, to apply various MCDA techniques based on fuzzy logic-AHP-WLC, integrated with GIS to produce a coastal vulnerability assessment of the Estonian coast at high resolution, (2) to integrate less obvious and less used parameters such as the location of nature protection areas, land tenure (ownership), and setbacks (the distance of the first infrastructure from the shoreline) to improve the coastal vulnerability analysis, and (3) to produce a vulnerability assessment for the whole Estonian coast
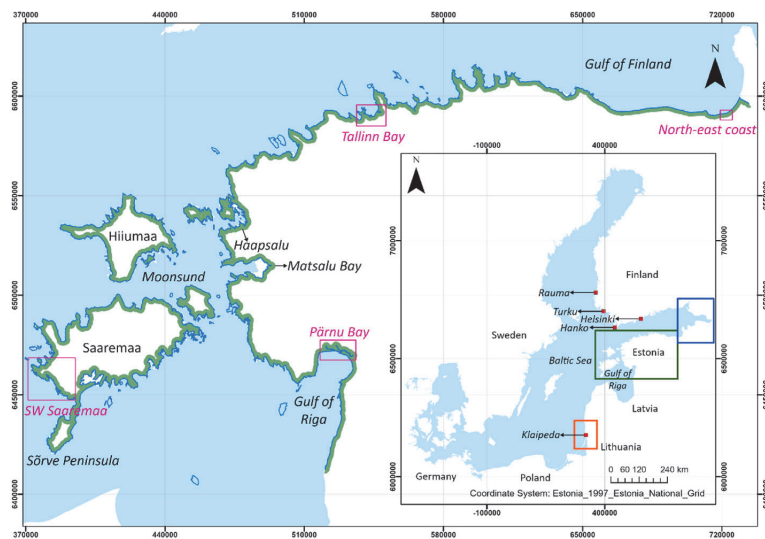
Fig. 1. The coast of Estonia. The axis units are in metres. The study area (wide green line) extends 2 km inland from the 1 m contour that describes the surface height above approximate long-term mean sea level (0 m in EH2000 datum). Pink boxes indicate sub-areas in which inland vulnerability is discussed. In the inset, the study area of Kovaleva et al. (2022) is shown using a blue box, the study area of Bagdanavičiūtė et al. (2019) using an orange box, while our study area is indicated using a green box. The red points represent the nearest calibrated tide gauge locations, where relative sea level rise was available (Table 1). (For interpretation of the references to colour in this figure legend, the reader is referred to the Web version of this article.)

extending to a distance of 2 km inland.

Consideration of this inland strip is significant in the vulnerability assessment for two reasons. Firstly, on many occasions estimates of vulnerability are relevant over a substantial distance from the shoreline, e.g., behind coastal dunes or along river valleys. Secondly, many parameters used in such assessment reflect various properties (e.g., the presence of vulnerable infrastructure or population density) over a quite wide coastal area. The resulting countrywide assessment is provided as an example of the application of a coastal vulnerability analysis at a scale not common in the literature. By addressing these three objectives this research aims to provide accurate and better analyses of coastal vulnerability in Estonia, and using this example, further develop the CVI approach as an important constituent of integrated decision support systems (DSSs) for sustainable coastal planning and management.

The vulnerability assessment of the study area employs multi-criteria decision analysis combined with the techniques of fuzzy logic, analytical hierarchy process, and weighted linear combination. The analysis is integrated with a geographical information system, to map the CVI of the Estonian coasts and the nearshore land strip in high resolution based on 16 parameters that express all three basic constituents of vulnerability – exposure, sensitivity, and resilience (Turner II et al., 2003). The resolution of description of these parameters varies from several kilometres (e.g., water level extremes) down to 10 m for the land elevation map.

We begin with descriptions of the study area and the methods used, the scheme of data acquisition and an overview of the justification, sources, resolution and properties of the 16 parameters that we consider. As the shoreline of the study area has quite a complicated shape and strongly varying properties, we provide maps of all of the used variables. We perform fuzzy standardization of the parameters, employ the analytical hierarchy process, verify the consistency of the outcome, and apply the weighted linear combination method. The methodology includes seeking the input of experts. Three of the parameters are regarded by experts as being the most influential with respect to coastal vulnerability, and we repeat the analysis using only those three parameters. Finally, we summarize the outcome and lessons from the performed analysis.

2. Material and methods

2.1. The study area

The study area is the entire coast of Estonia, including the major western islands (West Estonian Archipelago). We consider a 2 km wide region inland from the 1 m height isoline (top of the beach) over which parameters are mapped (Fig. 1). The required elevation data are extracted from a digital terrain model with 10 m spatial resolution generated from LIDAR elevation points 2018–2022 (Table 1). The intention is to ensure that not only the coastal environment but also critical infrastructure, crucial for regional resilience and community function, located up to 2 km away from the shoreline, is appropriately evaluated for vulnerability to coastal hazards. Both low-lying coastal areas, such as low-lying river valleys or coastal lakes, and infrastructure, such as roads, utilities, and buildings, may be significantly affected by hazards like coastal flooding, storm surges, depending on local geomorphological characteristics, even if they are located further inland.

Estonian coasts are mainly low in elevation and are dominated by moraine deposits, but with many different types of sedimentary coasts comprised of gravels, sands and silts. There are also areas with limestone coastal cliffs (Łabuz, 2015; Orviku, 2018). The western islands (the largest of which are Hiiumaa and Saaremaa) have mostly heights of 1–10 m above mean sea level (MSL). These islands have narrow gravel beaches and frequently visible erosion (Orviku et al., 2003; Suursaar et al., 2008). Landforms along the Estonian coast are strongly influenced by land uplift and as a result are generally prograding but many have

insufficient sediment (Łabuz, 2015) that significantly increases their vulnerability in the light of current and expected climate changes.

The majority of the study area experiences a deficit of fine sediment and gradual erosion (Orviku, 2018). As erosion is expected to dominate during times of high water level, water level extremes are commonly considered as a threat to the coast. The Baltic Sea is a microtidal water body, with tidal range 2–5 cm in most of the basin and up to 10 cm in some locations of the eastern Gulf of Finland (Leppäranta and Myrberg, 2009). The course of water level is thus almost completely governed by almost stationary halosteric effects and atmospheric impacts with time scales from a few hours to a few months. In the Baltic Sea, the course of water level is mainly influenced by the water volume of the sea, strong winds, and the effects of waves (Hünicke et al., 2015). Water levels in the entire Baltic Sea may be elevated up to 0.8 m above the long-term mean by large-scale water volume changes for periods up to a few weeks (Weisse et al., 2021). The local impact of storms may be largely enhanced due to the resulting high water level background (so-called preconditioning, Andrée et al., 2023) and may lead to catastrophic surges in the eastern part of the Baltic Sea (Suursaar et al., 2006).

Wave conditions are usually directly related to wind speed and direction, with long-period remote swell waves being virtually absent (Björkqvist et al., 2021). The wind direction can intensify wave set-up on certain sections of coast (Pindsoo and Soomere, 2015), which contributes to extremely high water levels (Eelsalu et al., 2014). The biggest documented storm surges were in Pärnu in 2005 and 1967, with maximum water levels of 2.75 m and 2.53 m, respectively (Suursaar et al., 2006; Suursaar and Sooäär, 2007). An increase in storm frequency coupled with sea level rise and a shorter duration of winter ice cover are other factors that contribute to coastal flooding (Harff et al., 2017).

Extreme events driven by climate change may have severe effects on coastal communities located along the Estonian coast (Kont et al., 2003). Many current and future social, economic, and environmental problems could also be exacerbated by such hazards (Rosentau et al., 2017). Therefore, vulnerability assessment of the Estonian coasts is needed, to assist with the mitigation of and adaptation to coastal hazards, and to facilitate plans for coastal community resilience.

2.2. Methods

2.2.1. GIS-multi-criteria decision analysis (MCDA)

2.2.1.1. Data acquisition. Determination of the parameters to be considered in a vulnerability assessment is an important first step of the analysis (Fig. 2 and Table 1). The classic approach of Gornitz et al. (1994) includes only five parameters: geomorphology, relative sea level change, shoreline displacement, tidal range and wave heights. However, tidal range is irrelevant in the microtidal Baltic Sea and relative sea level change may have almost negligible impact on coastal vulnerability assessments at the scale of a small country, such as Lithuania (Bagdanavičiute et al., 2015) or Estonia where country-scale variations in the rate of relative water level change are below 2 mm/yr (Suursaar and Kall, 2018). The number of parameters was increased to 13 in Gornitz et al. (1994). The most relevant parameters characterize the impact of oceanographic processes such as waves and surges, and express the contribution of coastal characteristics comprising elevation, coastal slope, geomorphology, human factors, etc., to the vulnerability of a particular coastal segment (Mullick et al., 2019).

We adopt the concept proposed by Turner II et al. (2003) identifying three core components of vulnerability: exposure, sensitivity, and resilience. A sensible measure of coastal vulnerability should include variables or parameters that contribute to all these components. Exposure refers to the degree, duration, and extent of hazards that a system is influenced by, and includes environmental and socio-political pressures (Adger, 2006). The selection of exposure parameters in this study follows the classic set of the relevant parameters that have been proved to
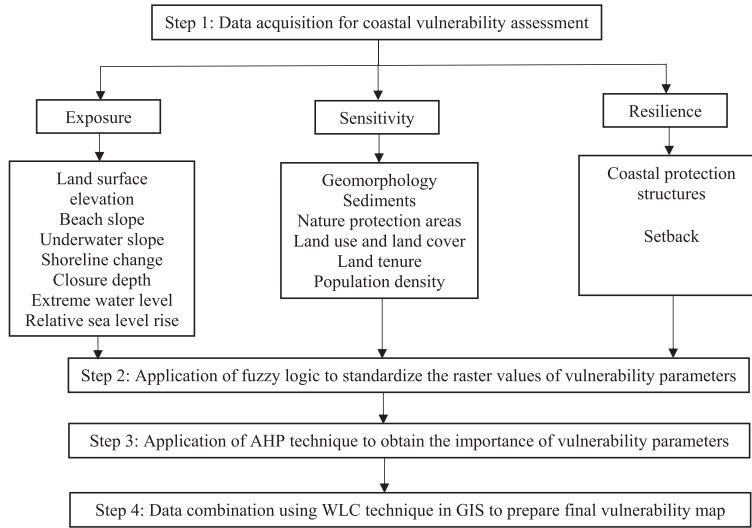
Fig. 2. An integrated DSS framework for coastal vulnerability assessment using GIS-MCDA showing the parameters used in this study.

adequately characterize vulnerability in largely different conditions (e. g., Bagdanavičiūtė et al., 2015; Kovaleva et al., 2022 in the context of the Baltic Sea): land surface elevation above MSL, beach slope, underwater slope, shoreline change, closure depth, extreme water level above MSL, relative sea level change, and maximum significant wave height. Sensitivity presumes that the resource is exposed to the hazard and characterizes the relative consequences of that exposure (Feng et al., 2021). The choice of such parameters depends on the particular coastal type and on whether the vulnerability is evaluated only for the shoreline and from the viewpoint of society, or is extended to some distance inland and includes values relating to nature. Our selection of the relevant parameters is to some extent dictated by the wish to extend the CVI analysis to the quasi-two dimensional case while not radically increasing the total number of parameters when compared with the classic studies, such as Gornitz et al. (1994). Thus, additionally to the classic parameters, such as geomorphology, sediments, we also included the presence of nature protection areas, type of land use and land cover, land tenure, and population density as two-dimensional sensitivity parameters to characterize vulnerability of the inland region. Resilience is the capacity of a system to withstand or recover from physical, economic, and infrastructure damage from a hazard (Mullick et al., 2019). The number of resilience parameters is limited. We chose the presence of coastal protection structures to characterize the situation at the shoreline and the measured setback from the shoreline to the first infrastructure.

The data for GIS analysis were processed and prepared with a spatial resolution of 10×10 m in ArcGIS Pro based on the 1997 Estonia National Grid reference coordinate system. The vertical datum system used is the European Vertical Reference Frame 2007. The 0 m contour (Estonian Land Board, maaamet.ee) was used as approximate mean sea level (MSL). In reality, MSL varies between $+19$ cm and $+27$ cm with respect to the local datum (Estonian Land Board, 2023) that is related to the Amsterdam Ordnance Datum. These large positive values mostly reflect low salinity of the Baltic Sea waters (Ekman and Mäkinen, 1996). In this study we apply 16 parameters (Figs. 3–10) that together reflect
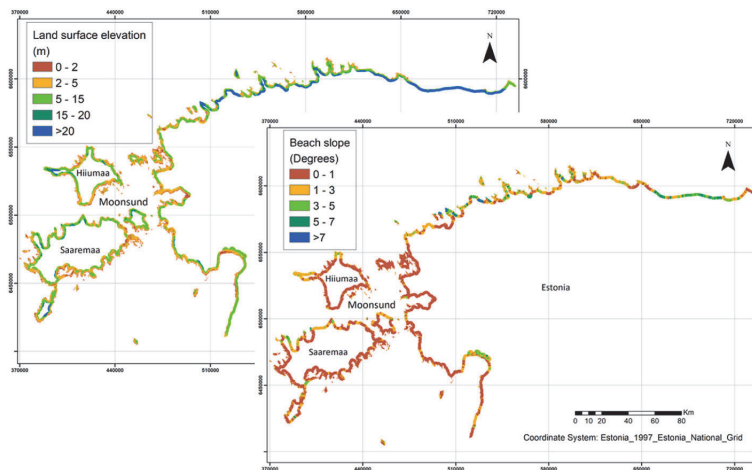
Fig. 3. Alongshore variation of land surface elevation (left) and beach slope (right).
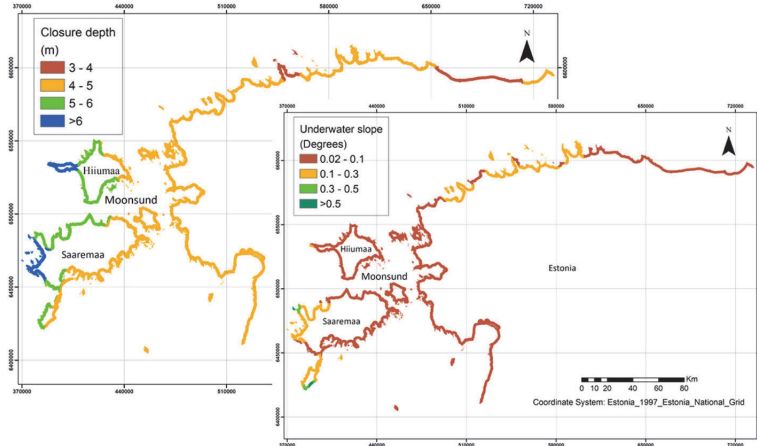
Fig. 4. Alongshore variation of closure depth (left) and underwater slope (right).
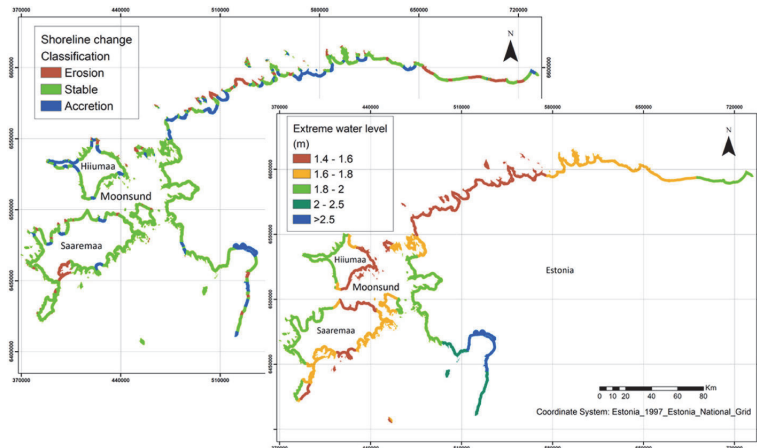
Fig. 5. Alongshore variation of shoreline change (left) and extreme water level (right).

the core aspects of exposure, sensitivity, and resilience (Turner II et al., 2003) (Table 1). Some parameters exhibit a clearly defined value at every specific coastal location that varies along the shore. These parameters include beach slope, closure depth, extreme water level, geomorphology, maximum significant wave height, relative sea level rise, setback, shoreline change, and underwater slope. These values are then applied to the entire 2 km wide nearshore stretch from the 1 m elevation isoline with respect to MSL, effectively creating a quasi-two-dimensional (2D) representation of what is essentially a one-dimensional (1D) variable. Several other parameters are naturally two-dimensional, particularly those related to land features such as coastal protection structures, land surface elevation, land tenure, land use and land cover, population density, the presence of nature protection areas, and type of sediments. All calculations were performed with a spatial resolution of 10 × 10 m. This resolution was applied to the entire shoreline of Estonia, including areas selected for more detailed analysis (Fig. 1). The values of parameters that were available at a coarser resolution were interpolated to 10 × 10 m raster using the inverse distance weighting method. The parameters that are intrinsically one-dimensional at the shoreline (e.g., closure depth) were extended to inland calculation cells along shore

normal.

2.2.1.2. Fuzzy standardization. The second step in the procedure (Fig. 2) is standardization of the parameters before they are combined due to the different scales on which they are measured or evaluated (Eastman, 2009). The fuzzy logic method analyzes data from any measurement scale, and experts in the field provide judgments to assign values for each factor (Pradhan, 2011; Ramesh and Iqbal, 2020). Fuzzy logic uses standardized (normalized) data in the range from 0 to 1, where 0 and 1 indicate lowest and highest values respectively. The ranges for very low (0, 0.2), low (0.2, 0.4), medium (0.4, 0.6), high (0.6, 0.8), and very high (0.8, 1) values are usually chosen as linearly increasing (Cheng et al., 2023).

The vulnerability increases with the assigned or observed values R_i of a selected parameter at a single location for extreme water level, sea level rise rate, maximum significant wave height, etc. (so-called increasing functions in Table 2) while it decreases for elevation, coastal slope, shoreline change, etc. (so-called decreasing functions in Table 2) (Barzehkar et al., 2021). It is therefore necessary to convert both increasing and decreasing functions of vulnerability into the
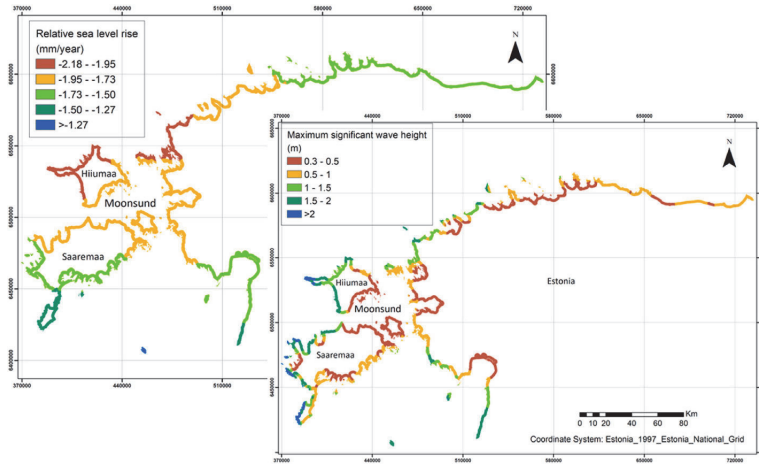
Fig. 6. Alongshore variation of relative sea level rise (left) and maximum significant wave height (right).
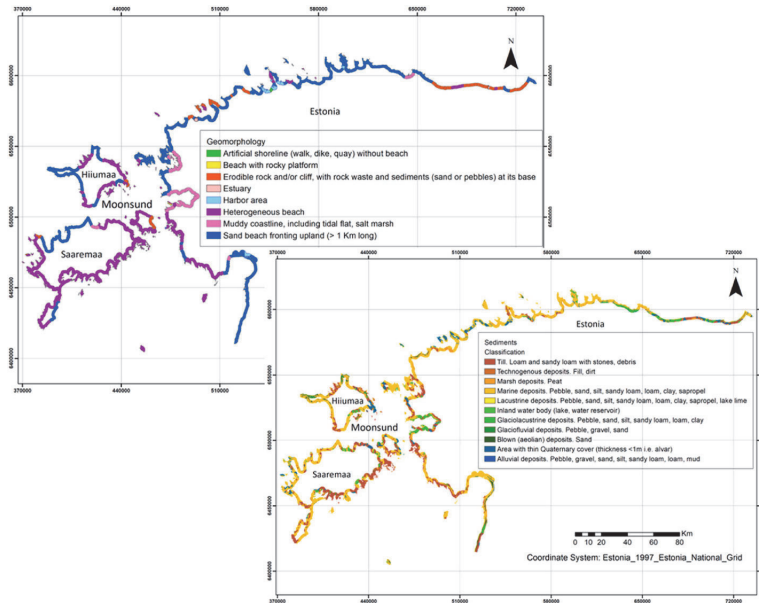
Fig. 7. Alongshore variation of geomorphology (left) and sediments (right).

standardized input of fuzzy logic. It may also occur that values over (or below) some (possibly expert-recommended) threshold R_{max} (R_{min}) do not further increase or decrease the associated vulnerability.

To do so, the input data for the use of fuzzy logic is built from the gathered data sets that represent increasing functions using a piecewise linear function $X(i)$ that is (i) set to 0 if the particular (pixel or assigned) value $R_i \leq R_{min}$, (ii) set to 1 if it is $R_i \geq R_{max}$, and (iii) increases linearly as $X(i) = (R_i - R_{min})/(R_{max} - R_{min})$ if it is between R_{min} and R_{max}. For decreasing functions, the function $X(i)$ is set to 0 if $R_i \geq R_{max}$, to 1 if $R_i \leq R_{min}$, and to $X(i) = (R_{max} - R_i)/(R_{max} - R_{min})$ for all other occasions (Kao, 2010).

The third class of input functions for fuzzy logic form custom user-defined functions expressed as discrete estimates that characterize

vulnerability associated with geomorphology, type of sediment, presence or absence of nature protection areas or coastal protection structures, land use, and land tenure. A proxy of standardized fuzzy layers is created for such parameters using literature sources and expert knowledge (expert judgement and literature in Table 2).

In some occasions (e.g., presence or absence of nature protection areas or coastal protection structures) the relevant input for fuzzy logic is like a Heaviside function with discrete values 0 and 1. The choice of, e. g., which land use correspond to 0 (low vulnerability) and which one to 1 (high vulnerability), or whether some intermediate values should be used, is often debatable and different types of the coast may require the use of different numerical values. In such aspects we rely on the opinions of local experts that is a common approach for modeling such variable-
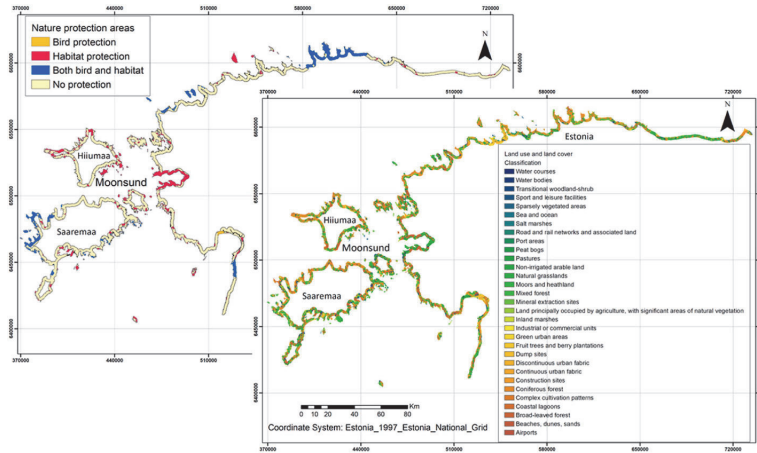
Fig. 8. Alongshore variation of nature protection areas (left) and land use and land cover (right).
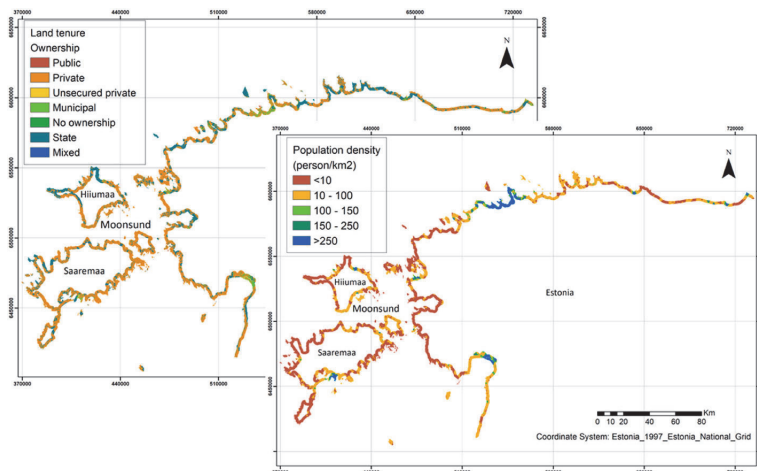
Fig. 9. Alongshore variation of land tenure (left) and population density (right).

category relationships in coastal vulnerability assessment (Teck et al., 2010).

The intermediate values based on the fuzzy logic approach are assigned to the parts of the coast with low-moderate or moderate-high vulnerability, e.g., areas with stable coasts, erodible cliffs, heterogeneous beaches, coastal lagoons, areas occupied with agriculture and plantations, etc. These parameters are specifically coastal protection structures, geomorphology, land use and land cover, land tenure, and sediments, where fuzzy intermediate values are assigned for categorical parameters.

2.2.1.3. Weighting of parameters. The third step in the analysis (Fig. 2) is to use the analytical hierarchy process (AHP), which is a popular approach that considers the relative importance of parameters in multicriteria decision analysis (MCDA) (Hadipour et al., 2020). This methodology relies on the subjective perception of experts on the relative importance of various parameters in the coastal vulnerability assessment (Ghosh and Mistri, 2022). It is based on a $n \times n$ pairwise comparison matrix of n parameters that represents the experts' qualitative

judgments of the importance of these parameters (Chai et al., 2013). The experts' ranking of parameters in this method is usually scaled from 1 to 9, where class 9 represents an extremely high level of prioritization, class 7 conveys a very strong prioritization, class 5 denotes strong prioritization, class 3 implies a moderate level of prioritization, and class 1 characterizes a neutral situation. Experts can also employ intermediate values like 2, 4, 6, and 8 (Saaty and Tran, 2007). The pairwise comparison matrix is completed by inserting reciprocal values (e.g., 1/3, 1/5, 1/7, 1/9) into the transposed positions (Saaty and Tran, 2007).

The pairwise comparison matrix (Table 3) was built in this study based on opinions of 10 experts from the academic and governmental sectors with expertise in coastal management. A geometric mean of all values assigned by experts for each pair of comparisons was used to compute an estimate of the "priority" of each parameter (Mu and Pereyra-Rojas, 2018) because it effectively accommodates the possibly diverging viewpoints of experts (Mu and Pereyra-Rojas, 2018). In the next step, these estimates were incorporated into a matrix to calculate the relative weights (importance) for each parameter (Mu and Pereyra-Rojas, 2018). Then, the entries in this matrix can be normalized
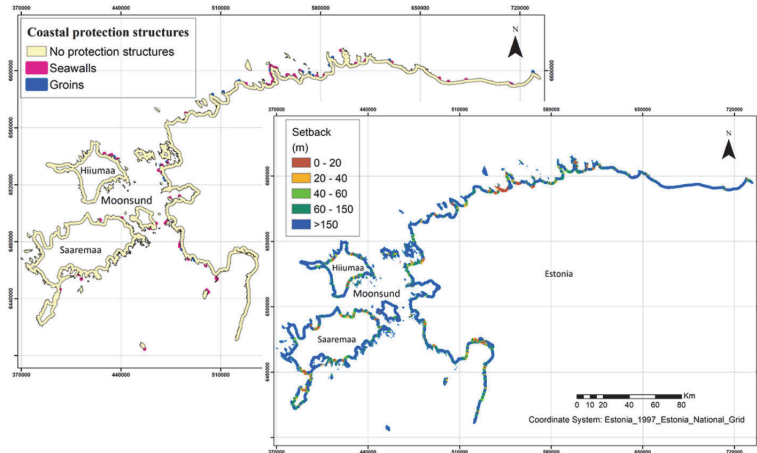
Fig. 10. Alongshore variation of coastal protection structures (left) and setback (right).

by dividing the values in each cell by the number of criteria, which is used to calculate the weights, representing the relative importance of parameters (Saaty, 1980).

2.2.1.4. Consistency of the estimates. The relevance of the pairwise comparison matrix is checked using the consistency ratio $CR = CI/RI$ (Saaty and Tran, 2007). The consistency index $CI = (\lambda_{max} - n)/(n-1)$ is defined by the largest eigenvalue λ_{max} of this matrix, where $n = 16$ in our study of 16 parameters. The so-called random index RI provides this value for the totally random input (Saaty and Tran, 2007). The RI value for $n = 16$ is 1.59 (Aguarón and Moreno-Jiménez, 2003). The outcome of weighting by the AHP method is acceptable if $CR \leq 0.1$ (Saaty and Tran, 2007). Otherwise, the consistency of the comparison may be questionable.

The calculated consistency ratio among experts' perspectives was $CR = 0.04$. Thus, it is reasonable to use the experts' opinions to weight the used parameters based on the AHP technique as the experts' judgements are consistent in terms of (Saaty and Tran, 2007). The most significant parameters based on the experts' perspectives for coastal vulnerability assessment of the Estonian coasts using AHP were extreme water level, shoreline change, and geomorphology, whereas closure depth, population density, and land tenure were the least important parameters for coastal vulnerability (Fig. 11).

Most experts used a limited range from 1 to 5 of the weighting scale (Table 3), when assigning weights to parameters through the AHP technique. This feature together with the effect of using the geometric mean to calculate the values presented in Table 3 tends to compress the range of values. This phenomenon is commonly encountered in applications of the AHP when the goal is to achieve consensus and agreement among experts (Mu and Pereyra-Rojas, 2018), but does not invalidate the approach as long as the consistency ratio is ≤ 0.1.

2.2.1.5. Data combination. The final step (Fig. 2) is to employ the weighted linear combination (WLC) technique in MCDA for the combination of spatial data in the GIS environment to calculate the coastal vulnerability index (CVI) using $n = 16$ parameters (Hadipour et al., 2020) as

$$CVI = \sum_{i=1}^{n} W_i X_i. \tag{1}$$

This map combination technique was used to combine the weights W_i of each parameter (raster layer) with the values X_i of this parameter in the raster layers (Malczewski and Rinner, 2015). A natural condition

is that the sum of the weights is 1. The WLC was also performed to obtain the final ranking of pixels (cells) for the output map, where the highest rank is 1 (Malczewski, 2000).

As an extra step, the analysis was repeated to evaluate vulnerability at all raster points of the study area using only the three parameters with the largest weights according to the full AHP analysis: extreme water level, shoreline change and geomorphology. The weights were then renormalized to have their sum equal to 1. These normalized weights were used in the WLC method to maintain consistency with the map reflecting all 16 parameters while focusing on the top three parameters.

To summarize the presented material, in this study, the CVI was calculated by integrating the standardized and weighted parameters to obtain a vulnerability score for each grid cell with dimensions of 10 × 10 m along the shoreline and within a 2 km wide inland strip. The spatial resolution for the CVI calculation was thus 10 × 10 m in the entire study area, including the areas selected for more detailed discussion. These areas were chosen based on their particular vulnerability properties or geographical significance. This high resolution was intrinsically present in some of the input data, such as land elevation, location of infrastructure and coastal protection, or natural protection areas. The data relating to hydrodynamic properties were of much lower resolution (e. g., relative sea level increase or maximum significant wave height) and were interpolated to the 10 × 10 m raster using the inverse distance weighting technique.

3. Results

3.1. Coastal vulnerability based on 16 parameters

The resulting CVI values are normalized between 0 and 1. They range from 0.24 (very low vulnerability in the context of the study area) to 0.72 (very high vulnerability). The entire range of the CVI values is 0.48 and thus covers almost half of the theoretically possible span. This wide span suggests that a sensible representation of spatial variations of coastal vulnerability is provided by the classic approach of dividing the CVI values for single locations into five equally spaced classes (Table 4).

Perhaps surprisingly, almost entire study area has either low or moderate vulnerability. As expected, several segments with very low vulnerability are located on the northern coast of Estonia in areas with stable limestone cliffs (Fig. 12). Also, many sections of the shores of Moonsund, the interior water body of the West Estonian Archipelago, have very low or low vulnerability. This feature apparently reflects gradual uplift of this archipelago and moderate values of extreme water

Table 1

The parameters used in the vulnerability assessment of the Estonian coast, the data sources and description.

Parameter and resolution	Data source	Description
Core component 1: Exposure		
Land surface elevation, 10 × 10 m	Digital terrain model (DTM) from Estonian Land Board, maaamet.ee	Elevation is defined here as the height of the land surface at a point, above approximate MSL. Land surface elevation is a significant parameter to determine land which is potentially inundated at a certain water level (Mullick et al., 2019). The areas with land surface elevation smaller than elevated water levels are flooded and are ranked high to very high vulnerability. The DTM was generated from LIDAR elevation points 2018–2021.
Beach slope, 10 m	DTM from Estonian Land Board. maaamet.ee	Beach slope is defined here as the average gradient from the waterline at the MSL to the 1 m elevation contour. Beach slopes typically >7° have very low vulnerability, and <1° very high vulnerability (Pantusa et al., 2018). Beach slope was calculated from the DTM.
Closure depth, from a wave model with a 5.5 km resolution	Soomere et al. (2013)	Closure depth is the offshore limit to significant cross-shore sediment transport (Masselink et al., 2011). The transportation of longshore sediments occurs over the beach profile down to this limit (Nguyen et al., 2021). This variable is estimated from the wave model. The larger closure depths (>5 m) are associated with the largest wave intensities in the Baltic proper. Smaller closure depths (≤5 m) are found in the Gulf of Riga and along the southern coast of the Gulf of Finland (Soomere et al., 2013).
Underwater slope, 10 m for shoreline data, 5.5 km for closure depth	DTM from Estonian Land Board, maaamet.ee and closure depth from Soomere et al. (2013)	Underwater slope, defined as the ratio of the closure depth to the distance from the waterline at the MSL to the location of the closure depth, is an important parameter for assessing the coastal vulnerability. Steeper underwater slopes are associated with higher vulnerability of the coast due to waves. Gentle underwater slopes can provide more capacity to dissipate wave energy and diminish the wave impacts on the shoreline (Bagdanavičiute et al., 2015; Bagdanavičiūtė et al., 2019). Larger underwater slope is ranked high and very high due to the dissipation of wave energy in a smaller area. Underwater slope was calculated using the MSL from the DTM and modelled closure depth.
Shoreline change, input data: about 2.5 km (at a 1:250,000 scale) and 3.5 km (at a 1:350,000 scale) along the shore interpolated to 10 m raster	Coastal migration from the European Marine Observation and Data network (EMODnet)	Shoreline change for this study is classified as one of three discrete values: erosion, accretion or stable. Accreting coastal areas are less vulnerable than eroding ones (Mohamed, 2020). The values for the shoreline vulnerability classification were obtained from the rate of mean annual shoreline change from 2007 to 2017 using satellite data for sandy beaches (Luijendijk et al., 2018), and field measurements for other coastline types from the EMODnet geology dataset, specifically within the field data category of 250k–350k (https://www.emodnet-geology.eu/, last access: November 24, 2022). The spatial resolution of this data along the shore is approximately 2.5 km and 3.5 km and depends on the scale of the maps. This data is interpolated to the 10 m raster using the inverse distance weighting (IDW) technique. Segments with observed erosion or accumulation rate within the margin of error, as per EMODnet measurements, were classified as stable. This ensures that areas with insignificant erosion are not inaccurately labeled as eroding.
Extreme water level, 3.7 km	Soomere et al. (2016)	Extreme water level is the maximum water level that can be reasonably expected at a coastal site due to joint impact of atmospheric pressure variations, storm surge, and wave driven effects (e.g. set-up and runup). This parameter in some ways replaces tidal range in this location. The coastal areas with expected elevated water levels >2 m above MSL have high vulnerability (Wolski et al., 2014). The extreme water level on Estonian coasts for a 50-year return period with a resolution of 2 nautical miles (about 3.7 km, Soomere et al., 2016) was used for the analysis.
Relative sea level rise, 10 m for shoreline	European Environment Agency, eea.europa.eu	Relative sea level rise is the balance at the shoreline between eustatic sea level change caused primarily by global eustatic sea level change and sea level change caused by isostatic (local and regional) mechanisms (Masselink et al., 2011). The Baltic Sea MSL level increased at a rate of around 2 mm per year over the past 50 years, which is faster than the global average (Weisse et al., 2021). The areas with relative sea level decrease are less vulnerable. The observed trend slope in sea level change relative to land since 1970 for tide gauges along the Europe coastline was used as this parameter. The closest properly calibrated tide gauges to the Estonian coast in Lithuania (Klaipeda) and Finland (Fig. 1) were used for analysis. The data from these tide gauge stations were interpolated using the Inverse Distance Weighting (IDW) method.
Maximum significant wave height, 2 km	Significant wave height (1993–2021) from Copernicus Marine Service, data.marine.copernicus.eu	Significant wave height (SWH) is a measure of the average height of the largest one-third of waves, reflecting the wave energy that influences the coastal sediment budget. The average SWH in the nearshore of Estonia is well below 1 m (Giudici et al., 2023; Najafzadeh et al., 2024). The coastal areas with SWH>1 m are

(*continued on next page*)

Table 1 (*continued*)

Parameter and resolution	Data source	Description
		classified as highly vulnerable. For this analysis, we used the maximum values 1993–2021 of hourly time series of SWH data with a spatial resolution of 2 × 2 km, in single nearshore wave model grid cells. The SWH data was interpolated into the 10 m alongshore resolution using the inverse distance weighting method.
Core component 2: Sensitivity		
Geomorphology, 2.5 km (at a 1:250,000 scale) and 3.5 km (at a 1:350,000 scale)	Coastal type from EMODnet, emodnet-geology.eu	The coastal geomorphology variable classifies coastal landforms by type (Woodroffe, 2002). The study area includes erosion resistant cliffed coasts, muddy coasts, beaches, etc. Geomorphology is important to determine the vulnerability of the coastal segments because of the different reaction of the materials in a landform to the coastal hazards (Mohd et al., 2019).
Sediments, 4 km (at 1:400,000 scale)	Quaternary Deposits Map from Estonian Land Board, maaamet.ee	In this study sediments are defined by their environment of deposition and grain size. There are various sedimentary environments in the study area with combinations of sediments including glacial and fluvial (pebble/gravel/sand), alluvial (pebble/sand/silt/loam/mud), lacustrine (pebble/sand/silt/loam/clay/sapropel) depositional environments, etc. Sediments affect the recession of the coast and are influenced by physical coastal processes. In reality, fine sediments, particularly gently sloping sandy beaches, may be less vulnerable because they dissipate much of the incoming wave energy during the wave breaking process across a broad surf zone (Woodroffe, 2002). In contrast, gravel beaches are associated with steep-gradient slope (Woodroffe, 2002). Sandy beaches are generally considered more vulnerable in coastal vulnerability assessments due to their susceptibility to long-term erosion, despite their ability to dissipate wave energy across a broad surf zone. This contrasts with gravel beaches, which have a steep-gradient slope and are more resistant to erosion but are less efficient at dissipating wave energy (Woodroffe, 2002). Our analysis employs this traditional perception, as sandy beaches experience significant changes over time and can thus be considered more vulnerable in the long term.
Nature protection areas, 1 km (at a 1:100,000 scale) from Natura (2000) dataset.	HELCOM, helcom.fi	Nature protection areas protect ecosystems which provide services for people and help protect the most valuable species and habitats (HELCOM, 2021). Such areas are designated as bird protection for endangered species (A), as habitat protection (B), and both bird and habitat protection for the most vulnerable species and habitats (C). The nature protection areas under six management categories of International Union for Conservation of Nature and Natural Resources (IUCN) including strict nature reserves and wilderness areas, national parks, natural monuments or features, habitat/species management areas, protected landscapes or seascapes, and protected areas with sustainable use of natural resources (Dudley et al., 2008) are assigned with a higher ranking of vulnerability than other ecosystems.
Land use and land cover, 100 × 100 m	Copernicus global land service, land.copernicus.eu	In this study land cover includes beaches and dunes, forests, wetlands, agriculture, etc. This property reflects the human activities on the land (Armenio et al., 2021), particularly for tourism, housing, industrial and commercial areas, construction sites, transportation networks, etc. Land use can characterize vulnerability of human infrastructure to coastal hazards (Mullick et al., 2019), and whether it is economically valuable to conserve the coast (Furlan et al., 2021). Thus, economic value is used for the vulnerability classification of land use. Urban and industrial areas are interpreted as regions with very high vulnerability (based on the value of their infrastructure) while barren lands, water bodies, marshes, sparsely vegetated areas, and bare rock are areas with very low vulnerability because of their very low economic value.
Land tenure, positional accuracy of 0.1 m in high-density areas and 0.35 m in low-density areas.	Cadastral data from Estonian Land Board, maaamet.ee	Land tenure is defined as who owns the land. Different land tenures (e.g., private vs state owned land) directly affect many things such as the ability and agility to react to hazard (e.g., Fetoui et al., 2021; Pérez-Valdez et al., 2021). Rules of tenure govern how land rights are distributed within societies and determine different land tenures (FAO, 2002). The access to the beach is generally open to anyone for public property, whereas e.g., forest lands may fall under the mandate of the state (FAO, 2002). For private property, individuals have exclusive rights to properties, and other members of the community are excluded from using these resources without the consent of those people (FAO, 2002). Private ownership makes it difficult for managers and decision-makers to allow for retreat measures or the construction of coastal protection and therefore privately owned land is classified as having higher vulnerability. The study area includes public property, state property, private property, etc. Natural disasters such as flooding, cyclones and hurricanes may contribute to insecure land tenure. The occurrence of such hazards can lead to a loss of rights in land (Reale and Handmer, 2011).

Table 1 (*continued*)

Parameter and resolution	Data source	Description
Population density, 1×1 km	Statistics Estonia, estat.stat.ee	The population density in the area adjacent to the coast is determined with respect to census blocks, measured as the number of people per unit area (km^2) (Mafi-Gholami et al., 2020). Mesh blocks are at a resolution of 1×1 km. All raster cells in our data set within the mesh block are recorded as having the same population density. The coastal areas with higher population density generally have higher economic importance and more human activities along the coast than areas with low population density. The mesh blocks with population density >250 people per km^2 were categorized as areas with very high vulnerability (Bagdanavičiūtė et al., 2019).
Core component 3: Resilience		
Coastal protection structures, 10×10 m	Orthophotos (2022) from Estonian Land Board, maaamet.ee	This parameter is defined as the absence or presence, and type of infrastructure meant to protect the shore from coastal hazards and thus to influence coastal resilience (El-Shahat et al., 2021). The coastal protection structures are primarily seawalls and groins in the study area. Seawalls and bulkheads eliminate or significantly reduce coastal vulnerability against storm surges and waves (Khazai et al., 2007). Properly constructed, this infrastructure comes at high cost, but reduces vulnerability to coastal hazards. In locations with no protection structures the vulnerability is high. Coastal protection structures were identified using orthophotos provided by the Estonian Land Board (2022), with each orthophoto map tile covering 5×5 km and having a ground sample distance (GSD) of 10–16 cm for low-altitude flights. These structures were digitized in ArcGIS Pro and then converted into a raster dataset with a spatial resolution of 10×10 m for further analysis.
Coastal setback, 1 m	Buildings and transportation infrastructure locations from Estonian Land Board and orthophotos (2022), maaamet.ee	Coastal setback in this study is defined as the distance between the shoreline and the first infrastructure on the landward side. The setback distance was measured perpendicular to the shoreline using orthophotos and was determined to the nearest meter. The study area contains buildings, roads, parking lots, port facilities, etc. Coastal setbacks facilitate the plans for sustainable coastal development and to conserve the coastal environments. A setback of 100 m to protect infrastructure and settlements from adverse effects of coastal hazards is often regarded as being reasonable (Sanò et al., 2011). Shorelines with a setback of at least 150 m to the first infrastructure have low and very low vulnerability to coastal hazards.

levels (Männikus and Soomere, 2023).

As expected, the most vulnerable areas are low-lying locations that experience very high water levels and gradual erosion, host harbour facilities, and where buildings or transportation infrastructure are located close to the coast. The areas characterized by high and very high vulnerability are mostly located on the western shore of Saaremaa and in the neighbourhood of Pärnu Bay. The main reasons for this categorisation are evidently the possibility of having very high water levels (Suursaar and Sooäär, 2007; Eelsalu et al., 2014), shoreline erosion in several spots of the eastern shore of the Gulf of Riga, or being open to westerly storm events (western coast of Saaremaa). This outcome provides confidence in the approach and techniques used.

3.2. Coastal vulnerability based on three most important parameters

Another view of coastal vulnerability becomes evident if only three parameters with largest priority by experts are taken into account (Table 4, Fig. 12). Most notably, this selection reflects the views of the particular group of experts and excludes all social and economic parameters, only using extreme water level, shoreline change and geomorphology (Fig. 12). Properties of extreme water level and shoreline change were systematically considered as most important properties (Fig. 12) while geomorphology was estimated as slightly more important than several other variables.

The range of CVI index using this approach increases to 0.64, much larger than when using all 16 parameters and thus covers almost 2/3 of the theoretically possible span. The proportion of areas with low vulnerability is much smaller than in the analysis based on 16 parameters (Table 4) and the proportion of locations with high vulnerability is clearly larger. The CVI-based map of coastal vulnerability based on these three parameters (Fig. 12) and the rightmost columns of Table 4 show a greater number of vulnerable locations than coastal vulnerability estimates based on all 16 parameters (Fig. 12). Areas with high vulnerability according to this criterion are mostly located in the south-west and in the north-east of Estonia.

The Gulf of Riga coast, including Pärnu Bay, has a generally high vulnerability to coastal hazards, evidently reflecting the possibility of highly elevated water levels during extreme events (Männikus et al., 2019) and the presence of many relatively low-lying areas. Frequent co-occurrence of elevated water levels and severe wave events (Männikus and Soomere, 2023) additionally contributes to the vulnerability of the eastern shores of the Gulf of Riga. Several locations of the western shore of Saaremaa, a segment on the eastern shore of the Sõrve Peninsula and several sections of gravel and sandy beaches in the north-eastern Estonia belong into areas with high vulnerability in this metrics.

The range of CVI values using only three parameters (from 0.2244 to 0.8688) is clearly larger than the similar range using all parameters (from 0.2441 to 0.7251). This is in line with the general perception that an increase in the number of parameters leads to a smaller range of the resulting CVI values in the Baltic Sea conditions (Soomere et al., 2024). Also, the standard deviation of the CVI values using three parameters (0.1015) is almost twice as large as the one using all parameters (0.0597). The point-to-point correlation of CVI values for these two cases is 0.565, indicating that the two sets of CVI values are clearly related but obviously contain a large portion of different information. This estimate reinforces the main message from Fig. 12: the two measures share some spatial pattern and overall structure but are not perfectly aligned.

3.3. Vulnerability of inland locations

The approach used in study involves 2 km wide nearshore region and thus leads to a quasi-2D coastal vulnerability index (CVI) map, to highlight vulnerability in low-lying areas where critical infrastructure may exist. For consistency we show results using both 16 parameters and the 3 most important parameters according to experts.

The properties of this map are represented in Table 4 but the relevant details of vulnerability are not visible in the scales of maps on Fig. 12. Coastal sections of very high and high vulnerability, both in metrics representing all parameters and three most important parameters, are few in terms of alongshore coverage, small in terms of percentage of the 2 km wide nearshore area, and scattered over different regions. However, these sections are likely those that eventually provide challenges for managers and local communities. We highlight for further discussion some areas (Pärnu Bay, south-western (SW) Saaremaa, Tallinn Bay and a selection of the north-eastern coast) that host several coastal segments with high vulnerability.

It is typical that land elevation increases relatively rapidly in the inland of Estonia, except for a few locations such as Matsalu Bay directly to the east of Moonsund (Fig. 1) or the vicinity of Haapsalu. It is thus natural that the inland, usually clearly elevated, parts of the 2 km wide nearshore area exhibit much lower vulnerability (Fig. 12) whereas the areas with higher vulnerability follow low-lying river valleys and other low-lying spots. The "impact" of several truly coastal parameters, such as wave height, is translated into a pattern of lower and higher values of vulnerability of inland areas. This pattern that is aligned along the shore normal provides for many locations a spurious effect and should be ignored in management decisions. This effect becomes particularly significant in CVI maps constructed using only three main parameters (extreme water level, shoreline change, and geomorphology) (Fig. 12). The resulting estimates are basically applicable to a narrow coastal strip along and cannot be used at any larger distance from the waterline.

The appearance of a spatial pattern of vulnerability substantially depends on the nature of the particular coastal area. While vulnerable areas mostly follow river valleys in delta regions (Fig. 13), they largely reflect the local elevation map and complexity of the coastline on the open, mostly limestone south-western shore of Saaremaa that is partially protected by pebble, cobble and boulder pavement (Fig. 14). As the land elevation slowly increases inland, patches of high vulnerability are found at a distance of 1–2 km from the shoreline. It is likely that this high vulnerability represent openness of this area to strong westerly winds that may create very high local water levels (Eelsalu et al., 2014). This vulnerability translates inland on in a few locations of the northern part of the coastal segment shown in Fig. 14. As above, the map based on three most important parameters (Fig. 14) has much less detail. Differently from the Pärnu case, this map provides to some extent reasonable generalisation of the map based on 16 parameters.

The northern coastline along the Gulf of Finland has lower vulnerability, due to the geomorphology and the coastal orientation. East of Tallinn, past coastal change and the frequency and magnitude of extreme events are lower, and there are cliffed coasts and areas with higher land surface elevation than in the south and west.

On the one hand, the vulnerability map of the vicinity of Tallinn (Fig. 15) correctly recognizes several well-known features, such as low-lying areas on the Paljassaare Peninsula and the city centre around the Old Harbour but fails to follow the major differences in the land elevation in the highlighted area. On the other hand, it declares as moderately vulnerable several areas near the Pirita River mouth that are actually elevated enough to compensate for any marine-driven hazards in this region. It is also surprising that the large proportion of coasts in the vicinity of Tallinn have moderate vulnerability (Fig. 15) and low vulnerability (Fig. 15) despite the more extensive infrastructure and higher population density in Tallinn than in Pärnu and on the western coast of Saaremaa. It is likely that the outcome is steered to some extent by the massive presence of coastal engineering (harbours) and

protection structures. It may be also the result of the methodology, where experts did not distinguish between sub-areas in their assessment, and did not regard the social and economic parameters as being overall of great importance, even though they may be in some small geographic areas.

The low to moderate vulnerability of shores on the north-eastern coast of Estonia, eventually attributed to the presence of cliffs (Fig. 16), is significantly influenced by land surface elevation. However, the relatively low ranking given to land surface elevation by experts resulted in very high CVI values for this coastal segment in metrics that is based on three most important parameters (Fig. 16).

4. Discussion

The results obtained for the coastal vulnerability index using the GIS-MCDA (multi-criteria decision analysis) technology first of all highlight the impact of parameter selection on coastal vulnerability mapping in Estonia. The 16 parameter analysis (Fig. 12, left) selected parameters based on diverse physical and socioeconomic aspects of coastal areas in Estonia. The alternative approach (Fig. 12, right) used only a few physical parameters (extreme water level, shoreline change, and geomorphology) chosen based on their perceived high importance according to experts' opinions. The results are qualitatively similar but clearly differ in quantitative terms and highlight differently vulnerability of some coastal segments.

Interestingly, experts did not prioritize some parameters that logic would suggest would be highly important, especially land surface elevation, coastal protection structures, and maximum significant wave height, as is evident from the pairwise comparison matrix of parameters (Table 3). They highlighted historical extreme water levels, and some parameters describing the physical environment (previous shoreline change and geomorphology) as being more significant. This choice reflects a methodological issue in analytical hierarchy process (AHP), where experts' preferences in selection of parameters differ from those that provide persuasive information or arguments that guarantee resilience of a certain location, for example, relatively high elevation at a certain distance from the shoreline. This highlights the complexity of experts' judgments in decision-making process, emphasizing the need for a detailed awareness of contextual biases when dealing with (quasi) two-dimensional estimates. This may also suggest that it is important to involve people whose priorities are outside of classic coastal science and whose opinions would increase the weight of socio-economic aspects, and possibly even that experts in some way be asked to suggest additional parameters and criteria.

The difference in the resulting vulnerability maps highlights the significance of incorporating a diverse set of parameters and possibly repeating exercises of this type with different selections of experts. This approach aims to provide a more reliable and dependable picture of coastal vulnerability in Estonia than only a few physical parameters for vulnerability assessment.

The use of decision support systems and systematic calculation of coastal vulnerability has proved to be very popular in coastal management decision making (Wong-Parodi et al., 2020; Barzehkar et al., 2021). While the results of such studies should be able to be used by managers and other stakeholders to focus attention on vulnerable areas for incorporation in spatial plans and for investment decisions, we have highlighted some significant shortcomings if too few parameters are used, and for whatever reason, certain parameters are preferred by the experts consulted. Confidence in the methodology and results is increased if they are consistent with other research undertaken at a more local scale. Many studies of processes on the Estonian seashore or in the region (Bagdanavičiūtė et al., 2015, 2019; Kovaleva et al., 2022) concentrate on small areas (Orviku et al., 2009; Tõnisson et al., 2018), or on single and sets of related coastal processes (Kont et al., 2008; Tõnisson et al., 2011; Männikus and Soomere, 2023), however, they identify some particular vulnerabilities for some areas that can be

Table 2

Fuzzy standardization for the quantification of parameters in the coastal vulnerability assessment. For decreasing functions any value below the minimum threshold R_{min} is associated with maximum vulnerability (1) and any value above the maximum threshold R_{max} with minimum vulnerability (0). In a similar manner, for increasing functions, any value below the minimum threshold is associated with minimum vulnerability (0) and any value above the maximum threshold with maximum vulnerability (1).

Criteria	Sub-criteria	Reference used for the determination of thresholds	Threshold values		Type of the function
			Minimum threshold R_{min}	Maximum threshold R_{max}	
Exposure	Land surface elevation	Tõnisson et al. (2013); Averkiev and Klevannyy (2010)	2 m	5 m	Decreasing
	Beach slope	Pantusa et al. (2018)	1°	7°	Decreasing
	Underwater slope	Calculated by the closure depth	0.02°	1°	Increasing
	Shoreline change	Luijendijk et al. (2018); emodnet-geology.eu/	−1 (Erosion)	1 (Accretion)	Decreasing
	Closure depth	Soomere et al. (2013)	3 m	6 m	Increasing
	Extreme water level	Wolski et al. (2014)	1 m	2.5 m	Increasing
	Relative sea level rise	Madsen et al. (2019)	−2 mm/yr	−1 mm/yr	Decreasing
	Maximum significant wave height	Giudici et al. (2023); Najafzadeh et al. (2024)	0.3 m	2.8 m	Increasing
Sensitivity	Geomorphology	Koroglu et al. (2019)	0 (Cliffs)	1 (artificial beach)	Expert judgement and literature
	Sediments	Woodroffe (2002)	0 (Sand)	1 (Gravel)	Expert judgement and literature
	Nature protection areas	Dudley et al. (2008)	0 (No protection)	1 (nature protection areas with most vulnerable species and habitats)	Expert judgement and literature
	Land use and land cover	Armenio et al. (2021)	0 (Forests, marshes, water bodies, sea and ocean)	1 (Industrial and commercial areas)	Expert judgement and literature
	Land tenure	Asante et al. (2017); FAO (2002)	0 (Public property)	1 (Private property)	Expert judgement and literature
Resilience	Population density	Bagdanavičiūtė et al. (2019)	<10 person/km^2	>250 person/km^2	Increasing
	Coastal protection structures	Mohamed, (2020)	0 (Seawalls)	1 (No protection structures)	Expert judgement and literature
	Coastal setback	Sanò et al. (2011)	20 m	150 m	Decreasing

Table 3

Pairwise comparison matrix of 16 parameters A–P for coastal vulnerability assessment. The geometric means of estimates by 10 experts are rounded to the nearest integer or the nearest inverse of an integer. The experts generally chose to use only part of the possible range of rankings of the parameters (from 1 to 9). The rankings >1 in a cell mean that the parameter shown in the relevant row is estimated as more important than the parameter in the relevant column. The larger the value, the more dominant the parameter with respect to the other parameter is, as considered by the experts. The fractional entries are reciprocals of the estimates ≥1, used to fill the comparison matrix (Saaty and Tran, 2007) for further analysis.

No	Parameters for coastal vulnerability assessment	A	B	C	D	E	F	G	H	I	J	K	L	M	N	O	P
1	A – Land surface elevation	1	2	1	1/2	2	1	1	1	1	1	1	2	2	1	1	1
2	B – Beach slope	1/2	1	1	1/2	1	1/2	1	1/2	1	1	1	2	2	1	1/3	1/2
3	C – Underwater slope	1	1	1	1/2	1	1/2	1	1	1	1	1	2	1	1/2	1
4	D – Shoreline change	2	2	2	1	5	1	2	1	2	5	1	2	3	2	1	1
5	E – Closure depth	1/2	1	1	1/5	1	1/3	1/2	1	1/2	1	1	1	2	1	1/2	1/2
6	F – Extreme water level	1	2	2	1	3	1	3	2	2	2	2	3	4	3	2	2
7	G – Relative sea level change	1	1	1	1/2	2	1/3	1	1	1	2	1	2	2	2	1	1
8	H – Maximum significant wave height	1	2	1	1	1	1/2	1	1	1	2	2	2	3	2	1	1
9	I – Geomorphology	1	1	1	1/2	2	1/2	1	1	1	2	4	2	3	2	1	1
10	J – Sediments	1	1	1	1/5	1	1/2	1/2	1/2	1/2	1	2	2	4	3	1	2
11	K – Nature protection areas	1	1	1	1	1	1/2	1	1/2	1/4	1/2	1	1	2	2	1	1
12	L – Land use and land cover	1/2	1/2	1	1/2	1	1/3	1/2	1/2	1/2	1/2	1	1	3	3	1	1
13	M – Land tenure	1/2	1/2	1/2	1/3	1/2	1/4	1/2	1/3	1/3	1/4	1/2	1/3	1	1	1/2	1/2
14	N – Population density	1	1	1	1/2	1	1/3	1/2	1/2	1/2	1/3	1/2	1/3	1	1	1	1
15	O – Coastal protection structures	1	3	2	1	2	1/2	1	1	1	1	1	1	2	1	1	2
16	P – Setback	1	2	1	1	2	1/2	1	1	1	1/2	1	1	2	1	1/2	1

compared to our results. One exception is Tõnisson et al. (2013), which takes a country wide approach but concentrates specifically on coastal erosion.

The core novelty of our study is a quasi-two-dimensional approach that considers a 2 km zone extending inland from the coast. This approach makes it possible to incorporate parameters that are 2-dimensional in nature, but which must be excluded from an analysis which is undertaken in one dimension (along the coast, which is typical in CVI research). Not all parameters of this type are appropriate for inclusion, but some variables, like land tenure and land use and land cover, are suitable for representation as areas within this framework. However, challenges arise when incorporating into this approach variables that are essentially one-dimensional such as significant wave height or setback. For example, high water levels may impact the area behind dunes along a low-lying valley that enters the sea kilometres away. An assumption in our analysis is that a single value of such variables (except for water level) along the shoreline is chosen to represent the entire 2 km wide coastal segment. We emphasize the need for a detailed understanding of how different interpretations of the impact range of such variables and measurement or evaluation methods of such impacts affect the interpretation of results.
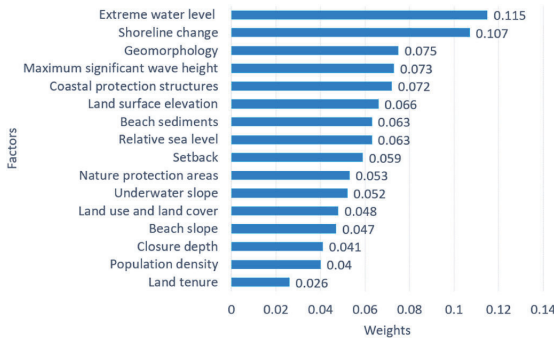
Fig. 11. Relative weights assigned to the employed parameters using the AHP method.

4.1. Limitations

In addressing limitations of the performed study and methodological concerns of the AHP methodology for coastal vulnerability assessment in Estonia, a critical examination of the significance of specific parameters, is necessary. Land surface elevation plays an important role in shaping vulnerability of the Estonian coast. The reason for a lower ranking given to this parameter by experts, when we expected it to be more highly ranked is not clear, but the impact on the outcome is significant, and is

particularly seen in the vulnerability rankings when using all parameters and the top three on the north-east Estonian coast. We believe that the description of the parameter given to experts is reasonable and clear. Some other parameters, such as the current setback distance to first infrastructure might also have been expected to be more highly ranked.

It is also clear that the spatial resolution of the available data relating to different parameters (Table 1) is a methodological issue worthy of further consideration. Some important parameters, such as the highly ranked shoreline change parameter only has three values (erosion, stable, accretion) and this is reflected in the blocky visual appearance of the outcome of the exercise with only three-parameters involved. In this study, the application of more MCDA techniques and a greater number of parameters based on fuzzy logic, AHP, and weighted linear combination (WLC) was meant to reduce uncertainty and provide more confidence in the results compared to other coastal vulnerability assessments (Armenio et al., 2021; Bagdanavičiūtė et al., 2015, 2019; Sekovski et al., 2020). The danger of relying on a few parameters that may be regarded as particularly important by experts, is highlighted by our work.

The determination of values of thresholds through MCDA using fuzzy logic for standardizing raster values in maps involves a judgment-based element. However, it is crucial to emphasize that the process of assigning values is not arbitrary, as it follows a systematic and reasoned approach (Robinson, 2003). This makes it a robust approach to implement the standardization based on the environmental and socioeconomic condition of the Estonian coasts and to deal with the uncertainty during coastal vulnerability analysis process. The results of this study align with

Table 4
Coastal vulnerability analysis using MCDA and two sets of parameters (all 16 versus the three most important as determined by experts). Areas are calculated for the coastal land up to 2 km from approximate MSL using the equal interval classification method in ArcGIS Pro.

Vulnera-bility class	CVI based on 16 parameters				CVI based on 3 most important parameters			
	CVI range	Area, km^2	%	Main locations	CVI range	Area km^2	%	Main locations
Very low	0.24–0.34	121	3.8	North-west	0.22–0.35	247	7.7	North-west
Low	0.34–0.44	1496	47.0	North-west and North-east	0.35–0.48	807	25.4	North-west and North-east
Moderate	0.44–0.53	1350	42.5	North-west, Pärnu Bay and western islands	0.48–0.61	1637	51.5	North-west, north-east, Pärnu Bay and western islands
High	0.53–0.63	207	6.5	Pärnu Bay and western islands	0.61–0.74	464	14.6	North-east, Pärnu Bay, and western islands
Very high	0.63–0.72	6	0.2	Pärnu Bay and western islands	0.74–0.86	25	0.8	Pärnu Bay and western islands
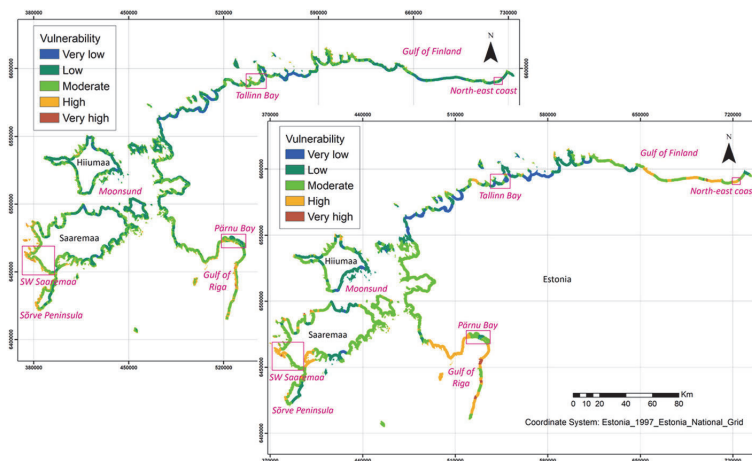
Fig. 12. Coastal vulnerability map using the MCDA technique (all 16 parameters, left) and three most important parameters (extreme water level, shoreline change and geomorphology, right) based on the perception of experts. Pink boxes indicate sub-areas in which inland vulnerability is discussed below. (For interpretation of the references to colour in this figure legend, the reader is referred to the Web version of this article.)
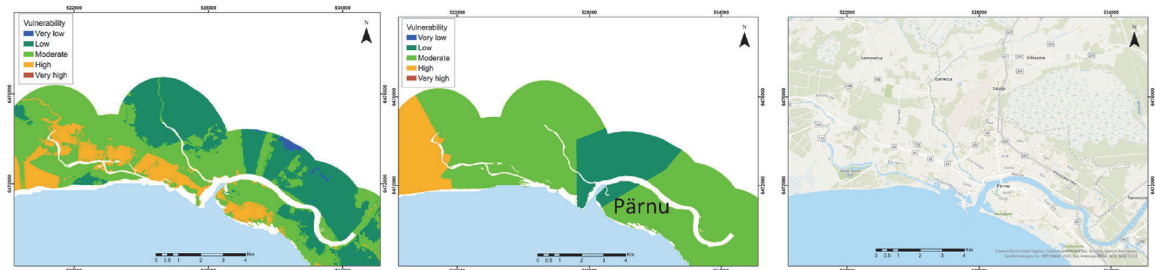
Fig. 13. Coastal vulnerability map of the vicinity of Pärnu (see Fig. 1) using MCDA based on all parameters (left), three most important parameters (middle), and topographic basemap (right).
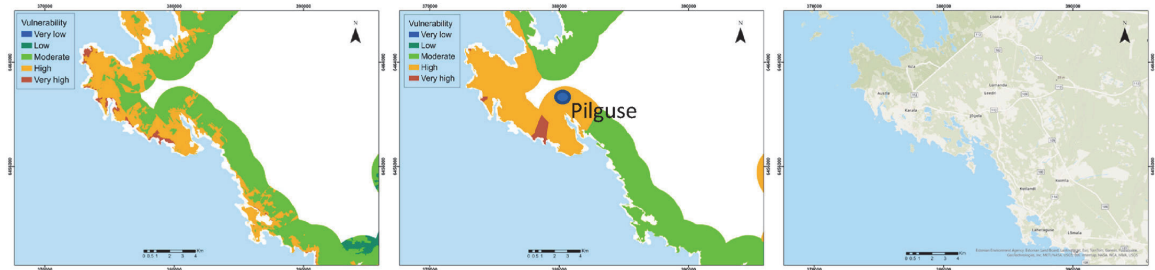
Fig. 14. Coastal vulnerability map of western Saaremaa (see Fig. 1) using MCDA based on all parameters (left), three most important parameters (middle), and topographic basemap (right). Pilguse is the birthplace of Fabian Gottlieb von Bellingshausen.
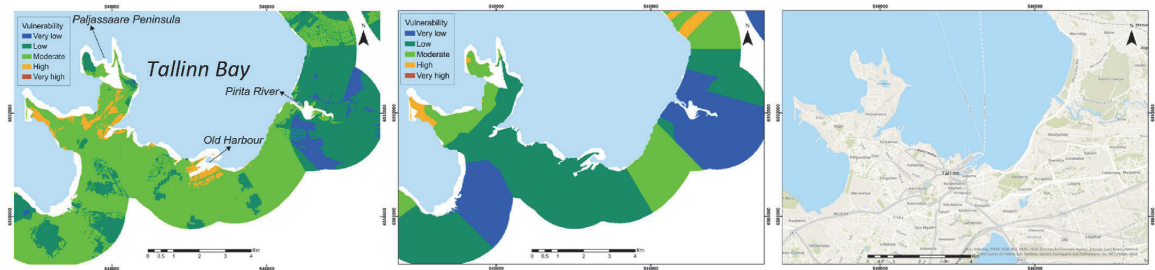
Fig. 15. Coastal vulnerability map of the vicinity of Tallinn (see Fig. 1) using MCDA based on all parameters (left), three most important parameters (middle), and topographic basemap (right).
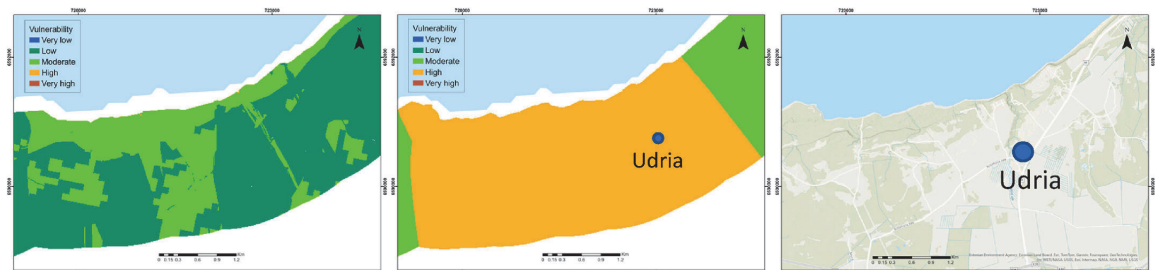
Fig. 16. Coastal vulnerability map of the north-eastern coast of Estonia (see Fig. 1) using MCDA based on all parameters (left), three most important parameters (middle), and topographic basemap (right).

the outcome of the study conducted by Mullick et al. (2019) for coastal vulnerability assessment in Bangladesh. Both studies highlight the effectiveness of fuzzy logic in providing detailed local-level vulnerability information, supporting its role in coastal planning and management.

Another implicit limitation of our study is that we have not performed a detailed statistical analysis of the numerical outcome of our research. This kind of analysis, albeit fairly complicated because of the use of a sequence of different methods, would provide much more confidence in the presented results, serve as important constituent of their proper interpretation, and offer a clearer view on the replicability of our study when upgraded datasets or another set of parameters will be used.

4.2. Recommendations based on country-wide approach

In this study, the coastal vulnerability analysis used a country-wide approach, helping coastal managers and decision-makers to plan for coastal hazards affecting coastal lands, infrastructure and inhabitants, rather than considering only coastal erosion, which is often considered synonymously with coastal hazard (Armenio et al., 2021; Bagdanavičiūtė et al., 2015, 2019). The coastal vulnerability analysis that includes areas up to 2 km inland provides possibilities to identify logically the interactions between the land and sea environments, particularly with respect to the lower reaches of rivers and estuaries, but must be used with care, considering that some parameters are 1-D in nature. The difference between the classic (1D) and our quasi-2D approach is almost immaterial for continuously cliffed or sandy areas with elevated inland, such as the north-eastern coast of Estonia (Fig. 16) where the situation in the 2 km wide inland strip is insensitive to what happens at the relevant location of the coastline. The difference is clearly evident in urban regions (Fig. 15) where socioeconomic parameters play more of a role. The pattern of vulnerability has an extensive cross-shore gradient in gently sloping locations, such as the western coast of Saaremaa (Fig. 14). This pattern is even more obvious in segments with low-lying (river) valleys oriented parallel to the shoreline (Fig. 13). In such places highly vulnerable locations may occur behind resilient high dunes.

A decision support analysis should not be used in isolation. There is no substitute for local knowledge interpreted by experts, but is a tool for decision makers that highlights areas that may be otherwise ignored. It provides another perspective on areas that may be thought to be highly vulnerable, which may not be, possibly due to them being well known (urban areas are an obvious example), or areas that are perceived as being safe, but have vulnerability that has not been identified. The response to a vulnerability assessment is another matter and must take into account various other factors including the availability of resources, environmental considerations, political considerations, etc. The range of responses is large, ranging from hard engineering through to do-nothing options (Masselink et al., 2011). The choice of strategy should be based on the specific needs and conditions of each coastal area, and should actively engage stakeholders, drawing upon their local knowledge and insights in the decision-making process. This collaborative effort will not only enhance coastal resilience but also provide trust and ensure the long-term sustainability of coastal environments.

The provided analysis and results lead to several recommendations and possibilities for further research. First of all, there is clear need for adequate express estimates of coastal vulnerability based on a few easily measurable or quantifiable parameters with sufficient resolution to properly describe the coastal segment in question or under planning consideration. This challenge includes not only an optimal choice of these few parameters but also a comprehensive understanding of how increasing the number of parameters influences the outcome when the number of parameter increases. Another crucial challenge is how to incorporate the impact of extreme water levels into the CVI analysis. There are currently several metrics of this parameter, from measured or modelled maximum values over some time period (used in our analysis)

up to variables with prognostic value, such as the slope parameter of the exponential distribution of local storm surge heights (Soomere et al., 2015) or the shape parameter of the generalized extreme value distribution (Soomere et al., 2018). A small selection of these variables have been recently discussed and tested for the Lithuanian shore (Soomere et al., 2024). There is also great potential for integrating advanced machine learning and deep learning techniques into CVI research (Barzehkar et al., 2024). These approaches could allow for better prediction and modelling of coastal vulnerability, particularly when incorporating large datasets. Future studies could focus on further enhancing the robustness of these models by combining environmental and socioeconomic data with advanced artificial intelligence techniques for improved decision-making and policy recommendations.

5. Conclusions

In this study we apply and extend widely used MCDA and GIS techniques to assess coastal vulnerability in Estonia, eastern Baltic Sea, at a high resolution thereby filling gaps in the literature while spatially extending previous analysis elsewhere in the region by Kovaleva et al. (2022) in the eastern Gulf of Finland and Bagdanavičiūtė et al. (2019) in Lithuania. The study shows that most (about 90%) of the Estonian has moderate, low or very low vulnerability, but there are areas, as expected, with high and very high vulnerability (slightly more when an analysis based on only 3 parameters regarded by experts as most important is used).

We added parameters to the analysis that are not typically used, particularly socio-economic parameters and parameters that are appropriately measured in 2D. We did not find a method to seamlessly integrate appropriately measured 1D and 2D data. Excluding 2D parameters leads to important parameters being excluded but including them leads to parameters that are necessarily measured only at the coast being over-emphasized inland, leading to some spurious results. Adding parameters provided some methodological challenges but excluding them limits the analysis significantly. This is clearly shown in our analysis using the only three most important parameters determined by experts. We did this to determine if it was feasible to reduce the inputs and still achieve reliable results. However, some spurious results became evident, e.g. with areas close to the coast being determined as being vulnerable, despite them being at relatively high elevation.

Very importantly, this vulnerability assessment is made for the whole Estonian coast extending to a distance of 2 km inland, considering vulnerability in areas, e.g., behind coastal dunes or along river valleys, where there may be significant populations and infrastructure. The resulting countrywide assessment provides some insights that may highlight locations of interest and importance that may be otherwise not be considered by coastal managers.

The AHP method typically uses the opinion of experts to produce weightings for the parameters. We highlight both advantages and problems of this approach. It was clear that the experts were only using about half of the ranking scale available to them, and were, with consistency as measured by the Consistency Ratios, making decisions, the reasons for which was not clear. This meant that some parameters that we thought should have been regarded as very important for coastal vulnerability (such as land surface elevation, coastal setback to infrastructure) were ranked lower than expected.

The CVI analysis and output maps provide an extra layer of information to coastal managers and policymakers when undertaking strategy assessments, including planning for infrastructure and coastal hazard mitigation. The outputs may also be effective for communication and consultation purposes. However, we emphasize the importance of interpreting the results in the context of local knowledge and on-site expert advice.

CRediT authorship contribution statement

Mojtaba Barzehkar: Writing – review & editing, Writing – original draft, Visualization, Software, Methodology, Investigation. **Kevin Parnell:** Writing – review & editing, Methodology, Conceptualization. **Tarmo Soomere:** Writing – review & editing, Methodology, Conceptualization.

Declaration of competing interest

The authors declare that they have no known competing financial interests or personal relationships that could have appeared to influence the work reported in this paper.

Acknowledgments

Data availability

Data will be made available on request.

References

Adger, W.N., 2006. Vulnerability. Global Environ. Change 16 (3), 268–281. https://doi.org/10.1016/j.gloenvcha.2006.02.006.

Adger, W.N., Hughes, T.P., Folke, C., Carpenter, S.R., Rockström, J., 2005. Social-ecological resilience to coastal disasters. Science 309 (5737), 1036–1039. https://doi.org/10.1126/science.1112122.

Aguarón, J., Moreno-Jiménez, J.M., 2003. The geometric consistency index: approximated thresholds. Eur. J. Oper. Res. 147 (1), 137–145. https://doi.org/10.1016/S0377-2217(02)00255-2.

Ahmed, M.A., Sridharan, B., Saha, N., Sannasiraj, S.A., Kuiry, S.N., 2022. Assessment of coastal vulnerability for extreme events. Int. J. Disaster Risk Reduc. 82, 103341. https://doi.org/10.1016/j.ijdrr.2022.103341.

Alcántara-Carrió, J., García Echavarría, L., Jaramillo-Vélez, A., 2024. Is the coastal vulnerability index a suitable index? Review and proposal of alternative indices for coastal vulnerability to sea level rise. Geo Mar. Lett. 44, 8. https://doi.org/10.1007/s00367-024-00770-9.

Andrée, E., Su, J., Dahl Larsen, M.A., Drews, M., Stendel, M., Skovgaard Madsen, K., 2023. The role of preconditioning for extreme storm surges in the western Baltic Sea. Nat. Hazards Earth Syst. Sci. 23, 1817–1834. https://doi.org/10.5194/nhess-23-1817-2023.

Armenio, E., Mossa, M., Petrillo, A.F., 2021. Coastal vulnerability analysis to support strategies for tackling COVID-19 infection. Ocean Coast Manag. 211, 105731. https://doi.org/10.1016/j.ocecoaman.2021.105731.

Averkiev, A.S., Klevannyy, K.A., 2010. A case study of the impact of cyclonic trajectories on sea-level extremes in the Gulf of Finland. Continent. Shelf Res. 30, 707–714. https://doi.org/10.1016/j.csr.2009.10.010.

Asante, W.A., Acheampong, E., Boateng, K., Adda, J., 2017. The implications of land tenure and ownership regimes on sustainable mangrove management and conservation in two Ramsar sites in Ghana. For. Pol. Econ. 85, 65–75. https://doi.org/10.1016/j.forpol.2017.08.018.

Bagdanavičiūtė, I., Kelpšaitė-Rimkienė, L., Galinienė, J., Soomere, T., 2019. Index based multi-criteria approach to coastal risk assessment. J. Coast Conserv. 23, 785–800. https://doi.org/10.1007/s11852-018-0638-5.

Bagdanavičiūtė, I., Kelpšaitė, L., Soomere, T., 2015. Multi-criteria evaluation approach to coastal vulnerability index development in micro-tidal low-lying areas. Ocean Coast Manag. 104, 124–135. https://doi.org/10.1016/j.ocecoaman.2014.12.011.

Barzehkar, M., Parnell, K.E., Soomere, T., Dragovich, D., Engström, J., 2021. Decision support tools, systems and indices for sustainable coastal planning and management: a review. Ocean Coast Manag. 212, 105813. https://doi.org/10.1016/j.ocecoaman.2021.105813.

Barzehkar, M., Parnell, K.E., Soomere, T., 2024. Incorporating a machine learning approach into an established decision support system for coastal vulnerability in the Eastern Baltic Sea. J. Coast Res. 113, 58–62. https://doi.org/10.2112/JCR-SI113-012.1. Special Issue.

Bell, M.L., Hobbs, B.F., Ellis, H., 2003. The use of multi-criteria decision-making methods in the integrated assessment of climate change: implications for IA practitioners. Soc. Econ. Plann. Sci. 37 (4), 289–316. https://doi.org/10.1016/S0038-0121(02)00047-2.

Björkqvist, J.-V., Pärt, S., Alari, V., Rikka, S., Lindgren, E., Tuomi, L., 2021. Swell hindcast statistics for the Baltic Sea. Ocean Sci. 17, 1815–1829. https://doi.org/10.5194/os-17-1815-2021.

Chai, J., Liu, J.K.N., Ngai, E.W.T., 2013. Application of decision-making techniques in supplier selection: a systematic review of literature. Expert Syst. Appl. 40 (10), 3872–3885. https://doi.org/10.1016/j.eswa.2012.12.040.

Cheng, Z., Zhang, Y., Wu, B., Soares, C.G., 2023. Traffic-conflict and fuzzy-logic-based collision risk assessment for crossing scenarios of a ship. Ocean Eng. 274, 114004. https://doi.org/10.1016/j.oceaneng.2023.114004.

Dudley, N. (Ed.), 2008. Guidelines for Applying Protected Area Management Categories. IUCN, Gland, Switzerland. WITH Stolton, S., Shadie, P., Dudley, N., 2013. IUCN WCPA Best Practice Guidance on Recognising Protected Areas and Assigning Management Categories and Governance Types, Best Practice Protected Area Guidelines Series No. 21, Gland, Switzerland: IUCN.

Eastman, J.R., 2009. IDRISI taiga: guide to GIS and image processing. Clark Labs. Clark University.

Eelsalu, M., Soomere, T., Pindsoo, K., Lagemaa, P., 2014. Ensemble approach for projections of return periods of extreme water levels in Estonian waters. Continent. Shelf Res. 91, 201–210. https://doi.org/10.1016/j.csr.2014.09.012.

Ekman, M., Mäkinen, J., 1996. Mean sea surface topography in the Baltic Sea and its transition area to the North Sea: a geodetic solution and comparisons with oceanographic models. J. Geophys. Res. Oceans 101 (C5), 11993–11999. https://doi.org/10.1029/96JC00318.

El-Shahat, S., El-Zafarany, A.M., El Seoud, T.A., Ghoniem, S.A., 2021. Vulnerability assessment of African coasts to sea level rise using GIS and remote sensing. Environ. Dev. Sustain. 23, 2827–2845. https://doi.org/10.1007/s10668-020-00639-8.

Estonian Land Board, 2023. Estonian topographic database. https://geoportaal.maaamet.ee.

Fannassi, Y., Ennouali, Z., Hakkou, M., Benmohammadi, A., Al-Mutiry, M., Elbisy, M.S., Masria, A., 2023. Prediction of coastal vulnerability with machine learning techniques, Mediterranean coast of Tangier-Tetouan, Morocco. Estuar. Coast Shelf Sci. 291, 108422. https://doi.org/10.1016/j.ecss.2023.108422.

FAO, 2002. Land tenure and rural development. FAO Land Tenure Stud. 3. https://www.fao.org.

Feng, Q., An, C., Chen, Z., Owens, E., Niu, H., Wang, Z., 2021. Assessing the coastal sensitivity to oil spills from the perspective of ecosystem services: a case study for Canada's pacific coast. J. Environ. Manag. 296, 113240. https://doi.org/10.1016/j.jenvman.2021.113240.

Fetoui, M., Aribi, F., Chouikhi, F., Sghaier, M., Sghaier, M., 2021. Vulnerability of rural households' livelihoods to climate change: comparative analysis of mountainous and coastal areas in Tunisian arid regions. New Med. 20 (4), 15–31. https://doi.org/10.30682/nm2104b.

Furlan, E., Pozza, P.D., Michetti, M., Torresan, S., Critto, A., Marcomini, A., 2021. Development of a multi-dimensional coastal vulnerability index: assessing vulnerability to inundation scenarios in the Italian coast. Sci. Total Environ. 772, 144650. https://doi.org/10.1016/j.scitotenv.2020.144650.

Gargiulo, C., Battarra, R., Tremiterra, M.R., 2020. Coastal areas and climate change: a decision support tool for implementing adaptation measures. Land Use Pol. 91, 104413. https://doi.org/10.1016/j.landusepol.2019.104413.

Ghosh, S., Mistri, B., 2022. Analyzing the multi-hazard coastal vulnerability of Matla–Bidya inter-estuarine area of Indian Sundarbans using analytical hierarchy process and geospatial techniques. Estuar. Coast Shelf Sci. 279, 108144. https://doi.org/10.1016/j.ecss.2022.108144.

Giudici, A., Jankowski, M.Z., Männikus, R., Najafzadeh, F., Suursaar, Ü., Soomere, T., 2023. A comparison of Baltic Sea wave properties simulated using two modelled wind data sets. Estuar. Coast Shelf Sci. 290, 108401. https://doi.org/10.1016/j.ecss.2023.108401.

Gornitz, V., 1991. Global coastal hazards from future sea level rise. Palaeogeogr. Palaeoclimatol. Palaeoecol. 89, 379–398. https://doi.org/10.1016/0031-0182(91)90173-O.

Gornitz, V.M., Daniels, R.C., White, T.W., Birdwell, K.R., 1994. The development of a coastal risk assessment database, vulnerability to sea-level rise in the U.S. southeast. J. Coast Res. 12, 327–338.

Hadipour, V., Vafaie, F., Kerle, N., 2020. An indicator-based approach to assess social vulnerability of coastal areas to sea- level rise and flooding: a case study of Bandar Abbas city, Iran. Ocean Coast Manag. 188, 105077. https://doi.org/10.1016/j.ocecoaman.2019.105077.

Harff, J., Furmańczyk, K., von Storch, H., 2017. Introduction. In: Harff, J., Furmańczyk, K., von Storch, H. (Eds.), Coastline Changes of the Baltic Sea from South to East, Coastal Research Library, vol. 19. Springer, Cham, pp. 363–386. https://doi.org/10.1007/978-3-319-49894-2_1.

HELCOM, 2021. Natura 2000 sites. https://metadata.helcom.fi.

Hinkel, J., 2011. Indicators of vulnerability and adaptive capacity: towards a clarification of the science–policy interface. Global Environ. Change 21 (1), 198–208. https://doi.org/10.1016/j.gloenvcha.2010.08.002.

Hoque, M.A.A., Ahmed, N., Pradhan, B., Roy, S., 2019. Assessment of coastal vulnerability to multi-hazardous events using geospatial techniques along the eastern coast of Bangladesh. Ocean Coast Manag. 181, 104898. https://doi.org/10.1016/j.ocecoaman.2019.104898.

Hünicke, B., Zorita, E., Soomere, T., Madsen, K.S., Johansson, M., Suursaar, Ü., 2015. Recent change - sea level and wind waves. In: The BACC II Author Team, Second Assessment of Climate Change for the Baltic Sea Basin, Regional Climate Studies. Springer, pp. 155–185. https://doi.org/10.1007/978-3-319-16006-1_9.

IPCC, 2022. In: Pörtner, H.-O., Roberts, D.C., Tignor, M., Poloczanska, E.S., Mintenbeck, K., Alegría, A., Craig, M., Langsdorf, S., Löschke, S., Möller, V., Okem, A., Rama, B. (Eds.), Climate Change 2022: Impacts, Adaptation, and

Vulnerability. Contribution of Working Group II to the Sixth Assessment Report of the Intergovernmental Panel on Climate Change. Cambridge University Press. Cambridge University Press, Cambridge, UK and New York, NY, USA, p. 3056. https://doi.org/10.1017/9781009325844.

IPCC, 2014. In: Field, C.B., Barros, V.R., Dokken, D.J., Mach, K.J., Mastrandrea, M.D., Bilir, T.E., Chatterjee, M., Ebi, K.L., Estrada, Y.O., Genova, R.C., Girma, B., Kissel, E. S., Levy, A.N., MacCracken, S., Mastrandrea, P.R., White, L.L. (Eds.), Climate Change 2014: Impacts, Adaptation, and Vulnerability. Summaries, Frequently Asked Questions, and Cross-Chapter Boxes. A Contribution of Working Group II to the Fifth Assessment Report of the Intergovernmental Panel on Climate Change. World Meteorological Organization, Geneva.

Kao, C., 2010. Fuzzy data standardization. IEEE Trans. Fuzzy Syst. 18, 745–754. https://doi.org/10.1109/TFUZZ.2010.2047948.

Khazai, B., Ingram, J.C., Saah, D.S., 2007. The Protective Role of Natural and Engineered Defence Systems in Coastal Hazards. Spatial Informatics Group, LLC. www.sig-gis.com.

Kont, A., Jaagus, J., Aunap, R., 2003. Climate change scenarios and the effect of sea-level rise for Estonia. Global Planet. Change 36, 1–15. https://doi.org/10.1016/S0921-8181(02)00149-2.

Kont, A., Jaagus, J., Aunap, R., Ratas, U., Rivis, R., 2008. Implications of sea-level rise for Estonia. J. Coast. Res. 24, 423–431. https://doi.org/10.2112/07A-0015.1.

Koroglu, A., Ranasinghe, R., Jimenez, J.A., Dastgheib, A., 2019. Comparison of coastal vulnerability index applications for barcelona province. Ocean Coast Manag. 178, 104799. https://doi.org/10.1016/j.ocecoaman.2019.05.001.

Kovaleva, O., Sergeev, A., Ryabchuk, D., 2022. Coastal vulnerability index as a tool for current state assessment and anthropogenic activity planning for the Eastern Gulf of Finland coastal zone (the Baltic Sea). Appl. Geogr. 143, 102710. https://doi.org/10.1016/j.apgeog.2022.102710.

Łabuz, T.A., 2015. Environmental impacts – coastal erosion and coastline changes. In: The BACC II Author Team, Second Assessment of Climate Change for the Baltic Sea Basin, Regional Climate Studies. Springer, pp. 381–396. https://doi.org/10.1007/978-3-319-16006-1_20.

Leppäranta, M., Myrberg, K., 2009. Physical Oceanography of the Baltic Sea. Springer Praxis, Berlin. https://doi.org/10.1007/978-3-540-79703-6.

Luijendijk, A., Hagenaars, G., Ranasinghe, R., Baart, F., Donchyts, G., Aarninkhof, S., 2018. The state of the world's beaches. Sci. Rep. 8, 6641. https://doi.org/10.1038/s41598-018-24630-6.

Madsen, K.S., Høyer, J.L., Suursaar, Ü., She, J., Knudsen, P., 2019. Sea level trends and variability of the Baltic Sea from 2D statistical reconstruction and altimetry. Front. Earth Sci. 7, 243. https://doi.org/10.3389/feart.2019.00243.

Mafi-Gholami, D., Jaafari, A., Zenner, E.K., Nouri Kamari, A., Tien Bui, D., 2020. Vulnerability of coastal communities to climate change: thirty-year trend analysis and prospective prediction for the coastal regions of the Persian Gulf and Gulf of Oman. Sci. Total Environ. 741, 140305. https://doi.org/10.1016/j.scitotenv.2020.140305.

Malczewski, J., Rinner, C., 2015. GIScience, spatial analysis, and decision support. In: Multicriteria Decision Analysis in Geographic Information Science. Springer, pp. 3–21. https://doi.org/10.1007/978-3-540-74757-4.

Malczewski, J., 2000. On the use of weighted linear combination method in GIS: common and best practice approaches. Trans. GIS 4 (1), 5–22. https://doi.org/10.1111/1467-9671.00035.

Männikus, R., Soomere, T., 2023. Directional variation of return periods of water level extremes in Moonsund and in the Gulf of Riga, Baltic Sea. Reg. Stud. Marine Sci. 57, 102741. https://doi.org/10.1016/j.rsma.2022.102741.

Männikus, R., Soomere, T., Kudryavtseva, N., 2019. Identification of mechanisms that drive water level extremes from in situ measurements in the Gulf of Riga during 1961–2017. Continent. Shelf Res. 182, 22–36. https://doi.org/10.1016/j.csr.2019.05.014.

Masselink, G., Hughes, M., Knight, J., 2011. Introduction to Coastal Processes and Geomorphology, second ed. Routledge.

Mclaughlin, S., Cooper, J.A.G., 2010. A multi-scale coastal vulnerability index: a tool for coastal managers? Environ. Hazards 9, 233–248. https://doi.org/10.3763/ehaz.2010.0052.

Mohamed, S.A., 2020. Coastal vulnerability assessment using GIS-Based multicriteria analysis of Alexandria-northwestern Nile Delta, Egypt. J. Afr. Earth Sci. 163, 103751. https://doi.org/10.1016/j.jafrearsci.2020.103751.

Mohd, F.A., Abdul Maulud, K.N., Karim, O.A., Begum, R.A., Awang, N.A., Ahmad, A., Wan Mohamed Azhary, W.A.H., Kamarudin, M.K.A., Jaafar, M., Wan Mohtar, W.H. M., 2019. Comprehensive coastal vulnerability assessment and adaptation for Cherating-Pekan coast, Pahang, Malaysia. Ocean Coast Manag. 182, 104948. https://doi.org/10.1016/j.ocecoaman.2019.104948.

Mullick, M.R.A., Tanim, A.H., Samiul Islam, S.M., 2019. Coastal vulnerability analysis of Bangladesh coast using fuzzy logic based geospatial techniques. Ocean Coast Manag. 174, 154–169. https://doi.org/10.1016/j.ocecoaman.2019.03.010.

Mu, E., Pereyra-Rojas, M., 2018. Practical decision making using super decisions v3. An introduction to the Analytic Hierarchy Process. Chapter 3: Build. AHP Model. Super Decis. v3, 23–42. https://doi.org/10.1007/978-3-319-68369-0.

Myers, M.R., Barnard, P.L., Beighley, E., Cayan, D.R., Dugan, J.E., Feng, D., Hubbard, D. M., Iacobellis, S.F., Melack, J.M., Page, H.M., 2019. A multidisciplinary coastal vulnerability assessment for local government focused on ecosystems, Santa Barbara area, California. Ocean Coast Manag. 182, 104921. https://doi.org/10.1016/j.ocecoaman.2019.104921.

Najafzadeh, F., Jankowski, M.Z., Giudici, A., Männikus, R., Suursaar, Ü., Viška, M., Soomere, T., 2024. Spatiotemporal variability of wave climate in the Gulf of Riga. Oceanologia 66 (1), 56–77. https://doi.org/10.1016/j.oceano.2023.11.001.

Nguyen, X.T., Tran, M.T., Tanaka, H., Nguyen, T.V., Mitobe, Y., Duong, C.D., 2021. Numerical investigation of the effect of seasonal variations of depth-of-closure on shoreline evolution. Int. J. Sediment Res. 36, 1–16. https://doi.org/10.1016/j.ijsrc.2020.03.016.

Nichols, C.R., Wright, L.D., Bainbridge, S.J., Cosby, A., Henaff, A., Loftis, J.D., Cocquempot, L., Katragadda, S., Mendez, G.R., Letortu, P., Le Dantec, N., Resio, D., Zarillo, G., 2019. Collaborative science to enhance coastal resilience and adaptation. Front. Mar. Sci. 6, 404. https://doi.org/10.3389/fmars.2019.00404.

Nicholls, R.J., Wong, P.P., Burkett, V.R., Codignotto, J.O., Hay, J.E., McLean, R.F., Ragoonaden, S., Woodroffe, C.D., 2007. Coastal systems and low-lying areas. In: Parry, M.L., Canziani, O.F., Palutikof, J.P., van der Linden, P.J., Hanson, C.E. (Eds.), Climate Change 2007: Impacts, Adaptation and Vulnerability. Contribution of Working Group II to the Fourth Assessment Report of the Intergovernmental Panel on Climate Change. Cambridge University Press, Cambridge, UK, pp. 315–356.

Orviku, K., 2018. Rannad Ja Rannikud (Beaches and Coasts). Tallinn University Press, Tallinn [in Estonian].

Orviku, K., Jaagus, J., Kont, A., Ratas, U., Rivis, R., 2003. Increasing activity of coastal processes associated with climate change in Estonia. J. Coast. Res. 19 (2), 364–375.

Orviku, K., Suursaar, Ü., Tönisson, H., Kullas, T., Rivis, R., Kont, A., 2009. Coastal changes in Saaremaa Island, Estonia, caused by winter storms in 1999, 2001, 2005 and 2007. J. Coast. Res. 56, 1651–1655. Special Issue.

Pantusa, D., D'Alessandro, F., Riefolo, L., Principato, F., Tomasicchio, G.R., 2018. Application of a coastal vulnerability index. A case study along the Apulian Coastline, Italy. Water (Switzerland) 10, 1–16. https://doi.org/10.3390/w10091218.

Pérez-Valdez, M.D., Parra-Galaviz, R.E., Macías-Segura, R., Díaz-Hernández, C.D.L.C., Félix-Tapia, R., 2021. Geospatial analysis for the delimitation of the federal maritime land zone in protected natural areas, case of El Maviri Beach, Sinaloa, Mexico. Revista RA Ximhai 17 (3), 405–424. https://doi.org/10.35197/rx.17.03.2021.17.mp.

Pindsoo, K., Soomere, T., 2015. Contribution of wave set-up into the total water level in the Tallinn area. Proc. Est. Acad. Sci. 64 (3S), 338–348. https://doi.org/10.3176/proc.2015.3S.03.

Pradhan, B., 2011. Use of GIS-based fuzzy logic relations and its cross application to produce landslide susceptibility maps in three test areas in Malaysia. Environ. Earth Sci. 63, 329–349. https://doi.org/10.1007/s12665-010-0705-1.

Rangel-Buitrago, N., Neal, W.J., Bonetti, J., Anfuso, G., de Jonge, V.N., 2020. Vulnerability assessments as a tool for the coastal and marine hazards management: an overview. Ocean Coast Manag. 189, 105134. https://doi.org/10.1016/j.ocecoaman.2020.105134.

Ramesh, V., Iqbal, S.S., 2020. Urban flood susceptibility zonation mapping using evidential belief function, frequency ratio and fuzzy gamma operator models in GIS: a case study of Greater Mumbai, Maharashtra, India. Geocarto Int. 37 (2), 581–606. https://doi.org/10.1080/10106049.2020.1730448.

Ramieri, E., Hartley, A., Barbanti, A., Santos, F.D., Gomes, A., Hilden, M., Laihonen, P., Marinova, N., Santini, M., 2011. Methods for assessing coastal vulnerability to climate change. In: European Environment Agency. European Topic Centre on Climate Change Impacts, Vulnerability and Adaptation, pp. 1–93. http://cca.eionet.europa.eu/.

Reale, A., Handmer, J., 2011. Land tenure, disasters and vulnerability. Disasters 35, 160–182. https://doi.org/10.1111/j.1467-7717.2010.01198.x.

Rehman, S., Jahangir, S., Azhoni, A., 2022. GIS based coastal vulnerability assessment and adaptation barriers to coastal regulations in Dakshina Kannada district, India. Reg. Stud. Marine Sci. 55, 102509. https://doi.org/10.1016/j.rsma.2022.102509.

Robinson, V.B., 2003. A perspective on the fundamentals of fuzzy sets and their use in geographic information systems. Trans. GIS 7 (1), 3–30. https://doi.org/10.1111/1467-9671.00127.

Rosentau, A., Muru, M., Gauk, M., Oja, T., Liibusk, A., Kall, T., Karro, E., Roose, A., Sepp, M., Tammepuu, A., Tross, J., Uppin, M., 2017. Sea-level change and flood risks at Estonian coastal zone. In: Harff, J., Furmańczyk, K., von Storch, H. (Eds.), Coastline Changes of the Baltic Sea from South to East, Coastal Research Library, vol. 19. Springer, Cham, pp. 363–386. https://doi.org/10.1007/978-3-319-49894-2_16.

Rutgersson, A., Kjellström, E., Haapala, J., Stendel, M., Danilovich, I., Drews, M., Jylhä, K., Kujala, P., Larsén, X.G., Halsnæs, K., Lehtonen, I., Luomaranta, A., Nilsson, E., Olsson, T., Särkkä, J., Tuomi, L., Wasmund, N., 2022. Natural hazards and extreme events in the Baltic Sea region. Earth Syst. Dynam. 13, 251–301. https://doi.org/10.5194/esd-13-251-2022.

Saaty, T.L., 1980. The Analytic Hierarchy Process. McGraw-Hill, New York.

Saaty, T.L., Tran, L.T., 2007. On the invalidity of fuzzifying numerical judgments in the Analytic Hierarchy Process. Math. Comput. Model. 46, 962–975. https://doi.org/10.1016/j.mcm.2007.03.022.

Sanò, M., Jiménez, J.A., Medina, R., Stanica, A., Sanchez-Arcilla, A., Trumbic, I., 2011. The role of coastal setbacks in the context of coastal erosion and climate change. Ocean Coast Manag. 54, 943–950. https://doi.org/10.1016/j.ocecoaman.2011.06.008.

Sekovski, I., Del Rio, L., Armaroli, C., 2020. Development of a coastal vulnerability index using analytical hierarchy process and application to Ravenna province (Italy). Ocean Coast Manag. 183, 104982. https://doi.org/10.1016/j.ocecoaman.2019.104982.

Serafim, M.B., Siegle, E., Corsi, A.C., Bonetti, J., 2019. Coastal vulnerability to wave impacts using a multi-criteria index: Santa Catarina (Brazil). J. Environ. Manag. 230, 21–32. https://doi.org/10.1016/j.jenvman.2018.09.052.

Sethuraman, S., Alshahrani, H.M., Tamizhselvi, A., Sujaatha, A., 2024. Assessment of coastal vulnerability using AHP and machine learning techniques. J. S. Am. Earth Sci. 147, 105107. https://doi.org/10.1016/j.jsames.2024.105107.

Soomere, T., Viska, M., Eelsalu, M., 2013. Spatial variations of wave loads and closure depths along the coast of the eastern Baltic Sea. Est. J. Eng. 19 (2), 93–109. https://doi.org/10.3176/eng.2013.2.01.

Soomere, T., Eelsalu, M., Kurkin, A., Rybin, A., 2015. Separation of the Baltic Sea water level into daily and multi-weekly components. Continent. Shelf Res. 103, 23–32. https://doi.org/10.1016/j.csr.2015.04.018.

Soomere, T., Pindsoo, K., Eelsalu, M., 2016. Extreme Water Levels and Their Return Periods on Estonian Coasts. Research Report. Institute of Cybernetics, Tallinn University of Technology [in Estonian].

Soomere, T., Eelsalu, M., Pindsoo, K., 2018. Variations in parameters of extreme value distributions of water level along the eastern Baltic Sea coast. Estuar. Coast Shelf Sci. 215, 59–68. https://doi.org/10.1016/j.ecss.2018.10.010.

Soomere, T., Bagdanavičiūtė, I., Barzehkar, M., Parnell, K.E., 2024. Towards implementing water level variations into coastal vulnerability index in microtidal seas. J. Coast. Res. 113, 48–52. https://doi.org/10.2112/JCR-SI113-010.1. Special Issue.

Suursaar, Ü., Sooäär, J., 2007. Decadal variations in mean and extreme sea level values along the Estonian coast of the Baltic Sea. Tellus 59, 249–260. https://doi.org/10.1111/j.1600-0870.2006.00220.x.

Suursaar, Ü., Kall, T., 2018. Decomposition of relative sea level variations at tide gauges using results from four Estonian precise levelings and uplift models. IEEE J. Sel. Top. Appl. Earth Obs. Rem. Sens. 11 (6), 1966–1974. https://doi.org/10.1109/JSTARS.2018.2805833.

Suursaar, Ü., Kullas, T., Otsmann, M., Saaremäe, I., Kuik, J., Merilain, M., 2006. Cyclone Gudrun in January 2005 and modelling its hydrodynamic consequences in the Estonian coastal waters. Boreal Environ. Res. 11 (2), 143–159.

Suursaar, Ü., Jaagus, J., Kont, A., Rivis, R., Tõnisson, H., 2008. Field observations on hydrodynamics and coastal geomorphic processes of Harilaid Peninsula (Baltic Sea) in winter and spring 2006-2007. Estuar. Coast Shelf Sci. 80, 31–41. https://doi.org/10.1016/j.ecss.2008.07.007.

Tanim, A.H., Goharian, E., Moradkhani, H., 2022. Integrated socio-environmental vulnerability assessment of coastal hazards using data-driven and multi-criteria analysis approaches. Sci. Rep. 12, 11625. https://doi.org/10.1038/s41598-022-15237-z.

Tanner, T., Lewis, D., Wrathall, D., Bronen, R., Cradock-Henry, N., Huq, S., Lawless, C., Nawrotzki, R., Prasad, V., Rahman, M.A., Alaniz, R., King, K., McNamara, K., Nadiruzzaman, M., Henly-Shepard, S., Thomalla, F., 2014. Livelihood resilience in the face of climate change. Nat. Clim. Change 5 (1), 23–26. https://doi.org/10.1038/nclimate2431.

Teck, S.J., Halpern, B.S., Kappel, C.V., Micheli, F., Selkoe, K.A., Crain, C.M., Martone, R., Shearer, C., Arvai, J., Fischhoff, B., Murray, G., Neslo, R., Cooke, R., 2010. Using expert judgment to estimate marine ecosystem vulnerability in the California Current. Ecol. Appl. 20 (5), 1402–1416. https://doi.org/10.1890/09-1173.1.

Thirumurthy, S., Jayanthi, M., Samynathan, M., Duraisamy, M., Kabiraj, S., Anbazhahan, N., 2022. Multi-criteria coastal environmental vulnerability assessment using analytic hierarchy process based uncertainty analysis integrated into GIS. J. Environ. Manag. 313, 114941. https://doi.org/10.1016/j.jenvman.2022.114941.

Tokunaga, K., Blandon, A., Blasiak, R., Jouffray, J.B., Wabnitz, C.C., Norström, A.V., 2021. Ocean risks in SIDS and LDCS. Ocean risk and resilience action alliance (ORRAA) report. https://oceanrisk.earth/documents/ORRAA-OceanRisks.pdf.

Tõnisson, H., Kont, A., Orviku, K., Suursaar, Ü., Rivis, R., Palginõmm, V., 2018. Application of system approach framework for coastal zone management in Pärnu, SW Estonia. J. Coast Conserv. 23, 931–942. https://doi.org/10.1007/s11852-018-0637-6.

Tõnisson, H., Orviku, K., Lapinskis, J., Gulbinskas, S., Žaromskis, R., 2013. The Baltic States. In: Pranzini, E., Williams, A. (Eds.), Coastal Erosion and Protection in Europe. Routledge, New York, 111130.

Tõnisson, H., Suursaar, Ü., Orviku, K., Jaagus, J., Kont, A., Willis, D.A., Rivis, R., 2011. Changes in coastal processes in relation to changes in largescale atmospheric circulation, wave parameters and sea levels in Estonia. J. Coast. Res. 64, 701–705. Special Issue.

Torresan, S., Critto, A., Valle, M.D., Harvey, N., Marcomini, A., 2008. Assessing coastal vulnerability to climate change: comparing segmentation at global and regional scales. Sustain. Sci. 3, 45–65. https://doi.org/10.1007/s11625-008-0045-1.

Turner II, B.L., Kasperson, R.E., Matson, P.A., McCarthy, J.J., Corell, R.W., Christensen, L., Eckley, N., Kasperson, J.X., Luers, A., Martello, M.L., Polsky, C., Pulsipher, A., Schiller, A., 2003. A framework for vulnerability analysis in sustainability science. Proc. Natl. Acad. Sci. USA 100 (14), 8074–8079. https://doi.org/10.1073/pnas.1231335100.

Uddin, M.N., Islam, A.K.M.S., Bala, S.K., Islam, G.M.T., Adhikary, S., Saha, D., Haque, S., Fahad, M.G.R., Akter, R., 2019. Mapping climate vulnerability of the coastal region of Bangladesh using principal component analysis. Appl. Geogr. 102, 47–57. https://doi.org/10.1016/j.apgeog.2018.12.011.

Weisse, R., Dailidiene, I., Hünicke, B., Kahma, K., Madsen, K., Omstedt, A., Parnell, K., Schöne, T., Soomere, T., Zhang, W., Zorita, E., 2021. Sea level dynamics and coastal Erosion in the Baltic Sea region. Earth Syst. Dynam. 12, 871–898. https://doi.org/10.5194/esd-12-871-2021.

WMO, 2021. WMO atlas of mortality and economic losses from weather. Clim. Water Extrem. 1970–2019. Chair, Publications Board, World Meteorological Organization (WMO), Geneva 2, Switzerland. https://library.wmo.int/doc_num.php?explnum_id=10902. (Accessed 5 January 2022).

Wolski, T., Wiśniewski, B., Giza, A., Kowalewska-Kalkowska, H., Boman, H., Grabbi-Kaiv, S., Hammarklint, T., Holfort, J., Lydeikaite, Ž., 2014. Extreme sea levels at selected stations on the Baltic Sea coast. Oceanologia 56, 259–290. https://doi.org/10.5697/oc.56-2.259.

Wong, P.P., Losada, I.J., Gattuso, J.P., Hinkel, J., Khattabi, A., McInnes, K.L., Saito, Y., Sallenger, A., 2014. Coastal systems and low-lying areas. In: Barros, V.R., Dokken, D. J., Mach, K.J., Mastrandrea, M.D., Bilir, T.E., Chatterjee, M., Ebi, K.L., Estrada, Y.O., Genova, R.C., Girma, B., Kissel, E.S., Levy, A.N., MacCracken, S., Mastrandrea, P.R., White, L.L. (Eds.), Climate Change 2014: Impacts, Adaptation, and Vulnerability. Part A: Global and Sectoral Aspects. Contribution of Working Group II to the Fifth Assessment Report of the Intergovernmental Panel on Climate Change. Cambridge University Press, Cambridge, United Kingdom and New York, NY, USA, pp. 361–409.

Wong-Parodi, G., Mach, K.J., Jagannathan, K., Sjostrom, K.D., 2020. Insights for developing effective decision support tools for environmental sustainability. Curr. Opin. Environ. Sustain. 42, 52–59. https://doi.org/10.1016/j.cosust.2020.01.005.

Woodroffe, C.D., 2002. Coasts: Form, Process, and Evolution. Cambridge University Press.

IV

Publication IV

Barzehkar, M., Parnell, K., Soomere, T. 2024. Incorporating a machine learning approach into an established decision support system for coastal vulnerability in the eastern Baltic Sea. Journal of Coastal Research, Special Issue 113, 58–62, doi: 10.2112/JCR-SI113-012.1.

Incorporating a Machine Learning Approach into an Established Decision Support System for Coastal Vulnerability in the Eastern Baltic Sea

Mojtaba Barzehkar[†*], Kevin Parnell[†], and Tarmo Soomere[†‡]

[†]School of Science, Department of Cybernetics
Tallinn University of Technology
Tallinn, Estonia

[‡]Estonian Academy of Sciences
Tallinn, Estonia

www.cerf-jcr.org

www.JCRonline.org

ABSTRACT

Barzehkar, M.; Parnell, K., and Soomere, T., 2024. Incorporating a machine learning approach into an established decision support system for coastal vulnerability in the Eastern Baltic Sea. *In:* Phillips, M.R.; Al-Naemi, S., and Duarte, C.M. (eds.), *Coastlines under Global Change: Proceedings from the International Coastal Symposium (ICS) 2024 (Doha, Qatar). Journal of Coastal Research*, Special Issue No. 113, pp. 58-62. Charlotte (North Carolina), ISSN 0749-0208.

Assessing coastal susceptibility to hazards is a critical input for coastal management for countries with long and greatly varying shorelines, such as Estonia. The use of different decision support systems eventually contributes to a better understanding of the functionalities and limitations of tools. The conventional multi-criteria decision analysis (MCDA) techniques using fuzzy logic, analytical hierarchy process, and weighted linear combination were applied to map the coastal vulnerability index (CVI) for the Estonian coast. As a promising alternative, we used machine learning based on the Random Forest (RF) algorithm based on the same set of 16 vulnerability parameters. The results of the MCDA methodology showed that about 47% and 42% of the Estonian coast were in the classes of low and moderate vulnerability, respectively. The estimate based on the RF technique indicates a much larger proportion of the coast (65.6%) in the class of low vulnerability and 24.9% in the class of moderate vulnerability. Almost all vulnerable locations identified by machine learning were in the south of the country. The differences may reflect the larger role of the opinions of experts in the MCDA analysis, providing a more detailed consideration of the local situation and the integration of qualitative data.

ADDITIONAL INDEX WORDS: *Coastal management, geographical information systems (GIS), multi-criteria decision analysis, Random Forest algorithm.*

INTRODUCTION

Coastal areas can experience negative consequences to changes in sea level and storm surges, and this can lead to flooding of low-lying regions (Nicholls *et al*., 2007). Infrastructure and human livelihoods may suffer adverse effects from these coastal hazards (Nichols *et al*., 2019; Tanner *et al*., 2014), potentially also leading to both the loss of ecosystem services and disruptions to biodiversity in marine and coastal ecosystems (Myers *et al*., 2019). Identifying hazards demands an appropriate approach that considers evaluating the exposure of people and assets to hazards, along with assessing the susceptibility of both human and natural systems to damage (IPCC, 2014). Vulnerability assessment is becoming popular among planners to assist coastal communities to enhance their resilience to hazards (Adger *et al*., 2005). A coastal vulnerability index (CVI) is widely used to assess coastal vulnerability (Rangel-Buitrago *et al*., 2020).

Using decision support tools (DSTs) provides a possibility to integrate coastal vulnerability estimates into adaptation planning (Gargiulo *et al*., 2020). A geographical information system (GIS)

is a decision support tool (DST) that facilitates spatial information representation, analysis, and visualization (Barzehkar *et al*., 2021). The combination of GIS with the multi-criteria decision analysis (MCDA) technique provides a methodology for integrating spatial data with experts' opinions to produce information for a decision-making process (Malczewski and Rinner, 2015). Numerous studies have employed GIS and MCDA techniques to assess coastal vulnerability (Armenio *et al*., 2021; Bagdanavičiūtė *et al*., 2019; Ghosh and Mistri, 2022).

In recent years, machine learning algorithms and geospatial techniques have become increasingly popular in mapping hazard susceptibility globally (Lei *et al*., 2020). Random Forest (RF) is a machine learning technique, which models intricate interactions between inputs and can handle large datasets (Wang *et al*., 2016). For example, machine learning techniques were used by Ennouali *et al*. (2023) and Fannassi *et al*. (2023) to integrate these models into coastal vulnerability assessment in Morocco.

However, there exists no systematic comparison of the outcome of MCDA and machine learning techniques for coastal vulnerability assessment. Also, the majority of the above-mentioned methodologies work successfully along relatively straight shorelines where smooth variation in coastal vulnerability is likely. The situation is different, e.g., in the eastern Baltic Sea with complex geometry, morphology, and

geology, and with a variety of coastal engineering structures (Kovaleva *et al.*, 2022).

Thus, three distinct gaps in the literature are addressed in this study using the example of the evaluation of coastal vulnerability in Estonia in the eastern Baltic Sea.

Firstly, the application of a machine learning technique based on Random Forest (RF) technique has been integrated with GIS and compared with well-established MCDA techniques with respect to their use in coastal vulnerability assessment. Secondly, the analysis incorporates less apparent and less explored variables, such as the location of nature conservation areas, land ownership, and setback (the distance between the initial infrastructure and the shoreline) extending up to 2 km over low-lying inland areas with high spatial resolution, to provide a comprehensive coastal vulnerability assessment. Finally, the implementation of a coastal vulnerability assessment covers the entire Estonian coastline. To delineate the study area, the eastern Baltic Sea coast was selected, extending 2 km inland from the line corresponding to the long-term mean sea level (0 m in EH2000 datum), as shown in Figure 1.

METHODS
Multi-Criteria Decision Analysis (MCDA)

The MCDA technique employed for coastal vulnerability integrates GIS with analytical hierarchy process (AHP), fuzzy logic, and weighted linear combination (WLC), organized into the following steps. Firstly, the significant environmental and socioeconomic parameters influencing the vulnerability are gathered and incorporated into GIS environment for data quantification and raster analysis mapping. Following the framework established by Turner *et al.* (2003) and applied by El-Shahat *et al.* (2021), we consider exposure, sensitivity, and resilience as the components of coastal vulnerability. Exposure parameters are land surface elevation, beach slope, closure depth, extreme water level, maximum significant wave height, relative sea level rise, shoreline change, and underwater slope. Sensitivity parameters are geomorphology, land use and land cover, land tenure, nature protection areas, population density, and sediments. Resilience parameters are coastal protection structures and coastal setback.

Vulnerability increases with higher values of specific parameters (e.g., extreme water level, sea level rise rate, maximum significant wave height) and decreases with higher values of other parameters (e.g., elevation, beach slope, shoreline change). Due to the different scales and meanings of an increase or decrease in the values of these parameters, it is essential to standardize (normalize) their numerical values before application of the technique (Eastman, 2009). Fuzzy logic is then applied to standardize the pixels of raster maps, assigning values between 0 and 1 (Barzehkar *et al.*, 2021). AHP is then used to obtain the relative importance (contribution) of each parameter, producing weights for individual parameters (Mu and Pereyra-Rojas, 2018). Parameter weighting values range from 1 to 9, following the methodology established by Saaty and Tran (2007), with validation employing a consistency ratio (*CR*) of equal to or less than 0.1 (Mu and Pereyra-Rojas, 2018). Weighted parameters are then combined in GIS using the WLC technique to produce the final map, achieved by multiplying the relative weight of each parameter by its normalized value (Malczewski and Rinner, 2015).

Machine Learning using RF Technique

The RF algorithm is a supervised machine learning technique that can be applied for classification or regression (Izquierdo-Horna *et al.*, 2022). This is a beneficial method to specify the weight of parameters through investigating the relationship between independent and dependent variables (Gigović *et al.*, 2019). In this study, the independent variables are the parameters involved in coastal vulnerability assessment and the dependent variables are the hazard and non-hazard locations for vulnerability analysis. The RF algorithm is a combination of numerous decision trees. Each tree is an individual model that makes predictions. They are constructed by using random samples from the original data (a technique called bootstrapping) and considering the available predictors (Izquierdo-Horna *et al.*, 2022). Each decision tree is built when both the predictive and target variables are defined (Rihan *et al.*, 2023).

To implement this technique, the parameters used for vulnerability assessment serve as predictors, and the hazard and non-hazard locations serve as target variables in a classification problem for categorizing and classifying other locations. Hazard and non-hazard locations must be specified and divided into two groups, typically based on a ratio of 70:30 to be used for training and testing of the model (Yariyan *et al.*, 2020). In this study, a total of 1000 samples were selected randomly from the MCDA map to be used in the RF technique, with 700 points for training of the model (coastal vulnerability classification) and 300 points for testing (validation) of the model.
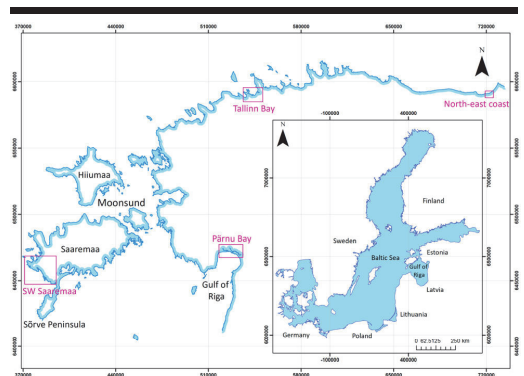
Figure 1. The location of the eastern Baltic Sea coast. The axis units are in meters. The study area (wide blue line) extends 2 km inland from the line corresponding to the long-term mean sea level (0 m in EH2000 datum).

Values >0.44 from the MCDA map were chosen as hazard locations and values ≤0.44 were chosen as non-hazard locations. The numbers of hazard and non-hazard locations were similar in order to avoid bias (Wang *et al.*, 2021; Rufat and Botzen, 2022). The coastal vulnerability parameters were used in the next step of training the model. The sixteen vulnerability parameters (in the format of raster maps) were incorporated in the GIS environment. In the final step, the pixel values of the raster

layers for vulnerability parameters were extracted for the hazard and non-hazard locations to obtain the training datasets and to proceed with the training process to classify vulnerability along a strip 2 km inland from the shoreline, defined as mean sea level.

RESULTS
Coastal Vulnerability based on MCDA and RF Techniques

The comparison between the MCDA and RF in coastal vulnerability assessment of the eastern Baltic Sea highlights the different outputs of the two techniques. In the MCDA framework, experts prioritized extreme water levels, shoreline change, and geomorphology, while giving less importance to closure depth, population density, and land tenure. The computed consistency ratio among experts' opinions was $CR = 0.04$, which shows the consistency of experts' perspectives (Saaty and Tran, 2007).

Despite the use of weighting scales from 1 to 5 by experts, the geometric mean for weight computation resulted in compression in the value range, which is a common practice to reach consensus. Across the study domain, the CVI map derived by MCDA indicated a high proportion of regions with low (47%) to moderate (42.5%) vulnerability. High-vulnerability areas, particularly those vulnerable to high water levels, gradual erosion, and proximity to human infrastructure, were concentrated along the western shoreline of Saaremaa and Pärnu Bay (Figure 2). The rationale relating to this pattern are attributed to (1) the frequent occurrence of elevated water levels in the Gulf of Riga (Suursaar and Sooäär, 2007; Eelsalu *et al.*, 2014) and associated shoreline erosion along various sections of the eastern Gulf of Riga, or (2) susceptibility to westerly storm events especially on western coast of Saaremaa.
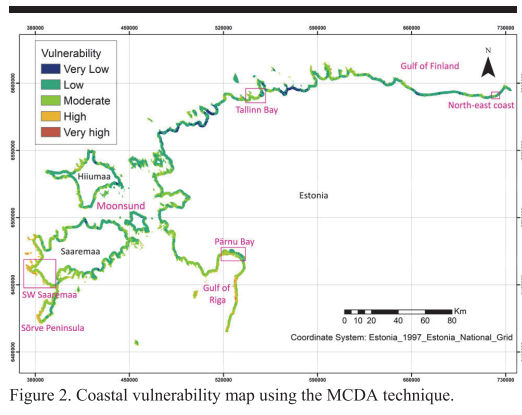
Figure 2. Coastal vulnerability map using the MCDA technique.

In contrast, RF technique produced a different vulnerability classification, with a much larger proportion of areas with low vulnerability (65.6%) than the MCDA technique. The high vulnerability areas identified by the RF technique are mainly located in the Gulf of Riga, including Pärnu Bay (Figure 3). The overall spatial pattern of vulnerability classes represented an

alignment between the two methodologies, providing some confidence in the results.

However, there are big discrepancies in categorizing vulnerable locations particularly in the Gulf of Riga, the western shore of Saaremaa, and Tallinn Bay. More vulnerable areas are mostly located in the south of the country on the shores of the Gulf of Riga. The most significant parameters based on the machine learning approach using RF technique, were geomorphology, maximum significant wave height, and shoreline change. Based on the results from both techniques (Table 1), very low vulnerability is in the North-west, low vulnerability is in the North-west and North-east, moderate vulnerability is in the North-west, Pärnu Bay, and western islands, high and very high vulnerability are found in Pärnu Bay and western islands. The detailed analysis using MCDA and RF techniques provides a comprehensive understanding of the spatial distribution of coastal vulnerability.

Table 1. *Coastal vulnerability analysis using MCDA (left two columns) and RF (right two columns) techniques.*

Vulnerability	Area (km²) MCDA	% MCDA	Area (km²) RF	% RF
Very low	121	3.8	15	0.5
Low	1496	47	2086	65.6
Moderate	1350	42.5	793	24.9
High	207	6.5	236	7.4
Very High	6	0.2	50	1.6
Sum of classes	3180	100	3180	100

Figure 3. Coastal vulnerability map using the RF technique.

DISCUSSION

Machine learning techniques, especially the RF approach, are beneficial for handling large datasets and identifying essential parameters through data-driven algorithms. However, they cannot integrate expert opinions or site-specific knowledge into the analysis. On the other hand, MCDA techniques offer a decision-support framework explicitly designed to incorporate experts' perspectives. Employing various MCDA techniques, such as fuzzy logic, AHP, and WLC provides greater flexibility to manage uncertainty and ensure a more accurate representation of vulnerability assessment in the eastern Baltic Sea (and

apparently in similar locations) than machine learning based on the RF technique.

Incorporating machine learning into the coastal vulnerability assessment typically enhances confidence in the outcomes when compared to other studies. Studies on coastal vulnerability assessment using machine learning commonly focus on small geographic areas (Ennouali *et al*., 2023; Fannassi *et al*., 2023) or specific coastal processes (Asiri *et al*., 2024). Hasan *et al*. (2023) chose a country-wide approach to coastal vulnerability assessment to flooding, although primarily emphasizing the physical parameters of vulnerability.

Our study presents a novel quasi-two-dimensional approach, examining a 2 km wide zone extending inland from the coast, which facilitates the mapping of parameters with inherent two-dimensional data types. By comparing MCDA techniques and machine learning based on RF, we demonstrate how machine learning adds value by providing a data-driven approach to analyzing coastal vulnerability. However, challenges arise for both methods when incorporating variables that are essentially one-dimensional, such as extreme water level, setback, etc., which naturally exist as line variables along the shoreline (Barzehkar *et al*., 2024).

Machine learning techniques like RF can still identify key parameters without explicitly modeling complex relationships. This means that these algorithms can automatically recognize patterns and correlations, allowing them to extract key parameters contributing to coastal vulnerability without relying on detailed prior knowledge or assumptions about the underlying relationships. This enhances the comprehensiveness and accuracy of coastal vulnerability assessment.

The response to vulnerability assessment requires consideration of resource availability, and environmental and political factors, with options ranging from hard engineering to doing nothing (Masselink *et al*., 2011). Coastal resilience and long-term sustainability are improved when using strategies for specific coastal conditions and actively engaging stakeholders.

CONCLUSIONS

The vulnerability assessment of the Estonian coast performed using two techniques (MCDA and machine learning based on RF) generated relatively different but still consistent vulnerability maps. The application of different techniques highlights in more detail the impact of different parameters and thus provides a better scientific basis and confidence for the interpretation of the results.

The most significant factors influencing vulnerability of the Estonian coasts based on the AHP were extreme water level, shoreline change, and geomorphology, whereas geomorphology, maximum significant wave height, and shoreline change influenced significantly the coastal vulnerability based on machine learning using RF technique. The output of the MCDA technique showed that more Estonian coasts have low and moderate vulnerability (which is aligned with the situation of the eastern Baltic Sea coasts) than does machine learning using RF technique. It is recommended that both techniques be applied in complex coastal environments to prepare coastal vulnerability maps and investigate further the results of those decision support systems for sustainable coastal planning and management.

LITERATURE CITED

Adger, W.N.; Hughes, T.P.; Folke, C.; Carpenter, S.R., and Rockström, J., 2005. Social-ecological resilience to coastal disasters. *Science,* 309(5737), 1036–1039.

Armenio, E.; Mossa, M., and Petrillo, A.F., 2021. Coastal vulnerability analysis to support strategies for tackling COVID-19 infection. *Ocean & Coastal Management,* 211, 105731.

Asiri, M.M.; Aldehim, G.; Alruwais, N.; Allafi, R.; Alzahrani, I.; Nouri, A.M.; Assiri, M. and Abdelaziz Ahmed, N., 2024. Coastal flood risk assessment using ensemble multi-criteria decision-making with machine learning approaches. *Environmental Research*, 245, 118042.

Bagdanavičiūtė, I.; Kelpšaitė-Rimkienė, L.; Galinienė, J., and Soomere, T., 2019. Index based multi-criteria approach to coastal risk assessment. *Journal of Coastal Conservation*, 23, 785–800.

Barzehkar, M.; Parnell, K.E.; Soomere, T.; Dragovich, D., and Engström, J., 2021. Decision support tools, systems and indices for sustainable coastal planning and management: A review. *Ocean & Coastal Management*, 212, 105813.

Barzehkar, M.; Parnell, K., and Soomere, T. 2024. Extending multi-criteria coastal vulnerability assessment to low-lying inland areas: examples from Estonia, eastern Baltic Sea. *Estuarine, Coastal and Shelf Science*.

Eastman, J.R., 2009. *IDRISI Taiga: Guide to GIS and Image Processing*. Clark labs: Clark University.

Eelsalu, M.; Soomere, T.; Pindsoo, K., and Lagemaa, P., 2014. Ensemble approach for projections of return periods of extreme water levels in Estonian waters. *Continental Shelf Research*, 91, 201–210.

El-Shahat, S.; El-Zafarany, A.M.; El Seoud, T.A., and Ghoniem, S.A., 2021. Vulnerability assessment of African coasts to sea level rise using GIS and remote sensing. *Environment, Development and Sustainability*, 23, 2827–2845.

Ennouali, Z.; Fannassi, Y.; Lahssini, G.; Benmohammadi, A., and Masria, A., 2023. Mapping coastal vulnerability using machine learning algorithms: A case study at North coastline of Sebou estuary, Morocco. *Regional Studies in Marine Science*, 60, 102829.

Fannassi, Y.; Ennouali, Z.; Hakkou, M.; Benmohammadi, A.; Al-Mutiry, M.; Elbisy, M.S., and Masria, A., 2023. Prediction of coastal vulnerability with machine learning techniques, Mediterranean coast of Tangier-Tetouan, Morocco. *Estuarine, Coastal and Shelf Science*, 291, 108422.

Gargiulo, C.; Battarra, R., and Tremiterra, M.R., 2020. Coastal areas and climate change: a decision support tool for

implementing adaptation measures. *Land Use Policy*, 91, 104413.

Ghosh, S. and Mistri, B., 2022. Analyzing the multi-hazard coastal vulnerability of Matla–Bidya inter-estuarine area of Indian Sundarbans using analytical hierarchy process and geospatial techniques. *Estuarine, Coastal and Shelf Science*, 279, 108144.

Gigović, L.; Pourghasemi, H.R.; Drobnjak, S., and Bai, S., 2019. Testing a new ensemble model based on SVM and Random Forest in forest fire susceptibility assessment and its mapping in Serbia's Tara National Park. *Forests*, 10(5), 408.

Hasan, M.H.; Ahmed, A.; Nafee, K.M., and Hossen, M.A., 2023. Use of machine learning algorithms to assess flood susceptibility in the coastal area of Bangladesh. *Ocean & Coastal Management,* 236, 106503.

IPCC, 2014. *Climate change 2014: impacts, adaptation, and vulnerability. Summaries, frequently asked questions, and cross-chapter boxes*. A contribution of working group II to the fifth assessment report of the intergovernmental panel on climate change [Field, C.B.; Barros, V.R.; Dokken, D.J.; Mach, K.J.; Mastrandrea, M.D.; Bilir, T.E.; Chatterjee, M.; Ebi, K.L.; Estrada, Y.O.; Genova, R.C.; Girma, B.; Kissel, E.S.; Levy, A.N.; MacCracken, S.; Mastrandrea, P.R., and White, L.L. (eds.)]. World Meteorological Organization, Geneva.

Izquierdo-Horna, L.; Zevallos, J., and Yepez, Y., 2022. An integrated approach to seismic risk assessment using random forest and hierarchical analysis: Pisco, Peru. *Heliyon*, 8(10), e10926.

Kovaleva, O.; Sergeev, A., and Ryabchuk, D., 2022. Coastal vulnerability index as a tool for current state assessment and anthropogenic activity planning for the Eastern Gulf of Finland coastal zone (the Baltic Sea). *Applied Geography*, 143, 102710.

Lei, X.; Chen, W.; Avand, M.; Janizadeh, S.; Kariminejad, N.; Shahabi, H.; Costache, R.; Shahabi, H.; Shirzadi, A., and Mosavi, A., 2020. GIS-based machine learning algorithms for gully erosion susceptibility mapping in a semi-arid region of Iran. *Remote Sensing*, 12, 2478.

Malczewski, J. and Rinner, C., 2015. GIScience, spatial analysis, and decision support. In: *Multicriteria Decision Analysis in Geographic Information Science*, pp 3–21. Springer

Masselink, G.; Hughes, M., and Knight, J., 2011. *Introduction to Coastal Processes and Geomorphology*. 2nd ed. Routledge.

Mu, E. and Pereyra-Rojas, M., 2018. *Practical decision making using super decisions v3. An introduction to the Analytic Hierarchy Process*. Chapter 3: Building AHP Models Using Super Decisions v3, pp. 23–42

Myers, M.R.; Barnard, P.L.; Beighley, E.; Cayan, D.R.; Dugan, J.E.; Feng, D.; Hubbard, D.M.; Iacobellis, S.F.; Melack, J.M., and Page, H.M., 2019. A multidisciplinary coastal vulnerability assessment for local government focused on ecosystems, Santa Barbara area, California. *Ocean & Coastal Management*, 182, 104921.

Nicholls, R.J.; Wong, P.P.; Burkett, V.R.; Codignotto, J.O.; Hay, J.E.; McLean, R.F.; Ragoonaden, S.; Woodroffe, C.D.; in:

Parry, M.L.; Canziani, O.F.; Palutikof, J.P.; van der Linden, P.J., and Hanson, C.E. (Eds.), 2007. *Coastal systems and low-lying areas. In: Climate Change 2007: Impacts, Adaptation and Vulnerability. Contribution of Working Group II to the Fourth Assessment Report of the Intergovernmental Panel on Climate Change*. Cambridge University Press, Cambridge, UK, pp. 315–356.

Nichols, C.R.; Wright, L.D.; Bainbridge, S.J.; Cosby, A.; Henaff, A.; Loftis, J.D.; Cocquempot, L.; Katragadda, S.; Mendez, G.R.; Letortu, P.; Le Dantec, N.; Resio, D., and Zarillo, G., 2019. Collaborative science to enhance coastal resilience and adaptation. *Frontiers in Marine Science*, 6, 404.

Rangel-Buitrago, N.; Neal, W.J.; Bonetti, J.; Anfuso, G., and de Jonge, V.N., 2020. Vulnerability assessments as a tool for the coastal and marine hazards management: An overview. *Ocean & Coastal Management*, 189, 105134.

Rihan, M.; Bindajam, A.A.; Talukdar, S.; Shahfahad; Naikoo, M.W.; Mallick, J., and Rahman, A., 2023. Forest fire susceptibility mapping with sensitivity and uncertainty analysis using machine learning and deep learning algorithms. *Advances in Space Research*, 72(2), 426–443.

Rufat, S. and Botzen, W.J.W., 2022. Drivers and dimensions of flood risk perceptions: Revealing an implicit selection bias and lessons for communication policies. *Global Environmental Change*, 73, 102465.

Saaty, T.L. and Tran, L.T., 2007. On the invalidity of fuzzifying numerical judgments in the Analytic Hierarchy Process. *Mathematical and Computer Modelling*, 46(7–8), 962–975.

Suursaar, Ü. and Sooäär, J., 2007. Decadal variations in mean and extreme sea level values along the Estonian coast of the Baltic Sea. *Tellus A*, 59(2), 249–260.

Tanner, T.; Lewis, D.; Wrathall, D.; Bronen, R.; Cradock-Henry, N.; Huq, S.; Lawless, C.; Nawrotzki, R.; Prasad, V.; Rahman, M.A.; Alaniz, R.; King, K.; McNamara, K.; Nadiruzzaman, M.; Henly-Shepard, S., and Thomalla, F., 2014. Livelihood resilience in the face of climate change. *Nature Climate Change*, 5(1), 23–26.

Turner II, B.L.; Kasperson, R.E.; Matson, P.A.; McCarthy, J.J.; Corell, R.W.; Christensen, L.; Eckley, N.; Kasperson, J.X.; Luers, A.; Martello, M.L.; Polsky, C.; Pulsipher, A., and Schiller, A., 2003. A framework for vulnerability analysis in sustainability science. *Proceedings of the National Academy of Sciences*, 100(14), 8074-8079.

Wang, L.; Zhou, X.; Zhu, X.; Dong, Z., and Guo, W., 2016. Estimation of biomass in wheat using random forest regression algorithm and remote sensing data. *The Crop Journal*, 4(3), 212–219.

Wang, S.; Zhang, K.; Chao, L.; Li, D.; Tian, X.; Bao, H.; Chen, G., and Xia, Y., 2021. Exploring the utility of radar and satellite-sensed precipitation and their dynamic bias correction for integrated prediction of flood and landslide hazards. *Journal of Hydrology*, 603, 126964.

Yariyan, P.; Avand, M.; Abbaspour, R.A.; Karami, M., and Tiefenbacher, J.P., 2020. GIS-based spatial modeling of snow avalanches using four novel ensemble models. *Science of the Total Environment*, 745, 141008.

Publication V

Soomere, T., Bagdanavičiūtė, I., Barzehkar, M., Parnell, K.E. 2024. Towards implementing water level variations into Coastal Vulnerability Indexes in microtidal seas. Journal of Coastal Research, Special Issue 113, 48–52, doi: 10.2112/JCR-SI113-010.1.

Towards Implementing Water Level Variations into Coastal Vulnerability Indexes in Microtidal Seas

Tarmo Soomere[†§*], Ingrida Bagdanavičiūtė[‡], Mojtaba Barzehkar[†], and Kevin E. Parnell[†]

[†]Wave Engineering Laboratory
Department of Cybernetics, School of Science
Tallinn University of Technology
Tallinn, Estonia

[§]Estonian Academy of Sciences
Tallinn, Estonia

[‡]Marine Research Institute
Klaipeda University, Lithuania
Nature Research Centre
Vilnius, Lithuania

ABSTRACT

www.JCRonline.org

Soomere, T.; Bagdanavičiūtė, I.; Barzehkar, M., and Parnell, K.E., 2024. Towards implementing water level variations into coastal vulnerability indexes in microtidal seas. *In:* Phillips, M.R.; Al-Naemi, S., and Duarte, C.M. (eds.), *Coastlines under Global Change: Proceedings from the International Coastal Symposium (ICS) 2024 (Doha, Qatar). Journal of Coastal Research*, Special Issue No. 113, pp. 48-52. Charlotte (North Carolina), ISSN 0749-0208.

We explore the potential of several quantities that reflect the magnitude of local water level variations to characterize the contribution of water level into estimates of the Coastal Vulnerability Index (CVI) in microtidal seas hosting substantial water level variations. The analysis is based on sea level time series reconstructed with the Rossby Centre Ocean model for 1961–2005 and an early version of the RCA4-NEMO model for 1961–2009. The projections of extremely high and low sea levels for return periods of 10 and 50 yrs are constructed using sea level extremes in 12 month long time intervals, block maximum method and several extreme value distributions. The focus is on the relatively straight Baltic proper shore of Lithuania. We show that projected extremely high and low sea levels once in 10 and 50 yrs provide certain independent information about vulnerability along this coastal segment. The use of a larger number of parameters shrinks the range of the output values of the CVI. The outcome provides important input for coastal management but also suggests that more elaborated quantities might better characterize the impact of varying water levels on coastal vulnerability.

ADDITIONAL INDEX WORDS: *CVI index, Generalized Extreme Value distribution, block maximum, Baltic Sea.*

INTRODUCTION

Coastal areas are under gradually increasing joint pressure by various hydrodynamic loads owing to climate change and different kinds of stresses stemming from growing concentration of people and escalating infrastructure. A particular concern is the increase in wave power (Kümmerer *et al*., 2024) or (compound) flood events over the whole European domain (Heinrich *et al*., 2023). These developments have reinforced the importance of the proper reaction of coastal communities to the amplifying pressures on sedimentary shores. In particular, the (geologically) young and rapidly developing shores of the Baltic Sea (Harff *et al*., 2017) serve as a significant coastal management challenge (Bagdanavičiute *et al.*, 2015) because of unusually strong wave impact (Viška and Soomere, 2013), presence of water level outliers (Suursaar and Sooäär, 2007) and spatial variability in the climate change driven modifications of drivers of coastal processes (Eelsalu *et al*., 2024; Soomere, 2024).

A natural way to meet this challenge is to develop an adequate measure of resilience or vulnerability of single beaches and coastal segments. This is a nontrivial task because the coastal zone is influenced by a large number of drivers. The first attempt to quantify the vulnerability of open ocean shores (Gornitz *et al*., 1991) includes seven parameters: elevation, lithology, geomorphology, relative sea level change, shoreline

displacement, tidal range and wave heights. Of these, tidal range is irrelevant in microtidal basins, such as the Baltic Sea or Caspian Sea, and has limited impact in many other sea areas, such as the Red Sea. Relative sea level change often varies insignificantly even on a country scale of many small countries, such as Latvia or Lithuania (Bagdanavičiute *et al*., 2015, 2019).

In essence, coastal vulnerability should incorporate exposure, sensitivity, and resilience (Turner *et al*., 2003). This means the necessity of involving many more parameters. Each of these components can be represented by several quantities. For example, the common exposure parameters are land surface elevation, beach slope, underwater slope, shoreline change, closure depth, extreme water level, relative sea level change, and wave loads. Geomorphology, sediments or population density could characterize sensitivity and coastal protection structures and coastal setback may indicate the level of resilience (e.g., Barzehkar *et al*., 2024).

While the use of an extended set of parameters but still following Gornitz *et al*. (1994) provides many more nuances to the pattern of coastal vulnerability also at small scales (Bagdanavičiute *et al*., 2015, 2019), the resulting pattern is sometimes controversial. A generic problem is that interpretation of alongshore variations of some parameters is not straightforward even for experts in the field. The classic example is tidal range: if this range is large, the shore has already adjusted to varying hydrodynamic loads and strong wave storms infrequently occur exactly at tide maximum. Therefore, many beaches with large tidal range are actually resilient to large variations in the water level while coastal sectors where water level variations are

smaller but sediment is mobile could be vulnerable with respect to even moderate elevations of water level.

It is thus not unexpected that the use of usual indicators of vulnerability may lead to controversial results. This feature becomes clear from the vulnerability of the entire shoreline of Estonia in the eastern Baltic Sea using a small selection of key parameters: modeled extreme water level, shoreline change and geomorphology (Figure 1). Several shore segments that are categorized as vulnerable (e.g., on Saaremaa) are naturally protected by numerous rocks and/or resilient vegetation. At the same time, highly sensitive bayheads and beaches, such as the interior of Pärnu Bay, formally have moderate or even low vulnerability (Figure 1).
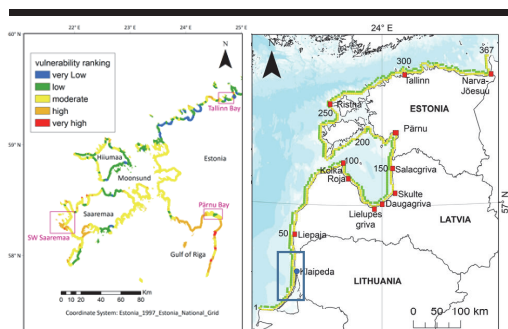

Figure 1. Left: Coastal vulnerability map of Estonia based on three most important parameters: extreme water level, shoreline change and geomorphology. See details in Barzehkar *et al.* (2024). Right: Circulation model calculation points for data in Figure 2. The blue box shows the area of evaluation of the CVI index in Figures 3, 4, and 5.

To shed more light on the challenge of the use of measures of alongshore water level variations in estimates of coastal vulnerability at the scale of a small country, in this paper we discuss the potential of several parameters that characterize water level variations. The focus is on projections for extremely high and low water levels for a selection of return periods. We show that alongshore variations of these projections along even fairly featureless (in terms of development of high and low water levels) coastal segments of Lithuania provide important additional information about coastal vulnerability. The benefits from the use of such quantities are discussed in the context of local and regional variations in the resulting coastal vulnerability index.

METHODS
Coastal Vulnerability Index

We employ here the framework of evaluation of coastal vulnerability index (CVI) adjusted to the conditions of the low-lying Lithuanian coast on the eastern shore of the microtidal Baltic Sea (Bagdanavičiūtė *et al.*, 2015, 2019) by modifying the approach of Gornitz *et al.* (1994) considering specific features of the study area. Specifically, we tested the "impact" of several quantities characterizing water level variations on the CVI values based on classic properties that portray coastal susceptibility: the historical shoreline change rate (HSC, m/yr),

beach width (BW, m), beach height (BH, m), beach sediment type (BS), underwater slope (US), number of sand bars (SB) and significant wave height (SWH, m) (Bagdanavičiūtė *et al.*, 2019).

Data for each of these variables was gridded into 500 m long sections of the coastline and analyzed using the ArcGIS 10.3 software as described in Bagdanavičiūtė *et al.* (2019). In this type of analysis, different criteria can contribute differently to coastal vulnerability. Each criterion's potential role in each grid cell was assigned a value from 1 to 5, indicating very low to very high vulnerability, respectively. We intentionally used the same data set (including significant wave height evaluated using the SWAN model for 2006–2009), except for adjusting the weights of individual parameters, as in Bagdanavičiūtė *et al.* (2019) to identify the potential of different characteristics of water level for the use as a constituent of CVI values. In this analysis, all criteria were presumed to have an equal contribution to coastal vulnerability, and the CVI was calculated using the arithmetic mean formula. Both the ranges of vulnerability with respect to each parameter and the resulting CVI values are divided into five classes of equal width, from very low (1) (lower 20% of the range) to very high (5) (upper 80–100% of the range) vulnerability.

Projections of Extremely High and Low Water Levels

The classic parameters to characterize vulnerability of a coastal sector are extremely high water levels in the past. In some applications, such as safety of shipping in shallow waterways, also the extremely low water levels could be decisive (Parker and Huff, 1998). A natural generalization of these quantities is the projection of extreme sea level maxima and minima for certain return intervals (Figure 2). These projections are built using two sets of modeled sea level time series for the entire Baltic Sea. The 6-hourly output of the Rossby Centre Ocean (RCO) model for 1961–2005 (Meier *et al.*, 2003) adequately replicates the course of water level in the eastern Baltic Sea (Soomere *et al.*, 2015) while the hourly output of an early version of RCA4-NEMO model (Hordoir *et al.*, 2013) for 1961–2009 follows well the average and lower water levels (Viigand *et al.*, 2024). Both models use the same family of primitive equations and a regular rectangular grid of 2×2 nautical miles (nmi) based on stationary topography. They have been extensively discussed in the above cited scientific literature.

We use projections of extreme sea levels for different return periods based on an ensemble of various reconstructions of parameters of extreme value distributions using the block maxima method and annual maxima and minima of sea level extremes as well as such maxima and minima during 12-month intervals from June to July of subsequent year. This ensemble includes the full Generalized Extreme Value (GEV) distribution, its particular case Gumbel distribution, and 2-parameter Weibull distribution to evaluate the lower threshold of sea level extremes for given return periods. The relevant procedures are provided in Soomere *et al.* (2018) and Viigand *et al.* (2024).

Figure 2 shows that the magnitudes of sea level extremes greatly vary along the shores of Lithuania, Latvia, and Estonia. For example, the projected extreme sea level with a return period of 50 yrs varies from about 1.2 m in the south of Lithuania up to values over 2 m in Pärnu Bay. The existing projections of this type qualitatively follow the observed water

level maxima but do not replicate the full range of water level extremes (Viigand *et al*., 2024).

Figure 2. Ensemble of projections of maximum (upper panel) and minimum (lower panel) sea level once in 50 yrs in terms of sea level with 50-yr return period along the shores of Estonia, Latvia and Lithuania. The bold red line indicates the ensemble average used in the analysis. The lower cluster of projections in the lower panel is based on the RCA4-NEMO model and the upper cluster on the RCO model. Graphics by Katri Viigand. See details in Viigand *et al*. (2024).

The projections of extremely low sea levels to some extent mirror projections of extreme elevations but have a clearly smaller range and less pronounced spatial variation. Both these quantities vary about 20% (±10% from their average values) along the Baltic proper shores of Latvia and Lithuania. This level of variation is apparently large enough to become evident in the CVI index. Similar variations are characteristic to extremely high and low sea levels once in 10 yrs (not shown).

RESULTS
Sea Level Maxima and Minima Once in 10 Years
The contribution of sea level maxima with a return period of 10 yrs (Figure 3) into the CVI index has a relatively contrasted appearance compared to the alongshore variations of its other 7 constituents mentioned above. It has a clearly defined maximum in the north of the Lithuanian shoreline, a minimum from Palanga to Klaipėda and in the northern part of the Curonian Spit, and values somewhat larger than average in the southern part of the Lithuanian sector of the Curonian Spit. The alongshore variation of this parameter to some extent follows a similar variation of other parameters used in the estimates.

However, it evidently provides information that is not present in other parameters. As sea level changes slowly along such a relatively straight coastline, it is natural that local variations in the 10-yr maximum sea level are clearly smaller than similar variations in several other parameters.

The situation is different with sea level minima with 10-yr return period (Figure 3, right panel). This parameter seems to provide information that is tangential to the majority of other parameters. The associated estimated vulnerability is the smallest in the north of the study area where its absolute values are smaller. Its largest values occur in the south of the study area.

Figure 3. Relative coastal vulnerability with respect to (a) historical shoreline change, (b) beach width, (c) beach height, (d) beach sediments, (e) underwater slope, (f) sand bars, (g) significant wave height, (I) CVI based on these criteria, equal weights, equal intervals classification, (II) CVI with equal weights but using also (h) sea level maxima (left) or minima (right) with a 10-yr return period. Note that line (I) is the same for both panels.

Interestingly, the contribution of both these parameters into the CVI is similar. Their use insignificantly changes the minimum CVI value from 1.71 to 1.75 for maxima, or to 1.88 for minima (Table 1). The changes to the CVI maxima are larger: from 4.57 to 4.125 for maxima or 4.25 for minima. Incorporation of sea level maxima slightly increases the resulting CVI values in the north while the use of sea level minima does the same in the south (as seen from a comparison of lines I and II in Figure 3). It is therefore likely that these parameters carry different information and are equally important constituents of a reliable CVI index.

The pattern and relative magnitude of spatial variation of extremely high and low sea levels once in 50 yrs largely follows these aspects for sea levels in 10 yrs (Figure 4). It is therefore expected that their contribution to the CVI index varies in a similar manner along the study area.

Figure 4 signals that these variations are still not exactly equivalent. This feature apparently reflects certain alongshore variations in the shape parameter of the generalized extreme

value distribution in the study area. Namely, its larger values indicate a faster increase in the projected sea level in the particular location (Coles, 2004).
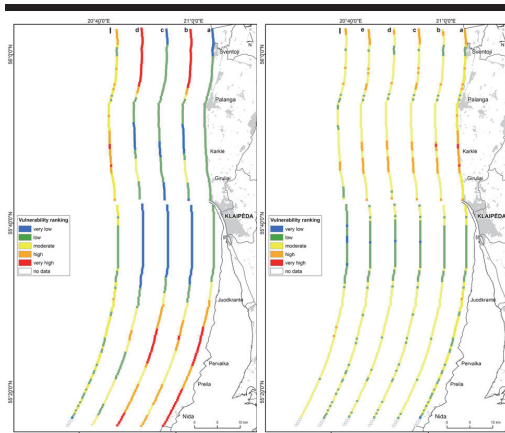

Figure 4. Left: Relative coastal vulnerability according to (a) minimum sea level with 10-yr return period, (b) maximum sea level with 10-yr return period, (c) minimum sea level with 50-yr return period, (d) maximum sea level with 50-yr return period based versus (I) the CVI values based on 7 criteria from Bagdanavičiūtė *et al*. (2019). Right: Relative coastal vulnerability (a) the CVI values based on 7 criteria from Bagdanavičiūtė *et al*. (2019), equal weights, equal intervals classification, (b) CVI with minimum sea level with 10-yr return period, (c) CVI with maximum sea level with 10-yr return period, (d) CVI with minimum sea level with 50-yr return period, (e) CVI with maximum sea level with 50-yr return period, (I) CVI index based on 11 criteria, equal weights.

All these parameters show agreement that the central part of the study area, about 15 km to the north and south of Klaipėda, has low vulnerability with respect to both high and low sea levels (Figure 4). They also agree that the southernmost part of the study area is more vulnerable to sea level variations than the central part. Intriguingly, the shore is less vulnerable with respect to sea level extremes that occur once in 50 yrs than with respect to those that occur once in 10 yrs. The four parameters reflecting sea level variations disagree with respect to vulnerability in the north of the study area. While this segment is characterized as very vulnerable with respect to sea level maxima, it has very low vulnerability with respect to sea level minima.

Table 1. *The range of CVI values in different CVI estimates in Figure 4.*

Index type	Number of variables	CVI index range	
		Min	Max
Reference CVI (RCVI)	7 (see above)	1.71	4.57
RCVI+10-yr minimum	8	1.88	4.25
RCVI+10-yr maximum	8	1.75	4.125
RCVI+50-yr minimum	8	1.75	4.125
RCVI+50-yr maximum	8	1.75	4.125
RCVI+all above	11	1.64	3.64

Integration of every single parameter as well as all the considered parameters into the CVI index using equal weights does not radically change the alongshore variation in the CVI index but still adds some nuance to its appearance (Figure 4). The length of segments with high and very high vulnerability decreases by 3–10% while the share of segments with moderate vulnerability increases by 9–21% (Table 2, Figure 5).

Table 2. *Distribution of CVI classes in coastal sections in Figure 3 and 4.*

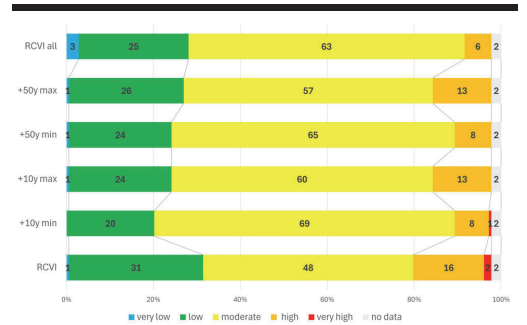| Vulnerability class	CVI range	%					
		RCVI	+10-yr min	+10-yr max	+50-yr min	+50-yr max	All
Very low	1.0–1.8	0.6	–	0.6	0.6	0.6	2.8
Low	1.8–2.6	30.9	20.2	23.6	23.6	26.4	25.3
Moderate	2.6–3.4	48.3	69.1	60.1	65.2	57.3	63.5
High	3.4–4.2	16.3	7.9	13.5	8.4	13,5	6.2
Very high	4.2–5	1.7	0.6	0.0	–	–	–
No data	–	2.2	2.2	2.2	2.2	2.2	2.2

Figure 5. Distribution of CVI classes in coastal sections in Figure 3 and 4.

DISCUSSION

We have made a first step towards systematic inclusion of water level variations into estimates of coastal vulnerability in microtidal water bodies in terms of modeled sea levels. The analysis first of all demonstrates that, not unexpectedly, water level variations serve as an important constituent of coastal vulnerability in such water bodies. Natural parameters characterizing these variations are the projections of extreme sea levels with various return periods. It is likely that these parameters are more stable than time series of modeled sea levels or observed water levels and provide important information that complements similar information provided by classic parameters that describe the geomorphology and history of the beaches.

Somewhat surprisingly, both sea level minima and maxima provide clearly independent information even though they agree in some parts of the study area. Also, projections of sea level extremes for different return periods seem to provide a certain amount of independent information. This feature signals that more elaborate parameters, such as the scale parameter or exponent of empirical probability distribution of sea levels (Soomere *et al*., 2015), or even the shape parameter of the generalized extreme value distribution, might carry even more

useful information even though their values are noisy and contain substantial uncertainties depending on the particular method of their evaluation (Soomere et al., 2018).

A general feature of the inclusion of one or more of the discussed parameters into the CVI is that the range of the resulting CVI values becomes smaller and in particular its highest values are reduced. This feature is not unexpected as different parameters intrinsically characterize vulnerability differently and the use of a larger selection of parameters tends to shrink the range of the resulting CVI values.

CONCLUSIONS

We have demonstrated that projected extremely high and low sea levels with 10-yr and 50-yr return periods provide certain independent information about coastal vulnerability even along fairly straight coastal segments of microtidal water bodies, such as the Baltic Sea. The use of a larger number of parameters naturally shrinks the range of the output values of the Coastal Vulnerability Index.

LITERATURE CITED

Bagdanavičiūtė, I.; Kelpšaitė, L., and Soomere, T., 2015. Multi-criteria evaluation approach to coastal vulnerability index development in micro-tidal low-lying areas, *Ocean & Coastal Management*, 104, 124–135. https://doi.org/10.1016/j.ocecoaman.2014.12.011

Bagdanavičiūtė, I.; Kelpšaitė, L.; Galinienė, J., and Soomere, T., 2019. Index based multi-criteria approach to coastal risk assessment. *Journal of Coastal Conservation*, 23, 785–800. https://doi.org/10.1007/s11852-018-0638-5

Barzehkar, M.; Parnell, K., and Soomere, T., 2024. Extending multi-criteria coastal vulnerability assessment to low-lying inland areas: examples from Estonia, eastern Baltic Sea. *Estuarine, Coastal and Shelf Science*.

Coles, S., 2004. *An Introduction to Statistical Modeling of Extreme Values.* 3rd printing. Springer, London.

Eelsalu, M.; Soomere, T.; Parnell, K., and Viška, M. 2024. Attribution of alterations in coastal processes in the southern and eastern Baltic Sea to climate change driven modifications of coastal drivers. *Oceanologia*, 66(3).

Gornitz, V., 1991. Global coastal hazards from future sea level rise. *Palaeogeography. Palaeoclimatology. Palaeoecology*, 89, 379–398. https://doi.org/10.1016/0031-0182(91)90173-O

Gornitz, V.M.; Daniels, R.C.; White, T.W., and Birdwell, K.R., 1994. The development of a coastal vulnerability assessment database, vulnerability to sea-level rise in the U.S. southeast. *Journal of Coastal Research*, Special Issue 12, 327–338.

Harff, J.; Deng, J.; Dudzińska-Nowak, J.; Fröhle, P.; Groh, A.; Hünicke, B.; Soomere, T., and Zhang, W., 2017. What determines the change of coastlines in the Baltic Sea? *In:*

Coastline changes of the Baltic Sea from South to East. Past and future projection. Harff, J.; Furmańczyk, F., and von Storch, H. (eds), Coastal Research Library, 19, Springer, Cham, Switzerland, 15–35, https://doi.org/10.1007/978-3-319-49894-2_2

Heinrich, P.; Hagemann, S.; Weisse, R., and Gaslikova, L., 2023. Changes in compound flood event frequency in northern and central Europe under climate change. *Frontiers in Climate*, 5, 1227613. https://doi.org/10.3389/fclim.2023.1227613

Hordoir, R.; An, B.W.; Haapala, J.; Dieterich, C.; Schimanke, S.; Höglund, A., and Meier, H.E.M., 2013. BaltiX: A 3D Ocean Modelling Configuration for Baltic & North Sea Exchange Analysis. SMHI-Report, Oceanography 48, 115 pp.

Kümmerer, V.; Ferreira, O.; Fanti, V., and Loureiro, C., 2024. Storm identification for high-energy wave climates as a tool to improve long-term analysis. *Climate Dynamics*, 62(3), 2207–2226, https://doi.org/10.1007/s00382-023-07017-w

Meier, H.E.M.; Döscher, R., and Faxén, T., 2003. A multiprocessor coupled ice–ocean model for the Baltic Sea: application to salt inflow. *Journal of Geophysical Research–Oceans*, 108(C8), 3273. https://doi.org/10.1029/2000JC000521

Parker, B.B. and Huff, L.C., 1998. Modern under-keel clearance management. *International Hydrographic Review*, 75(2), 143–165.

Soomere, T., 2024. Climate change and coastal processes in the Baltic Sea. *Oxford Encyclopedia of Climate Science.* https://doi.org/10.1093/acrefore/9780190228620.013.897

Soomere, T.; Eelsalu, M.; Kurkin, A., and Rybin, A., 2015. Separation of the Baltic Sea water level into daily and multi-weekly components. *Continental Shelf Research*, 103, 23–32. https://doi.org/10.1016/j.csr.2015.04.018

Soomere, T.; Eelsalu, M., and Pindsoo, K., 2018. Variations in parameters of extreme value distributions of water level along the eastern Baltic Sea coast. *Estuarine, Coastal and Shelf Science*, 215, 59–68. https://doi.org/10.1016/j.ecss.2018.10.010

Suursaar, Ü. and Sooäär, J., 2007. Decadal variations in mean and extreme sea level values along the Estonian coast of the Baltic Sea. *Tellus A*, 59(2), 249–260. https://doi.org/10.1111/j.1600-0870.2006.00220.x

Turner, B.L.; Kasperson, R.E.; Matson, P.A.; McCarthy, J.J.; Corell, R.W.; Christensen, L.; Eckley, N.; Kasperson, J.X.; Luers, A.; Martello, M.L.; Polsky, C.; Pulsipher, A., and Schiller, A., 2003. A framework for vulnerability analysis in sustainability science. *Proceedings of the National Academy of Sciences of the United States of America*, 100(14), 8074–8079. https://doi.org 10.1073/pnas.1231335100

Viigand, K.; Eelsalu, M.; Soomere, T., 2024. Quantifying exposedness of the eastern Baltic Sea shores with respect to extremely high and low water levels. *Coastal Engineering*.

Viška, M. and Soomere, T., 2013. Simulated and observed reversals of wave-driven alongshore sediment transport at the eastern Baltic Sea coast. *Baltica*, 26(2), 145–156, https://doi.org/10.5200/baltica.2013.26.15

VI

Publication VI

Barzehkar, M., Parnell, K.E., Dinan, N.M, Brodie, G. 2020. Decision support tools for wind and solar farm site selection in Isfahan Province, Iran. Clean Technologies and Environmental Policy, 23 (4), 1179–1195, doi: 10.1007/s10098-020-01978-w.

ORIGINAL PAPER

Decision support tools for wind and solar farm site selection in Isfahan Province, Iran

Mojtaba Barzehkar[1] · Kevin E. Parnell[1,2] · Naghmeh Mobarghaee Dinan[3] · Graham Brodie[4]

Abstract

Optimizing the location of wind and photovoltaic solar power plants is a significant environmental management problem. The effectiveness of the site selection process for renewable energy systems (RES) could be strengthened by flexible spatial and environmental planning strategies using decision support systems (DSS) to critically identify the most productive, environmentally friendly and acceptable sites for the production of sustainable and reliable wind and solar energy. This study discusses hybrid DSS, using multi-criteria evaluation based on the analytical hierarchy process (AHP), a geographical information system (GIS), fuzzy logic, and a weighted linear combination (WLC) approach to determine optimal locations for renewable energy generation infrastructure. In the first stage, the most decisive factors for evaluating the site suitability were identified, based on experts' opinions. Next, raster layers of ecological and socioeconomic sub-criteria were prepared GIS software. After incorporating the raster maps of each parameter, fuzzy membership functions were applied to normalize each raster layer between 0 and 1. The relative weights of different indicators were calculated using super decision software. Prioritizing vital elements were performed using AHP. In the final stage, the WLC approach was utilized to amalgamate layers in the GIS environment, which afforded the final site suitability maps. In Isfahan Province, Iran, 26% of the land area was found to be highly suitable for solar farms with 18% being highly suitable for wind farms. The results illustrate that using and comparing the results from combinations of computer-based DSS are more likely to result in better decisions than using individual DSS tools for the determination of the most suitable sites for RES location.

✉ Mojtaba Barzehkar
mojtaba.barzehkar@taltech.ee

1   Department of Cybernetics, School of Science, Tallinn
    University of Technology, Tallinn, Estonia

2   College of Science and Engineering, James Cook University,
    Townsville, Australia

3   Environmental Sciences Research Institute, Shahid Beheshti
    University, Tehran, Iran

4   Faculty of Agricultural Sciences, Melbourne University,
    Melbourne, Australia

Graphic abstract
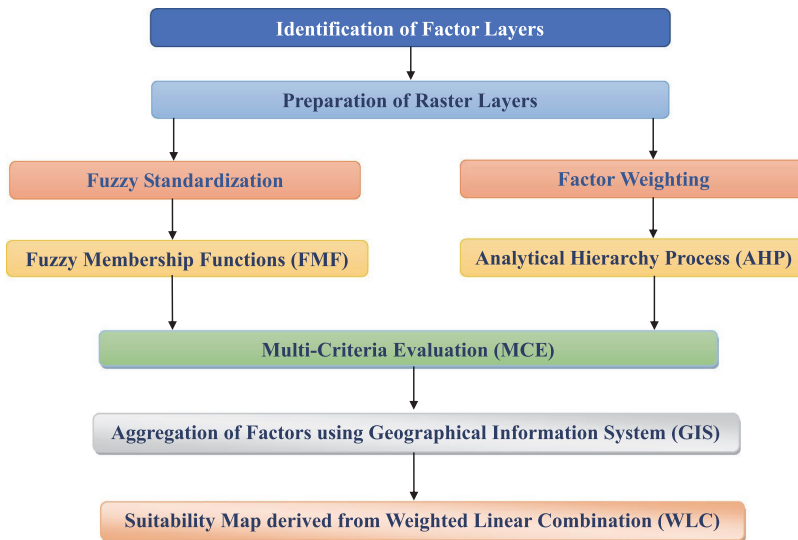
Introduction

Human communities have been subjected to global warming effects caused primarily by the increasing usage of fossil fuels (Amjad and Ali Shah 2020). Conventional energy resources such as coal, oil, and gas are becoming less attractive because they release substantial amounts of greenhouse gases, especially CO_2, into the atmosphere (Pambudi and Nananukul 2019). Furthermore, they have been considered as the major contributing factor in disturbing the ecological values of important natural ecosystems, particularly through air pollution or reducing the quality of ecosystem services (Giamalaki and Tsoutsos 2019).

Existing electric power plants have been recognized as drivers in damaging habitats and degrading the soil through their construction and maintenance phases (Suuronen et al. 2017). Many countries are now choosing sustainable sources of energy, which could contribute to environmental sustainability and provide alternatives to meet the energy demands of a community (Solangi et al. 2019). The majority of countries, particularly wealthy nations, have embraced renewable energy power plants, which are considered to be sustainable and environmentally friendly, and are often more affordable than using traditional energy resources (Konstantinos et al. 2019). Renewable energy sources, such as wind and solar farms, have paved the way toward innovative, affordable, long-term investments and created much more profitable and

economically viable solutions for the societies, as well as for the next generations, to satisfy energy needs and address climate change (Dhunny et al. 2019). In some instances, green jobs associated with renewable energy have been used to provide indigenous peoples with good employment opportunities and to tackle critical environmental challenges (Suuronen et al. 2017).

There has been a pressing obligation for environmental specialists and policy-makers to develop and apply new tools to help with these important energy priorities (Doorga et al. 2019), including developing strategies to find the most suitable locations for wind and solar energy infrastructure to both develop the energy potential and mitigate the consequences of climate change (Nait Mensour et al. 2019), in environmentally sustainable ways. A common and effective way to achieve these aims is to use decision support systems (DSS) to effectively and accurately identify the most suitable sites for the installation of wind and solar power plants, based on different indicator parameters (Villacreses et al. 2017).

Geographical information systems (GIS) have been commonly used as an efficient decision-support tool to store, analyze, and map the criteria regarding spatial planning for the renewable energy sector (Gasparovic and Gasparovic 2019). GIS is a tool that can help to minimize the time and cost of precise site planning while taking into consideration a database of information on the best possible sites. Another widely utilized method is multi-criteria decision-making

(MCDM), which is a powerful tool for specifying and prioritizing candidate locations in the site selection process for energy planning (Díaz-Cuevas 2018). The combination of GIS and MCDM provides a new possibility to devise an integrated approach to effectively investigate locations for the planning of wind and solar farms. This combined problem-solving model has high efficiency, flexibility, and inclusiveness in determining the environmental capacity of an area based on ecological, social, and economic factors to be applied to the site specifications (Baseer et al. 2017).

Since relying on only one kind of renewable energy cannot guarantee future generations' energy needs, it has become fundamentally important to consider both wind and solar farms to minimize intermittency problems. Based on the sustainable development goals for exploiting renewable energies, environmental sustainability and social welfare, indexes are incorporated into DSS for the identification of appropriate hybrid solar and wind generation sites (Aktas and Kabak 2019). It is feasible to develop both wind and solar farms at the same physical location (Ali et al. 2019).

There have been many studies regarding renewable energy plant site planning. Moradi et al. (2020) employed GIS and AHP as DSS for wind farm site selection in Alborz Province, Iran. Their research outcomes indicated that this method has high functionality to divide the spatial problem into smaller ones to achieve reliable results for site selection. Xu et al. (2020) undertook site selection for wind farms by considering stochastic VIKOR and interval analytical hierarchy processes (IAHP). They concluded that the integration of two methods could handle effectively the variability of weights given to the relative importance of parameters and the main calculations for selecting the candidate sites connected with diverse indicators. Koc et al. (2019) used GIS and AHP to identify desirable sites for solar and wind energy installations in Igdir Province, Turkey. They concluded that the best outcomes were obtained by comparing the results of the two methods. Dhunny et al. (2019) undertook wind and solar farm site selection by including fuzzy logic into the decision-making process. Their results showed that fuzzy logic assisted in the aggregation of qualitative and quantitative results for finding optimal locations.

Ali et al. (2019) applied GIS and MCDA, such as AHP, to determine areas that have the suitability for wind and solar installations in Thailand, advocating an integrated approach. Díaz-Cuevas et al. (2019) utilized an approach employing AHP and WLC in a GIS environment. They found this method useful for more sensibly prioritizing wind, solar, and biomass farm locations in Southern Spain. Uyan (2017) used GIS and AHP to optimize suitable locations for solar power plants in Karaman, Turkey. He found that the GIS-based MCE approach was a useful technique to determines feasible sites for solar farms from a range of alternatives.

Anwarzai and Nagasaka (2017) used MCDA and GIS to assess wind and solar energy farm locations in Afghanistan. They showed that the incorporation of MCDA applications in the ArcGIS environment could make a significant difference in determining better sites for energy development. Jahangiri et al. (2016) utilized Boolean logic to identify appropriate sites for the establishment of solar and wind power plants in the Middle-East. Their results indicated that this method was a more definitive approach to locate areas that have potential for energy exploitation. Watson and Hudson (2015) employed a GIS-based multi-criteria evaluation using Boolean logic and AHP to analyze the suitability of areas for large-scale wind and solar farm site assessments in England. They found that this method has the ability to make a significant contribution to the site selection process for renewable energy facilities in coastal regions. In a similar study, Janke (2010) used a GIS-based model using multi-criteria approaches to examine the potential areas for wind and solar farms in Colorado State, USA. The research results demonstrated that wind energy is more beneficial for large-scale farms, while solar power plants are more suited to small-scale farms.

As demonstrated above, the use of a decision support tool (or tools) to assist in site determination for renewable energy systems (RES) is now common. The main contribution and novelty of this study is the comparison and investigation of the diverse strategic, computer-based DSS available, and their use in combinations that can be implemented by experts and environmental authorities to help determine the best sites for RES location.

This research focuses on three objectives, and uses the case of Isfahan Province, Iran as a case study. Firstly, we identify areas that are environmentally preferred for the location of wind and solar farms. Secondly, we consider land use, where a balance between renewable energy expansion and environmental conservation must be considered and achieved, and where there must be a high-degree of community acceptance. Thirdly, we identify for the study area the optimal sites for wind and solar energy facility development. To achieve these goals, the most flexible and inclusive DSS for wind and solar power plant site selection are considered.

Site selection criteria

Site selection for wind and solar farms needs to incorporate a wide range of criteria to optimize electricity production and the protection of natural environments. As the goals of energy efficiency and environmental conservation are inextricably intertwined (Díaz-Cuevas et al. 2019), it is imperative to integrate both environmental and socioeconomic factors into decision-making to enable the generation of the required energy as well as respecting the natural ecosystems (Jahangiri et al. 2016).

Renewable energy farms should be at locations distant from protected areas. Areas which are prone to floods and soil erosion, and where there are steep slopes or nearby active faults should be excluded. Optimal sites should be in close proximity to power transmission lines and transport networks to avoid excess costs and maximize efficacy (Solangi et al. 2019). Obviously and most importantly, solar radiation and wind speed are key drivers for solar and wind renewable energy farm site selection. Potential sites for wind and solar energy farms are selected by considering several environmental specifications (Table 1) including wind speed, potential solar radiation, slope, probability of flooding, distance from faults, soil texture, geological formations, and distance from rivers. Protected areas, with high biodiversity values, are removed from consideration as possible sites. Socioeconomic factors (Table 1) such as distance from power transmission lines, distance from population centers, land use/cover, and distance from roads are incorporated in the analysis (Anwarzai and Nagasaka 2017). The importance of various parameters for site selection was determined through consultation with professional environmental and energy experts and scrutinizing reputable international publications on the identification of wind and solar farm sites. It has been universally recognized that the environmental and socioeconomic factors have different priorities (Dhunny et al. 2019) but with many commonalities, which may vary depending on local conditions. Data sources used for the parameters in this study are indicated: (1) Digital Elevation Model (DEM) derived from Isfahan Province Management and Planning Organization (2018); (2) Iran Energy Efficiency Organization (2018); (3) The World Bank (2017); (4) (5) (6) (7) (8) (9) (10) (11) (12) (13) Isfahan Province Management and Planning Organization (2018).

Materials and methods

The study area

The study area, Isfahan Province, is in the center of Iran. It covers an area of 107,017 square kilometers. The climate is generally described as arid and semi-arid, although there are a variety of physiographic regions. Due to densely populated cities and many industrial centers, satisfying the energy demands of the inhabitants of Isfahan is important (Zoghi et al. 2017). There are valuable wetlands and protected areas with high ecological values, in particular Ghomishloo National Park, Gavkhouni Wetland, Mouteh Wildlife Refuge, and Kolah Ghazi National Park, which must

be considered and protected when renewable energy power plant site selection is undertaken. It is generally believed that solar radiation and wind speed are sufficiently high for renewable energy to provide for the sustainable development goals of the province (Noorollahi et al. 2016). Figure 1 shows the location of Isfahan Province in Iran, and Fig. 2 is a land-use map of the study area.

Methodology

Fuzzy logic

The first stage of the research was to identify the most effective criteria and sub-criteria concerning wind and solar farms site evaluation through a comprehensive literature review. This was supplemented using the international standards and regulations required for renewable energy spatial planning (Yushchenko et al. 2018). After identifying the ecological and socioeconomic parameters for renewable energy site evaluation, each sub-criteria or spatial factor was quantified into obtain raster layers. This was implemented with the pixel size of 10×10 m using the raster analysis operator of ArcGIS 10.7 software (Asakereh et al. 2017) in the coordinate system WGS 1984/UTM Zone 39.

For solar energy, the long-term yearly average of diffuse horizontal irradiance (DHI) based on kilowatt-hours per square meter (KWh/m^2), covering the period of 1999–2015 was sourced from The World Bank (2017), who used satellite digital images and atmospheric datasets. Solar energy of at least 1500 $kWh/m^2/year$ is suitable. Wind energy was monitored by field measurements at large-scale (country level). Wind data were collected at 161 locations over the entire country (Iran) including 10 locations in Isfahan Province, and normalized to average annual wind speed 80 m above the ground (hub height). An inverse distance weighting (IDW) method was used to generate a wind raster map (Iran Energy Efficiency Organization 2018). Data for other parameters were obtained from Isfahan Province Management and Planning Organization (2018). Then, the raster layers of each parameter were standardized by applying a fuzzy membership function normalizing raster factors between the scales of 0 and 1, which relies heavily on fuzzy function types, whether it is increasing or decreasing (see below), for site suitability preferences (Wu et al. 2018). Table 2 shows the indicator parameters for wind and solar energy power plant site selection that were used.

In the fuzzy standardization method, the "membership" of a pixel in the raster map is evaluated from zero (lack of full membership) to one, (full membership). On

Table 1 The environmental, social, and economic criteria and sub-criteria for wind and solar farm site selection (Ali et al. 2019; Dhunny et al. 2019; Díaz-Cuevas et al. 2019; Naït Mensour et al. 2019; Solangi et al. 2019; Zoghi et al. 2017)

Criterion	Sub-criteria	Description	Data source
Environmental	Slope[1]	One of the natural factors with a significant impact on the selection of the optimum location of wind and solar power plants is the land slope. This is because the land potential for wind and solar energy usage, as well as wind and solar energy input, changes depending on the slope. Areas with slopes of 3–5% are the most appropriate sites for wind and solar power plants (Ali et al. 2019; Zoghi et al. 2017)	Digital elevation model (DEM) derived from Isfahan Province Management and Planning Organization (2018)
	Wind speed[2]	Wind speed is the first and the most fundamental variable with respect to wind energy potential and its assessment. Annual wind speed average, wind power density, and percentage of windy days are very important features for choosing a site for wind power plants. A wind speed map plays an important role in the selection of the optimal sites for the wind farms and this is the most influential factor supporting the financial evaluations of the installations. The range of 6–> 7 m/s for wind energy is suitable for site selection because it has been identified as achieving the best performance for wind turbines. This means that a minimum threshold of 6 m/s for wind energy measured 80 m above the land surface is required, with speeds at or above 7 m/s being optimal (Ali et al. 2019)	Iran Energy Efficiency Organization (2018)
	Solar radiation[3]	Solar radiation is measured as the yearly amount of solar energy intake at one point on the earth's surface which depends on various factors including latitude, longitude, sunshine hours, humidity, evaporation, air temperature, angle of the sun, and other factors. The minimum required diffuse horizontal irradiance (DHI) is 1500 kWh/m^2/year, with DHI at or above 1500 kWh/m^2/year desirable to optimize power generation (Solangi et al. 2019)	The World Bank (2017)
	Distance from rivers[4]	Since land near rivers may be subject to the risk of flooding, remoteness from the river will increase the safety of the construction project. A minimum distance of 500 m from rivers is considered appropriate (Naït Mensour et al. 2019)	Isfahan Province Management and Planning Organization (2018)
	Flooding[5]	Floods are among the most frequent natural phenomena that can jeopardize the safety of construction projects in riverine locations. To identify the flooding potential for the site, it is vital to know the topographic features of the region. In selecting sites, areas located on flood plains are generally unsuitable (Díaz-Cuevas et al. 2019)	Isfahan Province Management and Planning Organization (2018)
	Distance from fault lines[6]	Wind and solar power plants like other construction projects should be remote from fault lines. Faults that may be active must be at least 500 m from a site for both wind or solar energy systems (Zoghi et al. 2017; Noorollahi et al. 2016)	Isfahan Province Management and Planning Organization (2018)

Table 1 (continued)

Criterion	Sub-criteria	Description	Data source
	Soil texture[7]	The selection of suitable sites with the best soil texture is an important engineering decision in construction projects. Clayey textures, for example, are often more stable than sandy textures because they have a more suitable structure. Soil maps are a useful tool for helping decision-makers to determine the best location for renewable energies projects (Dhunny et al. 2019)	Isfahan Province Management and Planning Organization (2018)
	Geological formations[8]	Local geology must be considered with respect to providing the best foundations for the building of wind and solar energy farms (Dhunny et al. 2019)	Isfahan Province Management and Planning Organization (2018)
	Distance from wetland and protected areas[9]	Wetlands and protected areas, including protective buffers, are entirely unsuitable for the construction of wind and solar power plants. Sites at least 500 m distant may be considered in the analysis (Nait Mensour et al. 2019)	Isfahan Province Management and Planning Organization (2018)
Social	Distance from population centers[10]	Since cities are one of the main consumers of power, proximity to residential areas is an important factor in selecting the optimum locations of solar power plants. Electric power distribution costs and energy dissipation can be reduced by proximity to cities. Locating renewable energy facilities near residential areas can, however, cause adverse environmental impacts on the human communities. For this reason, areas at the distance of at least 500 m from residential areas are considered suitable (Díaz-Cuevas et al. 2019; Zoghi et al. 2017; Uyan 2017)	Isfahan Province Management and Planning Organization (2018)
Economic	Distance from roads[11]	Transport is one of the most important criteria for locating industries. The proximity to roads will reduce transportation costs of power plant equipment, personnel transport, and plant support. A distance of less than 500 m from roads is regarded as appropriate for wind and solar energy installations (Nait Mensour et al. 2019)	Isfahan Province Management and Planning Organization (2018)
	Distance from power transmission lines[12]	Solar and wind power plants require access to the transmission grid, and the grid connection is typically at high voltage. The high cost associated with constructing power transmission lines means that proximity to existing transmission lines avoids additional capital cost and power losses. However, due to environmental and efficiency considerations, wind or solar farms should be located at a minimum distance of 500 m from power transmission lines so that an efficient function affecting transmission lines will increase the safety of the energy facilities or protect the environment. A minimum threshold of 500 m would be required to avoid energy loss and to increase the productivity of power generation (Zoghi et al. 2017; Noorollahi et al. 2016)	Isfahan Province Management and Planning Organization (2018)

Table 1 (continued)

Criterion	Sub-criteria	Description	Data source
	Land use/cover[13]	In terms of ecological value and potential, as well as their role in environmental quality and agricultural/industrial production, the land use of regions is considered (Díaz-Cuevas et al. 2019)	Isfahan Province Management and Planning Organization (2018)

this scale, larger numbers are more desirable. There are diverse approaches for fuzzy standardization of data layers using minimum and maximum values. The logical way is using a linear scale, which has been applied to this study. The fuzzy membership approach using this method functions differently for any particular variable based on decreasing or increasing functions (Barzehkar et al. 2016). Some parameters such as slope, and distance from population centers, power transmission lines and roads, are of a decreasing type. This means that between a minimum threshold (*a*) and a maximum threshold (*b*) which is acceptable, the number assigned decreases. An increasing type is the opposite. Distance from rivers, fault lines and protected areas are of increasing type, which indicates that the anything above the maximum threshold is also suitable. Formulas (1) and (2) show how to calculate the fuzzy standardized degree. For example, for distance from fault lines, "*a*" is 500 m, which means less than 500 m from the fault lines is not acceptable and gives zero number. The number "*b*" is 1000 m and is assigned the value 1, and distances greater than 1000 m are also suitable and assigned the value 1. The fuzzy standardization of other parameters based on Table 2 was also calculated using Eqs. (1) and (2), where X_i is the value assigned to the fuzzy standardized layer, R_i is raw score of each pixel of the map, R_{min} is the minimum threshold and R_{max} is the maximum threshold, and whether the parameter is of increasing or decreasing type is shown in Table 2.

$$X_i = \frac{R_i - R_{min}}{R_{max} - R_{min}} \tag{1}$$

$$X_i = \frac{R_{max} - R_i}{R_{max} - R_{min}} \tag{2}$$

AHP approach

Because the significance of different factors varies based on experts' knowledge, it was crucially important to assign weights to each sub-criterion using the AHP before employing the WLC method. One of the most popular decision-making tools, an analytical tool based on super decision software (SDS) for prioritizing and weighting various factors, was used (Uyan 2017). The SDS was utilized to obtain the final weights of each parameter by applying a pairwise comparison matrix of distinct elements. Before implementing this vital step, the comments of highly qualified environmental and energy experts were sought using questionnaires regarding the relative importance of different parameters (values from 1 to 9). As can be seen from Table 3, twenty experts from the Iran Energy Efficiency Organization and
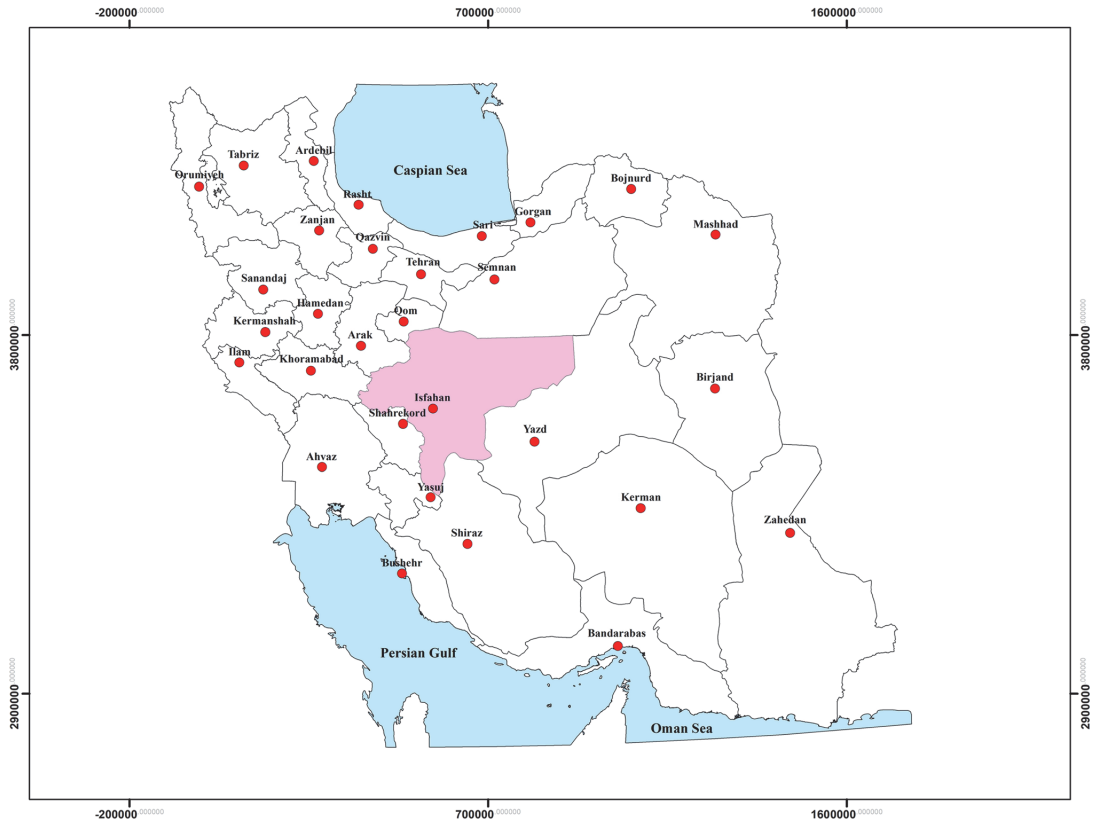
Fig. 1 Location of Isfahan Province (in pink), Iran (Isfahan Province Management and Planning Organization (2018))

Iran's Department of Environment, plus five others from academic institutions chosen based on their expertise were asked to prioritize factors. A matrix was developed based on the geometric mean values of the expert opinions, which reflects the importance of each factor compared to other factors. As shown in Table 4, for example, the distance from a protected area is 2 times more important than land use when assessing the sites of wind farms. The geometric mean of the responses to the questionnaires was utilized as an input to the super decisions software to attain the final weights of ecological and socioeconomic sub-criteria (Davtalab and Alesheikh 2018). Inconsistency between expert judgments was determined by obtaining an inconsistency ratio (IR) among a variety of factors. IR is determined by energy experts and environmental specialists using a prioritization process of parameters in SDS (Aydin et al. 2013). An IR > 0.1 represents a low evaluation of the criteria and the outcomes should not be accepted, while IR ≤ 0.1 indicates a consistency between specialists' judgments and the results are acceptable.

Table 5 represents the priorities of decision-makers for ranking of site selection factors concerning the importance of each parameter to others based on the scale 1–9.

WLC approach

One of the most widely used methods for the combination of different raster layers in ArcGIS is to employ the WLC approach (Barzehkar et al. 2016). In the following stage, the determination of the final site suitability map for either wind or solar farms was carried out by multiplying each fuzzy standardized factor and its weight, and aggregation of all factors using the raster analysis function based on WLC method in ArcGIS (Tavana et al. 2017). The multi-criteria evaluation (MCE), which was used in this research, used Eq. (3) (Ali et al. 2019) below, where S is the site suitability of the region, W_i is the relative weight of the sub-criteria, X_i is the fuzzy standardized layer, and n is the number of sub-criteria (Ali et al. 2019). Figure 3 shows the steps for wind and solar farms
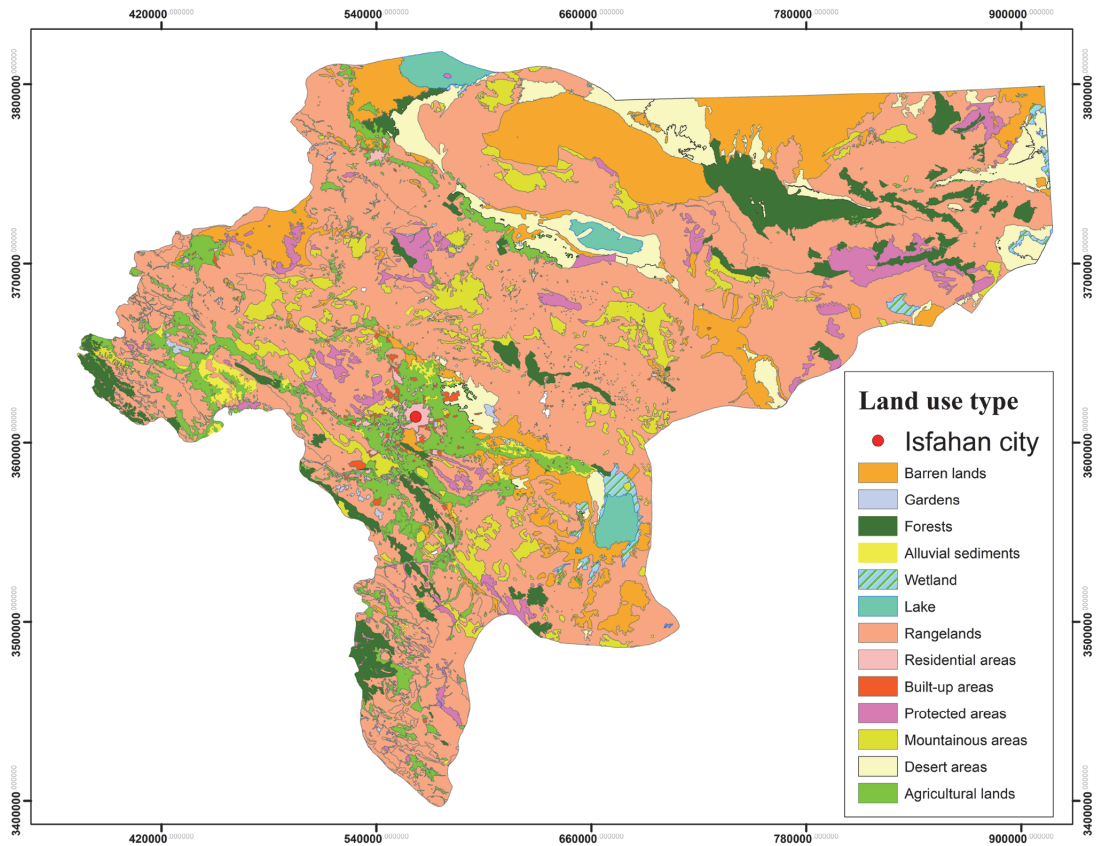
Fig. 2 Land-use map of Isfahan Province, Iran (Isfahan Province Management and Planning Organization (2018))

site selection using the fuzzy logic and WLC method in Isfahan Province.

$$S = \sum_{i=1}^{n} X_i W_i \tag{3}$$

Results and discussion

In this study, integration of GIS, multi-criteria evaluation based on AHP, fuzzy membership functions and the WLC approach has been employed to investigate and identify which sites have the feasibility to become wind and solar power plant locations. Since either wind or solar energy alone might not be able to address the energy shortages in a society and owing to the unpredictability of climate conditions in each region of Isfahan, both are considered.

An integrated site selection process is the best strategic decision-making system to equally prioritize both environmental protection goals and demands for socioeconomic development. An efficient site selection strategy could strengthen coordination in environmental conservation measures especially among energy efficiency organizations and other governmental corporations. Consequently, the land-use conflicts between renewable energy development

Table 2 Threshold values and fuzzy membership function to standardize different layers in fuzzy logic for (a) solar farm (Nait Mensour et al. 2019; Doorga et al. 2019; Solangi et al. 2019; Ali et al. 2019; Tavana et al. 2017) and (b) wind farm (Konstantinos et al. 2019; Díaz-Cuevas et al. 2019; Ali et al. 2019; Rezaian and Jozi 2016; Azizi et al. 2014), site selection

Row	Environmental and socioeconomic layers	Suitability	Threshold value		Type of the fuzzy membership function
			Minimum threshold a	Maximum threshold b	
1	Slope	3–5%	3%	5%	Decreasing
2a	Solar radiation	1500–2000 kWh/m^2/year	1500 kWh/m^2/year	2000 kWh/m^2/year	Increasing
2b	Wind speed	6–7 m/s	6 m/s	7 m/s	Increasing
3	Distance from rivers	500–1000 m	500 m	1000 m	Increasing
4	Flooding	Areas outside the flood plain	–	–	User-defined
5	Distance from fault lines	500–1000 m	500 m	1000 m	Increasing
6	Soil texture	Clay and silt clay textures	–	–	User-defined
7	Geological formations	Igneous, metamorphic, and sedimentary rocks	–	–	User-defined
8	Distance from wetland and protected areas	500–1000 m	500 m	1000 m	Increasing
9	Distance from population centers	500–2000 m	500 m	2000 m	Increasing
10	Distance from roads	500–2000 m	500 m	2000 m	Decreasing
11	Distance from transmission lines	500–1000 m	500 m	1000 m	Decreasing
12	Land use	Barren lands and areas with very low plant density	–	–	User-defined

Table 3 Demographics of the experts used for prioritizing the relative importance of parameters

	Governmental departments	University
Male/female (number)	13/7	3/2
Age range (years)	30–57	38–60
Education (degree)	Bachelors, Masters, PhD	PhD
Field of expertise	Energy management Energy engineering Environmental planning and management Environmental protection and education Environmental impact assessment	Land-use planning Environmental impact assessment

and environmental preservation would be substantially reduced.

Experts' perspectives, together with international regulations, were used for determining the parameters for wind and solar energy power plant site selection. Not surprisingly, experts and decision-makers assigned the highest weights to wind speed and solar radiation. Distance from power transmission lines and distance from population centers were

of secondary importance. Soil texture and geological formations had the lowest priorities, based on the specialists' perceptions.

Figure 4 shows the final weights and priorities assigned to the environmental and socioeconomic factors for wind farm site selection, and Fig. 5 presents the final weights and priorities assigned to the environmental and socioeconomic factors for solar farm site selection.

Figure 6 shows results from the fuzzy logic and WLC approach for wind farm site selection (range 0.015–0.9), and Fig. 7 shows the results for solar farm site selection (range 0.068–0.88). In this research, the IR was calculated to be 0.09 in the super decision software environment for the ecological and socioeconomic parameters of wind and solar power plants site evaluation. The consistency between experts' perspectives is acceptable. The final suitability map for either wind or solar farms was classified into five categories shown in Tables 6 and 7. For wind energy, 18% of the province has high suitability, and for solar energy 26% has high suitability.

In this research, fuzzy logic and WLC approach are employed to standardize the environmental and socioeconomic raster layers and the aggregation of them,

Table 4 Pairwise comparison matrix of parameters for wind and solar farm site selection

Parameters for wind and solar farm site selection	Pairwise comparison matrix												
	Slope	Wind speed	Solar radiation	Distance from river	Flooding	Distance from fault lines	Soil texture	Geological formations	Distance from wetland and protected areas	Distance from population centers	Land use	Distance from transmission lines	Distance from roads
Slope	1	1/6	1/8	1	1/3	2	3	3	1/6	1/6	1/5	1/6	1/5
Wind speed	6	1	1	6	4	7	8	8	4	4	5	4	5
Solar radiation	8	1	1	7	5	7	9	9	5	5	6	5	6
Distance from river	1	1/6	1/7	1	1/4	4	6	6	1/6	1/6	1/5	1/6	1/5
Flooding	3	1/4	1/5	4	1	5	7	7	1/5	1/5	1/4	1/6	1/3
Distance from fault lines	1/2	1/7	1/7	1/4	1/5	1	3	3	1/7	1/7	1/5	1/7	1/5
Soil texture	1/3	1/8	1/9	1/6	1/7	1/3	1	1	1/8	1/8	1/7	1/8	1/7
Geological formations	1/3	1/8	1/9	1/6	1/7	1/3	1	1	1/8	1/8	1/7	1/8	1/7
Distance from wetland and protected areas	6	1/4	1/5	6	5	7	8	8	1	1	2	1	2
Distance from population centers	6	1/4	1/5	6	5	7	8	8	1	1	3	1	2
Land use	5	1/5	1/6	5	4	5	7	7	1/2	1/3	1	1/3	1
Distance from transmission lines	6	1/4	1/5	6	6	7	8	8	1	1	3	1	3
Distance from roads	5	1/5	1/6	5	3	5	7	7	1/2	1/2	1	1/3	1

Table 5 The priorities of decision-makers for pairwise comparison of parameters (Saaty 1980)

Priorities of decision-makers	Numerical value
Extremely prioritized	9
Less important than the above priority	8
Very strongly prioritized	7
Less important than the above priority	6
Strongly prioritized	5
Less important than the above priority	4
Moderately prioritized	3
Less important than the above priority	2
Equally prioritized	1
Less important than the above priority	1/2
Moderately unprioritized	1/3
Less important than the above priority	1/4
Strongly unprioritized	1/5
Less important than the above priority	1/6
Very Strongly unprioritized	1/7
Less important between the above priority	1/8
Extremely unprioritized	1/9
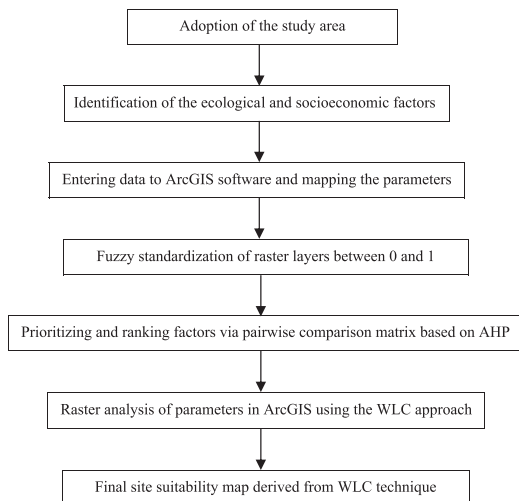
Fig. 3 Steps for wind and solar farms site selection using fuzzy logic and WLC method

respectively, leading to an estimate of the degree of site suitability on a continuous scale. The high class of land suitability is located in the areas where the probability of flooding is low, with low permeable soils such as clay, and which are far from the wetland and protected areas, fault lines and rivers. The potential locations are also located in the areas with proximity to cities, roads, and transmission lines, which is logical to guarantee the socioeconomic benefits of energy generation for the community. The suitable sites for wind farms are influenced by the wind speed of 6–7 m/s, and the appropriate sites for solar farm are influenced by a DHI of 1500–2000 kWh/m^2/year.

The previous studies implemented by Díaz-Cuevas et al. (2019) and Anwarzai and Nagasaka (2017) suggested that the combination of WLC, AHP, and GIS would be useful for ranking the potential sites of wind and solar farm. In this research, the application of fuzzy logic is also used to standardize the raster maps on a wider scale (from 0 to 1). This gives the decision-makers more choice with better information when considering wind and solar farm site selection. The fuzzy membership functions are also effective in reducing the uncertainty of site selection, by standardization of pixels in each raster layer. Therefore, the integration of fuzzy logic with AHP, WLC, and GIS is a flexible approach to the analysis of land suitability for either wind or solar energy.

As seen in Fig. 6, areas in the north and east of the province have generally higher suitability for wind farms than the areas located in south and west. The most suitable locations are generally areas that are sparsely populated with little vegetation, are distant from protected areas, and have generally higher wind speeds and a higher number of windy days. With respect to solar wind farm location, Fig. 7 shows that the north and east are even more favored than the south and west, with solar energy levels being higher than in other regions due to fewer cloudy and rainy days. For both wind and solar farm location, the north and east were also more favored by decision-makers than the south and west.

Using these methods, environmental authorities and planners have better tools to understand the energy generation capability of this diverse province, and increased ability to incorporate both environmental and socioeconomic capacity for renewable energy utilization into planning frameworks. Fuzzy logic, which has been utilized

Fig. 4 Final weights and priorities assigned to the environmental and socioeconomic factors for wind farm site selection
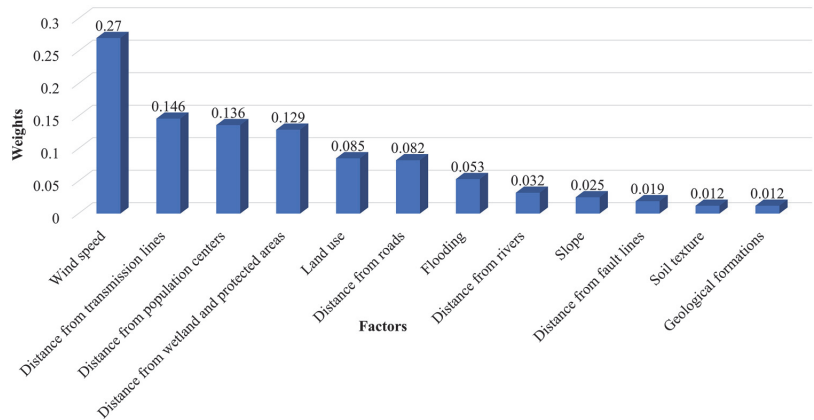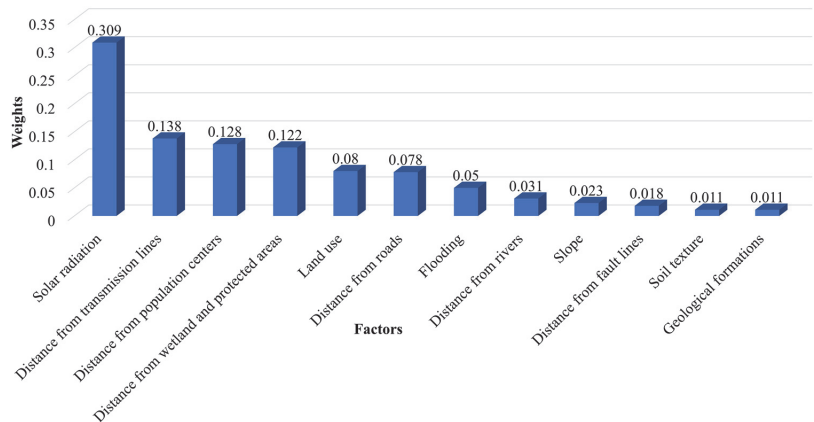

Fig. 5 Final weights and priorities assigned to the environmental and socioeconomic factors for solar farm site selection

in this study, is highly effective as a logical research framework for comparative assessment of possible sites of wind and solar power projects with great ability to handle the uncertainty of large-scale suitability analysis through the normalization of relevant factors. The appropriate prioritization of wind and solar farm sites is of importance with respect to land use for environmental protection and energy development. The proposed fuzzy approach, coupled with AHP, WLC, and GIS, is useful in ranking the suitability of different candidate sites. It has also been determined that the outcomes of an integrated approach, through the combination of diverse decision-making tools, may provide better information than using single tools.

Conclusions

This study highlights a combination of desirable decision support tools that encompass MCE based on AHP, fuzzy logic, the WLC method, and GIS models to formulate a meaningful research framework that incorporates environmental and socioeconomic data associated with site selection for wind and solar farm installations. The application of MCE enabled us to define a set of important parameters, which represent the site suitability for renewable energy power plants in the Isfahan Province, Iran. It may be possible to incorporate a wider variety of parameters including further ecological, social, and economic indicators to improve site selection even further.
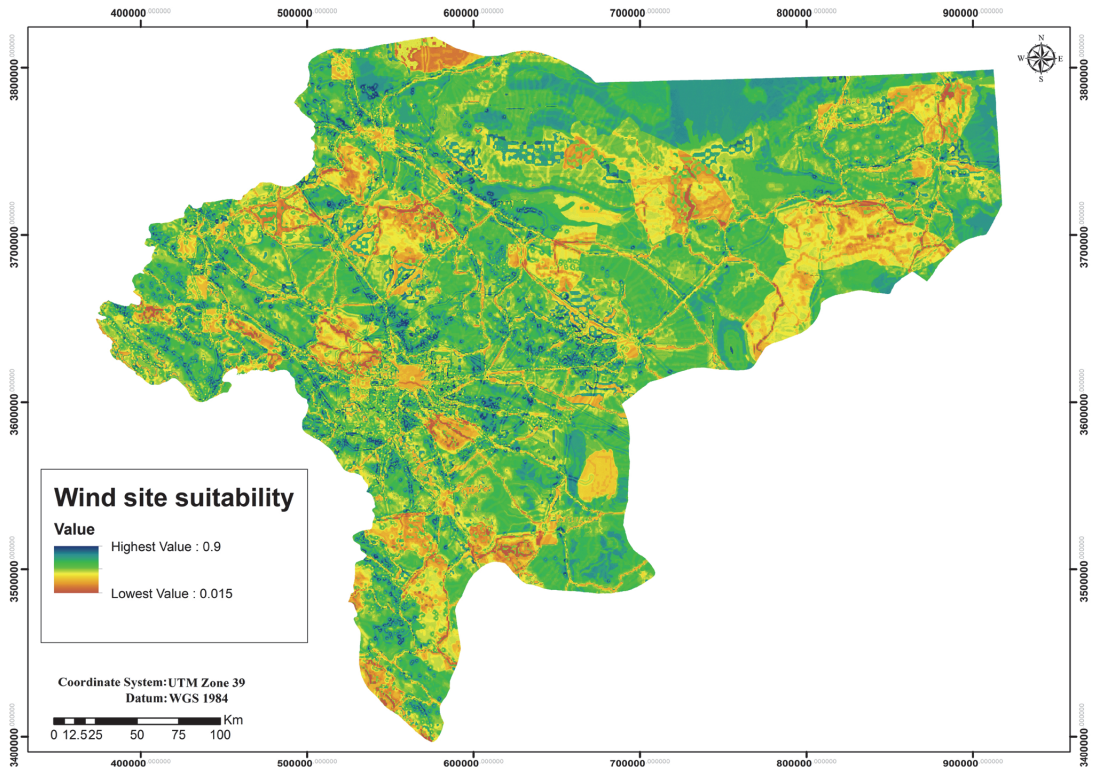
Fig. 6 Wind farm site suitability

The use of the high suitability sites selected may help rationalize the provision of energy to people in the community with protection of the environment for the next generations. Not only is this an intelligent problem-solving approach for decision-makers to tackle environmental issues of renewable energy system site selection, but it could also provide impetus for further development of wind and solar energy in a region.

It is concluded that the optimal energy systems are likely to be achieved by a mix of two or more renewable energy technologies to provide sustainable electricity in terms of satisfying the energy demands of people in the society and overcoming intermittency of supply, as well as providing a cost-effective way for energy expansion.

Blended decision support tools lead to more satisfactory and flexible environmental planning decisions. In this study, three main criteria and 12 sub-criteria for wind or solar farms were applied to the decision-making process, with the north and east of the province being found to be generally more suitable for both solar and wind farm location than the south and west, but with considerable local variability within the regions. The number of parameters considered can be increased in future research to enhance the performance of the site evaluations.
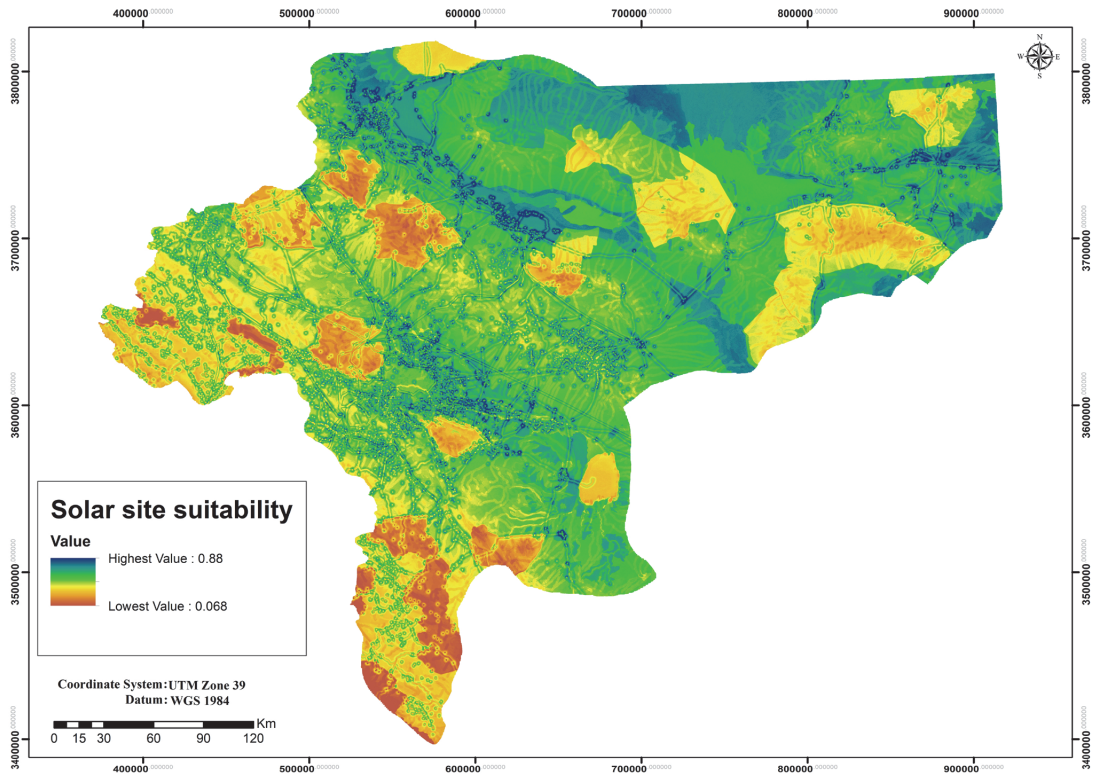
Fig. 7 Solar farm site suitability

Table 6 Land suitability as a percentage of the area of Isfahan Province for wind farm site selection using the fuzzy logic and WLC approach

Class of suitability	Area (km^2)	Percentage of area (%)
Very Low	15,771	15
Low	31,494	29
Moderate	40,959	38
High	18,793	18
Sum of Suitability	107,017	100

Table 7 Land suitability as a percentage of the area of Isfahan Province for solar farm site selection using the fuzzy logic and WLC approach

Class of suitability	Area (km^2)	Percentage of area (%)
Very low	7656	7
Low	26,813	25
Moderate	44,929	42
High	27,619	26
Sum of suitability	107,017	100

Compliance with ethical standards

Conflict of interest On behalf of all authors, the corresponding author states that there are no conflicts of interest for this project.

Ethical approval All those that answered the questionnaire were acting in their professional capacity and agreed to participate. Data gathered were anonymized, and no participants can be individually recognized.

References

Aktas A, Kabak M (2019) A goal programming model for grid-connected hybrid energy system operations. SN Appl Sci 2:71. https://doi.org/10.1007/s42452-019-1878-1

Ali S, Taweekun J, Techato K, Waewsak J, Gyawali S (2019) GIS based site suitability assessment for wind and solar farms in Songkhla, Thailand. Renew Energy 132:1360–1372. https://doi.org/10.1016/j.renene.2018.09.035

Amjad F, Ali Shah L (2020) Identification and assessment of sites for solar farms development using GIS and density based clustering technique—a case of Pakistan. Renew Energy 20:304. https://doi.org/10.1016/j.renene.2020.03.083

Anwarzai MA, Nagasaka K (2017) Utility-scale implementable potential of wind and solar energies for Afghanistan using GIS multi-criteria decision analysis. Renew Sustain Energy Rev 71:150–160. https://doi.org/10.1016/j.rser.2016.12.048

Asakereh A, Soleymani M, Sheikhdavoodi MJ (2017) A GIS-based Fuzzy-AHP method for the evaluation of solar farms locations: case study in Khuzestan province, Iran. J Sol Energ 155:342–353. https://doi.org/10.1016/j.solener.2017.05.075

Aydin NY, Kentel E, Sebnem Duzgun H (2013) GIS-based site selection methodology for hybrid renewable energy systems: a case study from western Turkey. Energy Convers Manag 70:90–106. https://doi.org/10.1016/j.enconman.2013.02.004

Azizi A, Malekmohammadi B, Jafari HR, Nasiri H, Amini-Parsa V (2014) Land suitability assessment for wind power plant site selection using ANP-DEMATEL in a GIS environment: case study of Ardabil province, Iran. Environ Monit Assess 186:6695–6709. https://doi.org/10.1007/s10661-014-3883-6

Barzehkar M, Mobarghaee Dinan N, Salemi A (2016) Environmental capability evaluation for nuclear power plant site selection: a case study of Sahar Khiz Region in Gilan Province, Iran. J Environ Earth Sci 75:1016. https://doi.org/10.1007/s12665-016-5825-9

Baseer MA, Rehman S, Meyer JP, Mahbub Alam M (2017) GIS-based site suitability analysis for wind farm development in Saudi Arabia. J Energy 141:1166–1176. https://doi.org/10.1016/j.energy.2017.10.016

Davtalab M, Alesheikh AA (2018) Spatial optimization of biomass power plant site using fuzzy analytic network process. Clean Technol Environ Policy 20:1033–1046. https://doi.org/10.1007/s10098-018-1531-5

Dhunny AZ, Doorga JRS, Allam Z, Lollchund MR, Boojhawon R (2019) Identification of optimal wind, solar and hybrid wind-solar farming sites using fuzzy logic modelling. J Energy 188:116056. https://doi.org/10.1016/j.energy.2019.116056

Díaz-Cuevas P (2018) GIS-based methodology for evaluating the wind-energy potential of territories: a case study from Andalusia (Spain). Energies 11(10):2789. https://doi.org/10.3390/en11102789

Díaz-Cuevas P, Domínguez-Bravo J, Prieto-Campos A (2019) Integrating MCDM and GIS for renewable energy spatial models: assessing the individual and combined potential for wind, solar and biomass energy in Southern Spain. Clean Technol Environ Policy 21:1855–1869. https://doi.org/10.1007/s10098-019-01754-5

Doorga JRS, Rughooputh SDDV, Boojhawon R (2019) Multi-criteria GIS-based modelling technique for identifying potential solar

farm sites: a case study in Mauritius. Renew Energy 133:1201–1219. https://doi.org/10.1016/j.renene.2018.08.105

Gasparovic I, Gasparovic M (2019) Determining optimal solar power plant locations based on remote sensing and GIS methods: a case study from Croatia. Remote Sens 11(12):1481. https://doi.org/10.3390/rs11121481

Giamalaki M, Tsoutsos T (2019) Sustainable siting of solar power installations in Mediterranean using a GIS/AHP approach. Renew Energy 141:64–75. https://doi.org/10.1016/j.renene.2019.03.100

Iran Energy Efficiency Organization (2018) Average annual wind energy speed at a height of 100 meters. In: Atlas of the country's renewable and clean energy sources, 1st edn. Tehran, pp 80–85

Isfahan Province Management and Planning Organization (2018). Land use planning. http://www.mpo-es.ir/index.aspx?sub=11

Jahangiri M, Ghaderi R, Haghani A, Nematollahi O (2016) Finding the best locations for establishment of solar-wind power stations in Middle-East using GIS: a review. Renew Sustain Energy Rev 66:38–52. https://doi.org/10.1016/j.rser.2016.07.069

Janke JR (2010) Multicriteria GIS modeling of wind and solar farms in Colorado. Renew Energy 35:2228–2234. https://doi.org/10.1016/j.renene.2010.03.014

Koc A, Turk S, Sahin G (2019) Multi-criteria of wind-solar site selection problem using a GIS-AHP-based approach with an application in Igdir Province/Turkey. Environ Sci Pollut Res 26:32298–32310. https://doi.org/10.1007/s11356-019-06260-1

Konstantinos I, Georgios T, Garyfalos A (2019) A decision support system methodology for selecting wind farm installation locations using AHP and TOPSIS: case study in Eastern Macedonia and Thrace region, Greece. Energy Policy 132:232–246. https://doi.org/10.1016/j.enpol.2019.05.020

Moradi S, Yousefi H, Noorollahi Y, Rosso D (2020) Multi-criteria decision support system for wind farm site selection and sensitivity analysis: case study of Alborz Province, Iran. Energy Strateg Rev 29:100478. https://doi.org/10.1016/j.esr.2020.100478

Nait Mensour O, El Ghazzani B, Hlimi B, Ihlal A (2019) A geographical information system-based multi-criteria method for the evaluation of solar farms locations: a case study in Souss-Massa area, southern Morocco. Energy 182:900–919. https://doi.org/10.1016/j.energy.2019.06.063

Noorollahi E, Fadai D, Akbarpour Shirazi M, Ghodsipour SH (2016) Land suitability analysis for solar farms exploitation using GIS and fuzzy analytic hierarchy process (FAHP)—a case study of Iran. Energies 9:643. https://doi.org/10.3390/en9080643

Pambudi G, Nananukul N (2019) A hierarchical fuzzy data envelopment analysis for wind turbine site selection in Indonesia. Energy Rep 5:1041–1047. https://doi.org/10.1016/j.egyr.2019.08.002

Rezaian S, Jozi SA (2016) Application of multi criteria decision-making technique in site selection of wind farm—a case study of Northwestern Iran. J Indian Soc Remote 44(5):803–809. https://doi.org/10.1007/s12524-015-0517-6

Saaty TL (1980) The analytical hierarchy process, planning, priority setting, resource allocation (decision making serious), 1st edn. McGraw-Hill, New York, pp 154–155

Solangi YA, Ali Shah SA, Zameer H, Ikram M, Saracoglu BO (2019) Assessing the solar PV power project site selection in Pakistan: based on AHP-fuzzy VIKOR approach. Environ Sci Pollut Res 26:30286–30302. https://doi.org/10.1007/s11356-019-06172-0

Suuronen A, Lensu A, Kuitunen M, Andrade-Alvear R, Guajardo Celis N, Miranda M, Perez M, Kukkonen JVK (2017) Optimization of photovoltaic solar power plant locations in northern Chile. J Environ Earth Sci 76:824. https://doi.org/10.1007/s12665-017-7170-z

Tavana M, Santos Arteaga FJ, Mohammadi S, Alimohammadi M (2017) A fuzzy multi-criteria spatial decision support system for solar farm location planning. Energy Strateg Rev 18:93–105. https://doi.org/10.1016/j.esr.2017.09.003

The World Bank (2017) Longterm yearly average of diffuse horizontal irradiation—Islamic Republic of Iran. Solargis 19115:2003/19139

Uyan M (2017) Optimal site selection for solar power plants using multi-criteria evaluation: a case study from the Ayranci region in Karaman, Turkey. Clean Technol Environ Policy 19:2231–2244. https://doi.org/10.1007/s10098-017-1405-2

Villacreses G, Gaona G, Martínez-Gómez J, Juan Jijón D (2017) Wind farms suitability location using geographical information system (GIS), based on multi-criteria decision making (MCDM) methods: the case of continental Ecuador. Renew Energy 109:275–286. https://doi.org/10.1016/j.renene.2017.03.041

Watson JJW, Hudson MD (2015) Regional Scale wind farm and solar farm suitability assessment using GIS-assisted multi-criteria evaluation. Landsc Urban Plan 138:20–31. https://doi.org/10.1016/j.landurbplan.2015.02.001

Wu B, Yip TL, Xie L, Wang Y (2018) A fuzzy-MADM based approach for site selection of offshore wind farm in busy waterways in China. Ocean Eng 168:121–132. https://doi.org/10.1016/j.oceaneng.2018.08.065

Xu Y, Li Y, Zheng L, Cui L, Li S, Li W, Cai Y (2020) Site selection of wind farms using GIS and multi-criteria decision making method in Wafangdian, China. Energy 207:118222. https://doi.org/10.1016/j.energy.2020.118222

Yushchenko A, de Bono A, Chatenoux B, Kumar Patel M, Ray N (2018) GIS-based assessment of photovoltaic (PV) and concentrated solar power (CSP) generation potential in West Africa. Renew Sustain Energy Rev 81:2088–2103. https://doi.org/10.1016/j.rser.2017.06.021

Zoghi M, Ehsani AH, Sadat M, Amiri MJ (2017) Optimization solar site selection by fuzzy logic model and weighted linear combination method in arid and semi-arid region: a case study Isfahan-IRAN. Renew Sustain Energy Rev 68:986–996. https://doi.org/10.1016/j.rser.2015.07.014

Curriculum vitae

Personal data

Name:	Mojtaba Barzehkar
Date of birth:	26.02.1988
Place of birth:	Dehaqan, Isfahan, Iran
Citizenship:	Iran

Contact data

Address:	Ehitajate tee 5, 12616 Tallinn
Phone:	(+372) 53679636
E-mail:	mojtaba.barzehkar@taltech.ee

Education

2020–2024	Tallinn University of Technology, PhD, Coastal Engineering
2012–2014	Shahid Beheshti University, MSc, Natural Resources Engineering – Environmental Pollution
2007–2011	The University of Tehran, BSc, Natural Resources Engineering – Forestry
2003–2007	Shahid Razavian, High school, Experimental Sciences

Language competence

English	Fluent
Azerbaijani	Native
Persian	Native

Professional employment

January 2020–to date	Tallinn University of Technology, School of Science Department of Cybernetics, Early stage researcher

Research activity

Articles indexed by the Web of Science database (1.1):

Barzehkar, M., Parnell, K., Soomere, T. 2024. Extending multi-criteria coastal vulnerability assessment to low-lying inland areas: examples from Estonia, eastern Baltic Sea. Estuarine, Coastal and Shelf Science, 311, 109014, doi: 10.1016/j.ecss.2024.109014.

Barzehkar, M., Parnell, K.E., Soomere, T., Koivisto, M. 2024. Offshore wind power plant site selection in the Baltic Sea. Regional Studies in Marine Science, 73, 103469, doi: 10.1016/j.rsma.2024.103469.

Barzehkar, M., Parnell, K.E., Soomere, T., Dragovich, D., Engström, J. 2021. Decision support tools, systems, and indices for sustainable coastal planning and management: A review. Ocean & Coastal Management, 212, 105813, doi: 10.1016/j.ocecoaman.2021.105813.

Barzehkar, M., Parnell, K.E., Mobarghaee Dinan, N., Brodie, G. 2020. Decision support tools for wind and solar farm site selection in Isfahan Province, Iran. Clean Technologies and Environmental Policy, 23, 1179–1195, doi: 10.1007/s10098-020-01978-w.

Barzehkar, M., Mobarghaee Dinan, N., Salemi, A. 2016. Environmental capability evaluation for nuclear power plant site selection: a case study of Sahar Khiz Region in Gilan Province, Iran. Environmental Earth Sciences, 75, 1016, doi: 10.1007/s12665-016-5825-9

Articles in other peer-reviewed international journals (1.2):

Barzehkar, M., Parnell, K., Soomere, T. 2024. Incorporating a machine learning approach into an established decision support system for coastal vulnerability in the eastern Baltic Sea. Journal of Coastal Research, Special Issue 113, 58–62, doi: 10.2112/JCR-SI113-012.1.

Soomere, T., Bagdanavičiūtė, I., Barzehkar, M., Parnell, K.E. 2024. Towards implementing water level variations into Coastal Vulnerability Indexes in microtidal seas. Journal of Coastal Research, Special Issue 113, 48–52, doi: 10.2112/JCR-SI113-010.1.

Abstracts of conference presentations (5.2):

Barzehkar, M., Parnell, K., Soomere, T. 2024. Integrating multi-criteria decision analysis and GIS for coastal vulnerability assessment: a case study in Estonia, Eastern Baltic Sea. *10th Nordic Geographers Meeting* (24–27 June 2024, Copenhagen, Denmark).

Soomere, T., Barzehkar, M., Parnell, K.E. 2024. In search for suitable parameters quantifying the contribution of water level variations into coastal vulnerability index of microtidal seas. *5th Baltic Earth Conference "New Challenges for Baltic Sea Earth System Research"* (13–17 May 2024, Jūrmala, Latvia).

Barzehkar, M., Koivisto, M., Parnell, K.E, Soomere, T. 2022. An integrated decision support system for offshore wind farm site selection in the Baltic Sea. *18th European Academy of Wind Energy (EAWE)* (2–4 November 2022, Bruges, Belgium).

Barzehkar, M., Parnell, K., Soomere, T. 2021. An integrated decision support system for the resilience assessment of eastern Baltic Sea coasts. *CoastGIS* (16–17 September 2021, Raseborg, Finland, online).

Elulookirjeldus

Isikuandmed

Nimi:	Mojtaba Barzehkar
Sünniaeg:	26.02.1988
Sünnikoht:	Dehaqan, Isfahan, Iraan
Kodakondsus:	Iraani

Kontaktandmed

Aadress:	Ehitajate tee 5, 12616 Tallinn
Telefon:	(+372) 53679636
E-post:	mojtaba.barzehkar@taltech.ee

Hariduskäik

2020–2024	Tallinna Tehnikaülikool, doktorantuur
2012–2014	Shahid Beheshti ülikool, Iraan, MSc, Loodusvarad – keskkonnareostus
2007–2011	Teherani ülikool, BSc, Loodusvarad – metsandus
2003–2007	Keskharidus, Shahid Razavian keskkool, loodusteaduste kallakuga

Keelteoskus

Inglise keel	Kõrgtase
Aserbaidžaani keel	Emakeel
Pärsia keel	Emakeel

Teenistuskäik

Alates jaanuarist 2020	Tallinna tehnikaülikool, küberneetika instituut, doktorant-nooremteadur

Teadustegevus

Publikatsioonide ja ettekannete nimistu on esitatud ingliskeelse CV koosseisus.